# Microbial carbonates: concepts, controls and distribution on Neoproterozoic carbonate platforms, Congo Craton

Erwan Le Ber

Thesis submitted to the University of London

for the degree of Doctor of Philosophy

Earth Sciences Department

Royal Holloway, University of London

2014

## Declaration of authorship

I Erwan Le Ber hereby declare that this thesis and the work presented in it is entirely my own. Where I have consulted the work of others, this is always clearly stated.

<div align="right">

Erwan Le Ber

February 2014

</div>

# Abstract

Despite more than one hundred years of research, microbialites and more specifically stromatolites present several conundrums. Stromatolites are the main constituents of Neoproterozoic platforms, and are components of frontier petroleum systems. Assessing the factors influencing microbial sediment geometries and distribution is a crucial step toward the evaluation of their potential role in petroleum systems. This thesis presents a multi-area, multi-scale and multi-disciplinary study of microbially dominated carbonate platforms located in Democratic Republic of Congo, Zambia and Namibia. Literature reviews, field data and sample analyses are synthesised, both leading to discussions on current knowledge and understanding of each study area.

At the inter-regional scale, it appears that the break-up of supercontinent Rodinia at the beginning of the Neoproterozoic was accompanied by the development of rift shoulders. Such a setting favoured the initiation of carbonate platforms along the edges of the Congo Craton. Aspects of three of these platforms are developed to a regional-scale by: 1) questioning platform orientation in the West Congolian Group of Democratic Republic of Congo; 2) illustrating the development of organic-rich shales deposited in the vicinity of stromatolites in the Roan Group of Zambia; and 3) presenting a substantial dataset, with new interpretations, for complex facies of the post-Sturtian Rasthof Formation of northern Namibia.

Outcrop analysis in northern Namibia favours the detailed analysis of microbial fabrics. Stratigraphically, the Rasthof Formation represents a cap carbonate deposited in the aftermath of the Sturtian glaciation. Based on regional to microscopic-scale observations, the features encountered in the cap carbonate sequence are discussed. The facies locally exhibit evidence for elevated energy levels compatible with shallow water conditions, questioning the amplitude of the supposed post-glacial flooding. Fundamental mesoscopic to microscopic observations are presented to explain the variety of the microbial facies and geometries found in the Rasthof Formation.

"Sometimes, I guess there just aren't enough rocks."

Forrest Gump

# Acknowledgments

This thesis is the result of an unexpected journey. At the beginning I was expecting to go straight from the point A to the point B, maybe with one or two detours. Reality has been more chaotic, and the thesis is closer to a point A to plan B then C, to reach the point X: a journey to the unknown. It has been difficult to accept and this is where I begin my acknowledgments: starting with my supervisors Daniel Le Heron and Bernie Vining who have taught to me how to always look on the bright side of research.

I express my gratitude to Daniel Le Heron for his daily enthusiasm and patience to face my anxiety and doubts. I thank him for having significantly improved my academic mind and writing.

Thanks to Bernie Vining for setting up this project and gathering all the institutions involved. The project was based at the Royal Holloway University of London (RHUL), but most of the data came from Namibia, Zambia and the Democratic Republic of Congo. Thanks to Sonangol and Namcor who have funded this project, Fred Kamona (University of Namibia), Imasiku Nyambe and Willy Nundwe (University of Zambia) who all have greatly helped with the logistics in the field. Thanks to Gerd Winterleitner (RHUL) for his help with logistics in Namibia, sample analyses and sample sharing; Marie Busfield for her time and help on the field in Namibia and Zambia. I wish I spent more time with Damien Delvaux and Luc Tack (Royal Museum for Central Africa) to discover more about the geology of the Bas Congo. Thanks to the many farmers from Namibia and to the staff from Zambian mines (Konkola Copper Mines, Mopani Copper Mines, Chibuluma Copper Mines) who have accepted our visits and data collection.

Several researchers and experts spent some minutes or hours to help and guide me during this project: Pete Burgess, Dan Bosence, David Alderton, Norman Oxtoby, Nathalie Grassineau, Trevor Burchette, Christina Manning, Jürgen Adam, Margaret Collinson, Chris Elders, David Waltham, Martin Jones, Wendy Kirk, Monique Mettraux and Joyce Neilson. To this list I can add all the staff from the RHUL that

helped me to make it through with samples preparation, advices, computers repairs and administration.

I wish to thank my colleagues and friends, starting with Maria Emilia Bertoni for her listening, support, input and help for so many things I will need another page to list. I am very grateful to Arnaud Gallois for his advices and comments on many things, including my microfacies. Thanks to them and many other research students, colleagues from the department for creating such a friendly atmosphere. I am grateful to my closest friends that I managed to see or who managed to see me during the project: Anna, Gigi, Julia, Maxime, Romain and Yann. Also thanks to my flatmates during the last third of the PhD, it was good to live in a friendly and relaxing environment.

I wish to thank my parents Pascal and Dominique for educating me, and my grandparents Joseph and Marie Louise who paid most of my studies until the beginning of this PhD. Finally, I want to thank Maéva for her permanent support and encouragements. Without her I would not have been able to find the strength during this project.

# Table of contents

# List of figures

**Chapter 6**

**Chapter 7**

**Chapter 8**

# List of tables

# Introduction

This project results from collaboration between Royal Holloway University of London (RHUL), the Royal Museum for Central Africa (RMCA), the University of Zambia (UNZA) and the University of Namibia (UNAM). The project has been funded by Sonangol and Namcor, Angolan and Namibian national companies of petroleum exploration.

The thesis synthesises a multi-scale and multi-field study of a region of central-southern Africa, encompassing the western Democratic Republic of Congo (DRC), northwestern Zambia and northern Namibia (Figure I). The project was not initially designed for such a large-scale study but several unforeseen events led to fieldwork focussing in different areas. The reasons for these changes are explained in each related chapter of the thesis. The Neoproterozoic series studied in each of these areas were deposited in basins created during the break-up of the supercontinent Rodinia and are now exposed in Pan-African aged belts. They are preserved on the edges of the Congo Craton, a stable Precambrian continental crust extending through the DRC and surrounding countries. The aim of the thesis is to synthesise the early stage knowledge of Neoproterozoic microbial platforms along the craton margins. As hydrocarbon exploration in the interior basins of Africa proceeds, this knowledge is essential to understand how potential petroleum systems components may have formed in these frontier settings.

The Neoproterozoic covers a long period of time (1000–542 Ma) and the three areas are all separated from each other by more than 1200 km (Figure I). For each area, a literature review identified the most relevant stratigraphic interval, associated with its potential for fieldwork. In the DRC, the late Neoproterozoic (Ediacaran) platform has been studied for decades but recent changes in geodynamic models question the orientation of the platform and consequently the interpretation of Neoproterozoic sediments in the area. In Zambia, the lower part of the Neoproterozoic (late Tonian – early Cryogenian) is better exposed and was well studied between the 1950s and 1970s because of its important economic interest. Ore bodies are widespread and are hosted in the sediments of mixed siliciclastic/carbonate margin. There, the platform is relatively well understood.

Finally, Namibia is an emblematic country for Neoproterozoic research, and high quality exposures occur widely over the country. The mid Neoproterozoic (Cryogenian) platform found in the northern part of the country remains poorly understood and exhibits extremely unusual and laterally continuous microbial facies, whose depositional environment and platform context is uncertain. This stratigraphic interval has been chosen for the main field based study to evaluate potential facies variation across the platform.
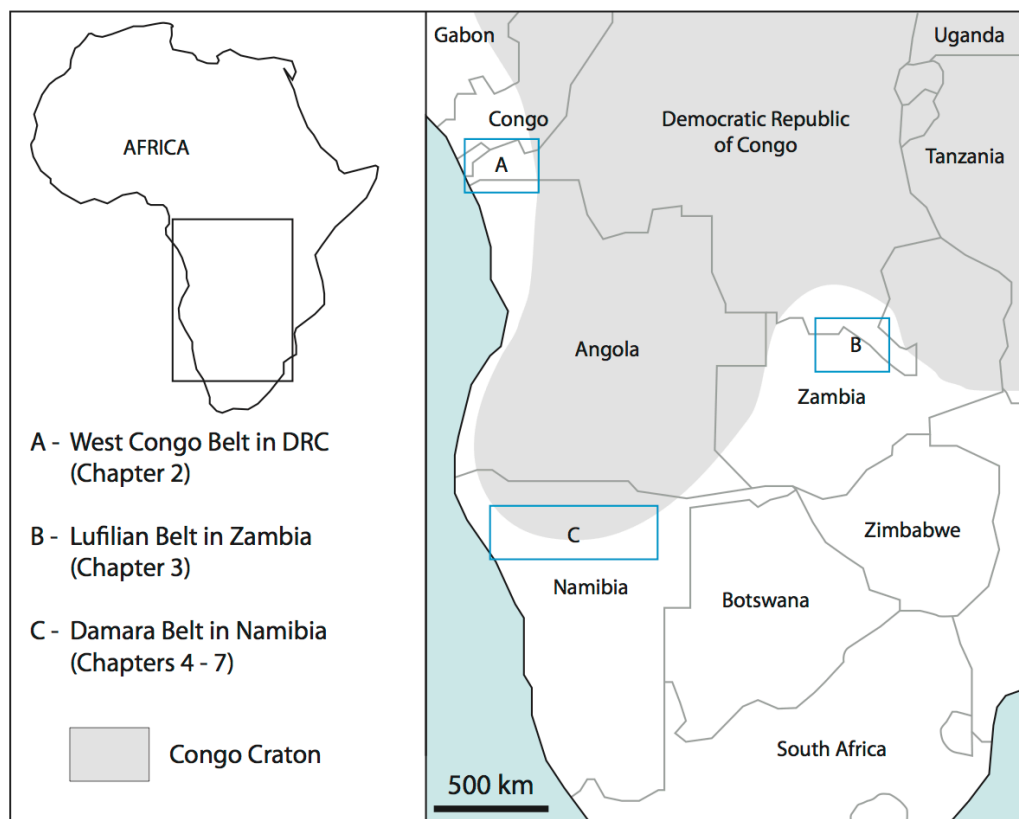


Figure I: Study area.

The overall area is complex to work in for several reasons that include quality/preservation of the sediments, safety and administration issues. The thesis deals with very spaced out areas and with disconnected stratigraphic intervals. The aim is therefore not to present integrated study of specific basins but to place all the intervals in a megaregional context, between the break-up of Rodinia and the Pan-African orogeny.

## Outline of the thesis

Before focussing on study areas, it is essential to introduce the Neoproterozoic. That is the aim of **Chapter 1**, to synthesise key features such as the geological context, knowledge about life and more specifically microbial carbonates. The chapter also explains why this era is important for frontier petroleum systems. Once the key Neoproterozoic features relevant to this study are presented, the rest of the thesis will address several problems, bearing in mind that the common theme of the studied areas are Neoproterozoic microbial dominated platforms.

The first Chapter, the second and the third are more based on literature data. They form the first part of the thesis. **Chapter 2** is a synthesis of the geology of the West Congo Belt (WCB) in the Democratic Republic of Congo (Figure I.A). Most of the Neoproterozoic is represented in this area, from the break-up of Rodinia to the Pan-African orogeny. The literature of the area points to the long-lived debate related to the interpretation of Neoproterozoic diamictites (mixtites of the Bas Congo in the DRC), and glacial vs. non-glacial modes of origin. Interpretations of the timing of the rifting and of the basement structure of the West Congo Belt are synthesised. This has implications for the orientation of the sedimentation. Timing and administration did not allow fieldwork in the DRC during this project; it has been decided to transfer the study to Zambia. **Chapter 3** focuses on the literature of the Roan Group (Tonian – Cryogenian) on the Zambian side of the Lufilian Belt (Figure I.B). This group records the local break-up of Rodinia, with the development of a microbially influenced platform on the southeastern margin of the Congo Craton. Interestingly, this part of the Lufilian Belt is well known for hosting one of the most important copper deposits in the world, giving its name to the area: the Copperbelt. The ore bodies are thought to be associated with organic rich sediments, deposited in the neighbourhood of stromatolites. This setting seems fairly well understood and illustrates how potential source rocks can be found in microbial environments. Results of the fieldwork in the area were limited and it has been decided to focus on a third area: northern Namibia (Figure I.C). The work done in Namibia is presented in the second part of the thesis because it is essentially based on field data, by contrast to the first part that is mainly literature-based.

In northern Namibia, a terminal Tonian – Ediacaran carbonate platform accumulated on the southwestern end of the Congo Craton (Angola Block). A specific stratigraphic interval of the platform, the Rasthof Formation, part of the Otavi Group, has been studied in details. The sedimentology of the formation and the setting of the platform are poorly understood. **Chapter 4** synthesises the knowledge of Neoproterozoic strata in the area. A more detailed review of previous descriptions/interpretations of the Rasthof Formation is also presented. The main interpretive challenges revolve around the microbial facies and the apparent lack of facies variations. Field observations are presented in **Chapter 5**, where facies variations are highlighted on the western part of the platform. Little has been published on microfacies from Cryogenian cap carbonates, **Chapter 6** focuses on establishing an inventory of notable microscopic features useful to understand the facies observed at a macroscopic scale, rather than focussing on diagenetic history only. The results of fieldwork on the eastern part of the same platform, evaluating facies variations, are presented in **Chapter 7**, with particular focus on stratigraphic conflicts and local facies interpretations. Finally, the last Chapter: **Chapter 8**, will wrap-up the outcomes of this project.

# Chapter 1 – The Neoproterozoic

## 1  Introduction

The Neoproterozoic (section 2) is a key Era in the history of Earth, which also involves many discussions and uncertainties related to large-scale tectonic (section 3), deposits of supposed large-scale glaciations (section 4) and the puzzling cap carbonates that overlie them (section 5). The scientific community tries to rebuild this old world, by understanding the break-up and amalgamation of supercontinents and their links with probable large-scale glacial events. Glaciations, tectonic activity or modifications of atmosphere and ocean composition are likely to be linked to major steps in the evolution of life (sections 6 and 7). The understanding of the Neoproterozoic Earth system is hence a real frontier and its visualisation requires multi-disciplinary efforts in all the fields of Earth sciences. A major component of Neoproterozoic carbonate platforms are microbialites but the interpretation of such facies has remained a real challenge for science for more than a century (section 7). Discoveries of Cenozoic microbialite petroleum systems offshore Brazil, and the constant need to access new oil and gas resources stimulate both industry and academia to investigate ancient sediments of microbial origin. In the Precambrian, microbial communities ruled the organic world and might represent major frontier for hydrocarbon resources (Craig et al., 2013, 2009). More generally, despite the lack of biodiversity and abundance compared to the Phanerozoic, icehouse/greenhouse transitions and microbial platforms of the Neoproterozoic are favourable settings for hydrocarbon source rock generation (section 8).

## 2  Stratigraphy

The Neoproterozoic is the terminal Era of the Proterozoic, preceding the Cambrian and the Phanerozoic Eon. Extending from 1000 to 542 Ma, the Neoproterozoic is split into three Periods (Ogg, 2009): the Tonian (1000–850 Ma); the Cryogenian (850–635 Ma) and the Ediacaran (635–542 Ma).

The study and the understanding of the Neoproterozoic are subject to several difficulties. The era is of long duration (ca. 458 Ma), yet only 3% of the world

outcrops are of Neoproterozoic age (Scotese, 2009). Moreover, most of them are metamorphosed or highly deformed. Due to the poor preservation or general lack of fossil assemblages, biostratigraphy is not applicable as in the Phanerozoic. Defining a stratigraphy and attempting correlations between different regions are not easy tasks.

## 3    Global tectonic

Building Neoproterozoic palaeogeographic models is a challenge because of poor palaeomagnetic data (Li et al., 2008; Pisarevsky et al., 2008). Furthermore, outcrops are scarce and mostly metamorphosed (Scotese, 2009). But considering the 458 million years of the Neoproterozoic, it is necessary to refer to the tectonic history of palaeocontinents. Two major configurations existed during the Neoproterozoic. Rodinia finished its amalgamation by 1000 Ma and started to break-up during the first half of the Neoproterozoic (Pisarevsky et al., 2003; Scotese, 2009). A short-lived supercontinent was then formed (650–500 Ma): Pannotia, also named Pan-African supercontinent or Greater Gondwanaland (Scotese, 2009). This second configuration is not always recognised as a supercontinent and most tectonic models consider it as a transition from Rodinia (~1000–750 Ma) to Gondwana (510–180 Ma) (Frimmel et al., 2011; Li et al., 2008; Pisarevsky et al., 2008). The Congo Craton has an uncertain history through the Neoproterozoic. This craton has a small counterpart now located in Brazil (São Francisco Craton) and in the following the term "Congo-São Francisco Craton" can be used to designate them as a single craton.

### 3.1    Rodinia

Rodinia (Figure 1.1.A) was amalgamated during the terminal Mesoproterozoic, between 1200 and 1050 Ma. Once assembled, the supercontinent persisted until the Cryogenian, when it broke-up in two parts: north and south Rodinia. This study focuses on sediments deposited along the edges of the Congo Craton, which has a poor palaeomagnetic dataset (De Waele et al., 2008). Latest studies consider several models for this craton (Li et al., 2008; Pisarevsky et al., 2008, 2003; Scotese, 2009). If Rodinia includes most of the palaeocontinents, the successive positions of the Congo-São Francisco Craton are uncertain. From geological synthesis and

palaeomagnetic data, De Waele et al. (2008) suggested that the Congo-São Francisco Craton could be independent or part of Rodinia. In the second possibility it is suggested that the Mwashya rifting (~765 Ma, Lufilian Belt) records the break-up between the Congo Craton and Rodinia.

Another model from Scotese (2009) suggests that the Congo Continent (i.e. Congo-São Francisco Craton and Saharan Shield) was separated from Rodinia by an ocean between 1100 and 900 Ma or between 1100 and 1050 Ma (Li et al., 2008 and references therein). Between 800 and 750 Ma the Congo Continent collided with Rodinia, this event triggered the break-up of the supercontinent into northern and southern Rodinia.

## 3.2    Pannotia

During and after the break-up of Rodinia, from 750 Ma onward, the Congo Continent (see Figure 1.1.A) was intercalated between north Rodinia (Kalahari, Mozambique, East Arabia, East Gondwana, Cimmeria, Sibumasu and Cathysia cratons) and south Rodinia (Laurentia, Amazonia, Rio Plata, West Africa, Baltica, Siberia cratons). This configuration is named Pannotia (Figure 1.1.D). Rodinia has broken-up and amalgamated Pannotia during the same geotectonic event. The collisions resulting from this amalgamation formed the Pan-African orogen around the Congo Continent. The first phase of collision involved the Congo Continent and north Rodinia (Figure 1.1.B), with the closure of the Mozambique Ocean (roughly 750–500 Ma, Grantham et al., 2003; Stern, 1994). The suture is in eastern Africa. Meanwhile, the Congo Continent started to collide with south Rodinia (Figure 1.1.C, D) with the closure of Pharusian–Adamastor Ocean between ca. 600 and 500 Ma (Gaucher et al., 2009 and references therein). Corresponding Pan-African belts are now located in southwest and west Africa. During the terminal Neoproterozoic – early Cambrian, Pannotia broke-up to form Gondwana, Laurentia, Siberia and Baltica palaeocontinents. The Congo Continent was then part of Gondwana.

The term "Pannotia" is not common in recent literature (Murphy et al., 2009; Scotese, 2009), yet it can be viewed as an inter-palaeocontinental stage between Rodinia and Gondwana. Synthesising all the local geotectonic history from Rodinia to Gondwana is a huge task limited by little and uncertain data. Timing and location

of cratons/basins are consequently highly uncertain. So far we can consider the following big picture: Rodinia was already formed in the early Neoproterozoic and broke-up around 750 Ma. During the terminal Neoproterozoic – early Cambrian, continental collisions led to the formation of the Pan-African orogen. This global scenario applies to the study area: basins were created during the break-up of Rodinia around the Congo Craton, the series deposited in these basins are now exposed in the Pan-African aged West Congo, Damara and Lufilian belts.
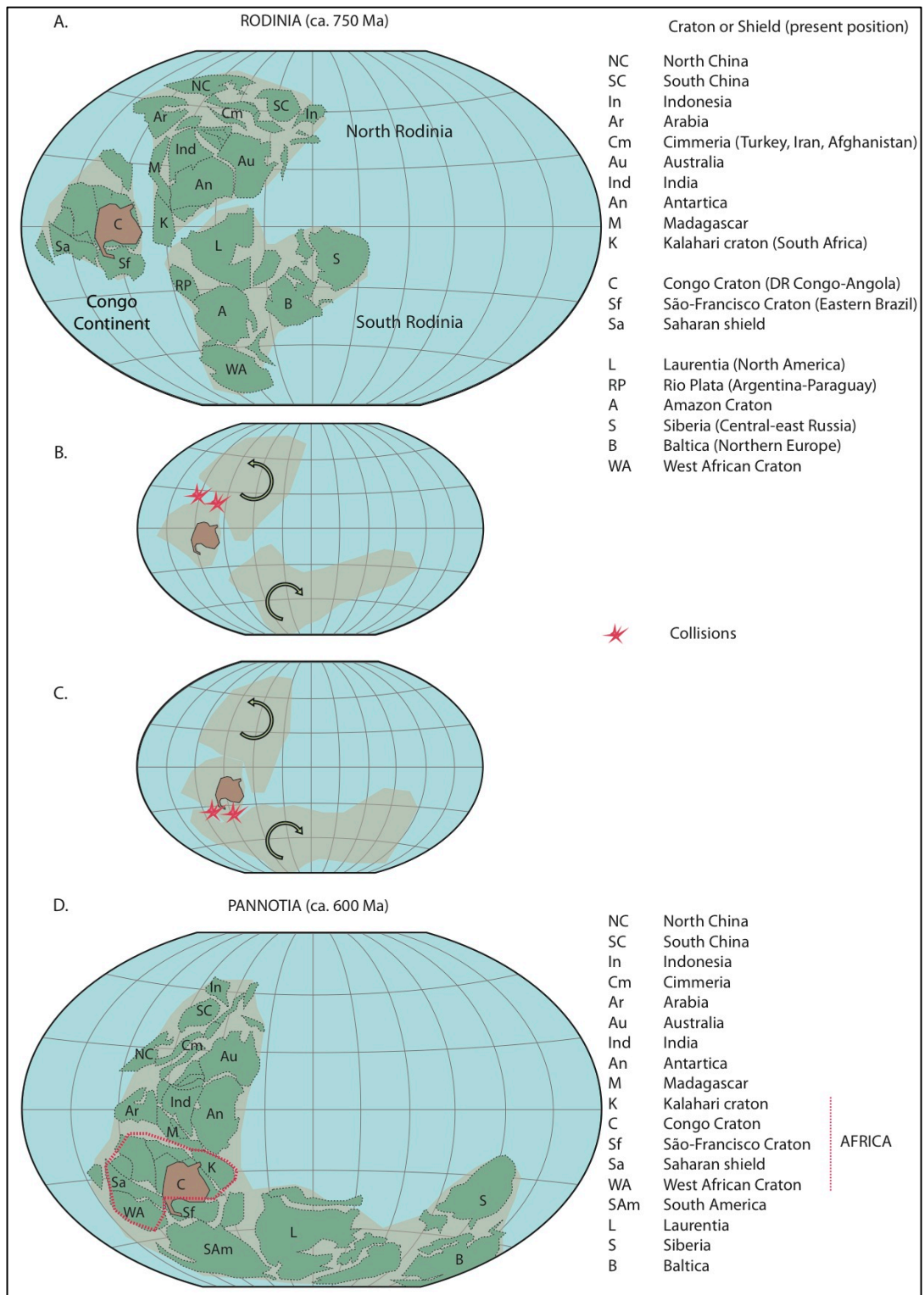
Figure 1.1: From Rodinia to Pannotia. Redrawn from Scotese (2009). **A**. Rodinia before break-up, with the Congo Continent independent from the supercontinent. Note the Congo-São Francisco Craton in red. **B** and **C**. Sketches of the break-up of Rodinia with collisions on the (modern) eastern then western edges of the Congo Craton. **D**. Pannotia with the highlight of the modern coastline of Africa (modern orientation is ~90° clockwise).

# 4 Cryogenian diamictites: glaciations vs. tectonics

## 4.1 Diamictites, glaciations and snowball Earth

One of the periods of the Neoproterozoic is named the Cryogenian from the Greek *cryos* "cold" and *genesis* "birth". Several Cryogenian diamictites (cf. Flint et al., 1969a, 1969b) are observed worldwide. Diamictites are non- to poorly-sorted, generally non-stratified terrigenous sediments. The term "diamictite" is purely descriptive, and hence diamictites can result from a variety of processes in environments ranging from marine to continental (e.g. Eyles and Januszczak, 2004). Kirschvink (1992), Hoffman et al. (1998a, 1998b and references therein), Hoffman and Schrag (2002) and many other authors suggest that several of these diamictites result from glacial processes. Typical features such as ice-rafted clasts and striated clasts are highlighted in support of this interpretation.

Furthermore, interpretations of palaeomagnetic data place some of these diamictites at low palaeolatitudes. The snowball Earth hypothesis proposed by Kirschvink (1992) and Hoffman et al. (1998b) suggests that during the Neoproterozoic, the Earth underwent at least two worldwide ice ages. These ice ages are often referred as the Sturtian (ca. 720–660 Ma) and Marinoan (ca. 650–635 Ma) glaciations (Arnaud et al., 2011; Hoffman and Li, 2009 and references therein). These two major glaciations are often used as rough correlative tools from one region to another because they are described on many palaeocontinents around the world (Hoffman and Li, 2009 and references therein). A third important glaciation is recognised, though less widespread: the Gaskiers event (c.a. 580 Ma, Hoffman and Li, 2009 and reference therein). In addition to those diamictites, the snowball Earth hypothesis suggests that after each glacial event, a cap carbonate sequence records a post-glacial flooding (e.g. Allen and Hoffman, 2005; Fairchild and Kennedy, 2007; Hoffman and Schrag, 2002; Hoffman et al., 2007, 1998b; Rose and Maloof, 2010; Shields, 2005). The snowball Earth hypothesis does not only rely on physical evidence: unusual isotopic records are also used to support this model (Hoffman et al., 1998b).

## 4.2    Other interpretations of the diamictites

The snowball Earth hypothesis and model are not universally accepted and other studies tend to interpret the Cryogenian diamictites or the related glaciations differently. Two aspects of the snowball Earth are criticised: 1) the global Earth context and 2) the sedimentological interpretation of the diamictites.

- The snowball Earth hypothesis is an extreme model, with a fully frozen Earth and no hydrological cycle. Whilst ice was probably present during the Cryogenian, a hard snowball Earth is often criticised and moderated with less extreme interpretations (e.g. Allen and Etienne, 2008; Fairchild and Kennedy, 2007; Le Heron et al., 2013a, 2011). Ice ages with a partially frozen Earth, an active hydrological cycle and ice-free areas are favourable settings to explain how life survived the Cryogenian icehouse periods (Le Heron, 2012). Still in relation with the global Earth context, the geodynamic events during the Cryogenian raise several questions regarding the origin of the diamictites, which leads us to the second point;

- Eyles and Januszczak (2004) and Eyles (2008) assume that many geologists misinterpret the environmental context of the Neoproterozoic diamictites. Those authors emphasise a rifting context, thus explaining the origin of diamictites via debris flow processes, turbidites or slumps. Some diamictites may have a glacial origin (sourced from glaciers that developed on rift shoulders during the break-up of Rodinia), whereas others may be simply tectonic in origin.

Sedimentological interpretation of diamictites is highly debated in the literature, with depositional environments ranging from strictly glacial to non-glacial. As an example, the interpretation of two distinct Neoproterozoic diamictites has been and is still debated in the West Congo Belt (western Democratic Republic of Congo) since the 1950's (see Chapter 2). Today, the glacial influence on sedimentation remains uncertain.

The study of the Cryogenian diamictites has generated a vigorous debate for more than 50 years, fuelled in the last two decades by the snowball Earth hypothesis (e.g.

http://snowballearth.org/bibliography). If one critically accepts the evidence for glaciation in each area, assuming that this evidence can be separated from tectonic processes, a major outstanding issue is that of geochronology. Whether three or more glaciations are recognised is open to debate as error bars for different dating techniques are often wide (Allen and Etienne, 2008). Using them as a correlative tool is therefore speculative. The snowball Earth hypothesis explains that after glaciations, a global sea level rise provoked the deposition of cap carbonates, another challenge for Earth scientists.

## 5    Cap carbonates, cap dolostones

### 5.1    Definition and context

The definition of a cap carbonate by Hoffman and Li (2009) is: "'**Cap-carbonate sequences**' (Hoffman and Schrag, 2002) refer to depositional sequences initiated by glacioeustatic flooding and ultimately accommodated by syn-glacial erosion and subsidence. **Cap dolostones** are the transgressive tracts of cap-carbonate sequences."

In the snowball Earth hypothesis, the sea level rise following the Neoproterozoic glaciations triggered the deposition of cap carbonate sequences (Hoffman et al., 1998a, 1998b). A cap carbonate generally starts with a 0–20 m-thick (but > 100 m in some areas) thinly laminated cap dolostone or basal cap carbonate (Corsetti et al., 2006; Hoffman et al., 2007), generally found in sharp contact above the diamictites. Post-Marinoan cap dolostone are more widely studied than the post-Sturtian examples (e.g. Hoffman et al., 2007 and references therein; Rose and Maloof, 2010; Shields, 2005).

If not considering the snowball Earth hypothesis (e.g. Eyles and Januszczak, 2004), cap carbonate could result from recycled carbonates or shallow-water carbonates accumulated when accommodation rates tended to decrease by the end of continental break-up. The association of shallower water setting and diminution of siliciclastic input would allow the formation of carbonate platforms. In the thesis, regardless of their origin (post-glacial flooding or late rifting stage setting), the

terms "cap carbonate" and "cap dolostone" are employed to designate these sediments.

## 5.2    Features

Cap carbonate sequences can reach up to several hundred m-thick. Facies can consist of shales to siltstones or limestones (Shields, 2005). Cap dolostones exhibit more exotic facies, and if underlying diamictites represent a complex sedimentological challenge, the cap dolostones are equally problematic from a sedimentological perspective, in addition to their unusual stable isotope geochemistry which is well recognised (Hoffman et al., 1998b; Kennedy and Christie-Blick, 2011; Shields, 2005). From one area to another, cap dolostones generally share common features such as a flat, mm-thick laminated fabric and a consistent lateral occurrence. Since they have been the subject of more detailed study, Marinoan cap carbonates are better documented than their Sturtian counterparts. Unusual sedimentary features are often described in the cap dolostones deposited in the aftermath of the Marinoan glaciation. They include sheet-crack cements, seafloor aragonite, giant wave ripples, seafloor barite, tube structures, and tepee like structures (e.g. Allen and Hoffman, 2005; Cloud et al., 1974; Corkeron, 2007; Corsetti and Grotzinger, 2005; Font et al., 2010; Hoffman and Macdonald, 2010; Jiang et al., 2003; Kennedy, 1996; Kennedy et al., 2001). Post-Sturtian cap carbonates and cap dolostones are far less studied and do not seem to exhibit such sedimentary features (Giddings and Wallace, 2009a, 2009b; Hood and Wallace, 2012; Le Ber et al., 2013; Tojo et al., 2007; Vieira et al., 2007).

Cap dolostones are mostly examined at the outcrop scale but some studies try to interpret them at a more regional scale, as post-glacial blankets. The reason for that is the need to understand the processes and timing involved in their deposition (Font et al., 2010; Hoffman et al., 2007; Rose and Maloof, 2010).

Another feature observed in the cap carbonate sequences overlying the diamictites (not only post-Marinoan) is their unusual isotopic record. Typical carbon isotope excursions are recognised during the Neoproterozoic: the Bitter Spring stage (ca. 800 Ma); the Islay anomaly (ca. 710 Ma); the Trezona anomaly (ca. 640 Ma) and the Shuram Wonaka anomaly (ca. 580 Ma) (Halverson et al., 2005; Macdonald et al.,

2010). Other isotopes such as O, Sr, and S are used to understand and evaluate the composition of Neoproterozoic ocean (Halverson et al., 2010, 2009 and references therein). Isotopic trends and interpretations were already studied before the snowball Earth hypothesis (Hoffman et al., 1998b and references therein). Since then, interest in Neoproterozoic stable isotope systems has increased exponentially, producing a dense literature with much discussion (Delpomdor and Préat, 2013; Derry, 2010; Frimmel, 2010; Giddings and Wallace, 2009a, 2009b; Halverson et al., 2010, 2009; Kaufman and Knoll, 1995; Le Guerroué and Cozzi, 2010; Macdonald et al., 2010; Rothman et al., 2003) about their use as correlative tools or proxies for oceanic/atmospheric composition.

## 6   Life

### 6.1   A transitional Era

In Neoproterozoic, the *Neo* prefix means "new", because it comes after the Mesoproterozoic (1600–1000 Ma) and the Paleoproterozoic (2500–1600 Ma). *Proterozoic* comes from the Greek *proteros* "fore, former" and *zoon* "animal, living creature", or all in all "earlier life". The Neoproterozoic is a transitional Era for the evolution of life. Direct evidences for early life (microfossils) are found in Archean sediments, deposited between ca. 3.5–3.0 Ga (Altermann and Kazmierczak, 2003; Brasier et al., 2006; Schopf et al., 2002) and possibly earlier, with geochemistry analyses, ca. 3.8 Ga (Mojzsis et al., 1996). The Ediacaran in particular is a crucial period of time for life evolution and the radiation of the metazoans (Canfield et al., 2007; Marshall, 2006; Peterson and Butterfield, 2005; Peterson et al., 2008).

Key biological events occurred during the Neoproterozoic, the most emblematic being the decline of stromatolite abundance in the rock record and then the appearance of the Ediacaran biota. Stromatolites (see section 7) are the earliest evidence for life in the fossil record, but their abundance decreased significantly during the Neoproterozoic (Grotzinger and Knoll, 1999; Grotzinger, 1990; Riding, 2011a). The second key event is the appearance of a variety of unusual macroscopic fossils, often referred as the Ediacaran biota (McCall, 2006; Narbonne, 2005; Peterson and Butterfield, 2005; Peterson et al., 2008; Seilacher et al., 2003). It is often considered as an unique fossil assemblage, an aborted biota specific to the

Ediacaran. But its status has more recently been criticised; MacGabhann (2014) explains that the fossils should not be looked as a whole and that they are not specific (geography, stratigraphy, biology, taphonomy) from this period.

The reasons for these major biological changes (i.e. stromatolite decline, metazoans radiation) remain unclear. They may be related to glaciations (Hoffman et al., 1998b); large-scale tectonic reconfigurations (Meert and Lieberman, 2008; Santosh, 2010); changes of hydrosphere and atmosphere compositions (Canfield et al., 2007) or genetics (Peterson et al., 2008). These hypothesis can be combined and interact.

## 6.2    Evolution in the Neoproterozoic

The Cambrian is a well-established step for metazoan radiation, with the appearance of both fossils and bioturbation in the sediment record (Marshall, 2006). Before that (except during the Ediacaran), indisputable body fossils are lacking from the fossil record. Any discovery of a possible multicellular fossil in the Precambrian record is thus subject to serious discussion and rigorous evaluation.

Evidence for Neoproterozoic eukaryotes, ranging from the micro- to macroscopic scale, tend to increase through time (Bosak et al., 2012, 2011; Butterfield, 2009, 2005; Corsetti et al., 2003; Dalton et al., 2013; Knoll et al., 2006; Maloof et al., 2010; Xiao, 2004). This indicates that radiation and rise of the metazoans may have started well before the Cambrian explosion or the Ediacaran, an interpretation that accords with evidence from molecular clocks (Peterson et al., 2008). Indeed, this rise of complex life is thought to be one of the causes of the stromatolite decline during the Neoproterozoic (Walter and Heys, 1985).

## 7    Microbialites: stromatolites

Note: two major publications dealing with all the questions related to definitions and understanding of stromatolites were published during this PhD: Riding (2011b) and Bosak et al. (2013a). Below, an overview about stromatolites is presented.

## 7.1    Definitions

"Microbialites are organosedimentary deposits that have accreted as a result of a benthic microbial community trapping and binding detrital sediment and/or forming the locus of mineral precipitation" (Burne and Moore, 1987).

Among microbialites, several categories are recognised according to their macrofabric: thrombolites, dendrolites, leiolites and the most common in the Precambrian literature: stromatolites (Figure 1.2). As Riding summarised (2011a, 2011b, 2000, 1999, 1991), the definition and concept of stromatolites have changed considerably since the term "stromatolith" was first introduced by Kalkowsky in 1908. The definitions proposed by Riding are: "Stromatolites are laminated benthic microbial deposits" (1991) and "Stromatolites are macroscopically layered authigenic microbial sediments with or without interlayered abiogenic precipitates" (2011b).
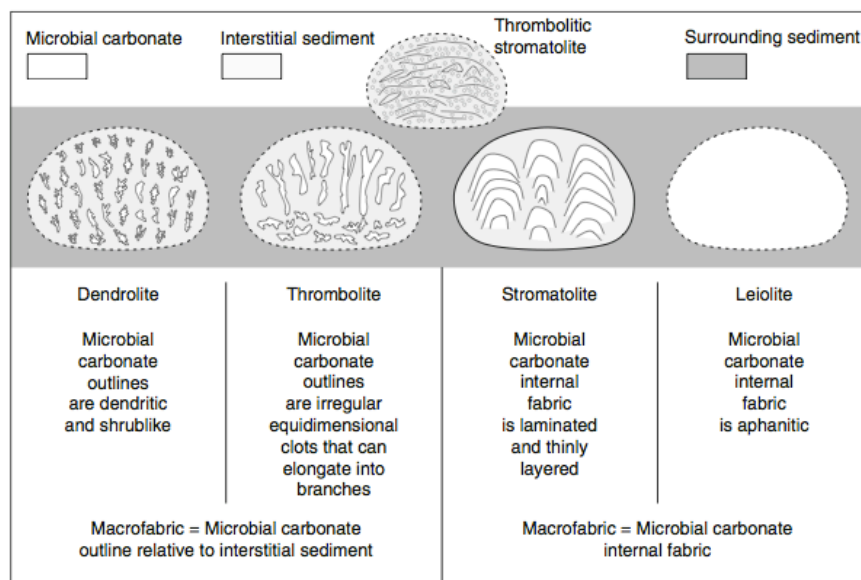


Figure 1.2: Microbial carbonates defined by macrofabric (Riding, 2011a).


## 7.2    Approaches in stromatolite interpretation

### 7.2.1    Evolutionary vs. environmental trends

Several approaches are used or have been used when studying stromatolites. Basically, two main "schools" exist. The first tends to view stromatolites as a potential biostratigraphic tool, adopting a Linnaean-style classification of forms (e.g. *Conophyton*, *Collenia*, *Baicalia*: Bertrand-Sarfati and Walter, 1981; Cloud and Semikhatov, 1969; Grey et al., 2011; Hill et al., 2000). This approach generally uses taxa, species and assemblage names to describe stromatolites. This classification is used as a reflection of evolutionary trend of microbial communities through

geological time, where one specific geometry or assemblage is typical from one period of time. This view of stromatolites is not proven but not impossible. However, stromatolites are not one organism; they are rocks resulting (in part) from microbial activity. Hofmann (1994, 1973) proposed more technical, quantitative ways to describe stromatolites. He considers they result from environmental processes but does not exclude a biostratigraphic use. Logan et al. (1964) viewed classification of stromatolites as confusing and complex; they proposed a more simple descriptive way where geometries of the stromatolites result from the environmental setting at the time of deposition. Since the 1990s, most studies view the stromatolite geometries as the result of a complex interaction between microbial communities and the environment (e.g. Allwood et al., 2009; Andres and Reid, 2006; Braga et al., 1995; Dupraz et al., 2006).

### 7.2.2  Modelling stromatolites

With this latter approach, the understanding of as many of the parameters and processes involved is used to establish a relationship between stromatolite geometries and depositional environment. In the field of microbiology, simple laboratory and modelling (cellular automaton, diffusion-limited aggregation) experiments show that a same type of bacterial colony can generate different patterns under different stresses (Lacasta et al., 1999; Matsushita et al., 1998; Wimpenny and Colasanti, 1997). Similar techniques have been used to simulate the growth of stromatolites and have produced geometries comparable to the fossil record (Dupraz et al., 2006; Grotzinger and Knoll, 1999). These simulations are still at an early stage and limited: it is extremely complicated to simplify a complex interactive ecosystem into a mathematic model with restricted variables. Also, if this kind of model can generate geometries extremely close to those observed in the rock record, one has to consider that similar geometries can form at different scales (mm–m) as well as in different environments. This approach is helpful to determine the controls influencing the growth of stromatolites but not sufficient to determine precisely the environment in which they have formed.

### 7.2.3 Modern vs. ancient stromatolites

Interpretation of ancient stromatolites is complex because there is no simple rule to illustrate how microbial communities interact with sediments and environmental controls. In Earth sciences, it is very common to refer to modern environments as analogues to understand the rock record. Several studies describe and interpret modern stromatolites (e.g. Andres and Reid, 2006; Jahnert and Collins, 2011; Papineau et al., 2005) but it is difficult to use them as analogues for ancient stromatolites (Grotzinger and Knoll, 1999). Considering the many parameters influencing stromatolite growths, similar shapes can be the result of different processes. Until the terminal Precambrian, the microbial communities were not exposed to grazing. Their growth was mainly influenced by physical and chemical factors. Today, microbial communities have to adapt their survival with other forms of life. Comparing ancient to modern stromatolites can allow the verification of some physical controls on the geometries but cannot guarantee their full comprehension. This kind of comparisons can also involve chemical and microbial controls. Given the lack of knowledge about 1) the nature and the metabolism of the microbes and 2) the seawater composition during the Neoproterozoic, analogy with modern stromatolites is complex.

## 7.3 Processes involved

Stromatolites are generally formed in a relatively shallow marine environment (Grotzinger and Knoll, 1999) and result from three processes: trapping of the sediments by microorganisms, biomineralisation and mineralisation (Flügel, 2004; Riding, 1991). All of these processes depend on several biological (microbial community, competition, cohesion), physical (topography, light, energy, grain size, hydrodynamic, accommodation, temperature, sediment input), chemical (salinity, nutrients, alkalinity) and time factors (Andres and Reid, 2006; Dupraz et al., 2006). Stacking of laminated fabric in stromatolites can result in a diversity of geometries such as tabular, columnar, domal or branching. These geometries range from the mm to the m-scale.

With favourable conditions, microbial communities will colonise the seafloor. Then, the environmental changes will force the microbial communities to adapt to survive

(Allwood et al., 2009). It is often accepted that water flow and scouring or sediment input lead to the branching of stromatolites (Bosak et al., 2013a; Dupraz et al., 2006; Johnson and Grotzinger, 2006; Planavsky and Grey, 2008). Abrasion by water or deposition of sediments will locally inhibit the growth of the mats, generating negative topography. Flow and sediments will preferentially follow the depressions, favouring the growth of columns on positive topography. The microbial communities are less exposed to such stress on the positive topography and can therefore continue growing.

The genetic input, the strategy and the behaviour of microbial communities at the time of deposition are difficult to evaluate when looking at the rocks. Nevertheless, organisation of the microbial communities at a microscopic scale may have influenced the growth patterns at a macroscopic scale. With unknown biological influence, stromatolites (and more generally microbialites) have to be tackled like any sediment, considering the rheology and cohesiveness of microbial mats before their lithification. A classic sedimentological approach, with the analysis of associated facies, is necessary to portray the depositional setting of stromatolites.

## 7.4    Geological record and Neoproterozoic decline

The oldest evidence of a stromatolite is at 3.4–3.5 Ga (Allwood et al., 2009, 2006). They were very common during the Precambrian but are scarce today and the most famous modern stromatolites are located in Shark Bay (Australia) and in Highbourne Cay and Lee Stocking Island (Bahamas).

Two trends are used to evaluate the stromatolites in the sediment record (Figure 1.3): their abundance (Grotzinger, 1990) and their morphologic diversity (Awramik and Sprinkle, 1999). The first one is based on the observation of stromatolites in the rock record while the second one is based on their diversity (different morphologies). A diversity trend is supposed to reflect possible evolutionary trend through time. But considering stromatolites as the result of a complex interaction between environmental and microbial controls, morphologic diversity trend is more likely to reflect the diversity of depositional settings.
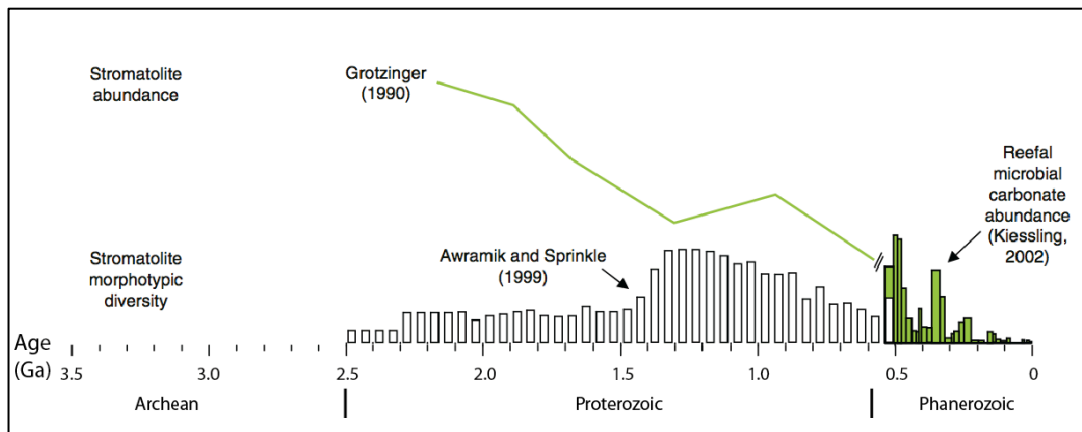
Figure 1.3: Stromatolite decline through time (Riding, 2011a).

Though constantly decreasing since the early Proterozoic, relatively high stromatolite abundance in the rock record from the Paleoproterozoic to the early Neoproterozoic might be due to a poor competition, a decrease in sediment production and high carbonate saturation in the seawater (Grotzinger, 1990). Indeed, without rivalry, microbial communities were able to develop easily without being consumed, disturbed or destroyed. Also, if the carbonate saturation in seawater was sufficient, microbial communities had enough supply to grow in platform settings.

The peak of the morphological diversity of stromatolites is estimated around 1.1–1.4 Ga (Figure 1.3) (Awramik and Sprinkle, 1999; Riding, 2006; Walter and Heys, 1985). Then during the Neoproterozoic, stromatolite diversity and abundance dramatically decreased (Grotzinger, 1990; Xiao, 2004). The demise of stromatolites probably results from the changing Earth system (supercontinent break-up bringing large amount of siliciclastics, large-scale ice ages, decrease of carbonate saturation in the ocean and changes in atmosphere composition) and the arrival of the first grazers (Walter and Heys, 1985). Finally during the terminal Neoproterozoic and the Phanerozoic, the intensive development of metazoans might have played a role in the decrease of stromatolite diversity and habitats (Riding, 2006).

## 7.5 Discussion

The approach to the study of stromatolites has evolved considerably in one century. For many decades, their study involved a palaeontological approach with the

recognition of different taxa and assemblages. The problem with this classification is that it is highly subjective. Stromatolites result from several generations of microbial communities, over thousands or millions years, and cannot be interpreted as one evolving organism. Today, most of the studies focus on understanding the controls and processes affecting stromatolite geometry, from a micro- to macroscopic scale.

At this stage, there is no indisputable evidence to use stromatolite morphodiversity as a biostratigraphic tool. Regardless of the human bias in recognising supposed different morphologies, the drop of morphodiversity through the Meso-Neoproterozoic might be related to their decreasing abundance in the rock record:

1) Fewer stromatolites in the rock record can mean fewer favourable environments for microbial communities to develop;

2) Reduced amount of favourable environments result in reduced variability/combination of environmental controls;

3) With fewer combinations of these controls, morphodiversity decreases, without involving any biologic evolutionary trend.

Geometry of stromatolites is thus more likely to reflect changing environmental controls. Sequences or patterns in stromatolite geometries can be identified at the outcrop scale (Chapter 5, Le Ber et al., 2013; Tucker, 1977), reflecting gradual changes in the environment. Microbial communities probably had an influence in determining the growth structures at a microscopic scale. In detail, understanding the microbiological interaction with sediments is challenging in terms of space and time scales. It is important to understand the factors influencing the growth of stromatolites (and other microbialites) because it helps to reconstruct the environments in which they have formed. Beyond the sedimentological challenges, microbialites are increasingly of interest to the hydrocarbon industry, as explored below.

# 8    Neoproterozoic petroleum systems

## 8.1    Proven and potential systems

Five elements are necessary to generate a viable petroleum system: 1) a source rock, 2) a reservoir, 3) a trap, 4) a seal and 5) timing. These five elements can occur in Neoproterozoic strata. The preservation of 1–4 and the probability they occur in a favourable configuration (5) to generate a petroleum system are more uncertain. The age of the rocks and their diagenetic/burial/metamorphic history cannot guarantee a good preservation of reservoir properties. With such long post-depositional history, potential source rocks are also likely to be over-mature as well.

The timing is a crucial point and therefore Neoproterozoic or even older rocks are a new frontier for petroleum exploration (Craig et al., 2013; Ghori et al., 2009). Several Neoproterozoic petroleum systems are already proven (Figure 1.4.A) in north Africa (Tindouf and Taoudeni basins), Australia (Amadeus, Officer and Mcarthur basins), India, China, Oman (Grosjean et al., 2009) and Russia (Frolov et al., 2011; Howard et al., 2012). The last three are even producing (Ghori et al., 2009; Lottaroli et al., 2009). Such proven and viable systems motivate both academic and industrial research to explore further time equivalent strata around the world. That is where this project starts, to study the sediments deposited along the margins of the Congo Craton. The studied area encompasses the Democratic Republic of Congo, Zambia and Namibia (Figure 1.4.B).
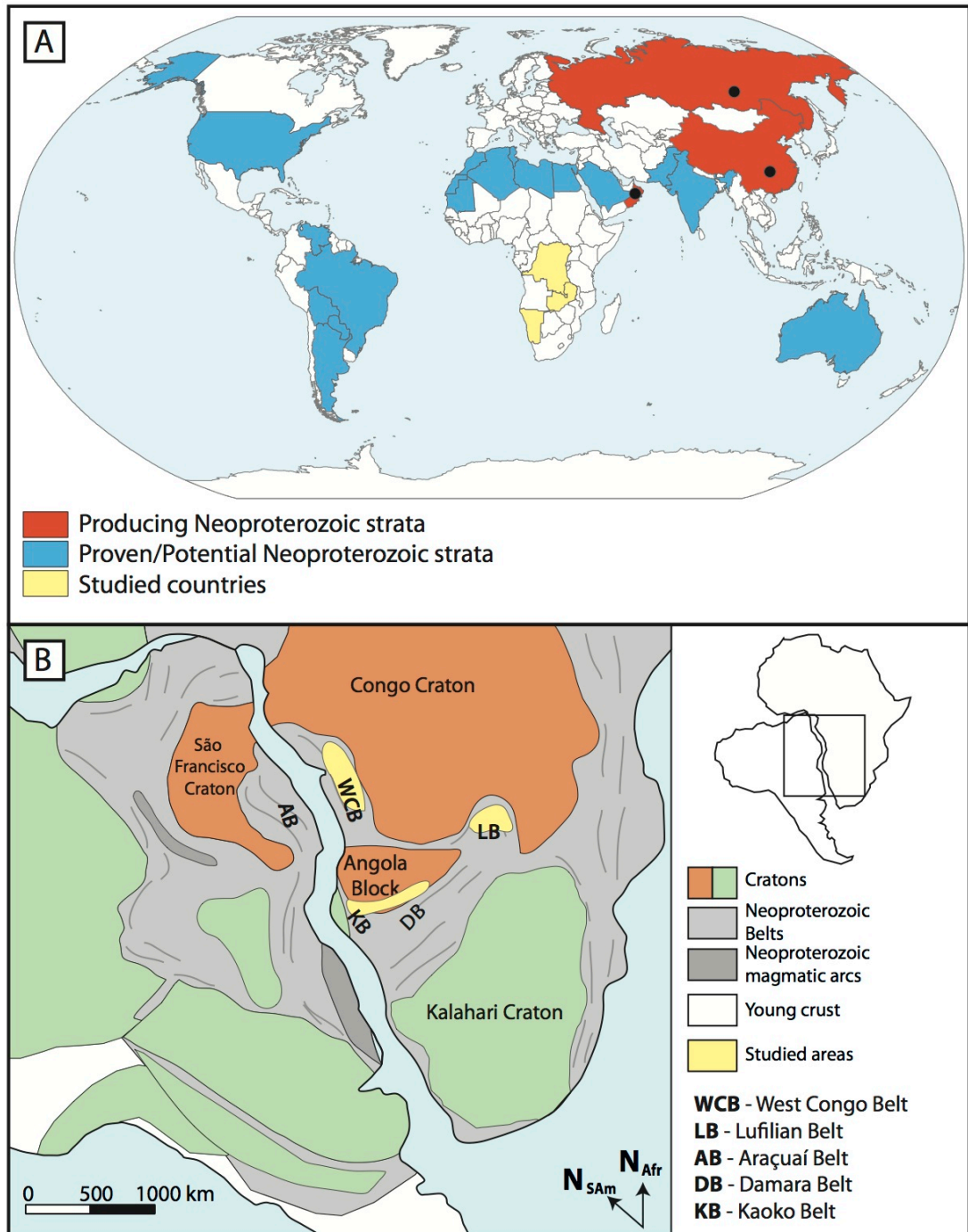
Figure 1.4: Neoproterozoic petroleum systems around the world. **A**. Synthetic map with producing and proven/potential systems (Lottaroli et al., 2009; Ghori et al., 2009). **B**. Setting of the studied area before the opening of the Atlantic. Brazil was grouped with the DRC, Angola, Namibia and Zambia, forming the Congo-São Francisco Craton (Modified from Frimmel et al., 2011).

## 8.2 Favourable environments during the Neoproterozoic

### 8.2.1 Microbialites and their potential

The widespread, microbially dominated platform environments represent favourable settings for the accumulation of hydrocarbon source rocks and reservoirs. Thus far, little is known in detail about the potential of microbial sediments as reservoirs. Microbial communities can build micro- to macroscopic frameworks creating porosity and permeability; sediments deposited between microbial buildups may also exhibit favourable reservoir properties (e.g. porous grainstones, vugs). The problem is that these textures are unlikely to be preserved over hundred million year timescales. In producing Precambrian carbonate strata of Russia, the main reservoir properties result from *secondary* features such as fractures, cavities or karsts (e.g. Frolov et al., 2011). In Neoproterozoic strata, it should be noted that petroleum system elements are not limited to the microbialites. Deeper water lateral equivalents of the microbial platform can consist of black shales, viewed as potential source rocks (Craig et al., 2009). Organic-rich facies can also be deposited in relatively shallow-water settings, in close association with microbial growths. For example in the Tonian strata of the Copperbelt, organic-rich shales that contain high TOCs (2–6%) are observed in close relationship with stromatolites (Garlick and Fleischer, 1972; Scott et al., 2006; Stanton, 1972).

### 8.2.2 Ice ages

Icehouse and greenhouse events create respectively favourable settings for the formation of sandy reservoirs (Huuse et al., 2012) and the deposition of source rocks during post-glacial transgression (Craig et al., 2009; Le Heron and Craig, 2012; Smith, 2009). The Neoproterozoic is known for its ice ages and is consequently an interesting Era for the investigation of potential petroleum systems. Glacial or not, diamictites are widespread in the global Neoproterozoic record (Fairchild and Kennedy, 2007; Hoffman and Li, 2009 and references therein). They are generally followed by cap carbonate sequences that can include post-glacial black shales (Huuse et al., 2012; Le Heron and Craig, 2012) and/or microbialites, deposited in a platform setting. Bechstädt et al. (2009) already suggested an analogy between Namibian Ediacaran post-glacial facies and North African late Ordovician – early

Silurian "hot shales" deposited in depressions after the melting of ice caps. Depressions can result from tectonic-related topography or valleys incised by ice during the glaciation (Lüning et al., 2000, 1999).

## 9    Conclusion

The Neoproterozoic is a key period on Earth, with important uncertainties and major events that may be connected between each other.

- The supercontinent Rodinia broke-up during the Neoproterozoic. The specific role and location of the studied Congo-São Francisco Craton is very uncertain in this setting;

- The break-up of Rodinia was accompanied by the deposition of widespread diamictites that have been interpreted as strictly glacial to strictly non-glacial. The break-up of Rodinia may have favoured the development of high rift shoulders, favourable to the development of ice bodies;

- In most of the case, diamictites are directly overlain by a cap carbonate sequence. These sediments are characterised by a specific set of facies (cap dolostones) and specific isotopic signatures;

- Severe icehouse/greenhouse transitions associated with major geotectonic events maybe linked to major steps in life evolution. The Neoproterozoic is a transitional Era before the Cambrian explosion;

- Microbialites, and more specifically stromatolites are the relics of dominant form of life during the Neoproterozoic Era. Interpretation of microbially influenced facies is fundamental to portray carbonate platforms during this era;

- As demonstrated in several countries, Neoproterozoic strata can represent significant economic value. Icehouse/greenhouse transitions and widespread carbonate platforms are interesting settings for the exploration of frontier hydrocarbon systems.

The aim of the thesis is not to give a local answer to all the uncertainties presented in this chapter. Because of different quantity of data, the author will present three Neoproterozoic platforms at different stratigraphic intervals and at different degrees of details. The three areas are connected by one common theme: microbial dominated platforms.

# Chapter 2 – The West Congo Belt, DRC

## 1    Introduction

This chapter provides a literature review of the West Congo Belt with the aims of highlighting 1) the problematic geodynamic timing and setting of the passive margin and 2) the setting of carbonate platform positioned at the western end of the Congo Craton. This review is essential for correctly framing the megaregional tectonic context. As explained in Chapter 1, it was originally intended that a substantial part of the project dataset would be obtained by fieldwork in the Democratic Republic of Congo (DRC), in collaboration with the Royal Museum for Central Africa (RMCA, Belgium). As it did not happen, the following focuses on literature data only.

Neoproterozoic sediments are exposed in three main areas in the DRC. They are located to the west of the country, in the West Congo Belt (WCB); to the southeast in the Lufilian/Copper Belt and to the north in the Lindian Basin. In this review, the author focuses on the WCB (Figure 2.1 to Figure 2.3) because it was connected to a Brazilian counterpart (the Araçuaí Belt) during the Neoproterozoic. Field comparisons were initially supposed to be done between those two counterparts during the project. The WCB is a stratigraphic tape-recorder for most of the Neoproterozoic; it includes sediments from a rifting stage preceding the breakup of Rodinia dated between ca. 1000 Ma and ca. 912 Ma to the Pan-African orogeny estimated at ca. 566 Ma in the area (Tack et al., 2001). Rocks deposited between these two major tectonic events constitute the West Congo Supergroup.

The geology of the WCB in the DRC is summarised in this chapter. A large amount of field descriptions are available at the RMCA, the majority made prior to the 1980s. Political instability in the DRC limited further field based studies until 2003. Therefore, there is a large time gap in the literature between early (pre 1980s) studies and later work. Other studies from neighbouring countries can be used. Later work reveals changes in methodologies, terminology, techniques (e.g. dating, provenance analysis) and interpretations applied to strata from the WCB. Earlier and later works propose a highly contrasting geological evolution for the WCB. Earlier work was focussed on the WCB within an African context, with

comparatively little attempt to consider the Neoproterozoic strata in the context of their Brazilian counterparts. This aspect is now more fully developed (e.g. Babinski et al., 2012; Pedrosa-Soares et al., 2008). A second change in approach that is applied to most of the Neoproterozoic sediments is the snowball Earth hypothesis (Hoffman et al., 1998b). This hypothesis suggests the occurrence of at least two worldwide distinct glacial intervals followed by cap carbonates during the Neoproterozoic. Prior to the 1980s, a glacial origin for two diamictites (Upper and Lower Mixtite formations) was vigorously debated in the WCB. But since the publication of the snowball Earth hypothesis, several studies undertaken on the stratigraphy of the WCB tend to consider large-scale glaciations to interpret and correlate local diamictites. These inferred interpretations and correlations are not always based on sedimentological evidence or direct datings.

## 2 Literature review

### 2.1 Geological setting

The WCB is located at the western end of the Congo Craton (Figure 2.1 and Figure 2.3). The Congo Craton is a Precambrian landmass now preserved under the form of several blocks: Angola, Kasai, Chailu-Gabon and North East Congo blocks. The Congo Craton is now mainly covered by Phanerozoic cover; it spreads through the DRC, Angola, Republic of Congo, Gabon, Cameroon, Central African Republic, Sudan, Zambia and Brazil (São Francisco Craton). Due to their ages and the long tectonic history, the extent of the blocks and more generally of the whole Congo Craton are not precisely defined and each author define the Congo Craton with some degree of freedom (e.g. De Waele et al., 2008; Frimmel et al., 2011; Kadima et al., 2011b). The WCB is not the only terminal Neoproterozoic – early Cambrian orogen that exposes Precambrian sediments in the DRC. The Lufilian Belt (LB), to the southeast, also results from a same terminal Neoproterozoic megaregional tectonic event: the Pan-African orogeny (Chapter 3). Both the WCB and LB occur on the edges of the Congo Craton. Other Neoproterozoic sediments are exposed to the north and northeast of the country (Lindi and Liki-Bebiam supergroups) but they will not be dealt with as they are out of the scope of this study. A thick pile of Neoproterozoic sediments also accumulated on the Congo Craton, but Phanerozoic sediments now cover

them. Subsurface studies (e.g. magnetism, gravimetry, seismic) with poor well dataset limit the interpretation of the Neoproterozoic sediments deposited on the Congo Craton. Most syntheses or studies focussing on the Central Cuvette retrace the Phanerozoic history of the craton (e.g. Kadima et al., 2011a, 2011b). Today, the overall depositional history of the Neoproterozoic sediments buried in the Central Cuvette remains poorly known. For field geologists, the WCB and LB appear to offer the best record of what happened during the Neoproterozoic, bearing in mind that "the best" refers to rocks that are old and have undergone various degrees of diagenesis and metamorphism that limit observations and interpretations.
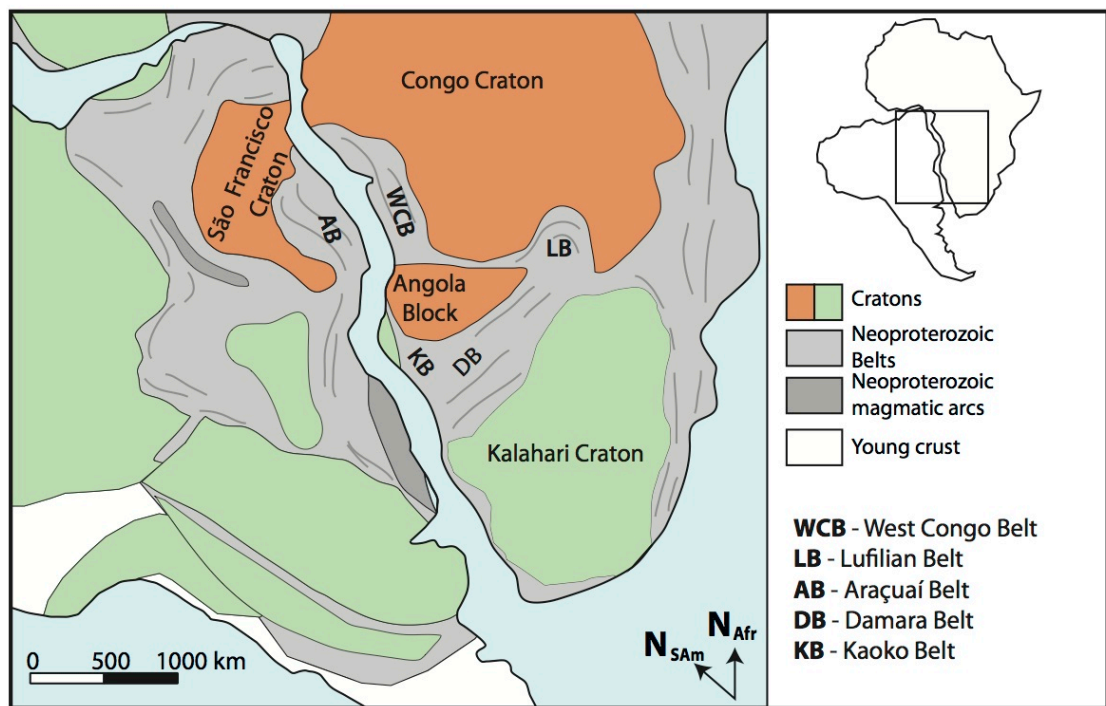


Figure 2.1: Location of the cratons in Africa and South America. Modified from Frimmel et al. (2011). Orange cratonic blocks highlight the study area of the project. Note the WCB, located in a gulf structure between the Congo and São Francisco cratons.

The WCB cuts from the north to the south through Gabon, Congo, the DRC and Angola (Figure 2.3). The West Congo Supergroup was uplifted during the Pan-African orogeny, with the oldest and most intensely deformed sediments located to the west, while intensity of the deformation and age of the sediments decreases towards the east (Tack et al., 2001). The sediments preserved in the WCB were deposited on the Congolian side of an intracratonic gulf, between the São Francisco

and Congo cratons (Pedrosa-Soares et al., 2008). During the Neoproterozoic, the Congo Craton was connected to the São Francisco Craton (now located in Brazil) by the Bahia-Gabon continental bridge. This long-lived feature existed from the Paleoproterozoic (Pedrosa-Soares et al., 2008) until the Cretaceous when the opening of the South Atlantic Ocean separated these cratons.

The West Congo Supergroup (Table 2.1, Figure 2.2) starts with the Zadinian Group, recording clastic sediments and syn-rift volcanic rocks (Tack et al., 2001). It is followed by the volcanic dominated Mayumbian Group. Then the West Congolian Group records siliciclastic sediments that change progressively to carbonates. By the end of the Neoproterozoic, the whole succession was uplifted and partly covered by the coarse clastics of the Inkisi Group (Cahen, 1978a). The time scale between the initial rifting (999 ± 7 Ma, Tack et al., 2001) and the Pan-African orogeny (566 ± 42 Ma, Frimmel et al., 2006) covers approximately 400 million years. Considering this long period, descriptions of the rocks presented in this chapter are extremely synthetic.

Table 2.1: Summarised stratigraphy of the West Congo Belt. Ages are from Tack et al. (2001) and Frimmel et al. (2006).

| Supergroup | Group | Subgroup | Formation |
|---|---|---|---|
| | Inkisi | | |
| West Congo | West Congolian (910–566 Ma) | Mpioka | |
| | | Schisto-Calcaire | Ngandu |
| | | | Bangu |
| | | | Lukunga |
| | | | Kwilu |
| | | | Upper Mixtite |
| | | Haut Shiloango | Sekelolo |
| | | | Petite Bembezi |
| | | | Lower Mixtite |
| | | Sansikwa | |
| | Mayumbian (920–910 Ma) | | |
| | Zadinian (1000–920 Ma) | | |

| | | |
|---|---|---|
| 558 ± 29 Ma ● | Inkisi Group | >920 m |
| 566 ± 42 Ma ● | Mpioka Subgroup | 1000 m |
| | Schisto-Calcaire Subgroup | 1100 m |
| | *Upper Mixtite Fm* | 150 m |
| | Haut Shiloango Subgroup | 1050 m |
| | *Lower Mixtite Fm* | 400 m |
| | Sansikwa Subgroup | 1650 m |
| 923 ± 43 Ma ● | | |
| 912 ± 7 Ma ● | | 3000 - 4000 m |
| 920 ± 8 Ma ● | | 1600 - 2400 m |
| | | < 1500 m |
| 999 ± 7 Ma ● | | |

West Congolian Gp.

Mayumbian Gp.

Zadinian Gp.

Legend:
- Volcanics
- Pelites
- Sandstones/conglomerates
- Diamictites
- Carbonates
- Anorogenic granites

Figure 2.2: Lithostratigraphy of the West Congo Belt (data synthesised from Frimmel et al., 2006; Pedrosa-Soares et al., 2008; Tack et al., 2001).
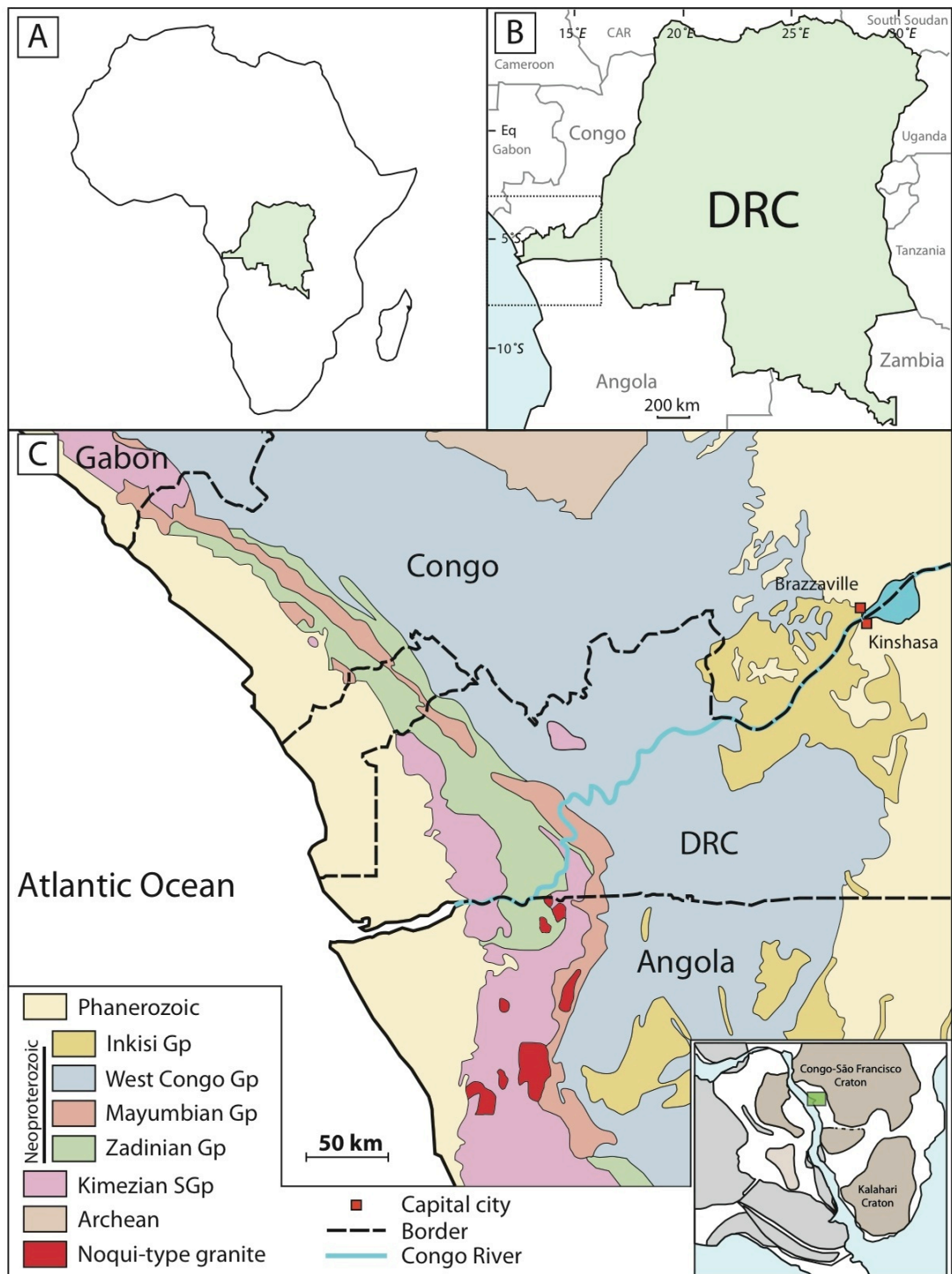
Figure 2.3: Study area, West Congo Belt. **A**. Location of the Democratic Republic of Congo. **B**. The Democratic Republic of Congo and neighbouring countries. Square is detailed in **C**. Geological map of the Bas Congo, West Congo Belt (Modified from Tack et al., 2001). C. Is also located on the map to the bottom right in relation with > 1 Ga cratons (details in Figure 2.1).

## 2.2    Rifting

The Neoproterozoic rifting on the western edge of the Congo Craton has to be considered together with its Brazilian counterpart (Figure 2.1). Syn-rift sedimentation on the Congolian side commenced at around 1000 Ma (Tack et al., 2001) and around 875 ± 9 Ma on the Brazilian side (da Silva et al., 2008, 2005, 2002). It is suggested that the locus of rifting migrated from the east to the west (Pedrosa-Soares et al., 2008). On the Congolian side, the Zadinian (1000–920 Ma) and Mayumbian (920–912 Ma) groups record this early rifting stage (Tack et al., 2001) before the break-up of Rodinia.

## 2.3    The Zadinian and Mayumbian groups

The Zadinian Group starts with a siliciclastic unit (< 1500 m) lying with an unconformity on a Paleoproterozoic basement, the siliciclastic sediments are associated with peralkaline rhyolites and are covered by the Gangila metabasalt (1600–2400 m) (Frimmel et al., 2006; Pedrosa-Soares et al., 2008; Tack et al., 2001). The Noqui granite intrusion at the base of the Zadinian Group gives a maximum age of sedimentation: the intrusion is dated at 999 ± 7 Ma using SHRIMP U-Pb analysis (Tack et al., 2001).

The Mayumbian Group is dated between 920 ± 8 and 912 ± 7 Ma with SHRIMP U-Pb (Tack et al., 2001). It is a thick magmatic succession (3000–4000 m in the Bas Congo) mostly consisting of felsic volcanic, plutonic rocks intruded by granites and few siliciclastic levels (Pedrosa-Soares et al., 2008; Tack et al., 2001). This group represents the early stage of the break-up of Rodinia between the São Francisco and the Congo cratons, however the Mayumbian Group is only present on the Congolian side.

The understanding of the geodynamic history – including the timing of rifting, break-up and collision stages – has considerably evolved during the past decades (e.g. Alvarez and Maurin, 1991; Boudzoumou and Trompette, 1988; Pedrosa-Soares et al., 2001, 1992; Porada, 1989; Vellutini et al., 1983). The more radically different model from modern interpretation suggests that an extension regime with an ocean was present west of the Congo Craton during the Paleo-Mesoproterozoic. Then the rocks were uplifted in an orogenic arc to form the Mayumbian orogen, resulting

from a late Mesoproterozoic – early Neoproterozoic collision (Vellutini et al., 1983). Younger sediments now preserved in the WCB were in turn deposited in a basin, between the orogen to the west and the Congo Craton to the east. This model also suggests that the collision that generated the Mayumbian orogen lasted until the Pan-African stage (i.e. terminal Neoproterozoic – early Cambrian). However it seems that a pre-Neoproterozoic extension regime cannot be fully demonstrated along the western edge of the Congo Craton due to insufficient data and analyses (Tack et al., 2001). An early Neoproterozoic extension regime was already proposed for the origin of the Mayumbian Group but Vellutini et al. (1983) rejected the hypothesis. They interpreted most of the magmatic series of the Mayumbian Group as calc-alkaline and assumed that the Mayumbian orogen may result from a collision stage around 1000 Ma, viewing the series as an ophiolite complex coming from the west to collide with the Congo Craton. More recent studies point out that ophiolites are lacking in the WCB (Pedrosa-Soares et al., 2008; Tack et al., 2001).

Tack et al. (2001) updated nature and age constraints for the Zadinian and Mayumbian groups: they formed during the Tonian and result from an early rifting stage, west of the Congo Craton. Collision occurred to generate the modern aspect of the WCB, but much later during the Pan-African orogeny at the end of the Neoproterozoic, probably after 600 Ma. It is now accepted that the Mayumbian does not result from a Paleo-Mesoproterozoic rifting followed by a Meso-Neoproterozoic orogeny: it records an early Neoproterozoic extension stage between the Congo and the São Francisco cratons.

Other models consider that the Mayumbian Group was uplifted during the mid-Neoproterozoic. The West Congolian Group then accumulated in an aulacogen, an aborted rift created during the Tonian – Cryogenian (950–700 Ma), a basin named the Mayumbian aulacogen (Alvarez and Maurin, 1991; Alvarez, 1999; Boudzoumou and Trompette, 1988). At the end of the Neoproterozoic, the Pan-African collisions closed this basin. Tack et al. (2001) suggests that there is no such aborted rift, but an initial rifting stage before the break-up of Rodinia.

All in one, the observations are similar for both models: there is an obvious NNW–SSE orogen to the west of the West Congo Belt. The core of this orogen exhibits the

Mayumbian Group. East from this orogen, there is the West Congolian Group, with the intensity of deformation that decreases eastward. From there, several models have been suggested. The most recent one suggests that on the western edge of the Congo Craton, rifting started between the Congo and São Francisco cratons at the beginning of the Neoproterozoic (Tonian). The break-up is estimated between 910 and 800 Ma (Tack et al., 2001). The West Congo Supergroup accumulated in this setting until the tectonic inversion of the Pan-African orogeny.

## 2.4 The West Congolian Group

The West Congolian Group has a much longer time record (923 ± 43 − 566 ± 42 Ma, Frimmel et al., 2006) than underlying groups: it represents more than 350 million years of continental rifting, passive margin and carbonate shelf sedimentation. It is succeeded by the Mayumbian Group after a hiatus (Frimmel et al., 2011) and is divided in five subgroups, overall poorly dated.

### 2.4.1 Sansikwa Subgroup

In the context of rifting, the Sansikwa Subgroup records the break-up phase with a filling with conglomerates, sandstones and shales. The maximum age for the deposition of this formation is 923 ± 43 Ma (detrital zircon, Frimmel et al., 2006). The maximum age is likely to be closer to 912 Ma or younger because it is the minimum age for the deposition of the underlying Mayumbian Group (Tack et al., 2001). Provenance analyses from Frimmel et al. (2006) suggest that a part of the siliciclastic input is derived from a continental late Mesoproterozoic island arc, possibly located to the west of the WCB. This hypothesis is highly speculative because there is no field evidence, but it could be compatible with older models that consider a landmass west of the basin located along the western edge of the Congo Craton during the Neoproterozoic (see section 2.3). This island arc does not seem to be considered in other recent studies of the rifting between the Congo and São Francisco cratons.

### 2.4.2 Haut Shiloango Subgroup

Frimmel et al. (2006) estimated the maximum age of sedimentation for this subgroup at 650 Ma. Delpomdor et al. (2014) suggested that the Haut Shiloango

Subgroup was deposited between 696 ± 4 Ma and ca. 635 Ma. The Haut Shiloango Subgroup starts with the Lower Mixtite Formation, interpreted as the local record of the Sturtian glaciation (Delpomdor et al., 2014 and references therein (U-Pb age 694 ± 4 Ma); Frimmel et al., 2006, 2002; Poidevin, 2007). It rests on the Sansikwa Formation along an unconformity of regional extent across the West Congo Belt (Cahen, 1978a; Vellutini and Vicat, 1983). The Lower Mixtite Formation was confused with the Upper Mixtite Formation (Schisto-Calcaire Subgroup) until the 1950s. They were both attributed to the same formation: "tillite of the Bas-Congo" (Cahen, 1954).

In the WCB, the Lower Mixtite Formation is generally well bedded and includes diamictites, conglomerates, greywackes, mudstones, quartzites and limestones intervals. In the diamictites, clasts can reach up to one metre large and are angular to well-rounded, they are locally striated (Angola, Schermerhorn and Stanton, 1963). In the WCB, it was first differentiated and interpreted as glacial (Cahen, 1954, "tillite inférieure"), then subaquatic non-glacial (Cahen and Lepersonne, 1976; Cahen, 1978a; Schermerhorn and Stanton, 1963; Schermerhorn, 1981, 1974; Vellutini and Vicat, 1983). This latest interpretation explains the deposition of the Lower Mixtite Formation by subaqueous mudflows that originated from uplifted areas. Later, Alvarez (1999) suggested that (in Congo) the Lower Mixtite Formation contains partially reworked sediments of glacio-fluvial origin. This interpretation is based on the observation of a shaly matrix with blocks and boulders, the lack of grading, interbedded varves, sandstones to conglomerates intervals. The same author suggests that the source of the detrial material maybe the Chailu Block, located north of the WCB.

The above interpretations are still open to discussion (Tack et al., 2006; Tait et al., 2011 and references therein). If the Lower Mixtite Formation seems to be synchronous to a Sturtian event (Delpomdor et al., 2014; Frimmel et al., 2006; Poidevin, 2007) it could be related to tectonic activity as well. The complex basement structure and consequent sub-basins formed along the western edge of the Congo Craton have been uncertain for decades. The palaeogeography consisted of a complex setting where both glacial and non-glacial sediments may have

accumulated. This would explain the interpretations of the Lower Mixtite Formation from deep-water non-glacial to glacial. With the present knowledge on this formation, it is extremely challenging to define where and to which extent ice bodies influenced the sedimentation of the Lower Mixtite Formation. Ice was probably present, but current data do not permit greater precision on the location of ice bodies or provenance of the sediments.

It is widely accepted that after a snowball Earth event, widespread cap dolostones accumulated during a post-glacial flooding (Chapter 1, section 5). After the Lower Mixtite Formation, no typical cap dolostone is described in the literature: a few m-thick conglomerate occurs instead, above a disconformity (Cahen, 1978a). The rest of the Haut Shiloango Subgroup consists of siliciclastic to carbonate sediments (Cahen, 1978a; Frimmel et al., 2006; Pedrosa-Soares et al., 2008). It is composed in its lower part of quartz/argillite-dominated sediments (Petite Bembezi Formation) and by carbonates (Sekelolo Formation) in its upper part. Cahen (1950) gave a detailed description of the Sekelolo Formation. In his work, he described a stromatolite reef succession and interpreted it as a deposited in a shallow-water environment, constantly growing in competition with a shale input. More recently Delpomdor et al. (2014) reinterpreted the uppermost part of the Haut Shiloango Subgroup as non-stromatolitic, deep-water sediments with reworking along a tectonically active margin. This new interpretation is based on the observation of hummocky cross-laminations, tempestites, syn-sedimentary slump structures and debrites.

### 2.4.3    Schisto-Calcaire Subgroup

The Schisto-Calcaire Subgroup starts with a second diamictite: The Upper Mixtite Formation. It is often correlated with the Marinoan (late Cryogenian) glaciation, estimated at 635 Ma in the sediments of the WCB (Frimmel et al., 2006; Poidevin, 2007). Because these rocks have not been dated, it is also plausible that they correlate with the Gaskiers (Ediacaran) glaciation (Babinski et al., 2012). Sedimentological interpretations of the Upper Mixtite Formation in the WCB have changed through decades, with different degrees of glacial influence and different environments enumerated in the following. An initial interpretation was that the

Upper Mixtite was deposited by a glacier developed on the Mayumbe orogen, advancing from west to the east (Cahen, 1950). Note, however, that the Mayumbian is now known to correspond to a zone of deformed strata that were uplifted during the Pan-African orogen (section 2.3), after the deposition of the Upper Mixtite Formation, and not an orogenic phase in itself. This does not exclude a high topography, such as a rift shoulder, as a source area for glaciers. Later, Cahen (1954) suggested that the Upper Mixtite Formation was less glacially influenced than the Lower Mixtite Formation. Schermerhorn and Stanton (1963), Schermerhorn (1974), Cahen and Lepersonne (1976) and Cahen (1978a) suggested that in Angola, the DRC and Congo, the mixtite exhibited poor evidence of a glacial influence, and resulted from tectonic activity. Yet, striated boulders are observed and several authors suggest that they are glacigenic. Vellutini and Vicat (1983) rejected a glacial origin for the formation and for the striated boulders. They interpreted the Upper Mixtite Formation as turbidites and mudflows. Alvarez (1999) interpreted its lateral equivalent in Congo ("Formation de la diamictite supérieure") as glacially influenced. This interpretation is based on 1) the interpretations from Cahen (1950) in the Bas Congo; 2) the observation of sandy to shaly matrix with polyhedric 2–40 cm large blocks 3) the stratification of the formation that increases upsection, meaning that it was deposited in a subaqueous environment. Here, it is suggested that the nearby lateral equivalent of the Upper Mixtite Formation was deposited in a lacustrine or marine setting, with an ice stream coming from the north of what is now the WCB (Chailu Block). Debates, correlations and interpretations of the formation continue into the more recent literature (Delpomdor et al., 2014; Frimmel et al., 2006; Poidevin, 2007). The most recent microscopic sedimentological observations (Tait et al., 2011 and references therein) suggest periglacial settings (fluvioglacial, glaciomarine, proximal subglacial and distal subaqueous) in the Bas Congo.

The Upper Mixtite Formation is followed by a < 10 m-thick finely laminated cap dolostone, commonly named "C1" or "SC I" in the literature. Cahen (1950) described a laminated pink dolomite and interpreted it as the deposit of a calm lagoon. Small low-angle cross stratification was locally described from this unit (Schermerhorn and Stanton, 1963). Based on outcrops in Angola, the previous

authors considered that the consistent thickness (~10 m) and the extent of the cap dolostone implied a deep-water environment. Cahen (1978a) restated that this pink dolostone was deposited in a calm shallow-water environment, probably a lagoon with rhythmic evaporation. In Congo, Alvarez (1992) suggested that the cap dolostone was the most distal facies (shallow subtidal, external ramp) of a carbonate ramp; more proximal facies consist of microbialites, evaporites, oolitic intervals and shallow siliciclastics.

Upsection, the cap dolostone is overlain by limestones, argillites, oolitic limestones and stromatolites, forming the > 600 m Kwilu Formation (Cahen, 1978a; Delmoitié-Nicolaï et al., 1972). It is in turn overlain by the ~300 m-thick Lukunga Formation, ~250 m-thick Bangu Formation and 90 m-thick Ngandu Formation. The present author is not aware of recent published field descriptions of these formations in the DRC. Sediments mainly consist of limestone, dolostone, stromatolites (e.g. Bertrand-Sarfati, 1972) with common oolitic and argillaceous intervals. Alvarez (1999, 1992), Alvarez and Maurin (1991), Alvarez et al. (1995) and Préat et al. (2011, 2010) published more detailed sedimentological descriptions of the Schisto-Calcaire, from exposures located further north (Congo, Gabon). The observation of evaporites, siliciclastics, stromatolites by the previous authors tend to support a relatively shallow-water setting (shallow subtidal to supratidal) for this formation.

### 2.4.4    Mpioka Subgroup and Inkisi Group

The Schisto-Calcaire Subgroup is covered by continental and shallow marine siliciclastic sediments: the Mpioka Subgroup. It was deposited during a collision stage around 566 ± 42 Ma (Frimmel et al., 2006; Tack et al., 2001); which corresponds to the Pan-African episode that deformed the strata present in the WCB. Later, the siliciclastic Inkisi Group covered the West Congolian Group. It is interpreted as post Pan-African (Tack et al., 2001) and dated at 558 ± 29 Ma using SHRIMP U-Pb (Frimmel et al., 2006).

# 3    Discussion

## 3.1    Study of the West Congo Belt

The origins of the Neoproterozoic rocks found in the WCB have always been intensely debated. Between the 1980s and the 2000s, the political situation limited field studies in the WCB. In fact, field studies were probably limited since the 1960s (independence of the DRC) and most of publications were based on older field observations and data. Many studies published in the 2000s focus on the stratigraphy of the strata preserved in the WCB (Alkmim et al., 2006; Frimmel et al., 2006; Pedrosa-Soares et al., 2008; Poidevin, 2007; Tack et al., 2001; Tait et al., 2011). These publications are probably related to a more stable political situation in the country since the 2000s, motivating new collaborations with the DRC and the RMCA. But also to catch up with the literature dealing with the snowball Earth hypothesis since Hoffman et al. (1998b); and the quest for new frontier petroleum systems in Precambrian successions around the world (Craig et al., 2013, 2009). Most recent work in the WCB updates key problems such as the origin of the diamictites (Tack et al., 2006; Tait et al., 2011), and they integrate new age constraints useful to the refinement of the global stratigraphy. Through decades, the extremely different interpretations suggested for the rocks of the WCB should intrigue Earth scientists. With a lasting stable political and safety situation in the Bas Congo Province, more field based studies and new interpretations in accordance with the megaregional context should be published (e.g. Delpomdor and Préat, 2013; Delpomdor et al., 2014).

## 3.2    Ice ages

Origins of the diamictites of the Bas Congo have been vigorously debated, from strictly glacial to non-glacial. The Lower and Upper Mixtite formations are respectively correlated with the Sturtian and Marinoan (Delpomdor et al., 2014 and reference therein; Frimmel et al., 2006; Poidevin, 2007) ice ages. Latest interpretations suggest periglacial settings (Tait et al., 2011). The source and extent of ice bodies remain uncertain.

Several have authors suggested the mixtite were deep-water debris flow deposits. In that case, debris flows may have originated from tectonic activity along the

margin or areas uplifted during the rifting. They might equally be sourced from ice masses delivering large volumes of sediment into the basin(s). Based on the literature, the different sedimentological interpretations and geotectonic models, it is extremely challenging to visualize the ice ages along the western, rifted margin of the Congo Craton. The structure of the basement probably played an important role by hosting ice bodies.

## 3.3    Platform orientation

Interpretations of the timing and nature of the tectonic events that formed the WCB has changed considerably through decades. It seems now well established that the Mayumbian Group has a Neoproterozoic age (920–910 Ma, Tack et al., 2001), and is interpreted as the result of a break-up stage on the western end of the Congo Craton. The sediments preserved in the WCB record rifting, followed by a passive margin and a platform setting, deposited between 1000 Ma and the Pan-African orogeny (Tack et al., 2001). The main depocenter was thus located towards the west of the Congo Craton.

Prior to the publication of these age constraints and this model, a failed rift basin (Alvarez, 1999; Boudzoumou and Trompette, 1988) was considered to be the depocenter of the West Congolian Group. A part of the sedimentation was shed from high topography towards the east (Figure 2.4.A), in the "aulacogen" or "geosyncline" (Vellutini and Vicat, 1983). Other sources were maybe located north of the WCB, on the Chailu Block (Alvarez, 1999).

The changes in the geotectonic models (section 2.3) do not mean that previous sedimentological interpretations and models are wrong. The early Neoproterozoic rifting (Tack et al., 2001) may have created grabens or half grabens, forming local depocenters before the main basin developed between the Congo and São Francisco cratons (Figure 2.4.B). This idea is similar to the one proposed by Boudzoumou and Trompette (1988), where an epeirogenic uplift occurred during the early Neoproterozoic, creating a topography west of the Congo Craton. It is in some way also compatible with the hypothesis of Frimmel et al. (2006): an island arc, or possibly even a Mesoproterozoic aged basement high, were maybe present to the west of the basin. This high topography separated the open ocean to the

west from the basin in which accumulated the West Congolian Group, with a depocenter located between the basement high and the Congo Craton.

On the southern edge of the Congo Craton, in northern Namibia, a similar setting may have occurred. There, Hoffman and Halverson (2008) recognised southward-directed sedimentation that accumulated in a rift basin between the Congo Craton/Angola Block and the Kalahari Craton (Northern Nosib Rift). The rift shoulders created a dipslope that favoured sedimentation towards the craton as well (northward). This setting possibly formed lagoon-like or intra- or epicratonic basins. Hoffman et al. (1998a, 1998b) suggested that the Congo Craton was a low-lying, Bahamas-type platform during the Neoproterozoic. The sea level was sufficiently high for sediments to drape the topography of the craton, allowing the formation of an extensive platform.

On the western edge of the Congo Craton, a part of the sedimentation was oriented towards the actual rifted basin (between the Congo and São Francisco cratons) and another part of sedimentation was oriented towards the Congo Craton, in an epicratonic setting. It is suggested here that this second basin is where the West Congo Supergroup accumulated, and where the Haut Shiloango and Schisto-Calcaire platforms have formed. Much more field observations would be necessary to confirm such model.
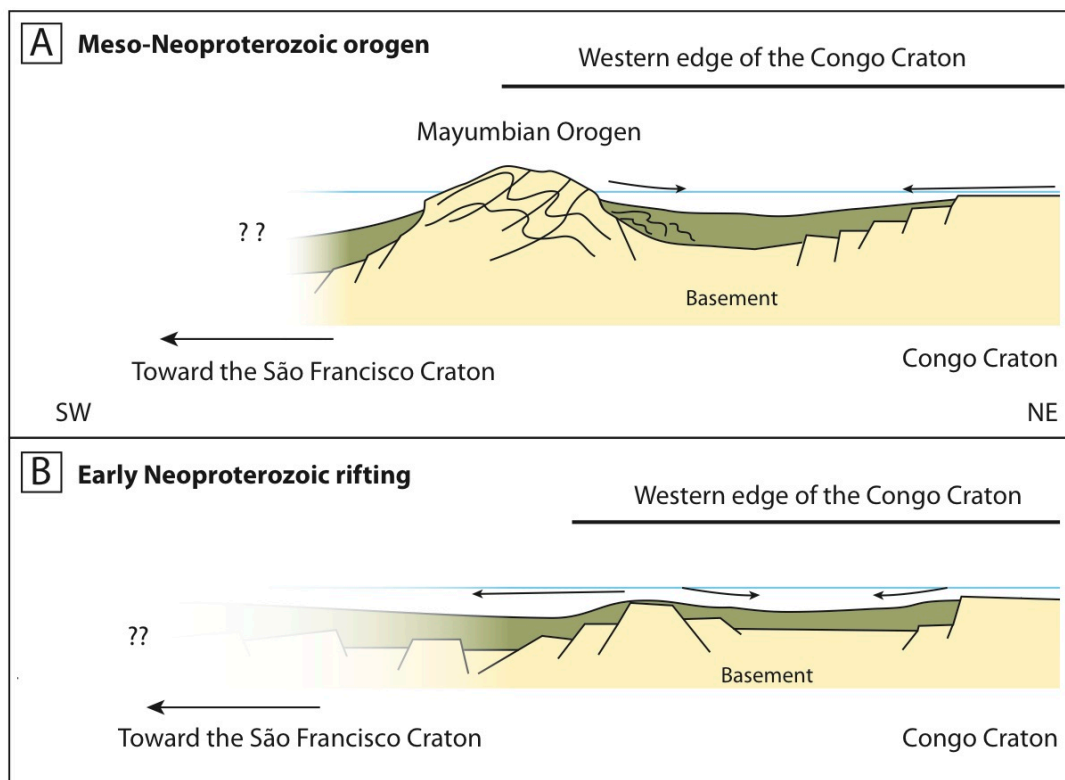
Figure 2.4: Schematic topography and orientation of the sedimentation on the western margin of the Congo Craton during the Neoproterozoic. **A**. Setting that interprets the Mayumbian Group as the result of an early Neoproterozoic collision. The high topography then present to the west through the whole Neoproterozoic is viewed as a source area for sedimentation. **B**. Setting considering an early Neoproterozoic rifting (Tack et al., 2001) associated with a high topography on the edge of the Congo Craton (Boudzoumou and Trompette, 1988). The Mayumbian Group results from a rifting stage. The sediments were thrusted at the end of the Neoproterozoic during the Pan-African orogeny, forming the West Congo Belt.

## 4    Conclusion

Despite more than a century of study, the exact setting in which the West Congo Supergroup accumulated is still poorly understood. The literature of the WCB can be confusing and disconcerting with highly contrasting interpretations and models. New dating and a better understanding of the megaregional context allowed the refining of the tectonic history in the Bas Congo Province. An early Neoproterozoic orogen can be replaced by invoking a rift-related basement high west of the West Congo Belt. In both settings, a basin was present along the western coast of the Congo Craton. This basin was separated by a high topography from the principal basin opened between the Congo and São Francisco cratons. In this setting, the West Congolian Group remains problematic because of the lack of sedimentological

observations and direct datings. This chapter does not bring new data, but it does illustrate the complexity and challenges to interpret Precambrian strata, often poorly preserved.

The collaboration between the RHUL and the RMCA allowed the access to all the data stored in the RMCA: samples, reports, annals, field notes, maps, etc. This dense dataset associated was, however, of limited use in answer to the questions addressed in this chapter. Finding samples for sedimentological description is dependent on the observations and interpretations from authors who have collected them. Furthermore a sample cannot document all the facies found on one outcrop, limiting the discussion with previous interpretations. Therefore, if one considers the sampling accurate in term of stratigraphy and location, samples can be used for other studies such as geochemistry (isotopes, dating, provenance; e.g. Frimmel et al., 2006; Poidevin, 2007; Tack et al., 2001). But to address solutions to the uncertainties encountered in the literature, fieldwork seems to be the best way to build up a new dataset of samples and observations.

# Chapter 3 – The Lufilian Belt and the Roan Group, Zambia

## 1    Introduction

Since data collection in the Democratic Republic of Congo (DRC) was not possible owing to administrative issues, focus was switched to a second area: the Lufilian Belt (Figure 3.1). This Pan-African aged belt sits astride the Katanga Province (southeast DRC) and the Copperbelt Province (Zambia). In this chapter, a specific part of the Lufilian Belt is studied: the Copperbelt. This area took its name from the mining activity, where copper ore is extracted since the beginning of the twentieth century. Mining activity centres on Neoproterozoic strata (Roan Group) and some authors suggest that former organic rich sediments may have play a role in the formation of ore bodies (El Desouky et al., 2008; Heijlen et al., 2008; Scott et al., 2006; Selley et al., 2005). Neoproterozoic sediments of the Copperbelt Province are highly deformed and metamorphosed. No petroleum systems are expected in this area or in these sediments. However, the depositional setting that later generated the ore bodies is a possible analogue for stromatolites associated with hydrocarbon source rocks.

In the Copperbelt Province of Zambia, field studies are challenging, with outcrops limited by the dense vegetation cover and also by intense tropical weathering. These factors limit field observations and sampling. The best outcrops are found in open pit copper mines and underground copper mines, though in the second, observations are limited by the lack of light. Also, due to ore exploration, many boreholes have been drilled. Cores are another way to access to the rock record. This chapter presents data collected in open pits and from shallow cores.

In the 1970s and earlier, research was logically oriented towards the ore bodies, their origin and economic potential. The number of research publications has decreased since the independence of Zambia in 1964. A factor that might have diminished the amount of research in the Lufilian Belt is its proximity to the Katanga Province (DRC) and Angola. Both countries faced several conflicts between the 1970's and 1990's. Since the beginning of the twenty-first century, a more stable and safe setting favoured the resumption of international collaborative projects and field-based research. As in the DRC, there is a time gap in the research, and modern

studies tend to catch up with recent literature related to the Neoproterozoic. In addition to the study of the formation of the ore bodies, literature of the Copperbelt sediments also compares the strata with worldwide time equivalent.

# 2    Literature review

## 2.1    Geological setting

The geodynamic history of the Lufilian Belt results from the same processes that formed the West Congo Belt: from a passive margin with the break-up of Rodinia to a collision stage with the Pan-African orogeny. These two major tectonic events are respectively dated at 883 ± 10 Ma using SHRIMP U-Pb on the intrusive Nchanga Granite (Armstrong et al., 2005) and 573 ± 5 Ma using $^{40}Ar/^{39}Ar$ technique on detrital grains from the foreland deposits of the Plateau Group (or Biano Group, Master et al., 2005). But the Pan-African orogeny is more widely estimated to occur between 590 and 512 Ma in the area (Master and Wendorff, 2011). In the Lufilian Belt, older rocks (Tonian – early Cryogenian) are located in Zambia and younger rocks (late Cryogenian – Cambrian) in the Katanga Province of the DRC.

In the Katanga Province of the DRC, North-Western and Copperbelt provinces of Zambia, the approximate time equivalent unit of the West Congo Group (Chapter 2) is named the Katanga Supergroup. The geotectonic context does not seem as problematic as in the West Congo Belt. However, the Katanga Supergroup is poorly dated and the stratigraphy of the area is rather confusing. The stratigraphic units observed and their names are not always the same and are not attributed to the same groups or subgroups (see Wendorff and Key, 2009, fig.2 and Muchez et al., 2010, fig.2). It is consequently difficult to synthesise the successions in terms of groups, subgroups and formations. The following stratigraphy (Table 3.1, Figure 3.2) is highly simplified, and despite the lack of homogeneity in the literature it is possible to divide the Katanga Supergroup in five groups: the Roan and the Nguba groups that record two successive rifting stages, and the Kundelungu, the Fungurume and the Plateau groups (Master and Wendorff, 2011) recording foreland basin deposits. The main tectonic stages are synthesised in Figure 3.3.

Table 3.1: Synthetic stratigraphy of the Katanga Supergroup (from Wendorff and Key 2009).

| Supergroup | Group | Subgroup | Formation |
|------------|-------|----------|-----------|
| Katanga | Plateau | | 62 |
| | Fungurume | | Dipeta |
| | | | Mutoshi |
| | | | Kambove |
| | Kundelungu | Kiubo | |
| | | Kalule | Calcaire Rose |
| | | | Petit Conglomérat |
| | Nguba | Monwezi | |
| | | Likasi | Kakontwe |
| | | | Grand Conglomérat (765–735 Ma) |
| | | Mwashya | |
| | | | Mufulira |
| | Roan (880–765 Ma) | Bancroft | |
| | | Kitwe | |
| | | Mindola | |
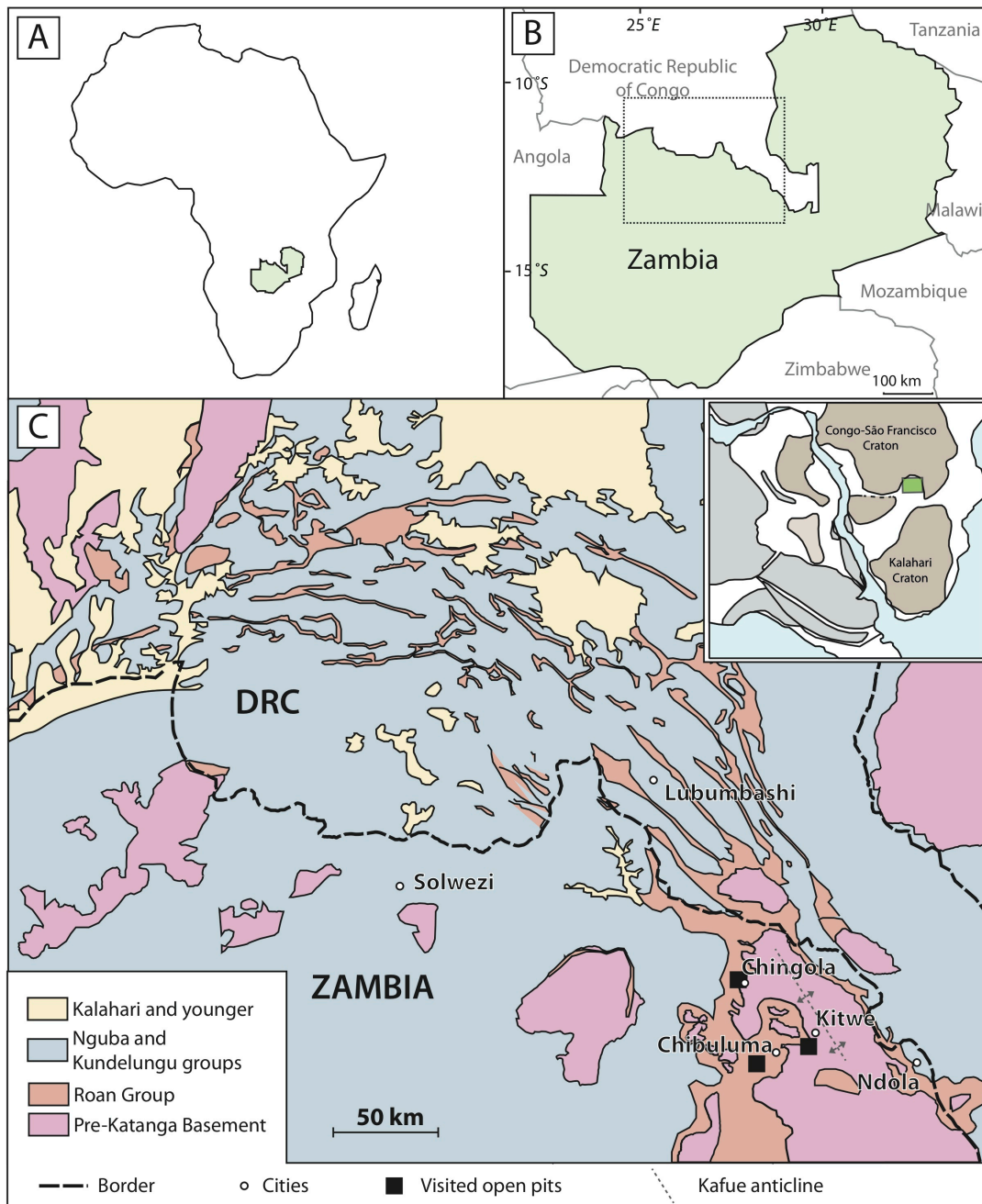
Figure 3.1: Study area, Lufilian Belt. **A**. Location of Zambia. **B**. Location of the study area. **C**. Geological map of the Lufilian Belt (modified from Wendorff, 2003). The map up right of C. locates the Lufilian Belt in a cratonic setting (green rectangle).
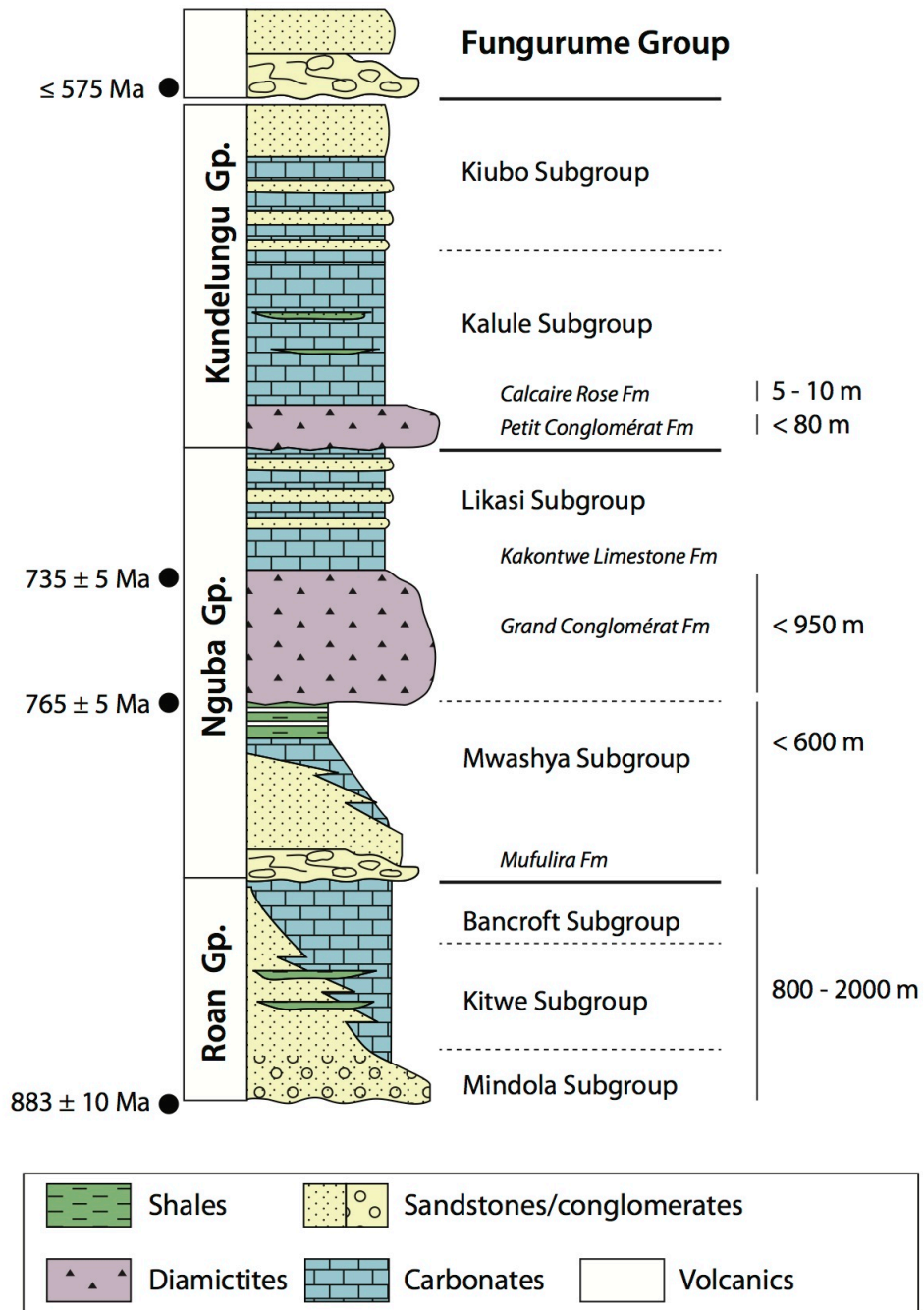
Figure 3.2: Lithostratigraphy of the Katanga Supergroup (based on Master and Wendorff, 2011; Master et al., 2005; Wendorff and Key, 2009). Note that the stratigraphy can change from one author to another.

## 2.2 Rifting

In Zambia, the rifting (Figure 3.3) was initiated later than in the West Congo Belt. Two different phases can be recognised in the extension process. First with the opening of the Roan rift, with a southwest – northeast expansion; second with the

Nguba rift, expanding northward, north of the first rift (Wendorff and Key, 2009). The oldest basin filling directly overlies the intrusive Nchanga granite, dated at 883 ± 10 Ma (Armstrong et al., 2005), this gives a maximum age for the beginning of the break-up of Rodinia on the SSE edge of Congo Craton. Rift shoulder uplift accompanied the second phase of rifting, dated at 765 ± 5 Ma with SHRIMP U-Pb technique on lava from the Mwashya Group (Key et al., 2001). These lavas are mafic andesitic and are interpreted as related to a rift–drift stage during the break-up of Rodinia.

## 2.3    Roan Group

The Roan Group is a succession of siliciclastic (Mindola Subgroup), mixed siliciclastic-carbonate (Kitwe Subgroup) and carbonate (stromatolites, dolomitic shales, anhydrite-bearing dolostones, Bancroft Subgroup) sediments (Porada and Druschel, 2010; Wendorff and Key, 2009). Instead of three subgroups, it is often divided into a ~1000 m-thick lower part consisting of siliciclastic and mixed siliciclastic-carbonate (equivalent of the Mindola and Kitwe subgroups) and a ~800 m-thick upper part consisting of carbonate sediments (equivalent of the Bancroft Subgroup). The Roan Group records a first rift setting on the SSE edge of the Congo Craton (Porada and Berhorst, 2000; Wendorff and Key, 2009), the maximum age of deposition is dated at 883 ± 10 Ma by the underlying intrusive Nchanga granite (Armstrong et al., 2005). The siliciclastic sediments were deposited during the first stage of the rifting and the overlying carbonate sediments were deposited in a more stable setting, probably on basement highs and/or where the competition with continental input was low or non-existent.

The ore bodies of the Copperbelt occur mainly in the Roan Group, but the processes that led to their formation are still uncertain. Due to its economic value, the Roan Group and its palaeogeography are well defined. Porada and Berhorst (2000) and Porada and Druschel (2010) proposed a model of a rimmed carbonate platform. This model is oriented northeast (proximal)–southwest (distal) and is located on the former northern margin of the Roan rift. The ore bodies occur in lagoonal deposits, sometimes in sandstones but mostly in lagoonal shales. The ore-shales were deposited in the neighbourhood of microbial buildups (Annels, 1984; Garlick and

Fleischer, 1972; Garlick, 1964; Malan, 1964; Porada and Druschel, 2010; Stanton, 1972), but microbial mats themselves may have played a role in the generation of ore (Porada and Druschel, 2010).

The genesis of the ore is still a complex question of research (Dewaele et al., 2006; McGowan et al., 2006, 2003; Muchez and Corbella, 2012) and it might be related to the presence of former organic-rich sediments (Scott et al., 2006; Selley et al., 2005). It can be explained by 1) fluid circulation through the organic-rich layers of the lower part of the Roan Group, 2) the proximity of the basement, 3) intense deformation during the terminal Neoproterozoic (Pan-African orogen) or a combination of the three. Although the Roan Group is accessible in Zambia, younger Neoproterozoic rocks are easier to find in the DRC. The following synthesis of the knowledge of Neoproterozoic strata in the Lufilian Belt is therefore based on publications focussing, in part, on the Congolian side of the orogen.

## 2.4    Nguba Group

### 2.4.1    Mwashya Subgroup

The Roan phase of rifting was succeeded by the Nguba rifting. At ca. 765 Ma (Key et al., 2001), the southern side of the Roan rift was uplifted, essentially on the Zambian side. The new rift expanded towards the north from this uplift (Wendorff, 2005). The Nguba Group starts with the Mwashya (or Mwashia) Subgroup and the Mufulira Formation at its base: a coarse clastic formation lying unconformably on the Roan Group and the Pre-Katangan basement (Master et al., 2005; Wendorff and Key, 2009; Wendorff, 2005). The Mufulira Formation is interpreted as syn-rift deposits derived from the uplifted Roan Group (Wendorff and Key, 2009). The Mwashya Subgroup changes to shallow-water siliciclastics and carbonates, and then to anoxic black shales in its upper part (Master and Wendorff, 2011). In the literature, the Mwashya Subgroup is sometimes associated to the uppermost part of the Roan Group (Cailteux et al., 2007; Muchez et al., 2010).

The Mwashya Subgroup is associated with a regional volcanic unit formed during the second rifting stage. Several ages have been provided for this volcanic unit: 765 ± 5 Ma in northwest Zambia (Key et al., 2001), 745 ± 7.8 Ma and 752.6 ± 8.6 Ma

(Armstrong et al., 2005; Borring et al., 2003). The 765 Ma age is widely regarded as the most reliable and is also used to constrain the maximum age of sedimentation of the Nguba Group.

### 2.4.2 Likasi Subgroup

The Mwashya Subgroup is overlain by the up to 1200 m-thick Grand Conglomérat Formation (Wendorff and Key, 2009). The contact is variably conformable to uncomformable. The Grand Conglomérat Formation has been interpreted as a glacigenic unit since the middle of the twentieth century (Cahen, 1978b, 1947). This formation typically composes the lower part of the Likasi Subgroup. Clasts found in the Grand Conglomérat Formation come from both southern uplifted and northern margins of the basin. A glacigenic input is demonstrated by the occurrence of faceted and striated clasts, diamictites but also outsized dropstones in laminated and finely-grained rocks (Wendorff and Key, 2009 and references therein). However, facies variations and evidence of ice-free and interglacial conditions such as cross-bedding or current-ripples indicate that it was not deposited in a "hard" snowball Earth setting (Wendorff and Key, 2009). The Grand Conglomérat Formation is estimated to have accumulated between 765 ± 5 Ma and 735 ± 5 Ma. The first age comes from the Mwashya Formation (see section 2.4.1), the second age was obtained with the SHRIMP U-Pb technique performed on brecciated mafic volcanic lenses, interpreted to occur above the Grand Conglomérat Formation (Key et al., 2001). The glacigenic formation is overlain by a cap carbonate: the Kakontwe Formation.

The Kakontwe Formation contains massive dolomites, limestones, some oncolites, an alternation of dark and light limestones, shales and microbial sediments (Key et al., 2001). The maximum thickness in the basin attains 600 m but is typically ca. 300 m (Batumike et al., 2007). Master and Wendorff (2011) gave more sedimentological details about the Kakontwe limestone, naming it "Kakontwe dolostone". They indicate distinctive features such as a laminated facies, soft-sediment deformation structures including roll-up structures which appear to be identical to those observed in the supposed time equivalent Rasthof Formation in Namibia (see chapters 4 and 5). However this cap carbonate does not seem to be present

everywhere: Wendorff and Key (2009) observed that the Kakontwe Formation was only present in the distal part of the basin, and its lateral equivalents are siliciclastic sediments deposited along the north and south margins of the basin. They suggested that this detrital material was derived from deglaciated land. This input was then too great on the margins to permit carbonate sedimentation.

## 2.5    Kundelungu Group and late Pan-African deposits

The Kundelungu Group marks the transition from an extensional to a compressional regime. It was deposited north of the rising Lufilian orogen. It starts with a second regional glacigenic formation: the Petit Conglomérat Formation, deposited in a foreland basin (Cahen, 1978b, 1954). It rests uncomfortably on the underlying Nguba Group (Wendorff and Key, 2009) and consists of a 30–50 m-thick unsorted to poorly sorted, matrix supported conglomerate. The clasts are derived from the older Nguba Group (Batumike et al., 2007). Master and Wendorff (2011) synthesised observations from various authors and explain that the observations of faceted and striated clasts support a glacial origin for this formation. However, they also refer to cross-bedded intervals and ripple marks, which in common with the Grand Conglomérat Formation exclude a "hard" snowball Earth setting. In terms of slope orientation, the size and abundance of the clasts decrease towards the south, they were derived from high topographies located in the DRC (the Mesoproterozoic Kibaran Belt and the Paleoproterozoic Bangweulu Block). In Zambia, periglacial facies are thought to have been shed northward from the uplifted southern shoulder of the Nguba rift (Master and Wendorff, 2011; Wendorff and Key, 2009). Deposits of the Petit Conglomérat Formation accumulated in a foreland basin now found in the DRC, along the border between the Copperbelt/North-Western provinces of Zambia and the Katanga Province of the DRC.

Considering these glacigenic interpretations but a lack of direct age constraints – the Petit Conglomérat Formation was deposited between 765 Ma and 620 Ma – several authors correlate it with the Marinoan glaciation (Batumike et al., 2007; Master and Wendorff, 2011). Like many other younger Cryogenian glacigenic formations, the Petit Conglomérat Formation is capped by a 5–10 m-thick finely laminated carbonate: the Calcaire Rose Formation (Master and Wendorff, 2011 and

references therein), no recent publications focus on the sedimentological description of this formation.

By the end of the Neoproterozoic, the Pan-African orogeny closed the sedimentary basins in which the Roan and Nguba groups accumulated. The Kalahari Craton pushed towards the Congo Craton and the timing of the collision ranged from ca. 590 and ca. 512 Ma (Master and Wendorff, 2011) but no direct age constraints exist yet. In this context, the Fungurume Group was deposited uncomformably on underlying units, to the north of the collision area. Most of the syn- to post-collisional sediments were deposited in a foreland basin, now located in the DRC. The Fungurume Group is composed of shallow marine to continental sediments derived from older Katangan groups coming from the south of the foreland basin. The group ends with shallow marine and carbonates strata and is followed by the undeformed Plateau Group, which records continental deposits (Master and Wendorff, 2011). Datings indicate that the Plateau Group was deposited after 573 ± 5 Ma (Master et al., 2005), using $^{40}$Ar/$^{39}$Ar on detrital grains.

## 2.6    Highlights

Most studies published since the 2000s retrace the geotectonic timing in the Lufilian Belt and try to synthesise a regional lithostratigraphy. In terms of sedimentology, the Grand Conglomérat and the Petit Conglomérat formations have been described and interpreted as glacigenic since the 1950s. Wendorff and Key (2009) suggest that the intensity of the glacial events in the Copperbelt was much more moderated than in the initial snowball Earth hypothesis (Hoffman et al., 1998b). The overlying cap carbonates are comparatively poorly described and no references to detailed work on microbialites was found in the literature. In terms of location and stratigraphic interval, the only relatively well-documented microbialites occur in the Roan Group. However, they have not been described for decades, except partly by Porada and Druschel (2010). The literature of the Copperbelt and more generally of the Lufilian Belt lacks of modern observations and studies of microbial carbonates. They appear to be well represented from the Tonian to the Cryogenian and describing them would be beneficial for the scientific

community; both for understanding the deposition of microbial carbonates in general and with regard to the cap carbonate conundrum.
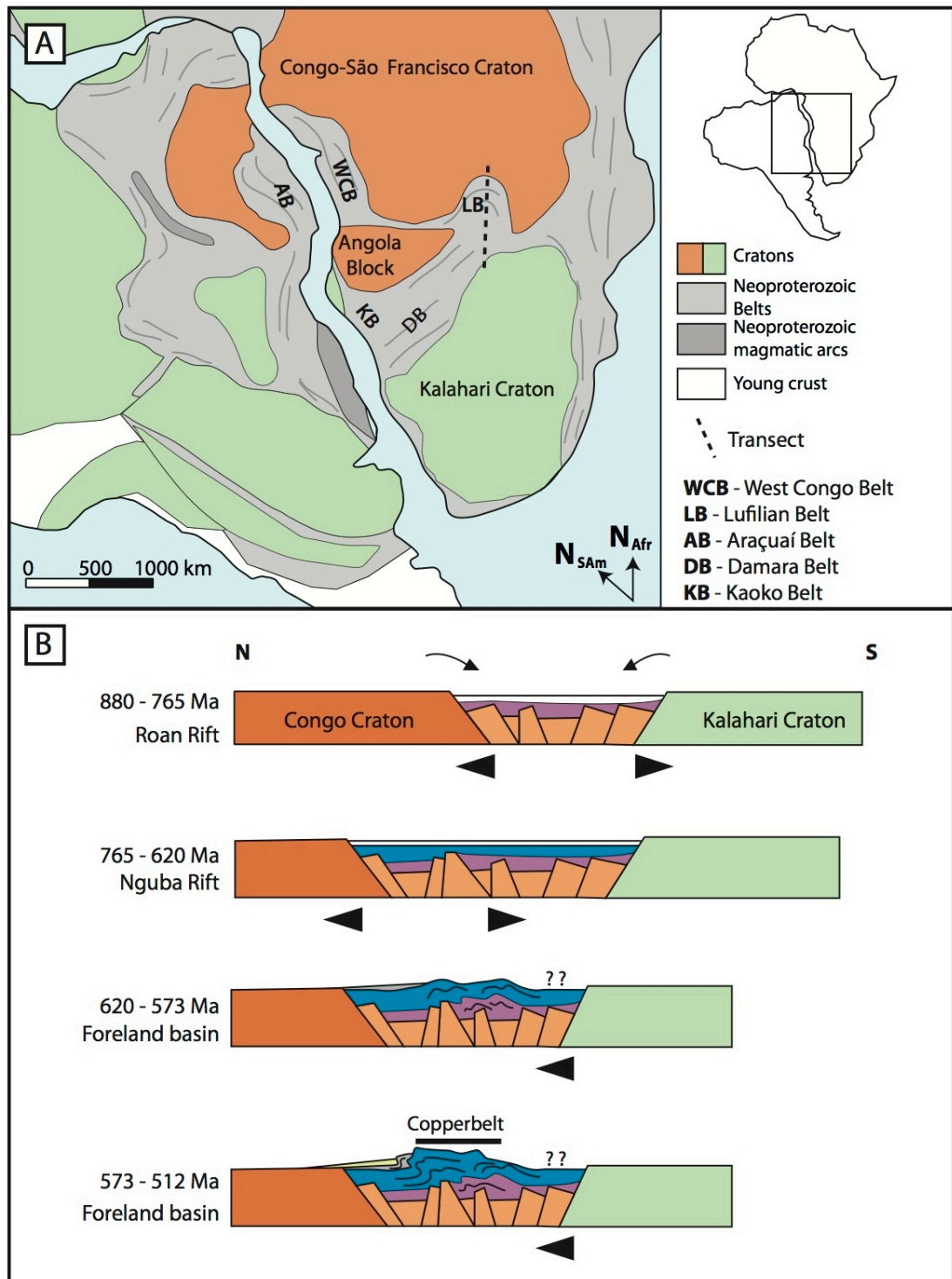


Figure 3.3: Tectonic history of the Lufilian Belt. **A**. Locations of the cratons in Africa and South America, modified from Frimmel et al. (2011). **B**. Summarised geodynamic history between the Congo Craton and the Kalahari cratons.

# 3    Fieldwork

## 3.1    Introduction and objectives

A field season was undertaken between the 12th September 2011 and the 18th October 2011. The initial objective was to locate and describe the stromatolites of the Roan Group and their relationship with organic-rich sediments (Porada and Druschel, 2010; Stanton, 1972). In this regard, controls on their geometry would be assessed. A second objective was to describe and sample the sediments from the Roan Group to the Kakontwe Formation. Sampling was to be targeted at organic rich shale intervals in the Roan Group and the Mwashya Subgroup. A third objective was to describe the Kakontwe Formation to compare it with its supposed time equivalent in northern Namibia: the Rasthof Formation. Note that this field season took place before the publication of Master and Wendorff (2011) that revealed strong similarities between the facies of the Kakontwe Formation and the Rasthof Formation. The latter is described in detail in chapters 5 and 6.

The two first points were the more feasible because the targeted sediments occur in Zambia. However, the description of the Kakontwe Formation, apparently more typical from the DRC was more an extra mission depending on time and logistics. Finding outcrops of the Kakontwe Formation in Zambia, which has no proven economic interest compared to older sediments, requires some exploration.

## 3.2    Field area

Fieldwork was targeted in the Copperbelt and North-Western provinces of Zambia. These provinces are close to the DRC, which was the initial country of interest for this project. In Zambia, natural Neoproterozoic outcrops are poor or difficult to locate and access owing of dense vegetation cover. Also, the geological maps are not detailed enough to trace potential outcrops. The regional mapping was made before the 1980s and many formation boundaries are inferred. Open pits, mines and cores resulting from ore exploration and production in Neoproterozoic strata represented the most feasible target for a first visit. Indeed, most of previous publications derive from such data sources.

The mining companies extract ore essentially from the Mindola and Kitwe subgroups (Roan Group), in shaly, siliciclastic and stromatolitic intervals (Garlick and Fleischer, 1972; Porada and Berhorst, 2000; Porada and Druschel, 2010; Stanton, 1972). The presence of shales and stromatolites at the base of the Neoproterozoic succession presented an opportunity to analyse potential hydrocarbon source rocks as already discussed by Scott et al. (2006). Moreover, determining relationship between stromatolites and organic rich shales may provide valuable comparisons to other nearby Neoproterozoic platforms from the DRC and Namibia.

## 3.3    Material and method

### 3.3.1    Sites

For administrative and communication reasons, the timing of the visits was not planned before but during the field season. Most of the visited sites are located in the heart of the industrial Copperbelt: in Chibuluma, Kitwe and Chingola mines (see Figure 3.1.C). Before the field season, the University of Zambia sent letters and made phone calls to request access to the open pits of mining companies for research purposes. Four institutions granted access to us, namely Konkola Copper Mines Plc (Chingola), Mopani Copper Mines Plc (Kitwe), Chibuluma Copper Mines Plc (Chibuluma, southwest of Kitwe) and the chamber of mines (Kalulushi, southwest of Kitwe).

According to the model suggested by Porada and Druschel (2010), the sites to which access was permitted expose lagoonal to marginal sediments from the Roan Group. From this publication it was expected that most of the author's observations would be related to siliciclastic and organic rich sediments deposited between a carbonate barrier and a siliciclastic margin. Facies of the Lower Roan Group in the area range from inter- to supratidal deposits, with local microbial mats. Extensive stromatolite buildups are more likely to be located southwest of the field area. It did not mean that no microbial sediments were accessible. Several mining geologists met during the project mentioned the existence of stromatolites occurring between the carbonate barrier and the border with the DRC.

### 3.3.2    Data collection and analysis

Access to mines in the Copperbelt is time consuming; also the author experienced a full health and safety induction for each visited open pit. The main risks are related to the driving in the open pits and to the possible rockslides. Most of the data that were acquired consist of field observations, core description and samples. The author had expected to visit several other sites, but this proved to be impossible for administrative reasons outside the author's control. Some samples were selected for Total Organic Carbon (TOC) analysis. These samples were sent to Gerd Winterleitner (RHUL) and Dr. Martin Jones (School of Civil Engineering and Geosciences, Newcastle University) for processing, and the results are presented in Figure 3.7.

## 3.4    Visited sites

### 3.4.1    Chibuluma Copper Mines

Location: 12° 54.800' S – 28° 04.800' E.

### *3.4.1.1    Description*

The first site is located 15 km WSW of Kitwe in the Chibuluma open pit. The now abandoned open pit is used as an entry to the underground mine that extracts bornite ($Cu_5FeS_4$) from sandstones of the lower part of the Roan Group. Outcrop quality in this open pit is poor owing to regional metamorphism and weathering, but the following data were obtained. The only non-metamorphosed outcrop found in the open pit was a 5 m-thick succession of shallowly dipping, fine-grained quartzitic sandstone (Figure 3.4). Beds are 0.2–2 m-thick, and they slightly thicken towards the west on the observed surface. The sandstone exhibits parallel bedding in the thinner beds, and low angle to moderately inclined trough cross-bed foresets in the thicker beds. Neither shales nor microbial mats were observed. Underground mining focuses on older sediments: sandstones and conglomerate. The upper part of the Roan Group does not seem to be exposed in the area.
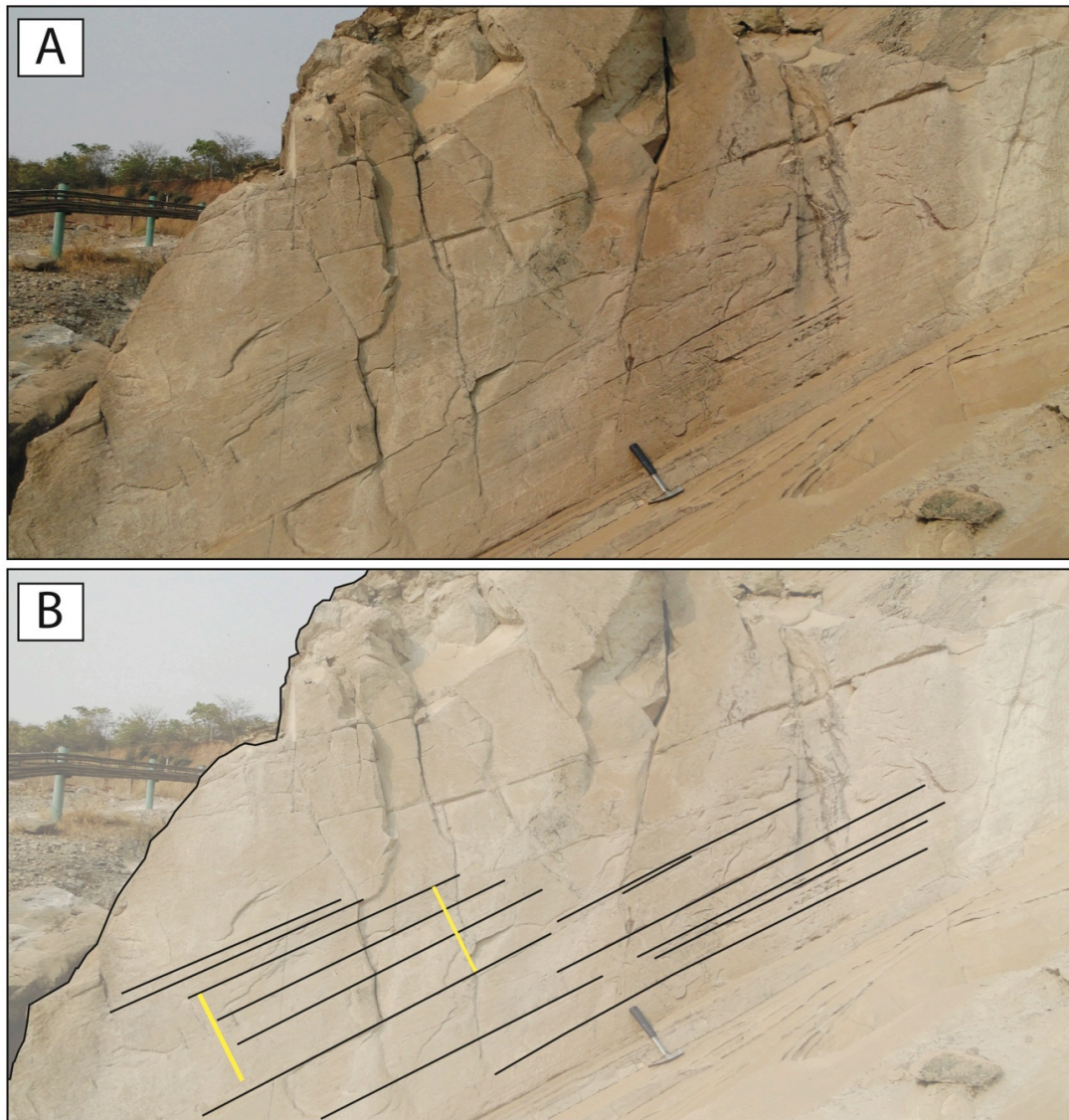
Figure 3.4: Sandstone from the Chibuluma open pit. **A**. Photography. **B**. Highlight of the thickening (yellow bars have the same length).

### 3.4.1.2    Interpretation

In the Copperbelt, this lower part of the Roan Group sandstone is often interpreted as very proximal to continental (e.g. Porada and Berhorst, 2000; Porada and Druschel, 2010). The sandstone could correspond to an aeolianite, an alluvial fan deposit or a playa flat environment (Robb et al., 2003). The author wishes to highlight the present day laterally restricted nature of these deposits, which preclude detailed testing of these hypotheses. However, the well-sorted nature of

the observed sandstones, in concert with the occurrence of parallel laminated to trough cross-bedded deposits, is not inconsistent with aeolian sedimentation.

### 3.4.2    Mopani Copper Mines – Nkana

Location: 12° 51.040' S – 28° 12.340' E.

#### *3.4.2.1    Description*

Several open pits are present on the MCM site. The younger pit at the time of the visit was the open pit J (Figure 3.5). This pit was chosen for reasons of accessibility. The copper is extracted from a 2–8 m-thick shale layer, representing the oldest observable unit in the open pit. Underlying sediments were described from a core (well SB0014) extending from the crystalline basement to the shales observed in the open pit.
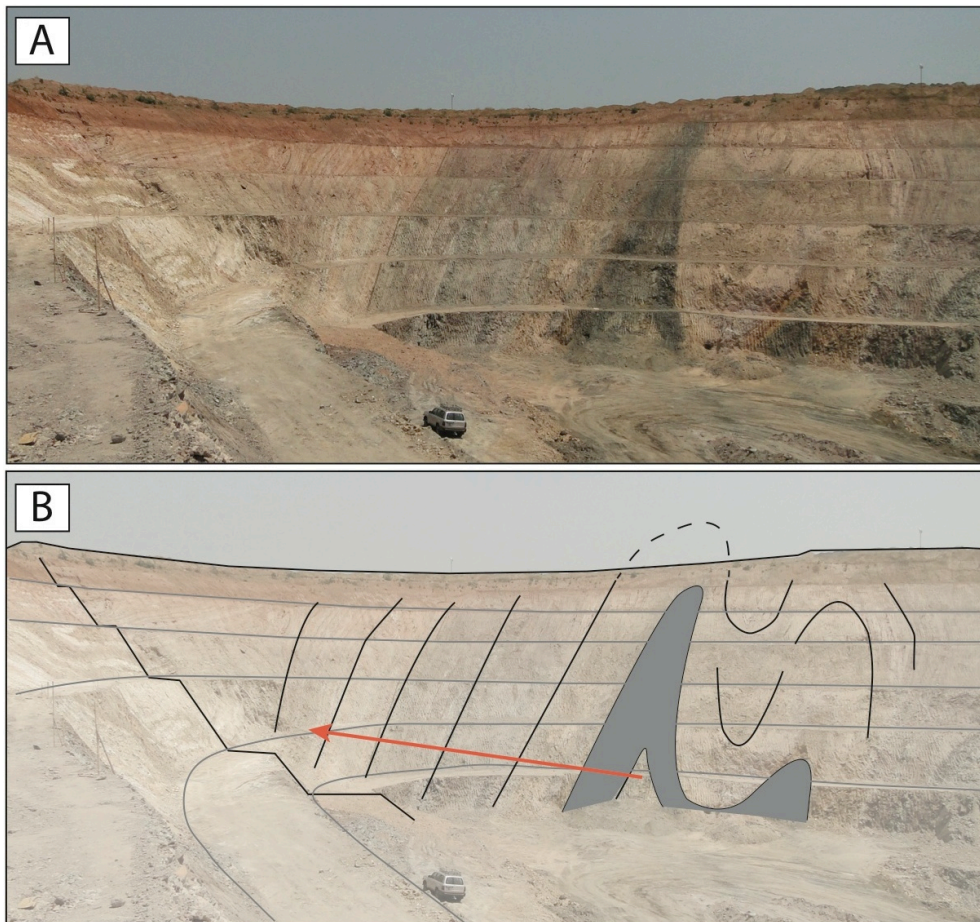


Figure 3.5: Open pit J, MCM. **A**. Outcrop. **B**. Sketch of the outcrop illustrating folded nature of the strata. The red arrow is the log presented in Figure 3.7.B.

In core, three main facies can be recognised. The first is a basal conglomerate (Figure 3.6.A), the facies is globally clast supported with local sandy matrix. Clasts are granule to cobble-sized, oblate to equant, rounded to subangular and derived from the crystalline basement. The size of the clasts tends to decrease upsection grading gently into the second facies, a fine to coarse-grained sandstones (Figure 3.6.B, C) with up to cm large lithoclasts. Marked cm-thick coarse mudrock intervals locally alternate with sandstones. The overall grains size decreases until the arrival into the third facies: shales associated with dolomite (Figure 3.6.D). Shales are associated with important development of pyrite, representing the ore body. It shows lateral thickness variation: it is thicker (~8 m) than in the open pit (~3 m). Overlying strata in the open pit are poorly preserved, sedimentological structures are rare and in most instance, the differentiation between shale and sandstone is the maximum detail that can be extracted. Rarely, cross-bedding is preserved. Alternation of medium to coarse-grained sandstones with shales also occurs. As noted previously, ore deposits can be generated from hydrocarbon replacement of organic-rich shales (Scott et al., 2006). Samples were thus collected from the shaly ore body from the open pit and the core for TOC analysis (Figure 3.7).

### 3.4.2.2    *Interpretation*

The core illustrates the classic succession of the Roan rift. With a basal conglomerate fining upward to sandtsones, shales and calcareous shales (TOC 1–2.6 %). No outstanding sedimentary structures were observed, although grain size variability clearly testifies to fluctuating energy levels. Maturity and poor to moderate sorting of the clasts in the conglomerate suggest a relatively short-lived transport and/or moderate reworking. The conglomerate records the most proximal facies and grain size diminishes into more distal and quiet settings with the deposition of shales. In the shales, diminution of detrital input punctually permitted the deposition of carbonates. The author suggests that the shales record a lagoonal setting, similar to that suggested by Porada and Berhorst (2000). It is emphasised that the restricted access to cores do not permit lateral facies variations to be assessed in detail. The shales are found again in the open pit and are overlain by sandstone-dominated facies. The lateral extent of the cross-bedded

sandstones observed in the open pit is uncertain, thus reducing confidence in any possible interpretation. They may correspond to beach, aeolian or fluvial deposits. It is noted that no channel-like bodies were observed at the outcrop scale, perhaps rendering a fluvial origin less likely. As a whole, the author envisages a similar interpretation to that suggested by Porada and Berhorst (2000) and Porada and Druschel (2010). Sediments of the Nkana site were deposited somewhere between a clastic margin and a lagoonal basin.
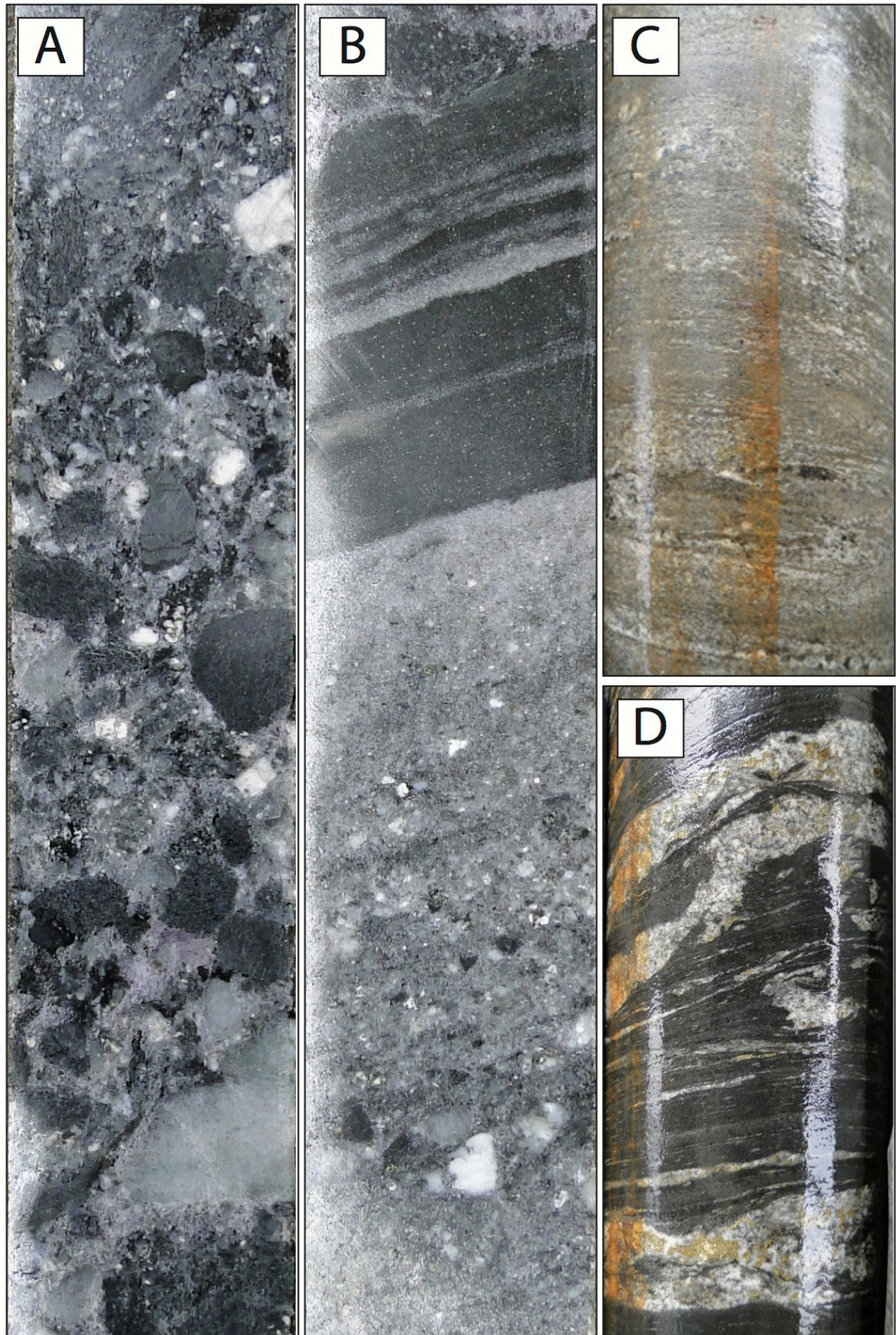
Figure 3.6: Typical facies from the lower part of the Roan Group. Cores are 7 cm large. **A**. Conglomerate. **B**. Coarse to fine-grained sandstone. **C**. Fine-grained sandstone. **D**. Dolomitic shale (ore body).

**A. WELL SB0014**
Nkana - Mopani Copper Mine

40 —

TOC
KC9.5 - 1.03%
KC9.4 - 1.01%
KC8.5 - 1.61%
KC8.4 - 1.62%

Pyrite rich calcareous shale (orebody)

30 —

20 —

Sandstones

10 —

Basal conglomerate

0 m —

Shale
Fine sandstone
Medium sandstone
Coarse sandstone
Conglomerate

**B. OUTCROP OPENT PIT AREA J**
Nkana - Mopani Copper Mine

30 —

20 —

10 —

TOC
S7C4 - 2.59%
K7.4 - 2.61%
S7C5 - 2.65%
K7.5 - 2.61%

orebody

0 m —

Shale
Fine sandstone
Medium sandstone
Coarse sandstone
Conglomerate

Figure 3.7: Logs from the Roan Group, MCM. **A**. From the basement to the ore body. **B**. Above the ore body.

### 3.4.3    Konkola Copper Mines – Nchanga

Location: 12° 30.530' S – 27° 52.800' E.

### 3.4.3.1    Description

The Nchanga KCM site forms a 11 km long fringe along the northwestern flank of the Nchanga granite. This granite is dated at 883 ± 10 Ma (Armstrong et al., 2005). This age is used as a reference for the beginning of the rifting in the area; it intrudes the Roan Group. Several open pits are in exploitation on KCM site and the visited one is the second biggest in the world with a maximum lateral extent of ~4 km and a maximum depth of ~400 m. McGowan et al. (2006) details the stratigraphy of the Nchanga open pit.

The sediments are mainly siliciclastic, and the lower part of the succession consists of a basal conglomerate overlain by a medium to coarse-grained sandstone. These lithologies were not observed at the time of the visit. The basal conglomerate is overlain by a shale interval ("Lower Banded Shale", Figure 3.8.A), in turn followed by a sandstone unit with 20–60 cm-thick sequences coarsening upward from siltstone to coarse sandstone. In the sandstones, foresets can be highlighted, dipping at 20° (Figure 3.8.B, C). The sandstone interval is overlain by a second shale interval ("Upper Banded Shale"). The deposits enumerated above are considered to belong to the lower part of the Roan Group. The upper part of the Roan Group consists of a dolomitic unit, shales interbedded with grits (Figure 3.8.D, E) and another dolomite. The latter was not observed.

In the open pit, the Lower Banded Shale was observed (Figure 3.8.A) together with shales with grits of the upper part of the Roan Group (Figure 3.8.D, E). These strata attain an approximate thickness of 200 m. Sedimentological features are poorly preserved and no stromatolites were observed. The uppermost visible sediments exhibit shaly undulated surfaces (Figure 3.8.E) and local 1–5 cm-thick lenses of coarse to very coarse-grained sandstones. No more sedimentological observations were collected during the visit.
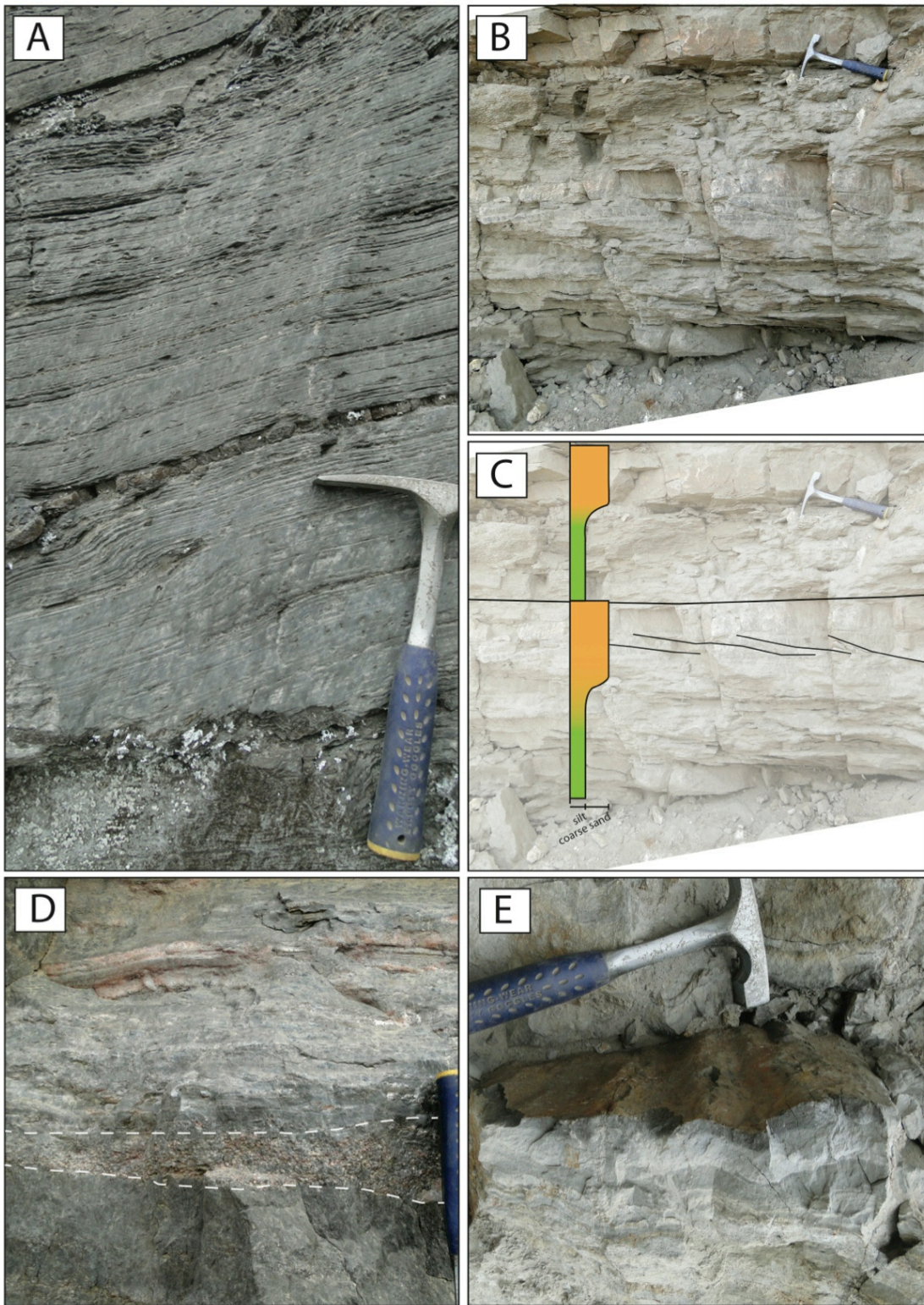
Figure 3.8: Facies from the Nchanga open pit. **A**. Lower Banded Shale. **B**. Fine to coarse sandstone. **C**. Interpretation of B with suggested foresets. **D**. Shale and grit (see lens in the dashed area). **E**. Shaly undulated surface, upper Roan Formation.

*3.4.3.2     Interpretations*

The very base of the Roan Group was not observed at the time of the visit. But the conglomerates and sandstones mentioned by geologists from KCM and their important thickness variation in the area (50 to 250 m, McGowan et al., 2006) suggest that these facies progressively filled the pre-Katangan negative topography. The conglomerate and overlying sandstones are compatible with proximal, syn-rift facies. Overlying finely laminated banded shales testify to a subaqueous, quiet setting. Sandstones deposited between the Lower and Upper Banded shales exhibit foresets, testifying to a more energetic setting. The coarsening upward profile exhibited by these forset-bearing units is equivocal, but could potentially correspond to localised prograding delta features of uncertain origin. Dolomites and shales with grits deposited above the Upper Banded Shale reflect an overall quiet setting. Diminution of detrital input allowed the precipitation of carbonates, and then overlying shales with grits indicate a quiet environment with occasional washing, probably from the coast. Uppermost shales observed exhibit an undulated surface, suggesting oscillatory motion in the water column. Overall, the size of the grains decreases from the base to the top of the succession. From the Lower Banded Shale to the shale with grits, a subaqueous proximal setting seems compatible with the facies observed.

# 4     Results and discussion

The sediments observed at the three localities record mainly the deposition of the lower part of the Roan Group. As already observed, most of the sediments of the lower part of the Roan Group are siliciclastic dominated, encompassing continental to sabkha and lagoonal settings. Some shales and rare carbonates occur, indicating relatively more distal, quieter lagoonal setting protected from continuous detrital input. The overall succession records the local break-up of Rodinia: the Roan rift.

Relatively coarse siliciclastic sediments dominate the lower part of the Roan Group. Rare 1–2.6 % TOC shales and calcareous shale intervals were observed and are likely to record facies deposited in a lagoon setting (Porada and Druschel, 2010). These organic rich facies were already mentioned in the literature and may have played an important role in the generation of ore (Scott et al., 2006; Selley et al., 2005). Some

authors (Garlick and Fleischer, 1972; Garlick, 1964; Malan, 1964; Stanton, 1972) have also referred to stromatolites in the lower part of the Roan Group. They are likely to have accumulated on basement highs (Annels, 1984) and where competition with siliciclastic input from the clastic margin was negligible. No stromatolites were observed during the field season. The rimmed platform model of Porada and Druschel (2010) places most of the ore bodies in a lagoonal basin located between a carbonate barrier to the southwest and siliciclastic system coming from the northeast (Figure 3.9). They have described some microbial mats nearby Kitwe (less than 10 km northwest from open pit J), again similar features were not observed during the field season.

The siliciclastic deposits observed at all the visited sections record a proximal setting that inhibited the development of microbial carbonates. These sites are located along the clastic margin of the Roan rift. The siliciclastic input is "diluted" towards the southwest, in the lagoon. Meanwhile, microbial communities developed in a more distal, or in protected settings and on local higher topography.
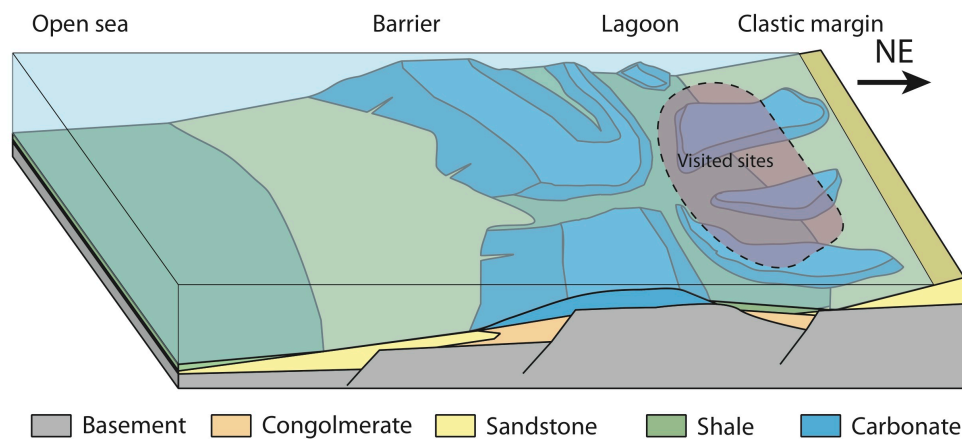


Figure 3.9: Synthetic model for the deposition of the Roan Group (modified from Porada and Druschel, 2010). All the visited sites are located between the clastic margin and proximal lagoonal facies.

# 5    Conclusion

Owing to the significant challenges faced in the course of this research (political upheaval, access issues, outcrop quality: all circumstances that were out of the author's control), a comparatively limited dataset was collected for analysis from the Copperbelt: 6 field days from 5 week's work. Those data that were collected lead to interpretations that are mostly compatible with previous studies published on the Roan Group. A total of three open pits were visited but observations were limited due to the preservation of the sediment (metamorphism, mining). Additional cores were available for description at Konkola Copper Mines and in the Chamber of Mines. These descriptions are not presented because, unfortunately, neither the location of the drill site in the Copperbelt, nor their stratigraphic position, were archived. Chibuluma Copper Mines also offered access to their coreshed but time constraints precluded both core selection and description. For the same reasons, no additional fieldwork has been undertaken in Zambia in the course of the author's research.

The ore bodies are hosted in shales and sandstones; shales revealed TOC values ranging from 1 to 3%. These values are not surprising considering previous studies (Scott et al., 2006). The description of the nearby microbialites (Annels, 1984; Garlick and Fleischer, 1972; Porada and Druschel, 2010; Stanton, 1972) and of their interval transition with the shales would have been a real benefit for the understanding of this setting and a good basis for comparison with other microbialite environments.

# Chapter 4 – The Rasthof Formation, Namibia

## 1    Introduction

The third study region is Namibia (Figure 4.1.A, B), a world-class country for Neoproterozoic geology. Late Precambrian sediments are well exposed in the north of the country (Figure 4.1.C) in the Damara and Kaoko orogenic belts of Pan-African age. The Neoproterozoic strata form a continuous series of outcrops along the southern, southwestern and western edges of the Owambo Basin. The aim of chapters 4–7 is to develop the knowledge about the Cryogenian Rasthof and Berg Aukas formations (Abenab Subgroup, Otavi Group, Damara Supergroup) located in northern Namibia.

The Rasthof and Berg Aukas formations are cap carbonates deposited in the aftermath of the Sturtian glacial event in northern Namibia. They represent a real puzzle in terms of geological context and sedimentological interpretation. The carbonate facies encountered over hundreds of kilometres through northern Namibia are extremely unusual, and finding analogues is challenging. It is thought that these formations were deposited in a platform setting: the Northern Platform (Hoffman and Halverson, 2008), an extensive microbial rich environment at Rasthof time. The precise nature of these sediments remains poorly studied and only partially understood (Bosak et al., 2013b; Hedberg, 1979; Hoffman and Halverson, 2008; Le Ber et al., 2013; Pruss et al., 2010). In northern Namibia, a large part of the platform is now preserved more than 2 km deep below the Owambo Basin (Hedberg, 1979). The buried part of the platform does not appear to have been subjected to deformation since the Pan-African orogeny (Miller et al., 2010).

Beyond the sedimentological challenge of the Rasthof Formation lies a potential petroleum system. First, it was deposited after the Sturtian glaciation, a setting that may have led to the deposition of organic rich shales (Le Heron and Craig, 2012) by analogy with more recent Paleozoic examples (Le Heron et al., 2009; Lüning et al., 2000, 1999). Such an hypothesis has already been suggested in northern Namibia for the younger Maieberg Formation cap carbonate (Bechstädt et al., 2009). Second, the supposed biotic nature of the sediments may represent potential hydrocarbon source rocks. In addition, Neoproterozoic strata from Zambia (Chapter

3) illustrate how a microbial platform setting can be associated with organic rich shales.

The Northern Platform lies north of the Nosib rift system, on the Angola cratonic block, but the details of its setting remain problematic. It is important to first provide an overview of the geological history of the region, between the break-up of Rodinia and the Pan-African orogeny, in northern Namibia. Once the general setting is defined, the previous studies focussing on the Rasthof Formation will be synthesised, outlining the main facies found on the platform.

## 2    Literature review

### 2.1    Geological setting

The sediments started to accumulate during the break-up of Rodinia, which is poorly dated, but products of rift-related magmatism provide age constraints (U-Pb) of $759 \pm 1$ Ma (tuff) and $752 \pm 7$ Ma (peralkaline intrusion) (Frimmel and Miller, 2009 and reference therein). The rifting is recorded by the siliciclastic dominated Nosib Group. Later, during a quiet interlude, a long-lived carbonate platform was established, recorded by the Otavi Group. By the end of the Neoproterozoic, a Pan-African collision stage led to the uplift and exposure of both Nosib and Otavi groups and to the deposition of syn- to late orogenic foreland sediments of the Mulden Group (Frimmel et al., 2011; Germs et al., 2009). The Nosib, Otavi and Mulden groups form the Damara Supergroup (Table 4.1, Figure 4.2). The Mulden Group is constrained between $575 \pm 10$ Ma and ca. 541 Ma by intrusive diorites (Miller, 2008) and between 580 and 541 Ma using $^{40}Ar/^{39}Ar$ (Gray et al., 2006). In their synthesis of the Neoproterozoic geodynamic in southwest Gondwana, Frimmel et al. (2011) estimate the Pan-African orogeny to have taken place between ca. 580 and 530 Ma on the edges of the Owambo Basin.

The Rasthof Formation crops out in a palaeo-shelf area called the Northern Platform, which is located on the Angola Block, southwest of the Congo Craton (Figure 4.3.A). Parts of the platform are exposed in the eastern Kaoko Belt and northern Damara Belt. There is a geographic continuity between these belts; they both result from the Pan-African orogeny, but developed diachronously in response

to different stress orientations. The Kaoko Belt developed in response to east–west compression, generated by a collision between the Rio De La Plata Craton and the Angola Block. The Damara Belt, meanwhile, was produced by a north–south compression, generated by a collision between the Kalahari Craton and the Angola Block. Thus, the orogens form belts resembling an arc of a circle that closed the Northern Platform and created the Owambo foreland basin (Figure 4.1). The main geotectonic events and their associated deposits are presented in this section. Time scale covers the break-up of Rodinia to the Pan-African orogeny, more than 200 million years.
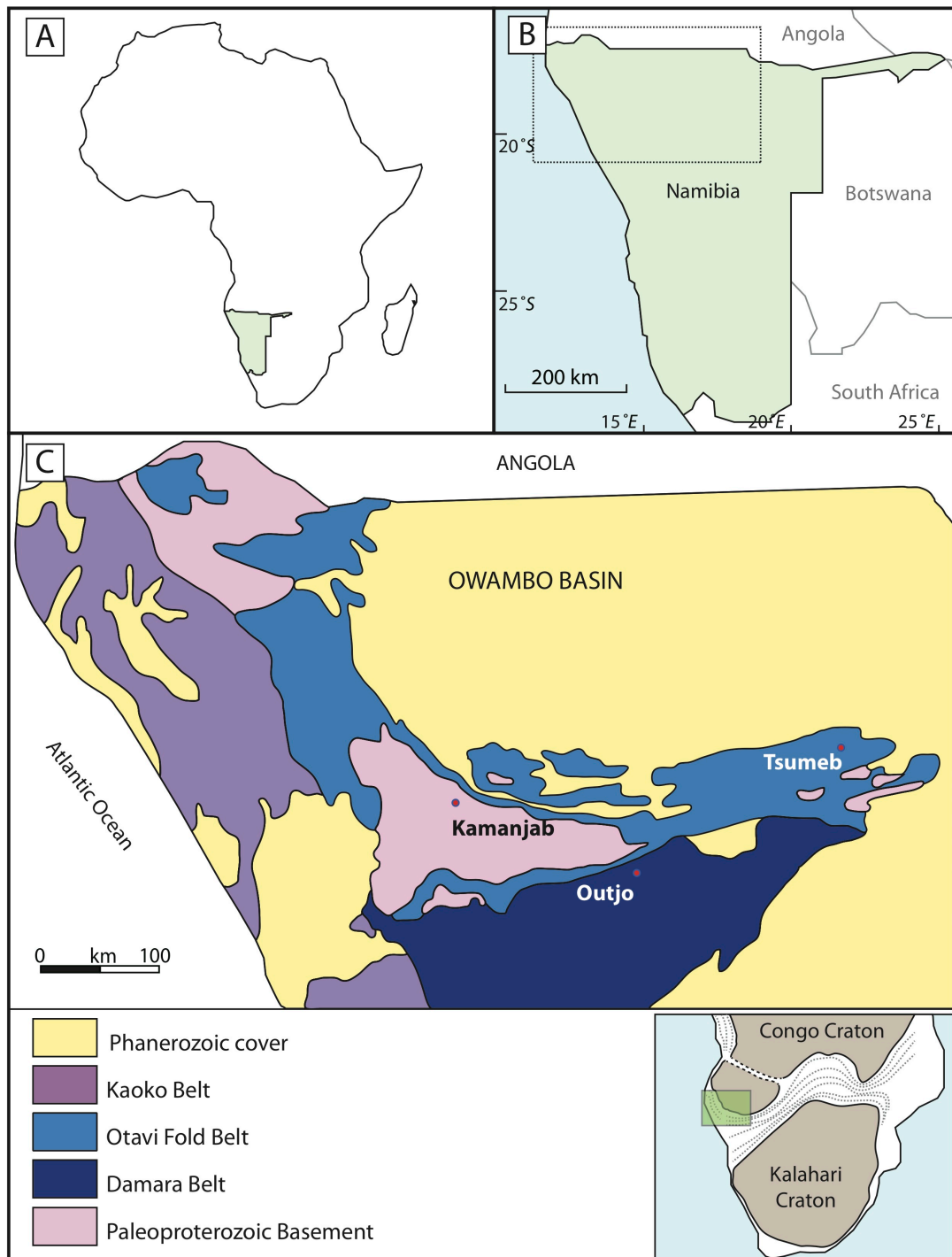
Figure 4.1: Study area, northern Namibia. **A**. Location of Namibia. **B**. Namibia and neighbouring countries. **C**. Geological map of northern Namibia (Modified from Hoffmann and Prave, 1996).

Table 4.1: Synthetic stratigraphy of the Damara Supergroup.

| | | Western Platform | | | Eastern Platform (Otavi Mountainland) |
|---|---|---|---|---|---|
| **Supergroup** | **Group** | **Subgroup** | **Formation** | | **Formation** |
| Damara | Mulden 580–541 Ma[1] | | Owambo | | |
| | | | Kombat | | Kombat |
| | | | Tschudi | | Tschudi |
| | Otavi 746–580 Ma[2] | Tsumeb | Hüttenberg | | Hüttenberg |
| | | | Elandshoek | | Elandshoek |
| | | | Maieberg | | Maieberg |
| | | | Ghaub | | Ghaub |
| | | Abenab | Auros | | Auros |
| | | | Ombaatjie | | |
| | | | Gruis | | Gauss |
| | | | Rasthof | | Berg Aukas |
| | | | Chuos | | Varianto |
| | | Ombombo | Okakuyu | | |
| | | | Devede | | |
| | | | Beesvlakte | | |
| | Nosib < 900–766 Ma[3] | | Nabis | | Nabis |
| Ages are from [1]Gray et al., 2006, [2]Halverson et al., 2005, Hoffman et al., 1996; Frimmel et al., 2011 and [3]Miller, 2008 | | | | | From Hoffmann and Prave, 1996 |
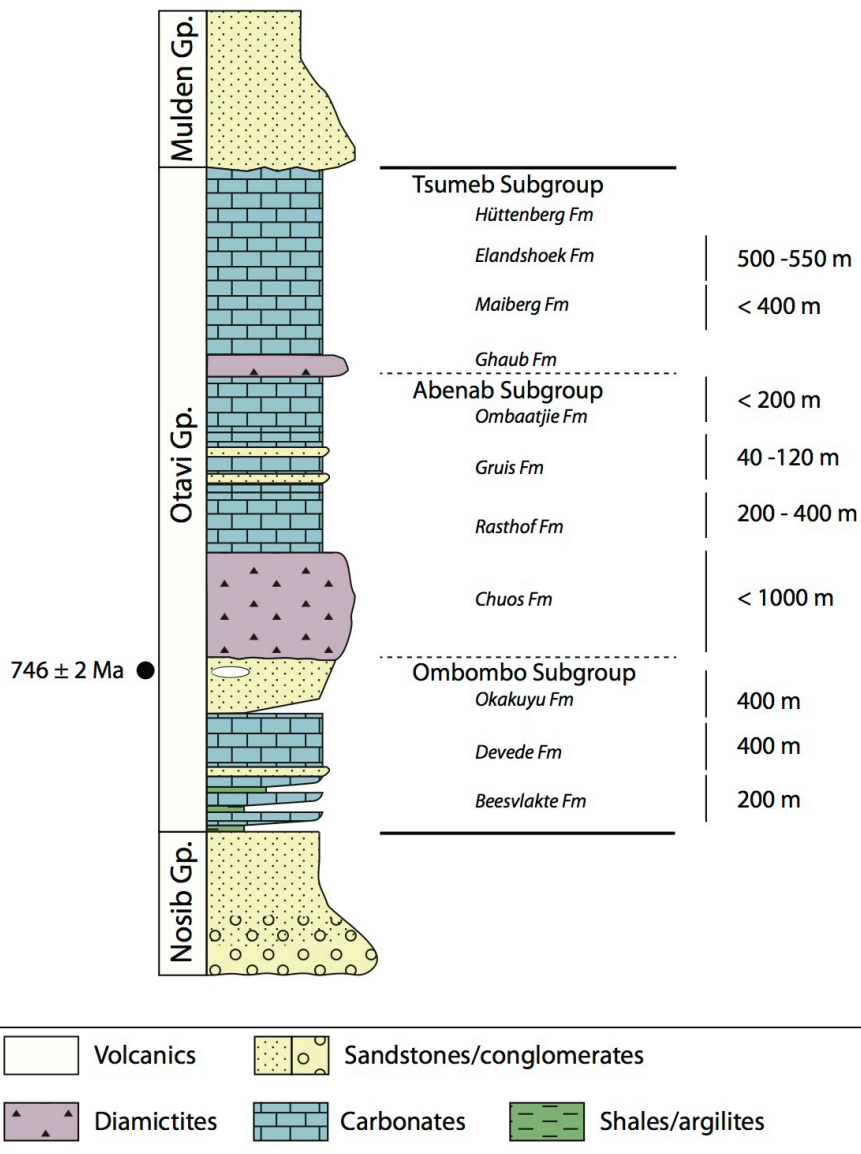
Figure 4.2: Simplified lithostratigraphy of the Damara Supergroup on the western part of the Northern Platform (data from Hoffman and Halverson, 2008).

## 2.2 Rifting

The beginning of the extension stage is not very well dated but the rift was active around 770–750 Ma along the southern edge of the Angola Block (Frimmel and Miller, 2009; Frimmel et al., 2011). The Northern Nosib rift opened the Outjo Sea (Figure 4.3.B). This rifting was aborted and another rift started to the south of the first one, opening the Khomas Sea (Frimmel et al., 2011 and references therein; Miller et al., 2009). The Damara Ocean is the association of the north and south rifts. On the western side of the Angola Block, rifting is not precisely dated either

but Konopásek et al. (2008) report U-Pb ages of ca. 840–805 Ma, suggesting they represent the oldest zircon specimen found in the Kaoko Belt. Rifting is likely to have developed in a zipper pattern, opening from the west of the Angola Block and migrating to the south. The Nosib Group was deposited south and also north of the Northern Nosib rift, on the Angola Block (Hedberg, 1979; Miller, 2008), which is the study area.

## 2.3 Nosib Group

The Nosib Group cannot be described from within the Owambo Basin, as it forms a deep siliciclastic basement, and has not hitherto been penetrated by wells. Sediments of the Nosib Group accumulated on and along the edges of the Angola Block are principally exposed in the Kaoko and Damara Belts (Hedberg, 1979). They consist of fine to coarse sandstones and conglomerates interpreted as continental to shallow-water deposits (Hedberg, 1979; Miller, 2008). More distal facies are expected southward in the north and south Nosib rifts.

## 2.4 Otavi Group

### 2.4.1 Ombombo Subgroup

After the rifting, a more stable setting is recorded by the Otavi Group. This unit contains a carbonate platform divided in three subgroups: the older Ombombo Subgroup, the Abenab Subgroup and the younger Tsumeb Subgroup (Hoffmann and Prave, 1996).

In the vicinity of the Kamanjab Inlier, the Nosib Group was deposited along a south dipping palaeoslope. The overlying mixed carbonate-siliciclastic Ombombo Subgroup recording a palaeocurrent reversal, with sediments shed in the opposite direction (Hoffman and Halverson, 2008). The former authors explain this change by a progressive rotation of the palaeoslope. From Ombombo times onward, the sediments deposited on the Angola Block follow a north dipping palaeoslope. The Northern Platform built-up on this slope, preceded by the continental deposits of the Nosib Group. This setting suggests a basin located north of the Nosib rift, the two basins being separated by uplifted ridges.

### 2.4.2    Abenab Subgroup

The base of the Abenab Subgroup is marked by a highly heterogeneous, diamictite-rich succession: the Chuos Formation. A range of ironstones, conglomerates, diamictites, sandstones and shales occur; clasts can be striated and dropstones occur, together with attenuated and deformed intervals interpreted to result from subglacial shearing (Busfield and Le Heron, 2013; Le Heron et al., 2013a). The maximum age of this glacial event is dated at 746 ± 2 Ma (Hoffman et al., 1996) with U-Pb from the underlying Nauuwport volcanics. It is interpreted as the local record of the Sturtian glaciation (Hoffman and Halverson, 2008; Hoffman et al., 1998b; Miller et al., 2009) punctuated by interglacial periods and ice-free conditions (Le Heron et al., 2013a). Post-glacial transgression triggered the deposition of the Rasthof Formation, also named Berg Aukas Formation in the eastern part of the Northern Platform (Hoffman and Halverson, 2008; Miller, 2008; Misiewicz, 1988). Both the Rasthof and Berg Aukas formations generally exhibit a basal cap dolostone followed by extensive microbial mats. The latter are in turn followed by fine-grained, epiclastic dolomite and grainstones (Hoffman and Halverson, 2008; Pruss et al., 2010). On the Northern Platform, the shallow-water, mixed carbonate and siliciclastic sediments Gruis Formation overlies the Rasthof Formation. The contact between these two formations is a regional subaerial exposure (Hoffman and Halverson, 2008). On the eastern part of the platform the lateral equivalent of the Gruis Formation is named the Gauss Formation. Upsection, limestones and dolostones of the Ombaatjie or Auros formations characterise the top of the Abenab Subgroup (Hoffman and Halverson, 2008; Miller, 2008). The facies of the Rasthof Formation will be developed in section 3 of the present chapter.

### 2.4.3    Tsumeb Subgroup

The base of the Tsumeb Subgroup is marked by the Ghaub Formation, often interpreted as the local record of the Marinoan glacial event (Hoffman and Halverson, 2008; Hoffman et al., 1998b; Miller et al., 2009). South of the Kamanjab Inlier, the glacigenic origin is supported by the observation of unstratified diamictites and ice-rafted dropstones (Hoffman and Halverson, 2008). Eyles and Januszcak (2007) question a glacial origin, highlighting the lack of sedimentological evidence, the rarity of striated clasts, the absence of a striated pavement, and

emphasising the texture: matrix supported diamictites, which could be interpreted as syn-tectonic mass flows of non-glacial affinity. Those authors conclude that there is no evidence for widespread ice cover during Ghaub times: if ice was present, it formed in uplifted source areas (Eyles and Januszczak, 2007). Rare striated clasts indicate however that ice was potentially locally present. Bechstädt et al. (2009) amplified the view of Eyles and Januszczak (2007) that most of the diamictites were ultimately of tectonic origin. These interpretations have been discussed by Domack and Hoffman (2011) who maintain the hypothesis of widespread ice at Ghaub time. Based on detailed sedimentological observations, they suggest that south of the Otavi Platform, the Ghaub Formation records an ice grounding line wedge. The diamictites are overlain by a cap carbonate: the Maieberg Formation. This formation starts with a cap dolostone, which presents most of the unusual facies of the post-Marinoan cap dolostones observed worldwide, e.g. tubestones, giant wave ripples and low angle cross-stratification (Hoffman and Macdonald, 2010 and references therein). Overlying facies of the Maieberg Formation consist of dolomite, carbonate and intraclast-ooids grainstones (Hoffman and Halverson, 2008). Upsection, the Elandshoek Formation is characterised by grainstone-dominated dolomite cycles and frequent stromatolites. It is in turn overlain by the Hüttenberg Formation, with very similar facies. However, a notable difference of the $\delta^{13}$C signatures allows a differentiation between the two formations (Hoffman and Halverson, 2008).

## 2.5    Collision stage and Mulden Group

The terminal Neoproterozoic collisions during the Pan-African orogeny led to the uplift of the Nosib and Otavi groups and to the deposition of the Mulden Group (Figure 4.3.B). It is thought that the closure of the oceans followed a zip-like movement that migrated from the west of the Angola Block to the south (Gray et al., 2008). Goscombe et al. (2005) dated the collision in the southern Kaoko Belt between 580 and 550 Ma, using a dense dataset of samples dated with U-Pb, Sm-Nd and $^{40}Ar/^{39}Ar$ methods. In the Damara Belt, Gray et al. (2006) estimated that the Pan-African orogeny occurred between 580 and 500 Ma, also using a dense set of $^{40}Ar/^{39}Ar$ ages. The same authors suggest a peak of deformation between 530 and 520 Ma in the Damara Belt.

The last group of the Damara Supergroup consists of foreland basin deposits: the Mulden Group is composed of conglomerates, sandstones and shales. Proximal facies are found to the west and distal facies to the east of the basin (Germs et al., 2009). First, the sandstone dominated Tschudi Formation rests with an angular unconformity on the Otavi Group (Bechstädt et al., 2009; Misiewicz, 1988) with erosion or karsts (Germs et al., 2009; Miller et al., 2009) or sometimes without evident unconformity ("paraconformity", Hoffman and Halverson, 2008). The overlying Kombat Formation consists of sandstones and siltstones. The last formation of the Mulden Group and of the Damara Supergroup is the Owambo Formation, giving its name to the foreland basin.
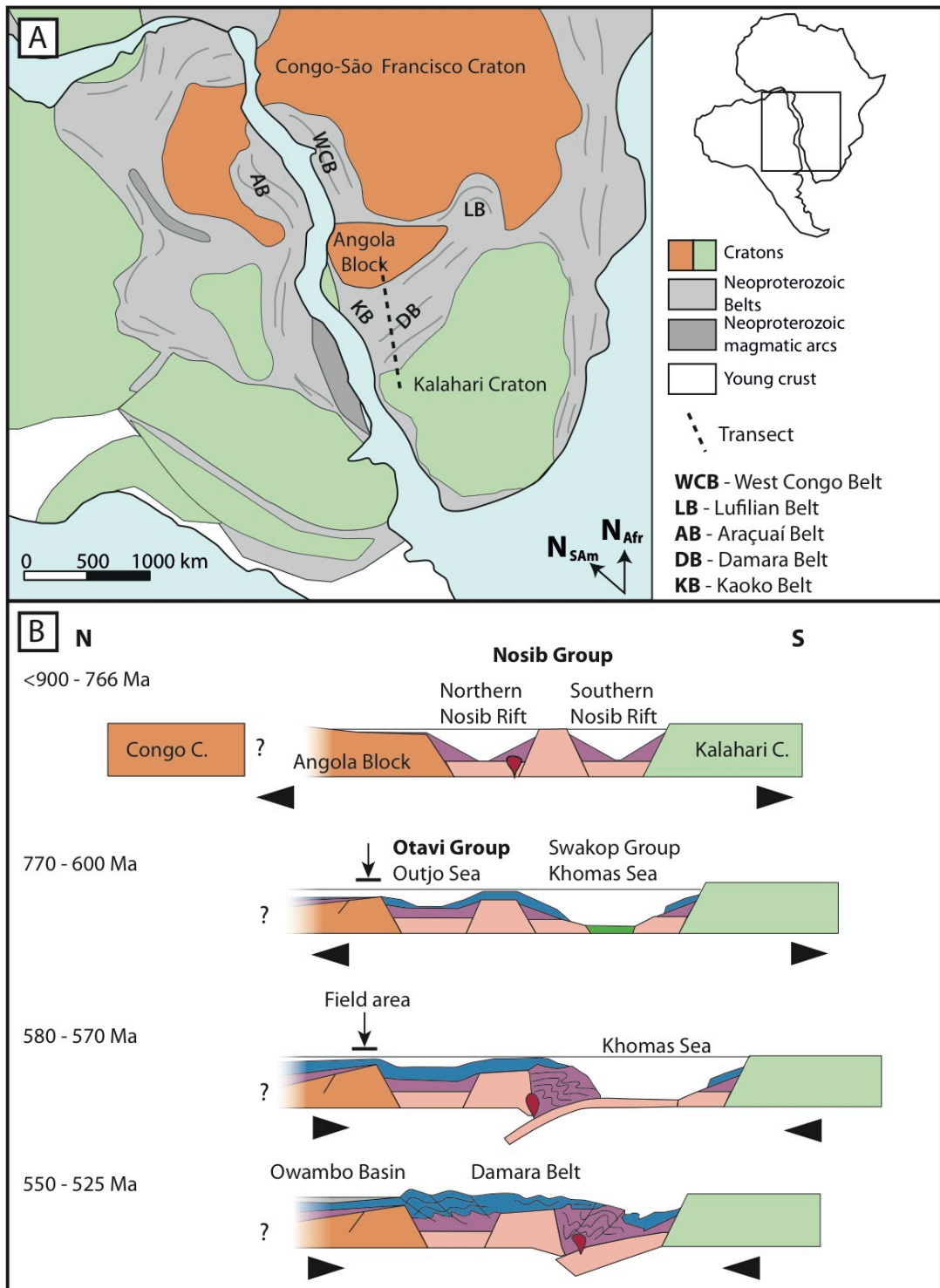
Figure 4.3: Tectonic history of the Damara Belt. **A**. Location of the cratons in Africa and South America (modified from Frimmel et al., 2011). **B**. Summarised geodynamic history between the Angola Block and the Kalahari cratons.

## 3    The Rasthof Formation

Now that the global geological context is set up, it is useful to look in closer detail at the previous work done on the Rasthof Formation. Hedberg (1979) first described the stratotype on the western part of the Northern Platform. Following an interval of non-activity, the interest around this formation has increased substantially since the late-1990s. Despite this, the number of publications directly related to the formation remains few. On the western part of the Northern Platform, a range of stratigraphic, macroscopic to microscopic studies were published (Bosak et al., 2012, 2011; Dalton et al., 2013; Hoffman and Halverson, 2008; Hoffmann and Prave, 1996; Le Ber et al., 2013; Pruss et al., 2010; Tojo et al., 2007; Yoshioka et al., 2003). The entire Otavi Group was more widely studied on the eastern part of the platform during the 20th century owing to its important ore deposits (Kamona and Günzel, 2007). The latter studies focus on to mineralisation processes and ore assemblages, rather than the general geology or sedimentology. In northwest Namibia, two other factors can explain the lack of study of the Rasthof Formation between its description as a stratotype (1979) and the renewed interest (mid-1990s). Firstly the political instability: Namibia was struggling to become an independent country from the 1970s to 1990. Independence installed more stability and therefore a safer environment to undertake geological fieldwork. Secondly, from a scientific point of view: the snowball Earth hypothesis (Hoffman et al., 1998), is essentially based on field observations from Neoproterozoic strata of northern Namibia. This stimulated an intense debate, and engendered an increasing interest in Namibian geology from the scientific community.

The Rasthof Formation is a post-Sturtian cap carbonate sequence deposited on the Northern Platform. It is exposed in the folded Neoproterozoic belts of northwest Namibia. It generally rests on the Chuos Formation and consists of a thin (0–70 m) basal cap dolostone, a thick (~150 m) microbial member and a final epiclastic member (20–50 m) (Hoffman and Halverson, 2008). The publications reviewed below focus on the cap dolostone and the microbial member only.

## 3.1 The Otavi platform at Rasthof time

Hoffman and Halverson's (2008) work focuses on the southern and western edges of the Kamanjab Inlier. They synthesised their work into a transect of the platform, adapted in Figure 4.4.A. Essentially, the present-day Owambo Basin occupies the former position of the Otavi Platform. The Kaoko and Damara belts, together with local inliers, meanwhile, correspond to present-day ridges/outcrops and a transition to the foreslope, located west and south of the Owambo Basin (Figure 4.4.B). In the following, locations of the specific areas are documented in Figure 4.5.
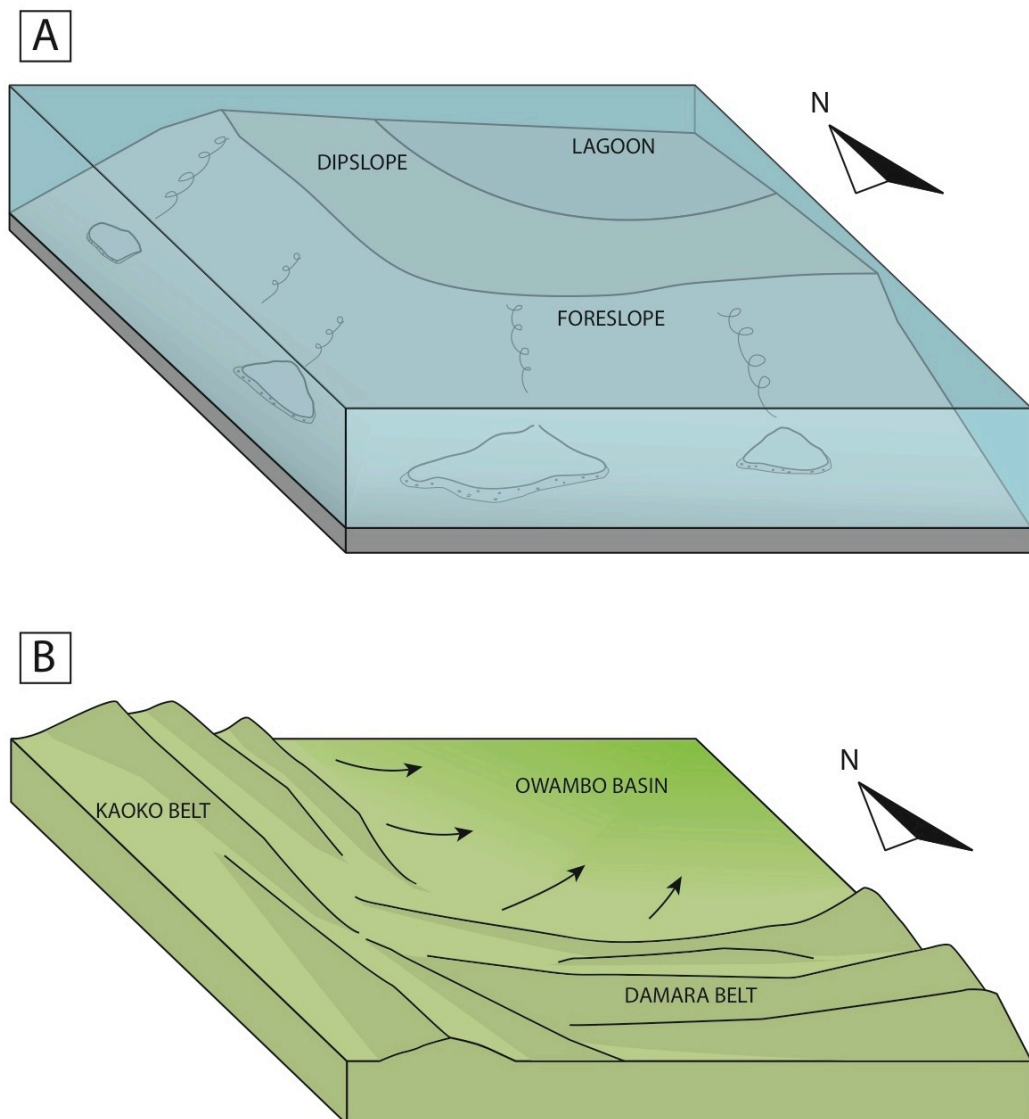


Figure 4.4: From the Northern Platform to the Owambo Basin. **A**. Schematic representation of the Northern Platform (Rasthof Time), water depths are difficult to evaluate. **B**. The Owambo Basin overlies the Otavi Platform and the Mulden foreland basin that resulted from the Pan-African orogeny. Limbs of the platform are exposed in the belts.

Exposures of the Rasthof Formation are poorly studied northeast of the Kamanjab Inlier (see Figure 4.1). A thin wedge of strata follows the edge of the basement before dipping beneath the strata that fill the Owambo Basin (Figure 4.5). This side of the Kamanjab Inlier was visited and locally described by Hedberg (1979) and Le Ber et al. (2013). Most of the other studies are located south (Fransfontein Ridge, Summas Mountains), west (Grootberg Syncline) and northwest of the Kamanjab Inlier (Khowarib Fold Belt). The margins and slopes of the platform are now exposed in the fold belts formed during the Pan-African orogeny: the Damara and Kaoko belts. The rest of the platform is likely to be mostly preserved below the Owambo Basin.
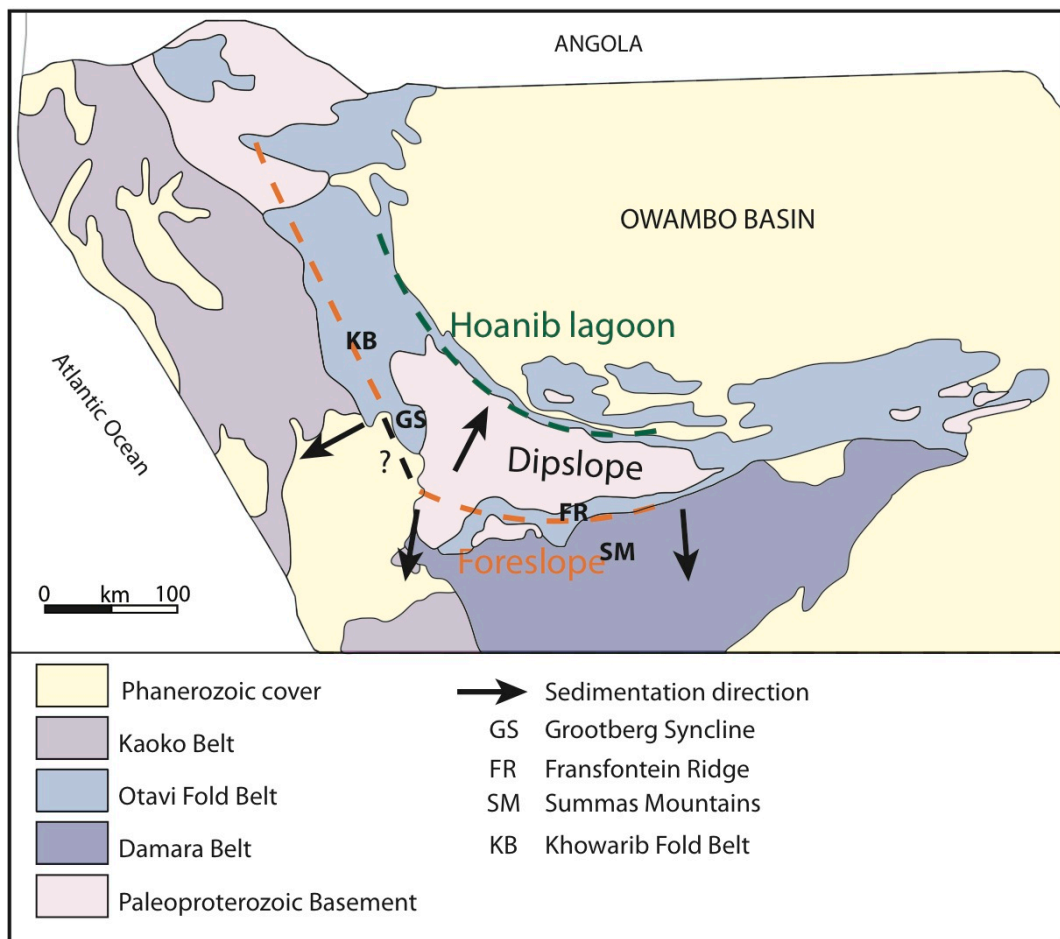


Figure 4.5: Map of the environments of the Rasthof Formation preserved in the Neoproterozoic Belts (modified from Hoffmann and Prave, 1996).

## 3.2    Facies of the Rasthof Formation

Hedberg (1979) first described the Rasthof Formation (Rasthof Member) at Rasthof Farm (see Chapter 5: section 3.3), NNE of the Kamanjab Inlier. It initially only included what is now called the microbial member. The cap dolostone was described as a separation between the Chuos Formation and the "Rasthof Member". The epiclastic member is not exposed at Rasthof Farm and was not initially included in the Rasthof Formation.

In northwest Namibia, the underlying Chuos Formation bears evidence of direct ice contact (subglacial shear zones, dropstones, ice-contact fans) with two glacial cycles preserved (Le Heron et al., 2013a). The overlying 200–400 m-thick Rasthof Formation is an archetypal, post-glacial, cap carbonate sequence. It generally starts with a cap dolostone, also locally termed "rhythmite" or "abiotic member" (Hoffman and Halverson, 2008; Pruss et al., 2010), in which cm–dm-thick allodapic beds alternate with m-thick delicately laminated dolostone (Hoffman and Halverson, 2008). The cap dolostone rests generally in sharp contact, but without any evident unconformity on the Chuos Formation. The abiotic member is concordantly overlain by the ~150 microbial member. Bizarre folds and local roll-up structures are characteristic from this member (Hoffman and Halverson, 2008; Pruss et al., 2010). Previous authors refer to the microbial laminae as microbialaminites or microbialites. Microbial mats were soft and cohesive at the time of deposition but they are now lithified. In this thesis, we refer to them as stromatolites on the basis of Riding's (2011b) definition: "Stromatolites are macroscopically layered authigenic microbial sediments with or without interlayered abiogenic precipitates."

In the Rasthof Formation, stromatolites are described as continuous, parallel to subparallel, often deformed mats. Miller (p. 13–58, 2008) noted that the formation can locally be stromatolitic, probably referring to individual morphologies (columns, cone, etc.) but not giving details about specific locations or geometries. At least two studies described individual stromatolite morphologies. First, Cloud and Semikhatov (1969) described a so-called *Baicala* morphotype in the lower Abenab Formation, together with a *Conophyton* morphotype in the upper Abenab, both in the Tsumeb

area (Figure 4.1.C, northeast Namibia, see Chapter 7). Hedberg (1979) observed "a peculiar algal growth which resembles the structure found in pillow lava" when describing facies variations along the northern flank of the Kamanjab Inlier. These "pillow lava" geometries could correspond to the dome stromatolites described by Le Ber et al. (2013) and in Chapter 5 (section 3.3.3.2), at Rasthof Farm. With the exception of the previous references, the most recent published literature (late 1990s–2010s) does not illustrate any similar dome stromatolites on the northwestern part of this post-Sturtian platform.

Hoffman and Halverson (2008) indicate that the cap carbonate sequence is terminated by an epiclastic member. The latter unit is present on the platform and facies is characterised by a coarsening upward motif that exhibits cross-bedding (Hoffman and Halverson, 2008). The same authors indicate that on the platform, subaerial exposure marks the top of the Rasthof Formation. Later, the Rasthof Formation was covered by the mixed siliciclastic/carbonate Gruis Formation.

### 3.2.1 South of the Kamanjab Inlier

South of the Kamanjab Inlier, along the Fransfontein Ridge (Figure 4.5), the Rasthof Formation is 15–150 m-thick (Hoffman and Halverson, 2008) and rests often directly on the basement – the Chuos Formation is missing. The cap dolostone can be described as a rhythmite associated with debrites. Intraclasts of microbial sediments are found in the debrites, probably derived from the platform located to the north (Hoffman and Halverson, 2008). The same authors do not provide further descriptions of the microbial facies in this area. In the Summas Mountains (Figure 4.5), the cap dolostone is also described as a rhythmite with debrites. However, no microbial member is observed. Argillites occur instead and the upper part of the Rasthof Formation is characterised by allodapic carbonates. Both Fransfontein Ridge and Summas Mountains sediments of the Rasthof Formation are interpreted as foreslope deposits deepening towards the south while the platform is interpreted to be located to the north. From the above, a gradation of lithofacies from distal/deep to proximal/shallow can be proposed: 1) argillites associated with debris-flows; 2) cap dolostone/allodapic carbonates; 3) microbial member (and 4) epiclastic member).

100

### 3.2.2    West and northwest of the Kamanjab Inlier

The renewed interest for the Rasthof Formation is highlighted by several recent studies (Bosak et al., 2013b, 2012, 2011; Dalton et al., 2013; Hoffman and Halverson, 2008; Pruss et al., 2010; Tojo et al., 2007; Yoshioka et al., 2003) undertaken in the Khowarib Fold Belt (Figure 4.5). Hoffman and Halverson (2008) recognised that north of the Fransfontein Ridge, the Rasthof Formation records a carbonate platform with a dipslope deepening towards the north into the Hoanib Lagoon. The latter is likely to be mainly preserved below the Owambo Basin, while the dipslope is located between the Hoanib Lagoon and the foreslope. The main observations and interpretations from previous authors are synthesised in Table 4.2.

#### 3.2.2.1    Cap dolostone

The cap dolostone thickness ranges from 0 m in the north (Ombepera: Pruss et al., 2010) to 75 m towards the south (Grootberg Syncline: Hoffman and Halverson, 2008). It is reported to consist of rhythmites associated with allodapic beds. In the Khowarib area, at least one carbonate turbidite bed was described (Tojo et al., 2007). This turbidite bed is less than 1.5 m-thick and tapers southward.

Microscopic study of the cap dolostone in the Khowarib–Ongongo area by Tojo et al (2007) revealed the nature of the laminated facies. First, they found that laminae can result from an alternation of horizontal "brick-shaped" calcite grains with subhorizontal laminae formed of fine clay particles. Second, they found that horizontally arranged, dark clay particles define the laminae in a white to grey micritic dolomite matrix. Thirdly, they observed similar clay laminae within a coarse crystaline dolomite. Thus, it appears that the laminae result from a sub-mm alternation of carbonate (dolomite or calcite) with relatively thinner laminae composed of clay particles.

#### 3.2.2.2    Microbial member

Pruss et al. (2010) described the microbial member in detail in the Khowarib area (Ongongo, Okaaru). They divided the microbial member in a thickly and thinly laminated facies. Thickly laminated stromatolites arrive generally after the cap

dolostone and are characterised by 1–4 mm-thick laminae. An abundance of soft-sediment deformation structures is observable throughout this facies. They form several dm–m-scale complex folds/dome like structures. This gives to the microbial facies a chaotic, bizarre aspect despite continuous sets of laminae. The lateral equivalent of the Rasthof Formation in northeast Namibia, the Berg Aukas Formation exhibits similar microbial sediments that were described as contorted dolomites (Misiewicz, 1988). This contortion-rich facies is laterally continuous for > 100 km throughout northern Namibia. In his description of the stratotype, Hedberg (1979) noticed that intensity of the deformations decreases upsection.

Often described above the thickly laminated facies, the thinly laminated facies is characterised by densely laminated (sub-mm) microbial laminae (Pruss et al., 2010). They are generally flat and less deformed than the thickly laminated microbialites. But they still exhibit unusual cm-scale roll-up structures (Hoffman and Halverson, 2008; Pruss et al., 2010). Similar structures, possibly more intensely deformed are observed at the stratotype section (Le Ber et al., 2013). Personal field observations revealed the occurrence of similar facies in the Berg Aukas Formation, northeast Namibia (Chapter 7, section 3.3). This indicates again the widespread occurrence of similar facies through more than one hundred kilometres on the Northern Platform.

Pruss et al. (2010) investigated the microfacies of the microbial member. They concluded that the thickly laminated microbialites are the result of an alternation of thin (~10 μm) dark organic rich, microbial laminae and much thicker (1–4 mm) light carbonate cement laminae. The latter are seen as intervals when cementation outpaced the growth of microbial mats. Composition of the laminae in the thinly laminated microbial member is the same, except that the light carbonate laminae are thinner (sub-mm). Note that no direct evidence of mat building organisms is preserved in the microbial member. However, also at the microscopic scale, Pruss et al. (2010), Bosak et al. (2011, 2012) and Dalton et al. (2013) described a variety of circular to elongated, walled features that they interpreted as fossil eukaryotes.

Table 4.2: Synthesis of the descriptions (D) and interpretations (I) of the Rasthof Formation.

| Member | | Hedberg, 1979 Rasthof Farm – Dipslope | Tojo et al., 2007 Khowarib Area – Hoanib Lagoon | Hoffman and Halverson, 2008 General facies | Pruss et al., 2010 Khowarib Area – Hoanib Lagoon |
|---|---|---|---|---|---|
| Thinly laminated | D | - regular lamination<br>- no contortion | - | - flat lamination<br>- roll-up structures | - sub-mm-thick, flat laminae<br>- roll-up structures |
| Thinly laminated | I | - shallow-water<br>- microbial origin | - | - cohesive microbial mats | - microbialites<br>- roll-ups due to fluid escape<br>- sub-storm, deep-water deposit |
| Thickly laminated | D | - dark/medium grey dolomite<br>- original facies highly contorted, with amplitude of one to four metres | - stromatolites with dome like structures | - convoluted intervals<br>- irregularly ballooned upward<br>- breccias | - 1–4 mm-thick laminae<br>- typical 10–50 cm large folds<br>- 0.1–0.5 m wide carbonate clastic dykes |
| Thickly laminated | I | - shallow-water algal mats<br>- contortions might be due to syn-depositional slumping; ice push; dissolutions of interstratified evaporates; removing of highly organic material during diagenesis | - | - cohesive microbial mats<br>- breccias due to dewatering or fluid escape | - microbialites<br>- folds due to fluid escape<br>- sub-storm, deep-water deposit |
| Cap dolostone | D | micritic medium-grey, tan and pink dolomite | light grey, finely laminated rhythmites interbedded with thin turbidites | dark grey fetid dolomite<br>mm-scale, parallel laminae<br>cm-scale turbidites | - rhythmite with allodapic wackestones |
| Cap dolostone | I | - | sub-storm wave base deposit | abiotic precipitation | sub-storm wave base deposit |
| | | **SHALLOW-WATER** | **DEEP-WATER** | **SUBLITTORAL** | **DEEP-WATER** |

(Microbial member comprises Thinly laminated and Thickly laminated rows.)

### 3.2.3 Interpretations

The Rasthof Formation is interpreted as a shoaling upward succession, with the cap dolostone deposited in the deepest environment (Halverson et al., 2005) (note that the deepest facies appears to be argillites found in the most distal settings, west and south of the platform). The cap dolostone is followed by sublittoral stromatolites of the microbial member. On the platform, the microbial member is overlain by the epiclastic member, which exhibits coarsening upward, into cross-bedded grainstones (Hoffman and Halverson, 2008). On the platform, regional subaerial exposure precedes the deposition of the Gruis Formation (Hoffman and Halverson, 2008).

#### 3.2.3.1 Cap dolostone

The cap dolostone is interpreted to record a sub-storm wave base setting on the western part of the Northern Platform (Tojo et al., 2007; Yoshioka et al., 2003). Common allodapic beds are mentioned (Hoffman and Halverson, 2008) and appear to be typical from this member. In the Khowarib Fold Belt, a turbidite has been described but its provenance awaits clarification. Tojo et al. (2007) interpreted the dolomitic laminated fabric of the cap dolostone as a primary feature.

South of the Northern Platform, a foreslope setting is supported by the occurrence of debrites with blocks of microbialites and oolitic grainstones. These blocks are likely to be derived from the Northern Platform (Hoffman and Halverson, 2008). The cap dolostone is also named "abiotic member" because the laminae do not result from biological processes by contrast with the overlying microbial member.

#### 3.2.3.2 Microbial member

The microbial member was first interpreted, on the northeast flank of the Kamanjab Inlier, on the dipslope of the Northern Platform. Hedberg (1979) suggested that the laminae were microbial in origin and deposited in a shallow-water environment. His interpretation was based on the observation of microbial mats, oolites and intraformational breccias. In northeast Namibia, shallow-water settings are also preferred to interpret the laterally equivalent facies of the Berg Aukas Formation on the Otavi Platform (Misiewicz, 1988). More recently, the strata in the Khowarib Fold

Belt area have been interpreted as sub-storm wave base deposits, i.e. indicating a comparatively deep-water environment. Pruss et al. (2010) justified this interpretation on account of the lack of bedforms, scour marks and intraclasts.

Several suggestions have been addressed to explain the widespread occurrence of deformation structures in the microbial member. Hedberg (1979, p.143–144), suggested several hypothesis: "syn-depositional slumping; […] ice-push; […] interstratified evaporites originally present may have been dissolved; […] failure of the formation to expel interstitial water until after considerable burial; […] the existence of highly organic material that collapsed and was removed during diagenesis". Despite this, the same author and Hoffman and Halverson (2008) explained that none of these hypotheses are supported by evidence.

Dewatering or gas escape are also suggested by Hoffman and Halverson (2008) and Pruss et al. (2010). The two first authors suggested this hypothesis after the observation of syn-sedimentary breccias in the thinly laminated microbialites. Pruss et al. (2010) supported this hypothesis with the observation of syn-sedimentary dykes cutting through the laminae of the microbial member.

## 3.3    The Berg Aukas Formation

Located on the eastern part of the Northern Platform, the Berg Aukas Formation is the lateral equivalent of the Rasthof Formation. Sedimentological studies related to this formation are rare (Cloud and Semikhatov, 1969; Miller, 2008; Misiewicz, 1988). Facies consist of undulated to contorted dolomitic laminae, with evidence of proximal and high-energy environment (oolitic grainstone, siliciclastic input, stromatolites, intraclasts of stromatolites). The work done in this area is not sufficient to allow precise comparisons with the Rasthof Formation.

From a stratigraphic perspective, the Berg Aukas was deposited after the Sturtian glacial epoch. The cap carbonate can rest either on the basement, the Nosib Group or the Chuos Formation. It is possible to divide the cap carbonate into 1) a basal cap dolostone unit and 2) overlying microbial-dominated units. The lack of recent studies implies a poor understanding of the internal stratigraphy and of the facies. More details about this formation are developed in Chapter 7.

# 4 Discussion

## 4.1 Context

The study area is located north of the Nosib rift system. On the Angola Block, the Nosib Group records continental deposits. Interpretation of the diamictites found upsection might differ between authors. If we consider widespread ice during the Sturtian glaciation, ice load may have increased the subsidence of the cratonic block, but the accumulation of ice on land may have triggered a sea level fall. Such considerations are amply illustrated by sequence stratigraphic approaches to Quaternary glacial successions produced by regional ice sheets (Brookfield and Martini, 1999). At the end of the ice age, melting of land-based ice logically led to a sea level rise, flooding the Angola Block. The Northern Platform succession was deposited in this context. No typical siliciclastic-rich facies are reported in the cap dolostone and microbial member of the Rasthof Formation. This indicates that 1) no source is present; or 2) the platform is protected from siliciclastic input; or 3) the platform is too far from the source (compatible with 2).

Note that despite sea level rise, the melting of the ice present on the craton must also have triggered a post-glacial rebound. The combination of these two post-glacial phenomena probably limited the amplitude of the flooding. If the diamictites of the Chuos Formation do not record the existence of widespread ice bodies but are rift-related instead (Eyles and Januszczak, 2004), the development of carbonate facies in the Rasthof Formation are linked to a diminution of siliciclastic input. Fewer siliciclastics would be compatible with the end of an extension regime and the development of a platform. Note that some of the latest interpretations of the Chuos Formation point at a glacial origin on strong textural grounds, as summarised in this chapter (Busfield and Le Heron, 2013; Le Heron et al., 2013a). It is therefore appropriate to consider the cap carbonate sequence as the record of a post-glacial setting.

## 4.2 Cap dolostone

Hoffman and Halverson (2008) named the cap dolostone "rhythmite" or "abiotic member". Their work focuses essentially on the foreslope and partly on the dipslope of the Northern Platform. On the foreslope, the cap dolostone is rich in

debris flows with blocks derived from the Northern Platform. On the dipslope, the allodapic beds are extremely common and often < 10 cm-thick (Fig.13.59.a, Hoffman and Halverson, 2008).

The nature of the allodapic beds is debatable. They are called "allodapic", but none of the authors (Hoffman and Halverson, 2008; Tojo et al., 2007; Yoshioka et al., 2003) who have worked on these features on the dipslope establish typical facies associations that may be used to present an allodapic interpretation with a reasonable level of confidence (see Flügel, 2004; Meischner, 1964), except for one clast-rich bed (Tojo et al., 2007), also described in Chapter 5, section 3.4.1.

## 4.3    Microbial facies

The main challenge to interpret the setting in which the microbial member of the Rasthof Formation was deposited is that no evidence support the initial hypotheses formulated to explain the unusual facies observed (Hedberg, 1979; Hoffman and Halverson, 2008). In a deep-water environment, Pruss et al. (2010) invoke fluid escape during the early compaction of the sediments to explain the widespread occurrence of deformation observed in the microbial member. This interpretation is plausible and is difficult to discount. A problem however is that their illustrations do not illustrate well a direct link between the fluid escape features and the deformations. The authors provided two illustrations (Pruss et al., 2010, fig.3.B and fig.6.D) with obvious up to 10 cm wide features cutting through the laminae. If these structures created the deformation of the mats during early compaction, we should expect the nearby laminae to be dragged upward. But in the illustrations, laminae point downward or remain perfectly flat. Also, deformations are extremely common but not necessarily associated with these dykes. The dykes probably result from fluid escape but do not seem to be the cause of the deformation. Dykes as well as widespread deformations appear to result from other stresses that need to be investigated.

If mats were cohesive at the time of deposition as previous authors suggested, breakage of beds to form clasts would be retarded, limiting the occurrence of intraclasts. No important clastic input is reported and any grain or small intraclast should be trapped, at some point, by the microbial mats covering the platform floor

at Rasthof time. This limits the transport of potential grains and the creation of bedforms. If exposed to occasional hydrodynamic energy, the cohesive mats were maybe more likely to bend instead of being dug and form scour marks. This hypothesis will be discussed more in details in Chapter 5 (sections 4 and 5). Given the supposed nature of the sediments before full lithification, wave percussion is a candidate as a factor for the deformation of the microbial mats (Le Ber et al., 2013).

## 5    Conclusion

The Otavi Platform was deposited north of the Nosib rift. At the base of the Damara Supergroup, widespread, coarse siliciclastic sediments of the Nosib Group record a continental to shallow-water environment. The Ombombo Subgroup records the transition from a rifting to a spreading stage. The overlying Chuos Formation records a glacial event, followed by the cap carbonate Rasthof Formation.

In the Rasthof Formation, the description of the cap dolostone and the microbial member has not changed significantly since they were first described as the stratotype. At the regional scale, facies are extremely continuous over hundreds of km across the platform. Hedberg (1979) described the cap dolostone as a micritic medium-grey, tan and pink delicately laminated dolomite and the microbial member as highly contorted with amplitude of the deformations from several dm to a few m (thickly laminated microbialites). Upsection, contortion of the mats decreases and passes into regular laminae (thinly laminated microbialites). More recent authors use the same background description at different locations. They have added local observations such as allodapic beds in the cap dolostone (Hoffman and Halverson, 2008; Tojo et al., 2007; Yoshioka et al., 2003) and sedimentary dykes as well as roll-up structures in the microbial member (Hoffman and Halverson, 2008; Pruss et al., 2010). The top of the formation is marked by shallow-water facies and a regional exposure on the platform.

We have seen that previous studies are placed on a north–south transect, on the southern edge of the Angola Block. On the foreslope of the Northern Platform, the sediments of the Rasthof Formation record a slope setting with deep-water deposits (argillites, debris flow, platform-derived blocks). These facies are expected southward and westward of the Angola Block (Hoffman and Halverson, 2008; Pruss

et al., 2010), in the basins separating the Angola Block from the Kalahari and Rio De La Plata cratons. These basins apparently never produced oceanic crust (Frimmel et al., 2011; Miller et al., 2009). On the platform, interpretations of the typical facies of the Rasthof Formation range from shallow to deep-water.

Three chapters (5, 6 and 7) focus in detail on the post-Sturtian cap carbonate in northern Namibia. Three different chapters are presented because scale of study and the areas visited raise a different set of problems and discussions. The aim of Chapter 5 is to present field data made on the western part of the Northern Platform, including new sedimentological observations. The Chapter 6 decrypts a part of the microfacies found in the cap dolostone and the microbial member. Since sedimentological observations and interpretations of the Berg Aukas Formation (eastern part of the platform) are rare and not as well established as the Rasthof Formation, a different approach is used in Chapter 7, with more general reflections on the local stratigraphy and facies interpretations.

# Chapter 5 – Macrofacies of the Rasthof Formation

## 1    Introduction

Most of the data and observations presented in this thesis come from northwest Namibia where two field seasons have been undertaken. The reason for focussing on the Rasthof Formation is that this specific stratigraphic interval (post-Sturtian) is poorly documented and understood, at both the local and international scale. Chapter 4 explains why the Rasthof Formation represents a sedimentological challenge. The unusual facies described in the Rasthof Formation have been interpreted to reflect both shallow and deep-water origins. In this chapter, new sedimentological observations from the Rasthof Formation are presented, in addition to the study published by Le Ber et al. (2013). This chapter focuses exclusively on the cap dolostone (i.e. abiotic member, Hoffman & Halverson, 2008) and the microbial member of the Rasthof Formation.

## 2    Material and method

In order to get a better understanding of the Rasthof Formation, a multi-scale approach was planned for this research, with intended integration of subsurface data (wells, seismic), field and microscopic observations (as well as chemical analysis). Prior to fieldwork, the first dataset accessible consisted from 5 wells data and about 50 seismic lines shot in the late 1960s in the Owambo Basin. None of the wells reach the Rasthof Formation and no check-shot allows any stratigraphic constraints on the horizons observed on the seismic lines. A synthetic seismogram was generated from the deepest well logs that reach the top of the Otavi Group. But even this technique did not produce any confident result, as the quality of the lines around this well is not good enough to be correlated with the synthetic seismogram. The overall poor quality and vertical resolution of the data as well as the global lateral discontinuity of the record (missing lines, > 50 km gaps) did not permit precise observations and consistent interpretations. From these obstacles, it was decided not to continue further work on the subsurface dataset and to focus on macroscopic to microscopic observations at outcrop.

The Rasthof Formation will be described and compared in three areas of northwest Namibia: Rasthof Farm, Omutirapo and Okaaru areas. Its lateral equivalent, the Berg Aukas Formation, is also studied in northeast Namibia (Chapter 7); the method presented below applies both to the present chapter and Chapter 7. Two field seasons were undertaken. During the first (July 2011), the author joined as a field assistant to describe and sample exclusively the cap dolostone, north of Kamanjab. The aim of the second field season (May–June 2012) was to:

- Trace, understand, and compare the main facies (cap dolostone, thickly and thinly laminated microbialites) at different locations, and to evaluate potential facies variations;

- Sample for microscopic study and TOC analyses.

## 2.1 Fieldwork

### 2.1.1 Planning

In Namibia, the year is divided in two seasons: summer (August–April) and winter (May–September). Temperature during summer can reach 40°C and thus winter fieldwork is preferable, with day temperatures of 25–35°C. However winter daytime is much shorter than summer, and it is too dark to work after 6 PM. It is sometimes preferable to leave outcrops early (e.g. 4–5 PM) to avoid night walks/drives.

The remote nature of the field area means travelling at all times with a satellite phone, a first aid kit and a hand held GPS. During long walks with low visibility or dangerous paths, the GPS is also essential to record which path was used on the way in.

A .kml file of the tracks that do not appear on the road maps was generated. The principal roads and some tracks are shown on the geological maps, but the tracks are not precise. Furthermore, some of the tracks shown on the geological maps are long since abandoned. For exploration of new outcrops, a precise and complete track file can therefore be created and exported from Google Earth. It can then be imported on a GPS to help with orientation, avoiding any "adventurous" off-track drives.

### 2.1.2 On-site

#### 2.1.2.1 Orientation

An all-terrain, four-by-four vehicle is highly recommended to access all the visited outcrops. Many are located on private lands and it is preferable to have the authorisation from the owner to drive around on their land. Organizing a visit in a farm can take several days; some farms are only accessible after crossing another farm, requiring the permission and sometimes the presence of several owners to guide the geologists through the numerous tracks.

#### 2.1.2.2 Communication

If most of the residents from Namibia speak an excellent English, the use of local languages such as Oshiwambo, Herero or Afrikaans can be indispensable to access some remote properties or to seek help and orientation. The University of Namibia (UNAM) offered the help of field assistants whose local language skills were essential to access outcrops. Some farmers can be suspicious because mining companies try to buy or explore their land. The UNAM also provided an essential official letter explaining the purpose of the fieldwork and research, facilitating the access to the farms.

#### 2.1.2.3 Risks

Several risks have to be considered when going on the field. Beyond all the classic risks related to field geology, the nature of the sediments and the field areas can limit observations.

- **Drives**: driving to the outcrops can require more than one hour. It is important to anticipate risks or unforeseen events such as road quality, punctures, dead-ends, unexpected closed fences, poor fuel supply. It is therefore advised to allow an extra time window to avoid any night drive or worse; getting stuck hours walk from the nearest village. Namibia has a low population density and in case of difficulty, help might be difficult to find. It is important to make sure all the tyres are ready to use and to take time to repair them if necessary. Ideally, at least two cars are needed to drive in the

most remote areas. Progression can be slow, especially in northeast Namibia where tracks are often damaged by warthog's holes, seasonal heavy rains and finally, football-sized boulders. The latter are left on the road by baboons, who roll them in search of insects.

- **Walks**: reaching and visiting the outcrops can involve long walks, sometime including steep climbs (average 16% slopes in the Omutirapo area but up to 30% + short climbing). Considering the temperatures (often ~30°C) it is advised to take as much water as possible. The vegetation in northwest Namibia is low and shade can be rare. Thorny trees and bushes (e.g. acacias) are commonplace and care must be taken. In northeast Namibia, while keeping an eye on the thorns, special care has to be taken to avoid warthog holes. They can be wide (up to 50 cm across) and deep (> 50 cm) but are often hidden by relatively long grass. Finally, the last risk to consider is wildlife. Most of the animals tend to run away and will not be encountered, but some of them can be dangerous: snakes, baboon hordes and possibly big cats. The probability to face these animals is very low but does exist.

- **Outcrops**: the outcrops of the Rasthof Formation present some risks due to weathering and instability. The weathering and dissolution have produced a razor sharp texture, continuous all along the exposures. Outcrops are most often weathered into 5–10 m large blocks, some of them can be smaller (< 2 m) and very unstable when stepping on them.

### 2.1.3 Descriptions

Once on an outcrop, the rock succession is described (facies, lithology, size of the structures, etc.), and a measured section made where possible. Sampling strategy is influenced by the main facies exposed and interesting features therein. Each sample needs to be large enough to allow the production of thin sections and geochemical analyses as necessary (e.g. TOC, Rock-Eval), thus samples are typically between 100 and 300 g. Difficult access to outcrops tends to limit the samples that can be carried. Bigger samples (up to 3 kg) have occasionally been selected in the microbial member (only at Rasthof Farm, section 3.3) to create slabs for a better description

of remarkable structures. Samples were sent back to the UK by colleagues in Namcor, the national Namibian oil company.

## 2.2    Sample preparation

Weathering and diagenesis may obscure sedimentary features in the field. To complete field observations with more precise macro- to microscopic descriptions, samples were cut to produce slabs and thin sections. Details of the samples preparation and methods used (plane polarised/cross polarised light microscope, cathodoluminescence, fluorescence, scanning electron microscope) for microscopic descriptions are presented in the Chapter 6.

Large samples (> 10 cm) of key facies from the Rasthof Farm were cut and polished for more precise descriptions. Colours of the laminae range from light to dark grey and colour variations can occur at a mm-scale. This makes observation, capture and digital interpretation of the facies problematic. Several methodologies were tried to capture and describe the polished samples. First, surface of the samples were oiled, then photographed with a SLR camera mounted with a macro lens (Figure 5.1.A). This technique did not produce good results, with problems of light reflection and a non-homogenous focus at the surface of the sample.

The second technique was the production of acetate peels from the polished samples (Figure 5.1.B). This technique theoretically allows detailed sedimentological descriptions under a hand lens or a microscope. Preparation of acetate peels follows 4 steps:

- The polished side of the sample is hold face-down in a 10% Hydrochloric Acid (HCl) solution for 20–40 seconds;

- The same side is cleaned with tap water then acetone, left face-up to dry for 1 hour;

- Once dry, the face is flooded with acetone and an acetate film is delicately rolled out on the surface, evacuating any air bubble;

- After 1 hour, the film can gently be peeled and is ready.

This second technique did not produce a satisfactory result for description. Peels are fragile and highly undulated. Contrasts between laminae remain poor and quality of the transferred surface is not good enough for microscopy, scanning or photography.

The last technique was to scan the samples (Figure 5.1.C). The polished face of the sample is moistened, placed on a transparent plastic sheet, on the glass of a scanner (e.g. Epson Perfection V500). The software Epson Scan allows choosing the area to scan as well as the resolution. Resulting pictures are good enough for image processing and detailed description.
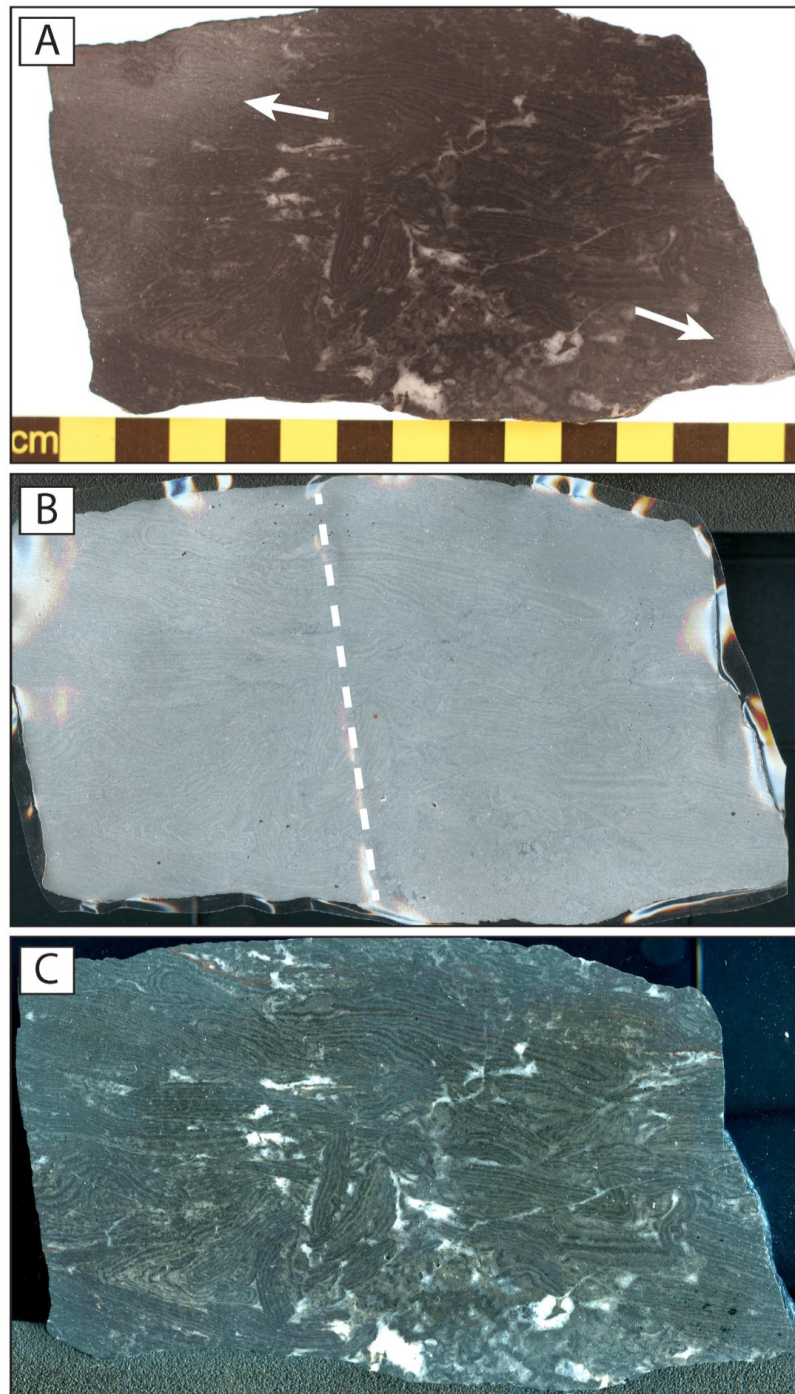
Figure 5.1: Preparation of polished samples. **A**. Photography. **B**. Acetate peel. **C**. Scan.

## 2.3    Total organic carbon

Samples from the cap dolostone and the microbial member were sent for total organic carbon (TOC) analysis to the School of Civil Engineering and Geosciences, University of Newcastle. The 24 samples all have ≤ 0.1% TOC. Owing to the low TOC

values, further analyses of the source rock potential of the Rasthof Formation were not undertaken.

# 3 Field Observations

## 3.1 Outcrop locations

Three areas were visited in the Kunene Region: Rasthof Farm, Omutirapo and Okaaru (Figure 5.2). They both show the same units but with some variations in thicknesses and facies. The first area visited is located 30–40 km NNW of the city of Kamanjab, where the Rasthof Formation forms an almost continuous ridge cutting through several farms. The ridges are surprisingly poorly described in the literature, although the type section for the Rasthof Formation is located in this area: at Rasthof Farm. The stratotype was first described by Hedberg (1979) as the Rasthof Member, the same outcrop was described again more recently by Le Ber et al. (2013) (Appendix A). In this chapter, other outcrops are presented around the Rasthof Farm area, at the Pioneer and Rustig farms. All the above outcrops are suggested to be located on the dipslope of the Northern Platform (Hoffman and Halverson, 2008).

The two other areas are located north of a veterinary cordon fence (the Red Line) separating the livestock of Namibia. This fence was built in the late nineteenth century and was later used to control and prevent wild animals from the north of the fence transmitting foot-and-mouth disease to the cattle from the south. North of the veterinary fence, there are no farms and the lands are more open. One of these is Omutirapo, 15 km northeast from Warmquelle. Several studies focus both on the cap dolostone and microbial member in the vicinity of this outcrop (Bosak et al., 2012, 2011; Dalton et al., 2013; Pruss et al., 2010; Tojo et al., 2007; Yoshioka et al., 2003). The last area is located close to the Okaaru village, 40 km north from Sesfontein on the road C43.
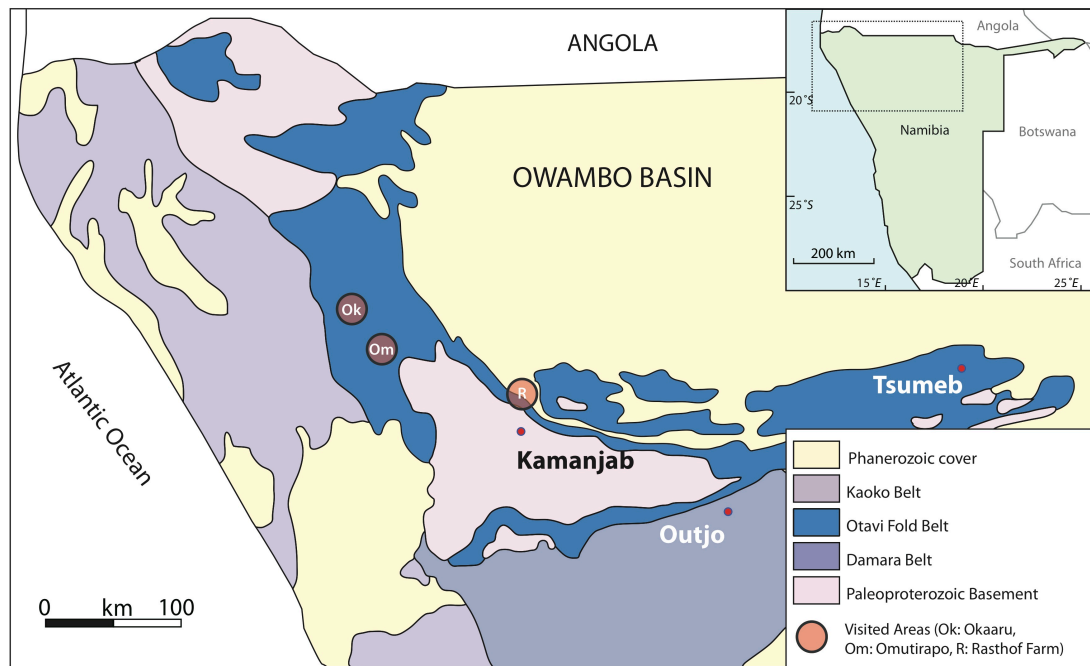
Figure 5.2: Location of visited sections. Simplified geological map of northern Namibia (modified from Hoffman and Prave, 1996).

## 3.2    General observations

### 3.2.1    Cap dolostone

The cap dolostone (CD) is present at the three locations, always lying on the Chuos Formation diamictite. Thicknesses range from 3 m (Okaaru) to 14 m (Omutirapo). The typical facies of the basal unit of the Rasthof Formation is delicately laminated. The sub-mm-thick laminae are generally perfectly horizontal, smooth and parallel. Deformation can occur, forming various < 50 cm-scale features including folds, kink-bands, and thrusts.

### 3.2.2    Microbial member

The colour, weathering and intense fracturing give to the microbial member a characteristic aspect. Hedberg (1979) used the excellent expression "elephant-hide weathering" to qualify this aspect of the Rasthof Formation. From afar, a recurrent observation is the apparent subdivision of the lower part of the microbial member (microbial member 1: MM1) into < 4 m-thick parallel beds (Figure 5.3 and also in Hoffman and Halverson, 2008, fig.13.58.a). No obvious sedimentological change is observed at the interface between beds. However the bedding is obvious, especially

118

at Rasthof Farm where most of the microbial member is exposed in one continuous section. Beds appear to become thinner upsection until they become indefinable owing to an intense fracture pattern (microbial member 2: MM2).
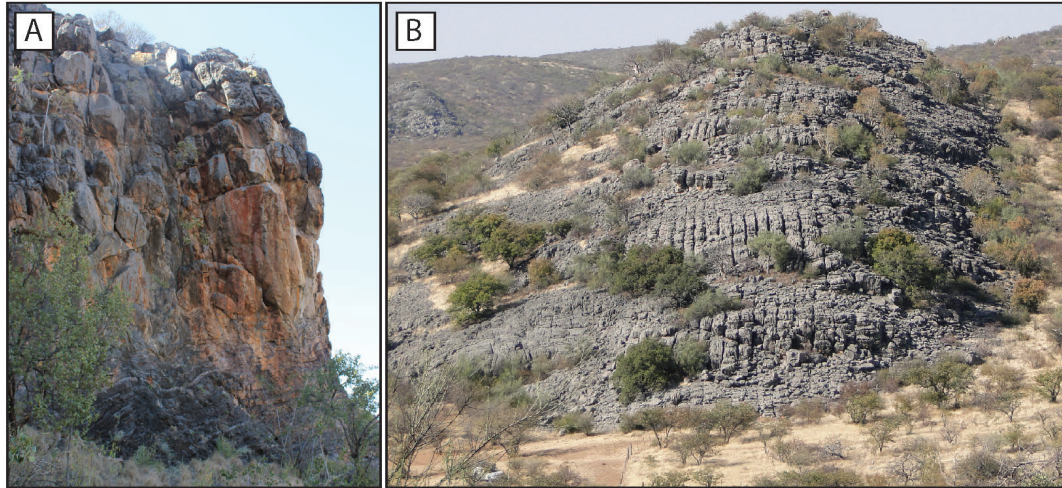


Figure 5.3: Illustration of the layer cake aspect of the Rasthof Formation. **A**. Omutirapo. **B**. Rasthof Farm. Note that the succession is vertical at Rasthof Farm.

The microbial member has been divided into two units, MM1 and MM2 (Le Ber et al., 2013), corresponding to the thickly and thinly laminated facies of Pruss et al. (2010). Laminae are laterally continuous and facies do not change significantly for hundreds of kms. MM1 consists of crinkly, horizontal undulated 1–5 mm-thick laminae. Contortions and folding of sets of laminae are typical from this facies and occur anywhere the formation is described. Description and quantification of the deformation is made difficult by the weathering that creates a surface pattern, partly hiding the laminated fabric. The transition to MM2 is gradual, no abrupt sedimentological change is observed except the thickness of the laminae as already noticed by Pruss et al. (2010). Also, in MM2, laminae are < 1 mm-thick and are not crinkly or massively contorted like in MM1. Local but typical < 10 cm large roll-up structures are intercalated between non-disturbed intervals.

## 3.3    Rasthof Farm area

North of the Kamanjab Inlier, a northwest–southeast range of small hills formed by the Rasthof Formation crosses several farms (Die Vlakte 634, Rustig 632, Rasthof 631, Elandslaagte 651, Pioneer 648 and Robyn 647). In addition to Hedberg's work at Rasthof Farm, the present work adds new sedimentological observations. The Rasthof Formation is exposed for more than 30 km along these hills, but a long and dense network of tracks often interrupted by fences and gates limits the visit of the outcrops. Three farms were visited: Rustig, Rasthof and Pioneer. The range of hills continues 20 km more towards the northwest, in the Etosha National Park. A campsite (Dolomite Camp) is even built on the outcrop but an extensive bush fire in the western part of the National Park (Kasaona, 2012) made fieldwork impossible at the time of the visit.

In the following, observations come from the following sites (Figure 5.4):

① Rustig Farm outcrop (MM1): 19°23.430' S – 14°50.950' E.

② Rasthof Farm outcrops (CD, MM1 and MM2): 19°20.000' S – 14°44.248' E to 19°21.000' S – 14°45.405' E.

③ Pioneer Farm outcrop (CD and MM1): 19°16.730' S – 14°40.110' E and 19°17.667' S – 14°42.000' E.

Most of the observations come from the Rasthof Farm where the formation is exposed vertically diving abruptly under the Owambo Basin (Figure 5.5). Exposure is better and more stratigraphic record is exposed than at the other farms. At Rustig Farm, the Rasthof Formation is overturned and only MM1 was observed. At Pioneer Farm, sediments are dipping at 30° towards the northeast, only the cap dolostone and MM1 are exposed.
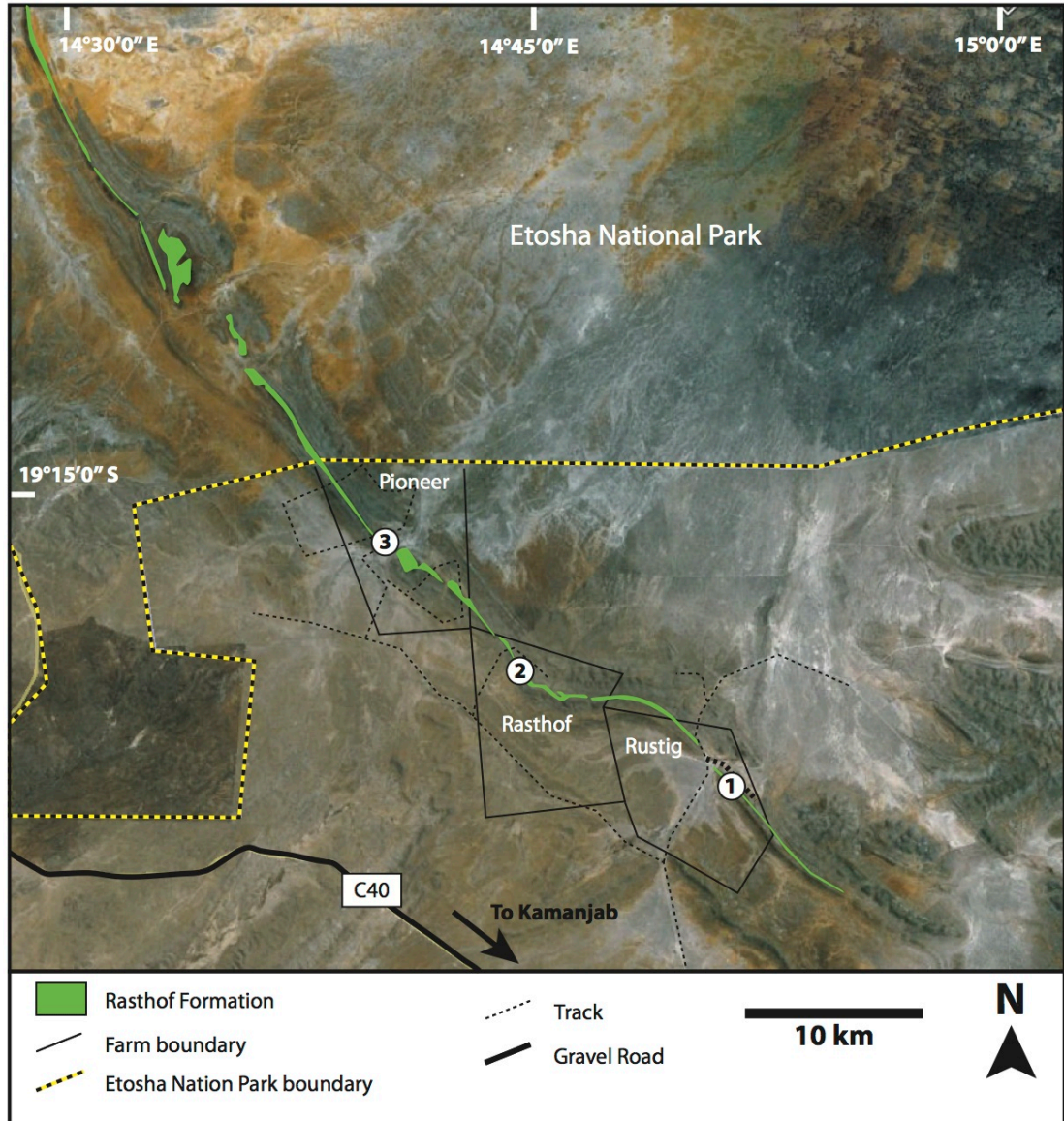
Figure 5.4: Satellite view of the Rasthof Farm area. The Rasthof Formation cuts through several farms before arriving in the Etosha National Park. Only the boundaries of the visited farm are traced. (Modified from satellite image (Google Earth): © 2013 DigitalGlobe; © 2013 Google; © 2013 Cnes/Spot Image).
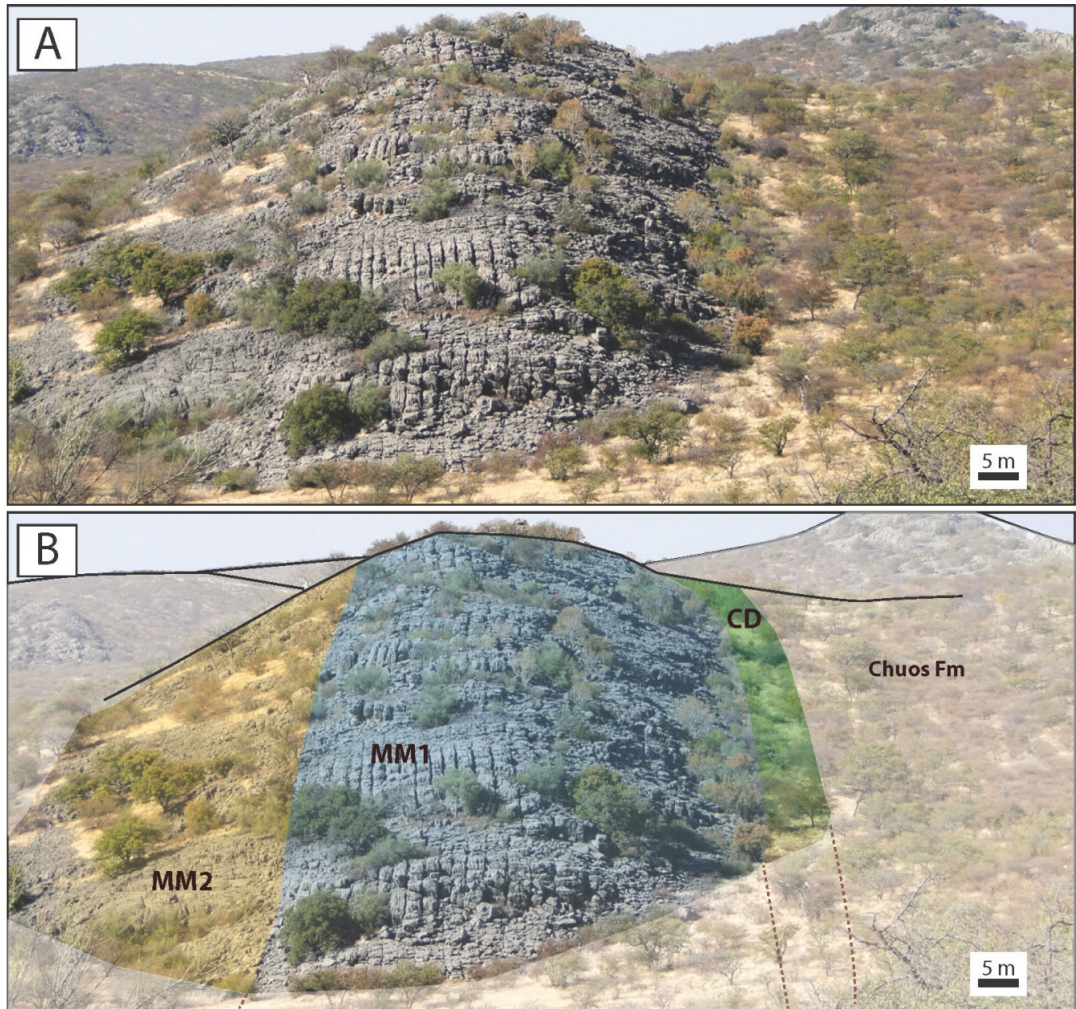
Figure 5.5: Type section of the Rasthof Formation. **A**. Outcrop, looking southeast. Note that the formation is vertical, base is at the right, top is at the left. **B**. Subdivision of the Rasthof Formation (cap dolostone, microbial member 1, microbial member 2).

### 3.3.1 Cap dolostone

The cap dolostone is exposed at Rasthof and Pioneer farms. Its exact thickness is difficult to evaluate because of the recent cover; the measured sections are generally between 9.50 and 10 m-thick. Recent cover and vegetation usually conceal the contact with the underlying Chuos Formation. The very base of the cap dolostone is locally pink coloured but changes to grey upsection.

Facies of the cap dolostone consist of mm-thick, perfectly parallel and flat laminae (Figure 5.6.A, B). Rare < 10 cm-thick, light intervals with less obvious to non-laminated fabric occur (Figure 5.6.C, D). These beds pinch out laterally. For example at Rasthof Farm, a 10 cm-thick of these bed is observed at one outcrop but is

122

missing 500 m along strike on the next hill. Overlying laminae can rest with a low angle (i.e. downlap) on these intervals (Figure 5.6.C).

In the upper 2 m of the cap dolostone, the outcrop can exhibit intrabed deformation structures (Figure 5.6.E). These do not exceed 50 cm-scale and occur between non-deformed sets of laminae. Disturbed intervals include 1) dm-scale overturned folds, with wavelengths of < 10 cm and short limbs dipping at 45–90° and 2) dm-scale fault-bend folds, with a low angle thrust ramp.

Local cross-stratified intervals are locally observed in the upper 2 m of the cap dolostone (Figure 5.7). Some of them can be subtle but others form obvious concave and convex bounding surfaces. Laminae in these bedforms are approximately parallel to the bounding surfaces, with subtle lateral variation in dip angles and laminae thicknesses. Dip directions are scattered. A short distance above these intervals, the microbial member occurs. Whilst the contact with the microbial member does not appear to be abrupt, and a transitional relationship is inferred, weathering has obscured the nature of the contact. Compaction and dissolution of the sediments as well as recent weathering has created several dm-thick breccias and the microbial member often appears with vertical laminae, discordant on the underlying horizontal laminae of the cap dolostone.
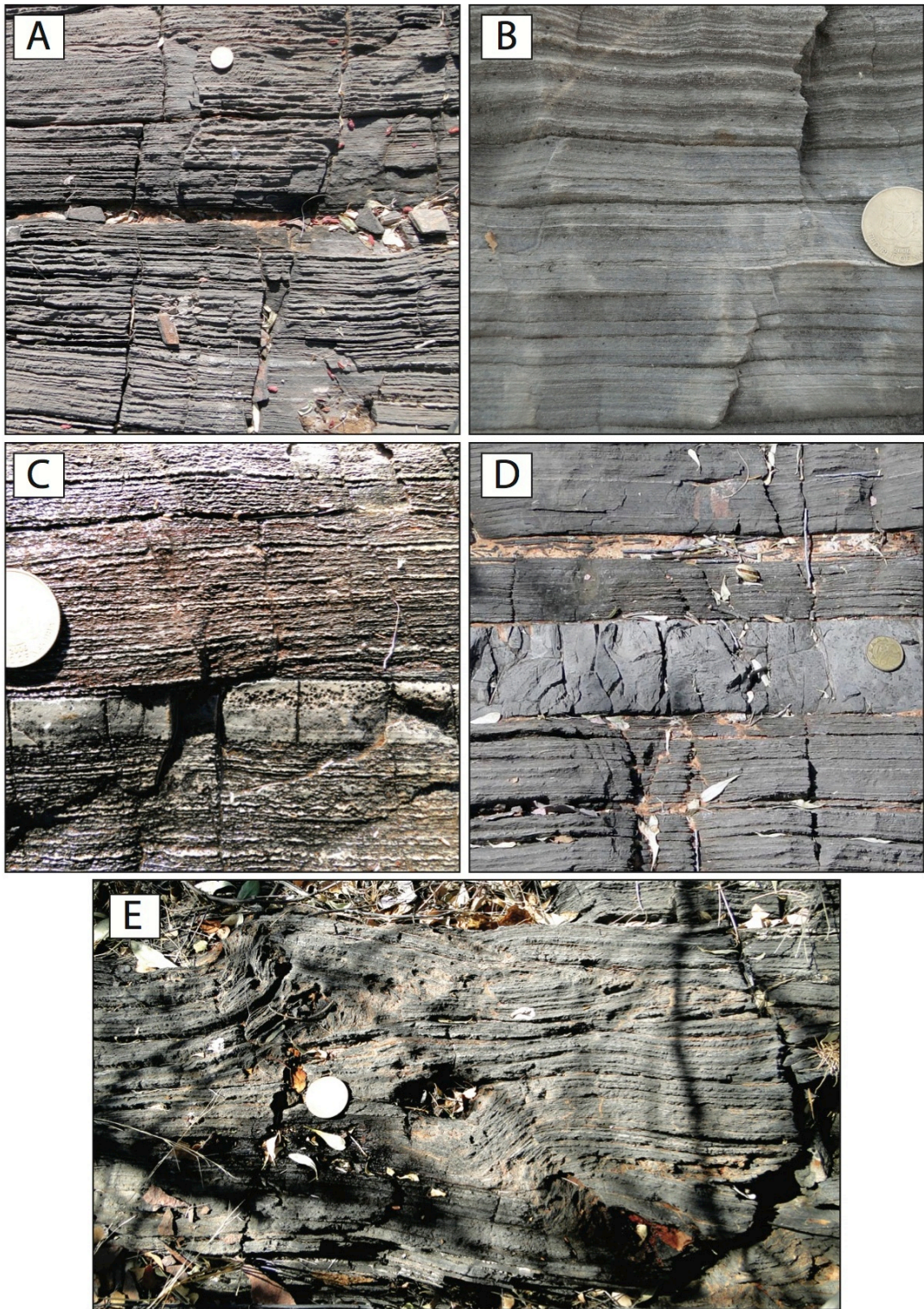
Figure 5.6: Cap dolostone, Rasthof Farm area (1/2). **A**. Thinly laminated facies. **B**. Idem at Pioneer Farm. **C**. Downlap of the laminae on a "non-laminated" interval, Rasthof Farm, note that a laminated fabric is still discernible. **D**. Similar type of interval but no laminated fabric is visible. **E**. Folds in the upper half of the cap dolostone. Coin is 23 mm Ø
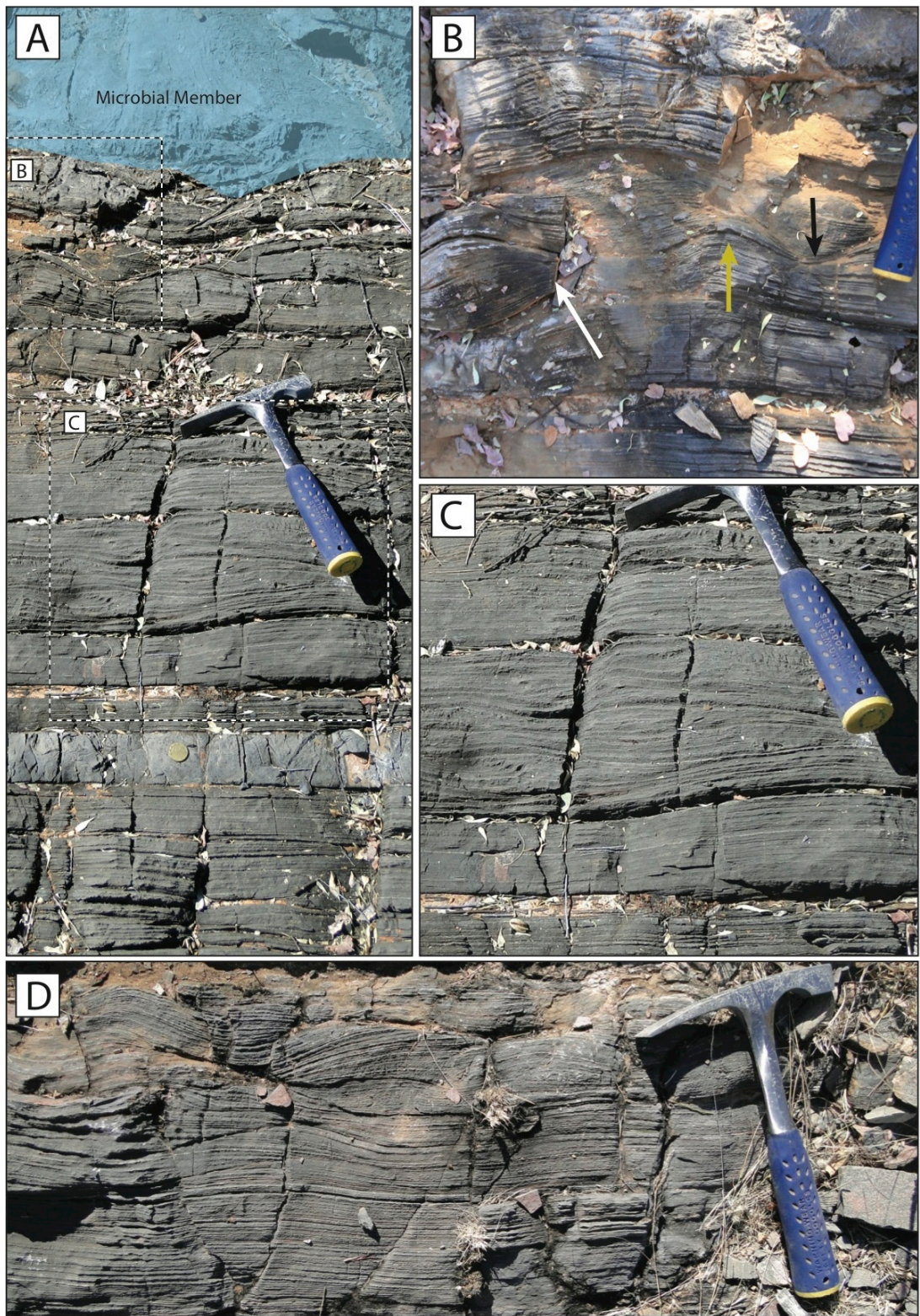
Figure 5.7: Cap dolostone, Rasthof Farm area (2/2). **A**. Last metre of the cap dolostone at Rasthof Farm, with cross-stratified intervals (B and C). **B**. Detail of concave up (black arrow), concave down (yellow arrow) bounding surfaces, and scattered dip directions (left of white arrow). **C**. Uncertain, low angle cross-stratification. **D**. Detail of hummocky cross stratifications.

### 3.3.2 Microbial member 1

MM1 is 60 m-thick and consists of relatively thickly laminated, crinkly, chaotic mats. Laminated fabric results from of an alternation of 1) sub-mm-thick dark, dolomicrite laminae with 2) light to mid grey, 1–5 mm-thick dolosparite laminae. Individual dark laminae are not perfectly laterally continuous: they can exhibit thickenings or a micro-clotted aspect at a sub-mm-scale (Figure 5.8).
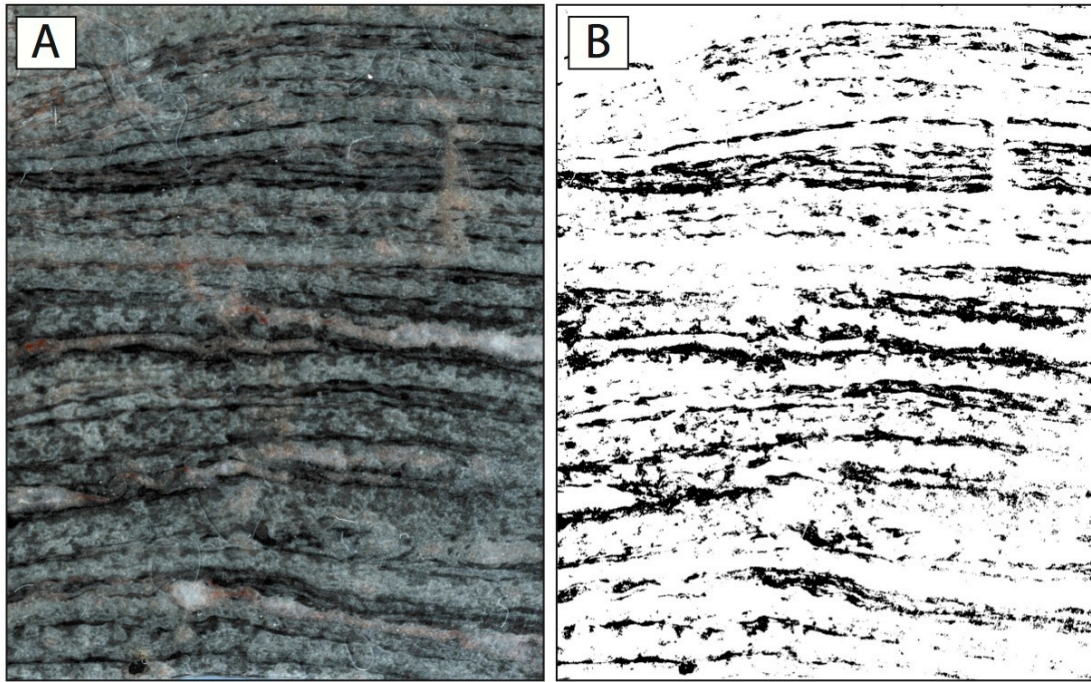


Figure 5.8: Laminated fabric of MM1, Rasthof Farm. **A**. Polished sample from MM1, Rasthof Farm. **B**. Threshold on the dark laminae, showing their local thickening. Image is 4 cm high.

When following a horizontal trend, laminae are undulose with a dm wavelength and a < 5 cm amplitude. What makes the Rasthof Formation characteristic is that MM1 is deformed through most of the section (Figure 5.9.A, B). Rare break-ups are observed (Figure 5.9.C); even rarer is the occurrence of possible dm large intraclasts (Figure 5.9.D). The deformation structures include dm–m-scale antiform, asymmetrical to recumbent folds and more complex contorted intervals (Figure 5.10). There is no consistent orientation to these structures. Above each folded interval, the strata assume a horizontal and undulating trend.

The chaotic aspect of MM1 decreases upsection. Towards the top of MM1, non-chaotic, clear undulations are observed, with large amplitudes (> 30 cm) and

wavelengths (> 30 cm) (Figure 5.11.A, B). In the last metres of MM1, the development of individual vertical cones can locally be observed. They are differentiated from the chaotic deformations observed below by their constant orientation, pointing upward. The 20 cm large cones are still surrounded by thick and slightly chaotic laminae (Figure 5.11.C, D).

The transition to MM2 is progressive and it is actually difficult to point at a precise boundary between the two units. In addition to the lack of obvious layer cake aspect, the change in laminae thicknesses is a key observation to differentiate MM1 from MM2. In MM1, laminae are 1–5 mm-thick while in MM2 they are < 1 mm. Also in MM2, there is no intense folding and laminae tend to be flat.
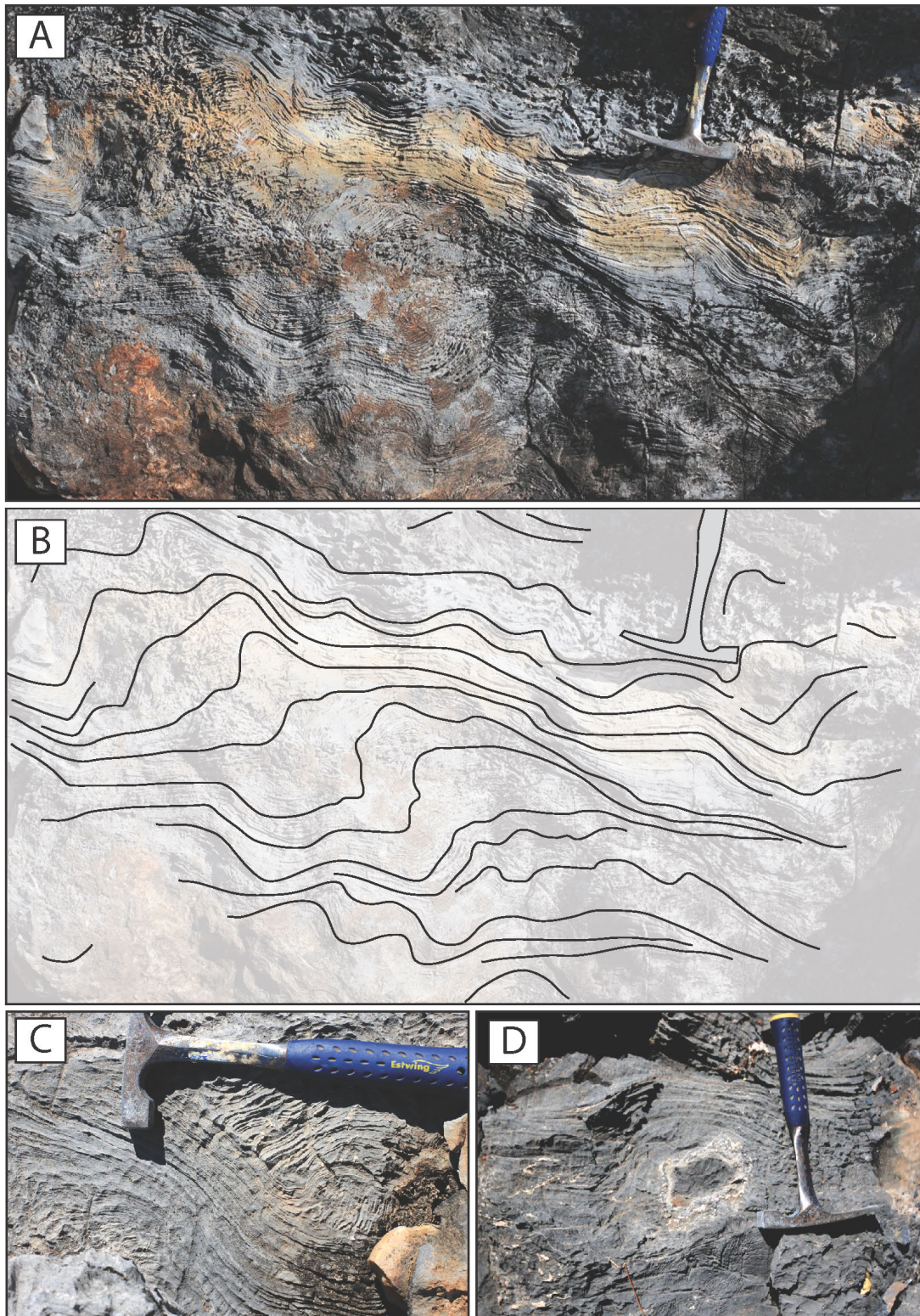
Figure 5.9: Facies of MM1, Rasthof Farm area (1/3). **A**. Typical facies observed at Rasthof Farm, with a recumbent fold associated to undulation of the laminae (Rasthof Farm). **B**. Sketch of A. **C**. Angular unconforimity between two sets of laminae (Rasthof Farm). **D**. Intraclast with laminae deposited above forming a small dome (Pioneer Farm).
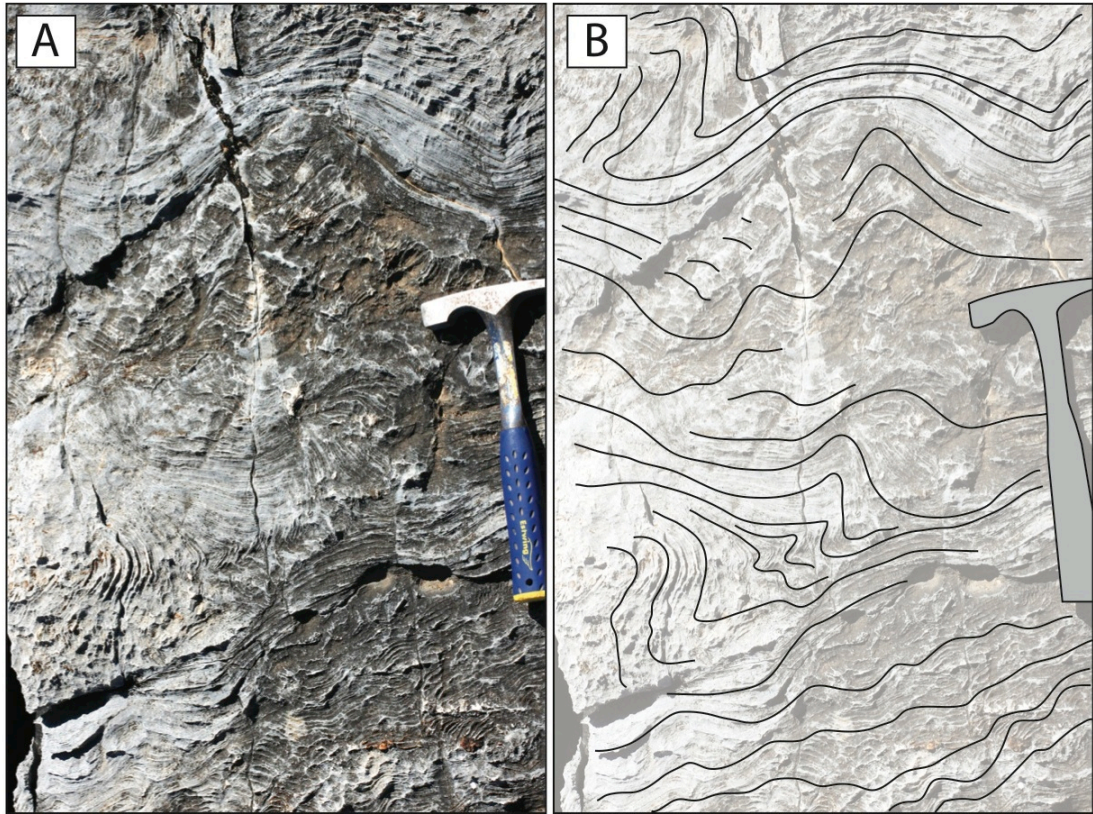
Figure 5.10: Facies of MM1, Rasthof Farm area (2/3). Example of typical deformation structures. **A**. Photograph. **B**. Sketch.
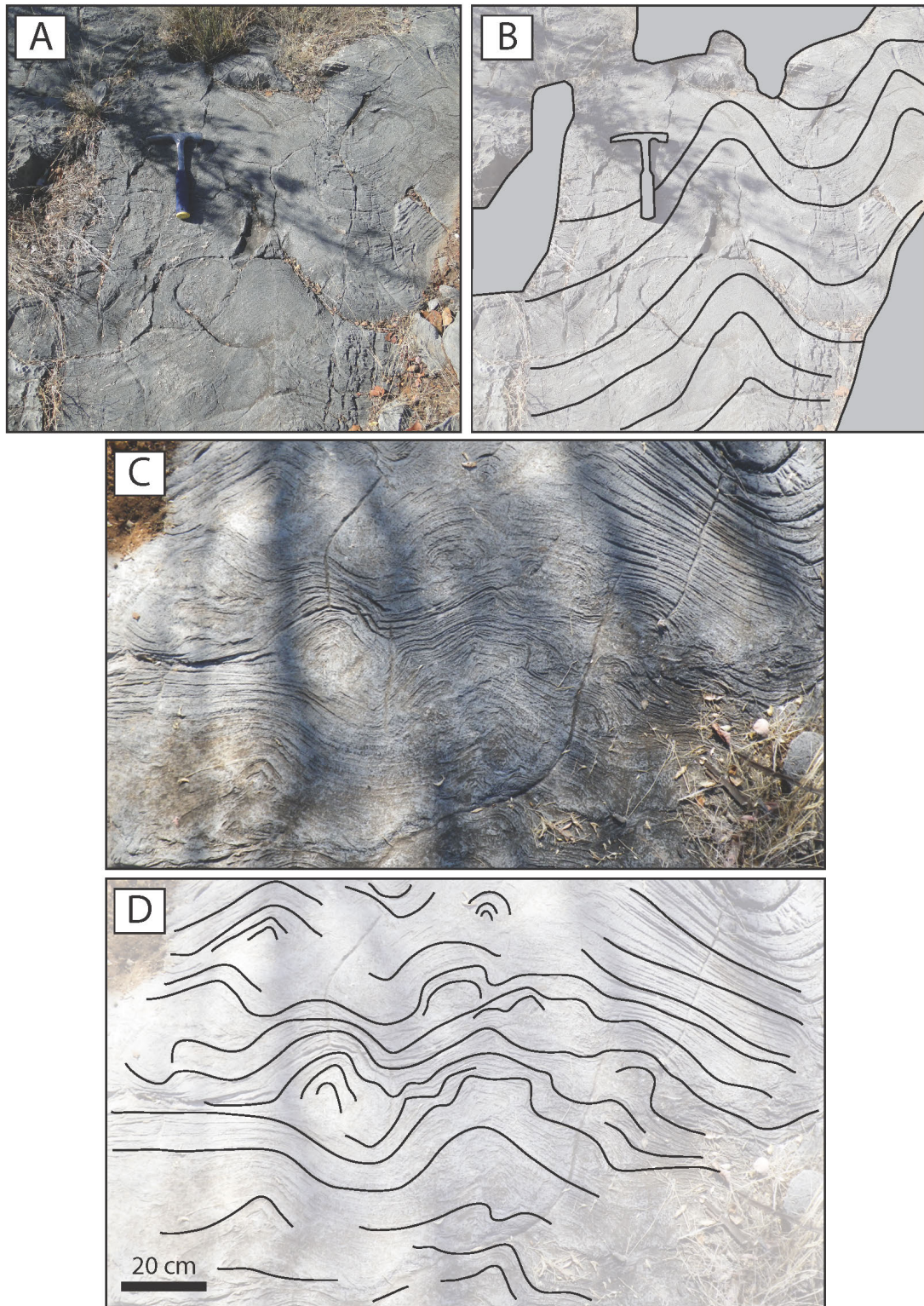
Figure 5.11: Facies of MM1, Rasthof Farm area (3/3). Transition before MM2. **A**. Intensity of the deformation decreases and large amplitude and wavelength undulations develop. **B**. Sketch. **C**. Local cones, constantly pointing upward. **D**. Sketch.

### 3.3.3   Microbial member 2

Laminae of MM2 are sub-mm-thick. They tend to be horizontal and undeformed but occasional rolled-up intervals characterise this facies (Hoffman and Halverson, 2008; Pruss et al., 2010). At Rasthof Farm, to an extreme degree, sets of laminae can be broken and form *in situ* cm large intraclasts. This degree of disturbance is observed only nearby the vertical growths presented later and in Le Ber et al. (2013) (Figure 5.12).
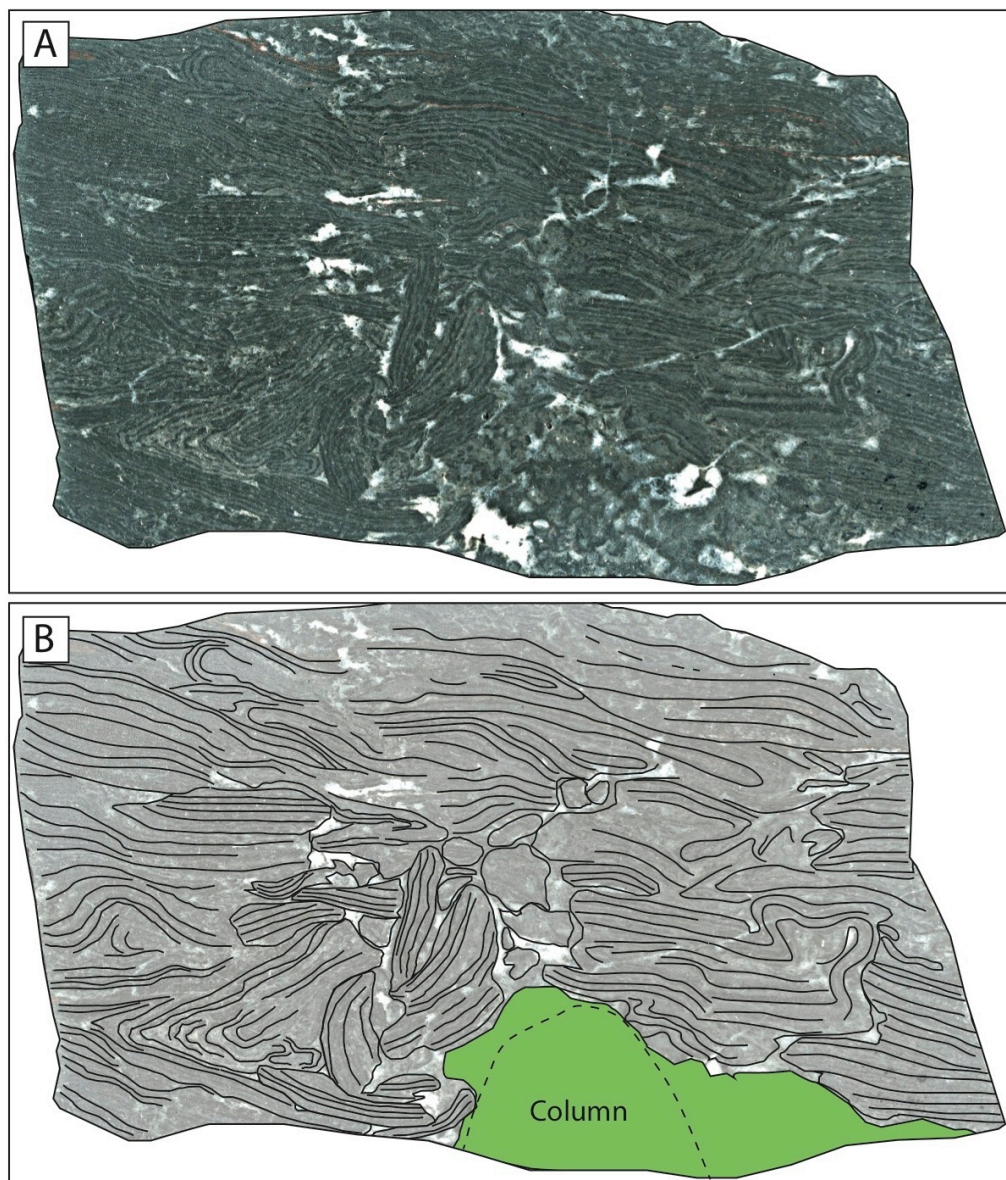


Figure 5.12: Rolled-up facies, Rasthof Farm. **A**. Polished slab. **B**. Details of the rolled-up intervals and cm-sized intraclasts formed around a columnar stromatolite. Intraclasts are much smaller very close to the top of a column (green area). This slab comes from the top of the specimen shown in Figure 5.14. The slab is 13 cm wide.

At Rasthof Farm, thinly laminated facies of MM2 shows variations from what is described elsewhere on the platform. Several individual growths are described (Le Ber et al., 2013), developing vertically and surrounded by thin laminae and/or intraclasts. Geometries start with dome structures, developing a few metres above the cones observed in MM1. Upsection, columns and different degree of branching columns follow.

Observations are scarce and establishing a clear relationship or facies variations between the different growths was not possible during the fieldwork. From the base to the top, geometries are observed as follow: 20 cm high cones (top MM1); 20–30 cm wide domes; wide columns (30–40 cm wide), columns with some branching (10 cm wide) and finally, branching columns (10 cm wide). Individual growths are generally thinly laminated (sub-mm), with darker and partly clotted dolomicrite laminae alternating with lighter dolosparite laminae. Details for each geometry are presented in the following paragraphs.

### 3.3.3.1   Transition growth-intergrowth

The individual growths are not always well differentiated from the surrounding sediments, partly explaining why Hedberg (1979) apparently missed them when describing the same section. In the domes and the larger columns intervals, laminae continue outside of the geometries (Figure 5.13.A). This gives a general laterally linked (Logan et al., 1964) aspect. Where the columns start to become narrower (e.g. < 10 cm), or to branch, there is often a clear differentiation between the growths and the surrounding sediments (Figure 5.13.B, C).

Recrystallisation and weathering of the outcrop can limit detailed observation of the sediments deposited between the growths. Where observed, intergrowth laminae are characteristic of thinly laminated facies described elsewhere on the platform. Some rolled-up to broken sets of laminae can occur at a cm-scale (Figure 5.12; Figure 5.14). Sediments deposited between the growths are not always laminated; they can consist of different degrees of broken mm–cm large intraclasts of lamina (Figure 5.20).
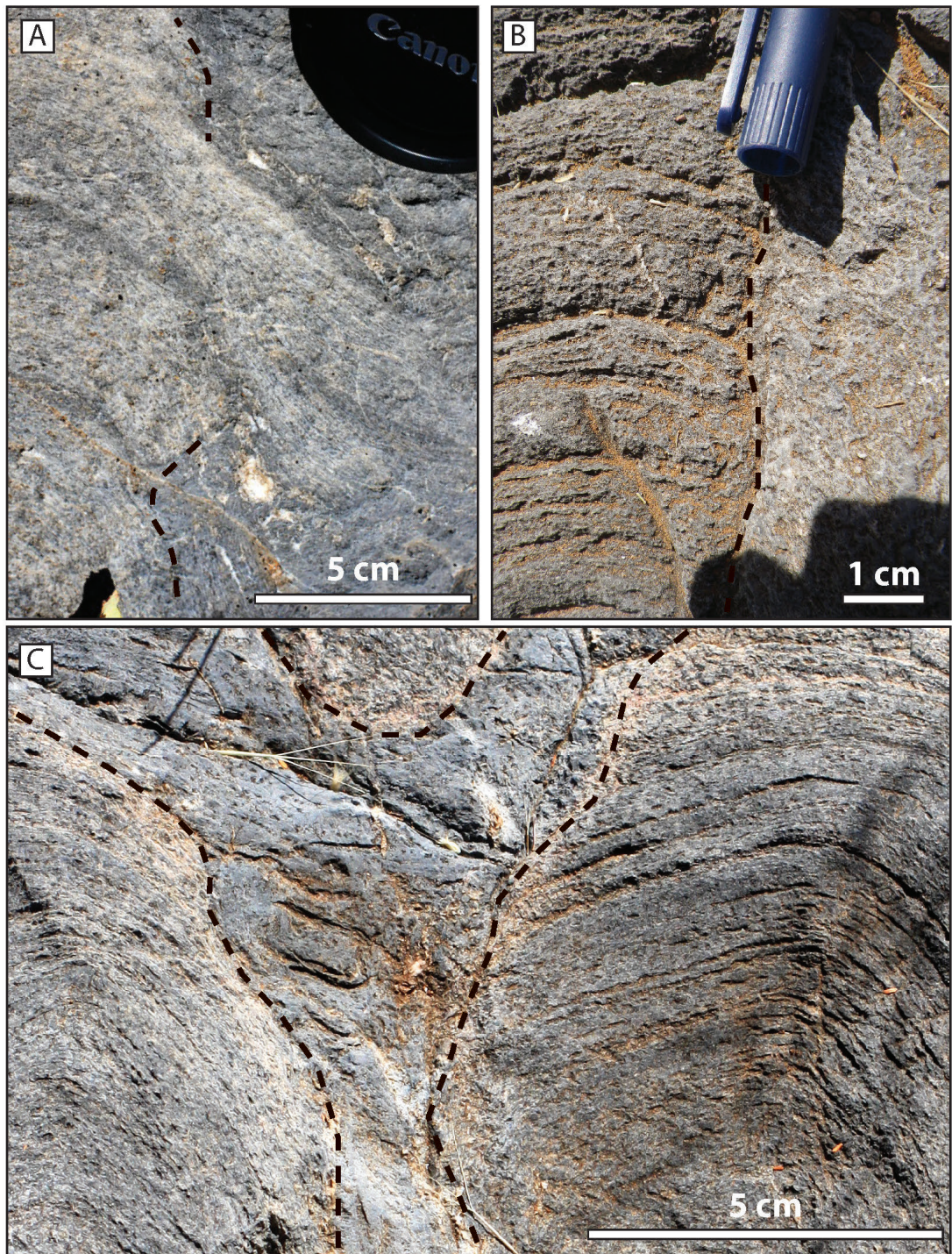
Figure 5.13: MM2, transition between growths and surrounding sediments, Rasthof Farm. **A**. A bridge between a large column (left) and the surrounding sediments. **B** and **C**. Well expressed boundary between columns and surounding sediments.
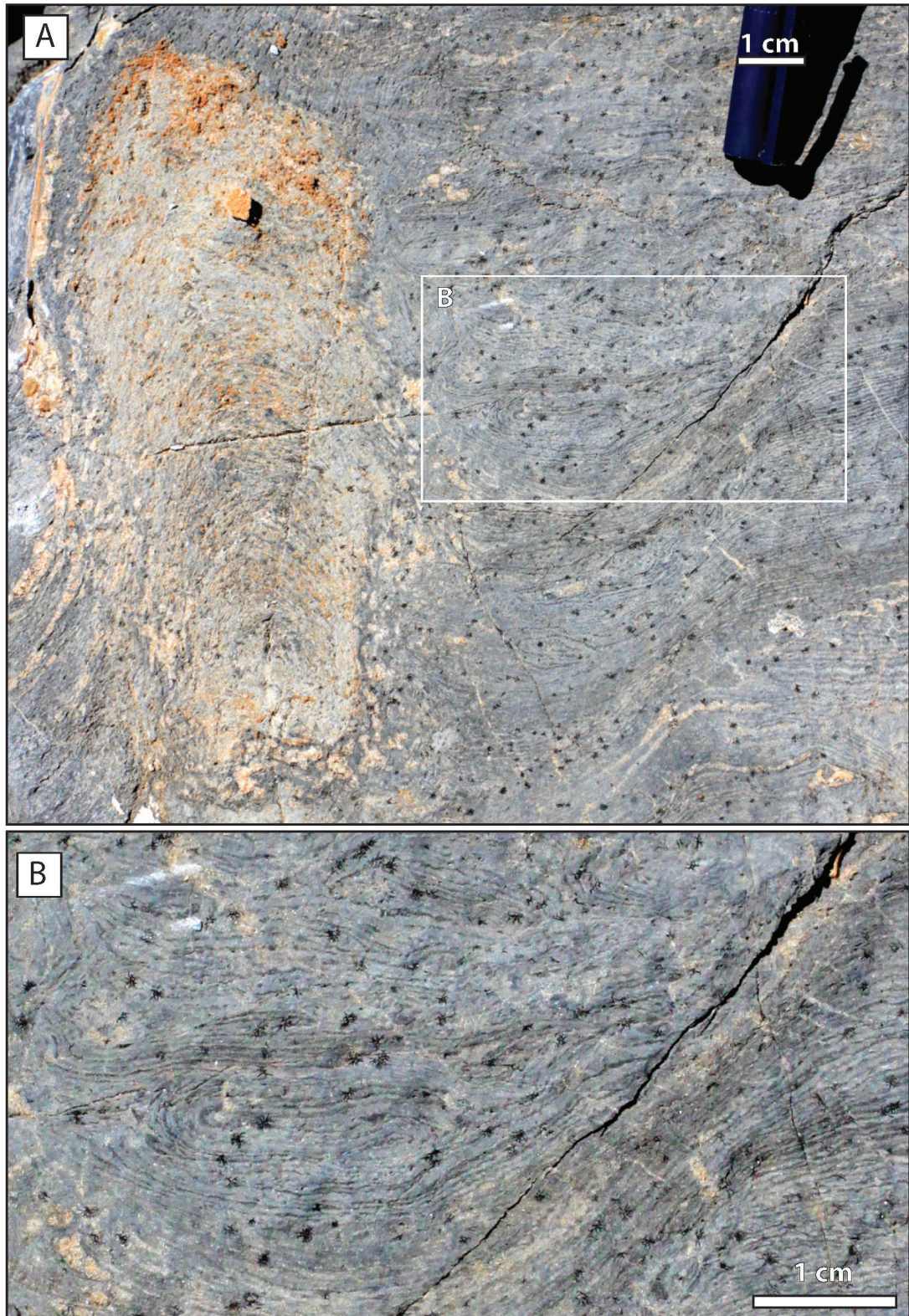
Figure 5.14: MM2, roll-up structure nearby a column, Rasthof Farm. **A**. Large view showing a clear column to the left, with convex upwad laminae and thinly laminated sediments next to the column. **B**. Detail of the contorted thinly laminated sediments, forming a roll-up structure.

### 3.3.3.2    *Domes*

Domes consist of laminae developing into large, half-circular convex upward structures (Figure 5.15). The diameter of the resulting geometries does not exceed 30 cm. They are laterally linked by clear and unbroken laminated facies. On the observed outcrops, the distance between domes can be 10 cm to more than 1 m.

In the domes, laminated fabric is generally easily observable but thickness of one lamina is not laterally constant. At a cm-scale (Figure 5.16), dark laminae reveal a clotted fabric (Figure 5.16.C). Clots are mostly elongated and follow the orientation of the laminated facies, alternating with sub-mm-thick light laminae.

Between the domes, thinly laminated facies is more constant and easier to follow than in the domes. However, dark laminae still exhibit a micro-clotted aspect, producing thickness variation of one single lamina (Figure 5.16.D). Sometimes, mm–cm wide rolled-up facies or intraclasts of thin laminae occur close to the interface with the dome (Figure 5.16.E).
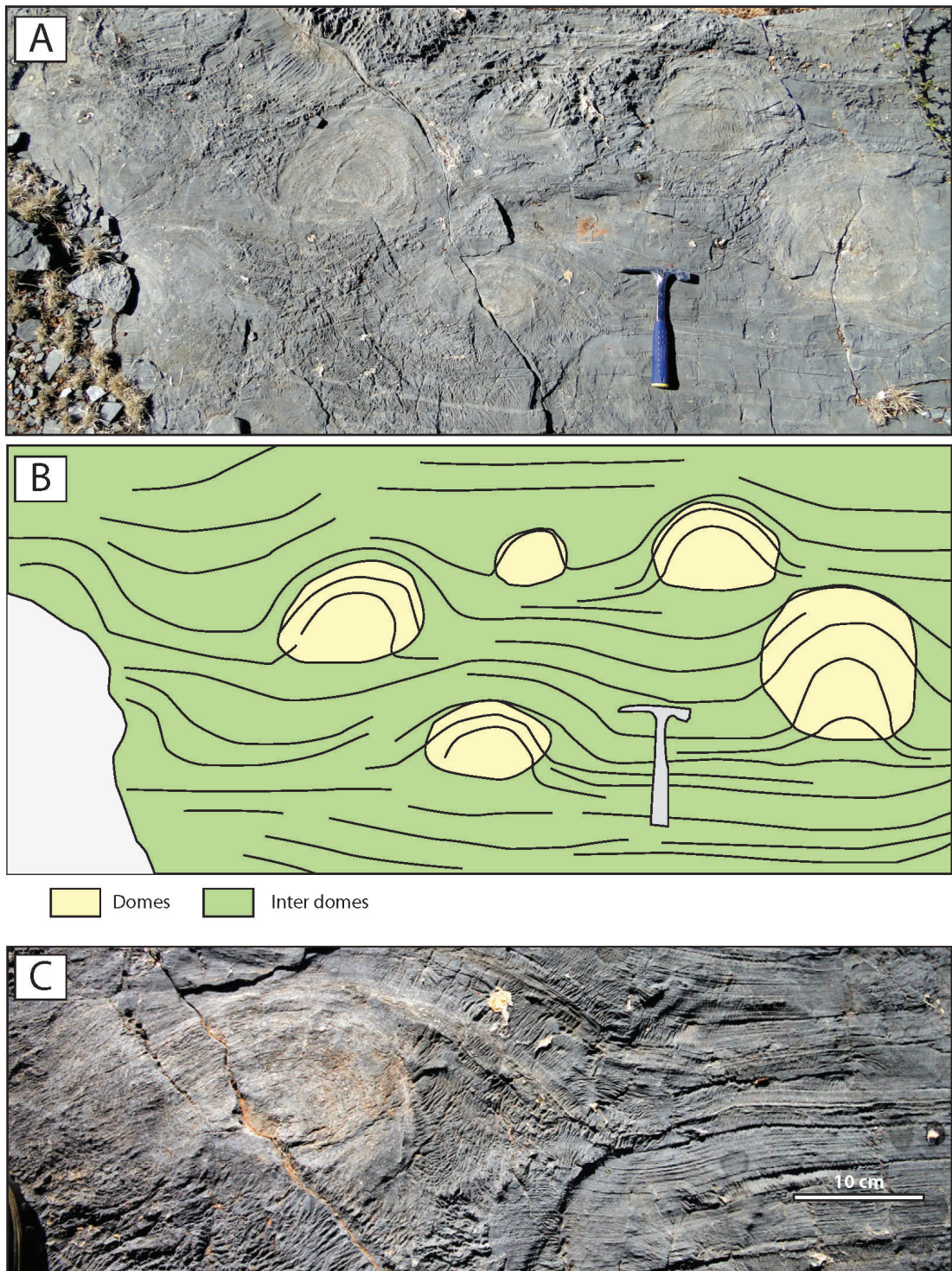
Figure 5.15: MM2, domes (macroscopic scale), Rasthof Farm. **A**. Photography. **B**. Sketch. **C**. Detail of the transition dome-interdome, with countinuous laminae.
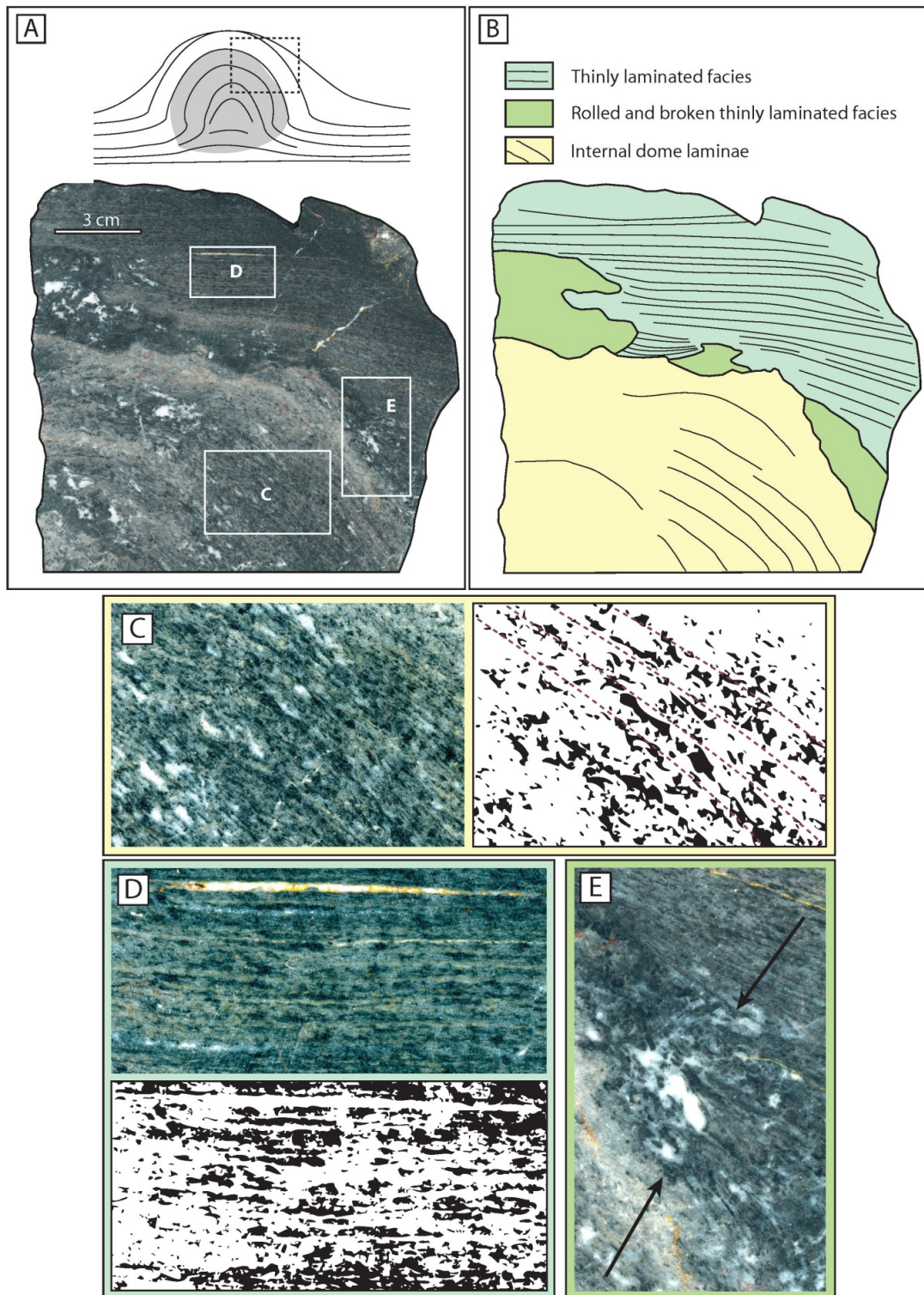
Figure 5.16: MM2, domes (mesoscopic scale), Rasthof Farm. **A**. Polished slab of a dome and overlying laminae. **B**. Sketch. **C**. Detail of the laminae within the dome (left) and highlight of the dark micritic sediments in black (right). **D**. Detail of the laminae above the dome (top) and highligh of the dark micritic sediments in black (bottom). **E**. Rolled-up and broken laminae at the interface with the dome.

### 3.3.3.3   Columns

Columns (Figure 5.17; Figure 5.18) can have a 5–40 cm diameter. The wider columns (> 20 cm diameter) can be vertically continuous for up to half a metre, forming single massive trunks. The narrower columns (< 20 cm diameter) are also vertically continuous for up to 1 m, they also can branch. Laminae in the columns are convex upward but, like in the domes, they are not perfectly continuous (Figure 5.18.D). Dark laminae have a partially clotted microstructure creating thickness variation in one single lamina.

Towards the sides of a column, the lamination becomes indistinct (Figure 5.18.D) and a 1–2 cm large, poorly laminated interval preceeds the edges of the column. Between the columns, laminae are convex downward and often broken (Figure 5.18.C). Rare preserved laminated bridges occur between two columns. Intraclasts are up to 5 mm large and they coexist with sub-cm large voids filled by dolosparite.
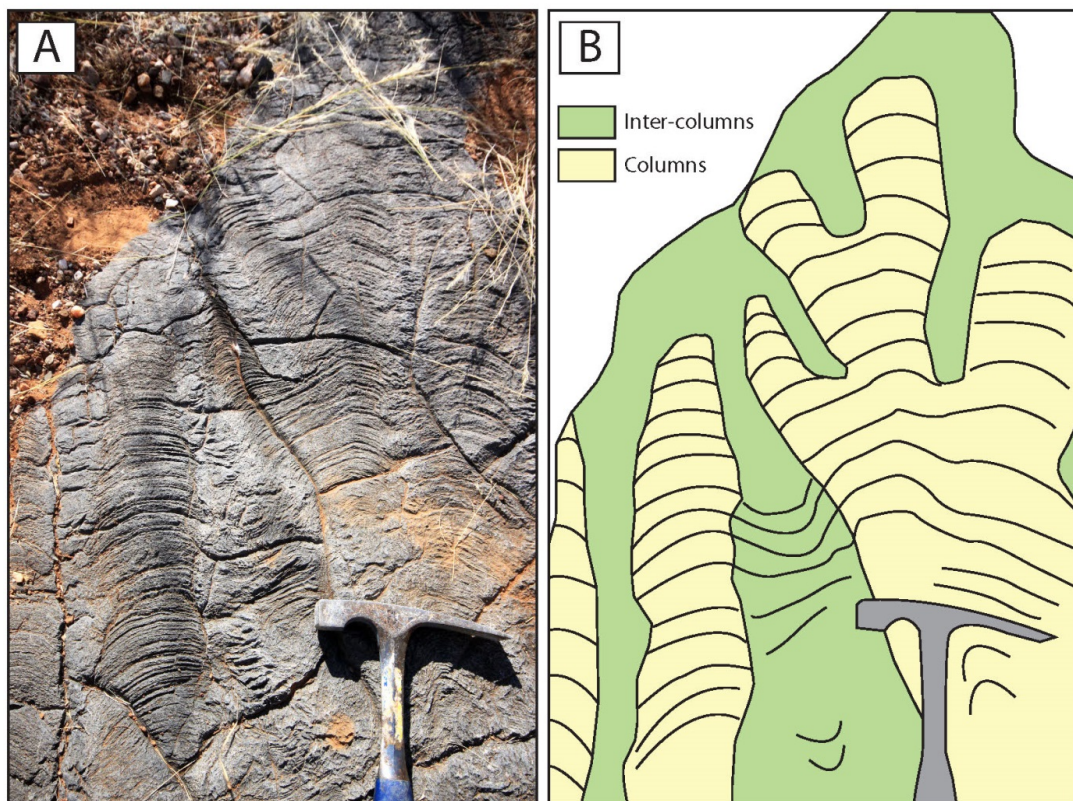


Figure 5.17: MM2, columns (macroscopic scale), Rasthof Farm. **A**. Photography. **B**. Sketch.
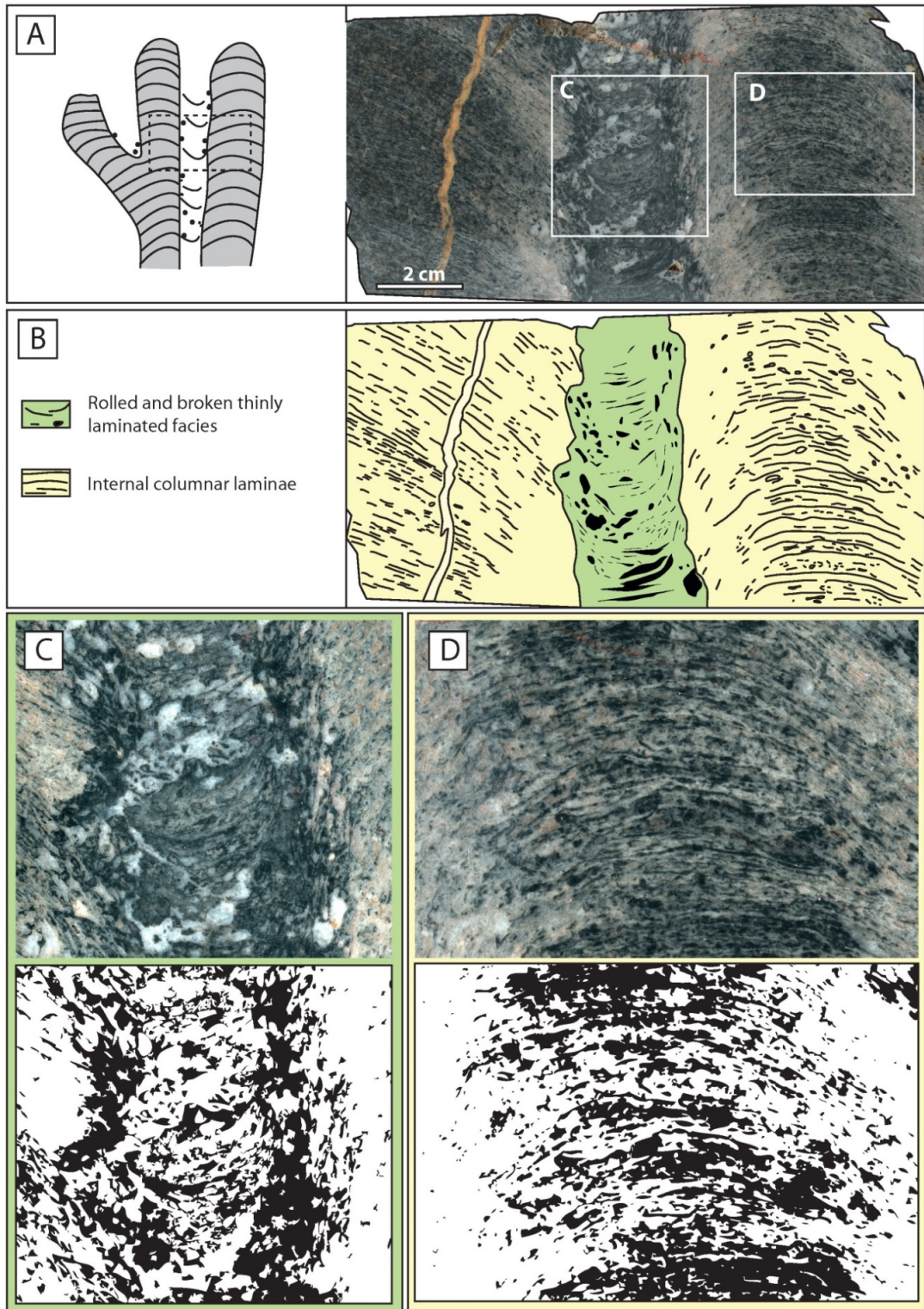
Figure 5.18: MM2, columns (mesoscopic scale), Rasthof Farm. **A**. Polished slab of two, closely spaces columns and intercolumnar sediments. **B**. Sketch. **C**. Detail of the sediments between the columns (top) and highlight of the darker sediments in black (bottom). Note the preserved convex downward trend. **D**. Detail of the laminae in one column (top) and highligh of the darker sediments in black (bottom). Note the micrite fades towards the edges of the column.

### 3.3.3.4    Branching columns

Branching columns form a relatively dense network of 5–20 cm wide and up to 30 cm high geometries (Figure 5.19) and are likely to be conntected in 3D. They are separated from each other by 5–30 cm intervals. On the outcrop, sediments deposited between the growths are often difficult to distinguish due to recent weathering and dissolution. Polished samples allow the observations of these sediments (Figure 5.20). Similarly to intercolumnar facies, they can consist of thinly laminated facies (Figure 5.20.C) but mostly of intraclasts (Figure 5.20.D).

### 3.3.3.5    End of the outcrop

Recent cover hides the top of the Rasthof Formation and it is not clear how the facies evolve upsection. Latest facies were non-laminated, massive but scarce and impossible to sample with a hammer where observed. Hoffman and Halverson (2008) note that, on the Northern Platform, the microbial member is followed by a fine- to coarse-grained epiclastic member. Facies include grainstones, teepee structures, cross-bedding and channels.
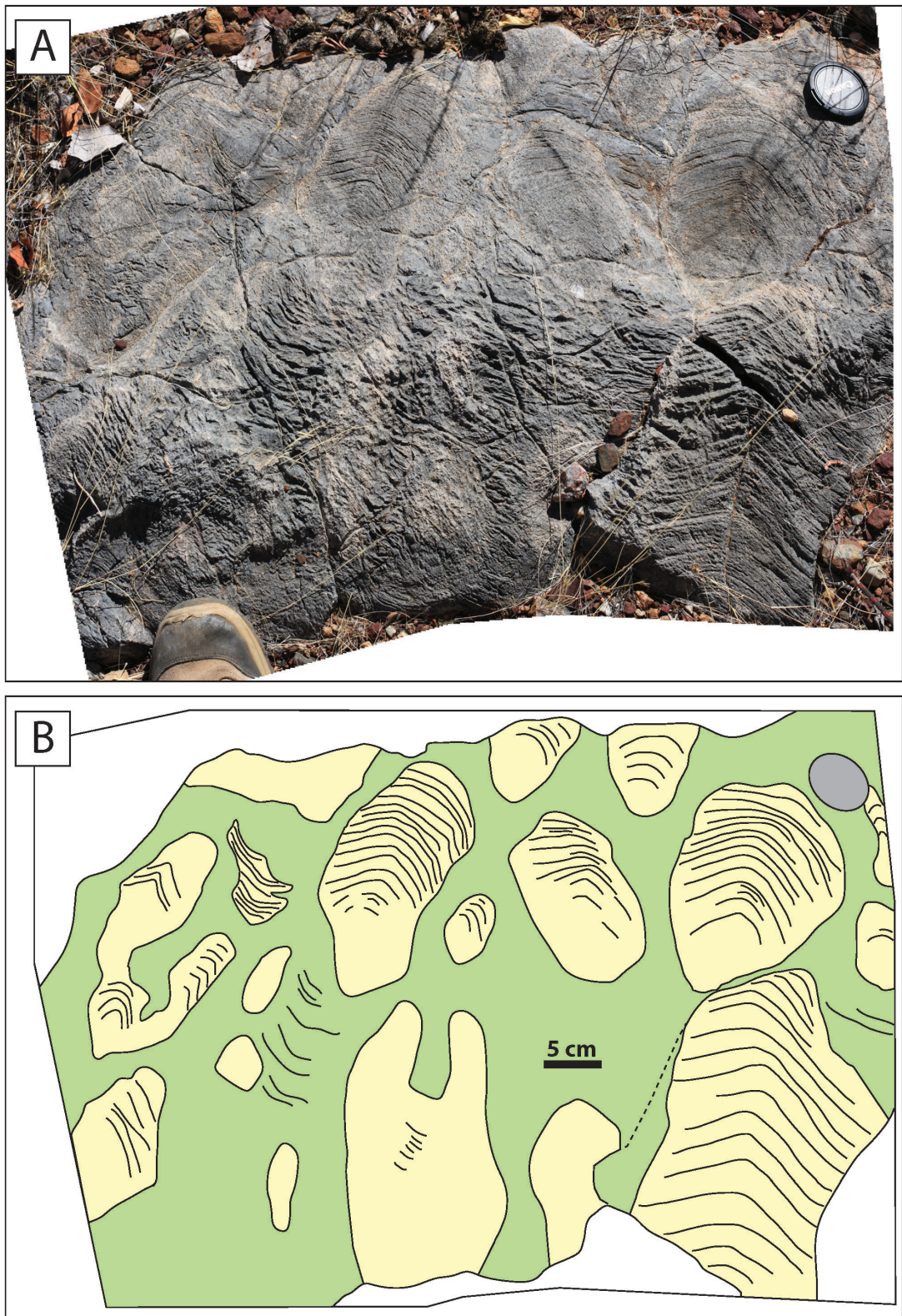
Figure 5.19: MM2, branching columns (macroscopic scale), Rasthof Farm. **A**. Outcrop. **B**. Sketch, the columns and branching columns are coloured in yellow. Sediments deposited between are coloured in green. They can consist of micrograinstones–packstones along the columns or of preserved laminae.
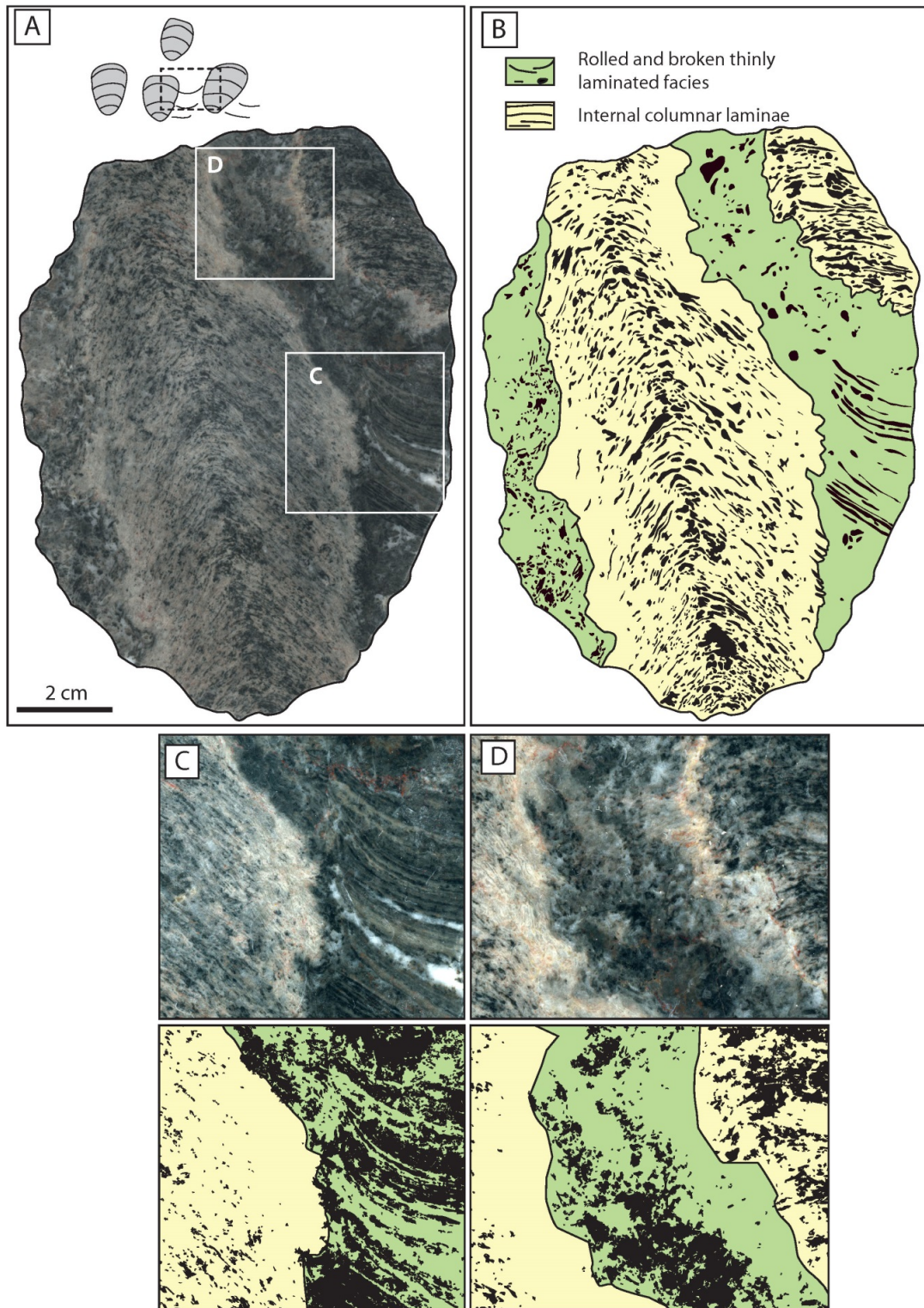
Figure 5.20: MM2, branching columns (mesoscopic scale), Rasthof Farm. **A**. Polished slab of a column and surrounding sediments. **B**. Sketch. **C**. Detail of preserved, convex downward laminae between columns (top) and highlight of the darker sediments in black (bottom). **D**. Detail of intraclasts between the columns (top) and highlight of the darker sediments in black (bottom).

142

## 3.4    Omutirapo area

The field observations were made on a hill (Figure 5.21) located directly to the north of Omutirapo waterhole. The Red Cross installed this well along the road D3710. Here, the Rasthof Formation is regionally dipping 15–20° WNW and forms a 3.5 km long plateau oriented southwest–northeast. Recent cover and vegetation mask sediments on the top of the plateau, but the cap carbonate is exposed along a ridge, on the top of the eastern side of the hill.

Previous works in the same area (Ongongo/Warmquelle (8 km to the W) and Khowarib (17 km to the SSW), Pruss et al., 2010; Tojo et al., 2007) allow comparisons with the sediments observed at Omutirapo. For this study, the plateau was visited along a 2 km transect, with descriptions made on the cap dolostone or the microbial member depending on the accessibility of the outcrop. Overall, facies are unchanging all along the ridge.
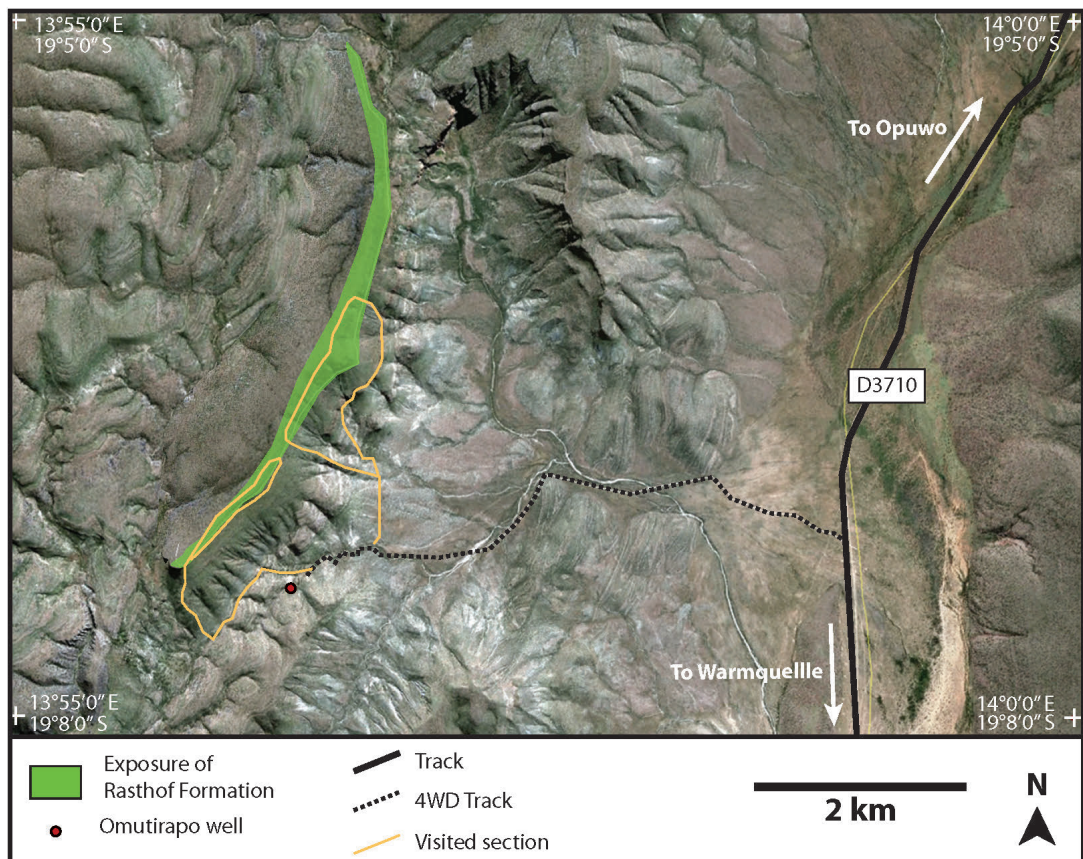


Figure 5.21: Satellite view of the Omutirapo area (Modified from satellite image (Google Earth): © 2013 DigitalGlobe; © 2013 Google).

### 3.4.1 Cap dolostone

At Omutirapo, the cap dolostone is 14 m-thick. It rests in sharp contact on the Chuos Formation. The latter was deposited in a km-scale and up to 350 m deep incised palaeovalley, formed during the Sturtian glacial event (Le Heron et al., 2013a). Above the diamictite, facies is typical from a cap dolostone, with mm-thick, smooth and flat laminae. Sub-m-scale deformations are common all along the exposure, with several kink-band, box-folds and thrust folds occurring between non-deformed intervals (Figure 5.22).

Seven metres above the contact between the diamictite and cap dolostone, a dramatic sedimentological change occurs. A 1.5 m-thick, non-laminated bed is observed all along the outcrop (Figure 5.23). Tojo et al. (2007) have also described this bed and it pinches out southward. The lower and upper contacts are sharp (Figure 5.23.A, B). Several mm to 10 cm large white carbonate clasts are incorporated in a light grey to black microcrystalline matrix (Figure 5.23.B–D). There are no obvious scour marks, truncation or angular unconformity at the base of the bed. A cm-thick clast-rich interval composes the base of the bed, with elongated < 3 cm large clasts, lying parallel to the bedding (Figure 5.23.B). Density of clasts decreases upsection but local larger clasts (< 10 cm), elongated to rounded or angular can be concentrated in other intervals. There is no orientation of the clasts in these intervals (Figure 5.23.C). Colour variations within the matrix show dm–cm-scale convolute features (Figure 5.23.D). At 1.20 m from its base, the bed is truncated and a second 30 cm-thick bed ends the non-laminated sequence. This bed has a similar facies to the one below, but more homogeneous, without convolutions and with relatively small clasts (< 1 cm).
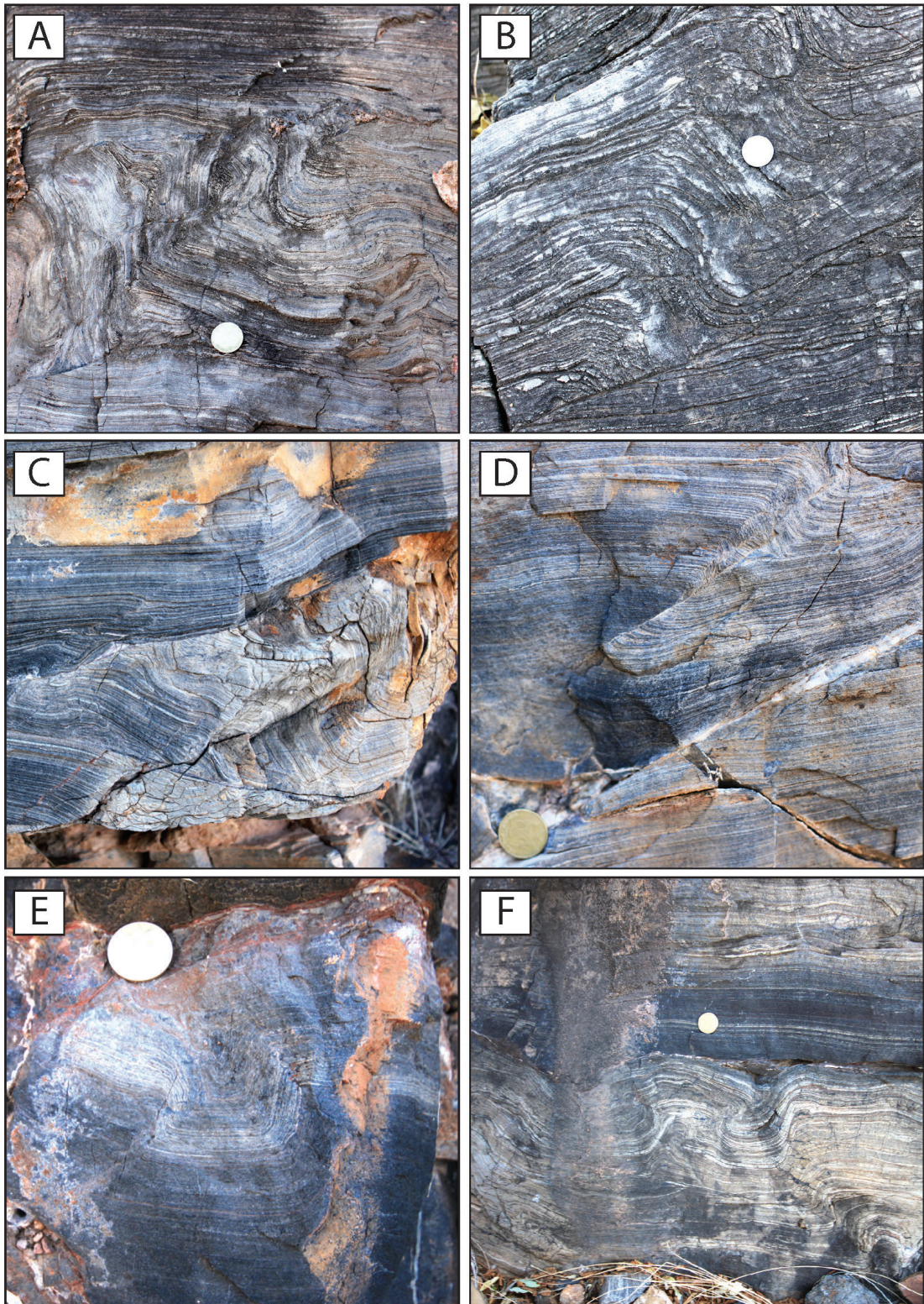
Figure 5.22: Cap dolostone, Omutirapo area (1/3). Soft-sediment deformations. **A** and **B**. Overturned folds. **C** and **D**. Fault bend folds. **E** and **F**. Kink-band/box folds. Coin is 23 mm Ø.
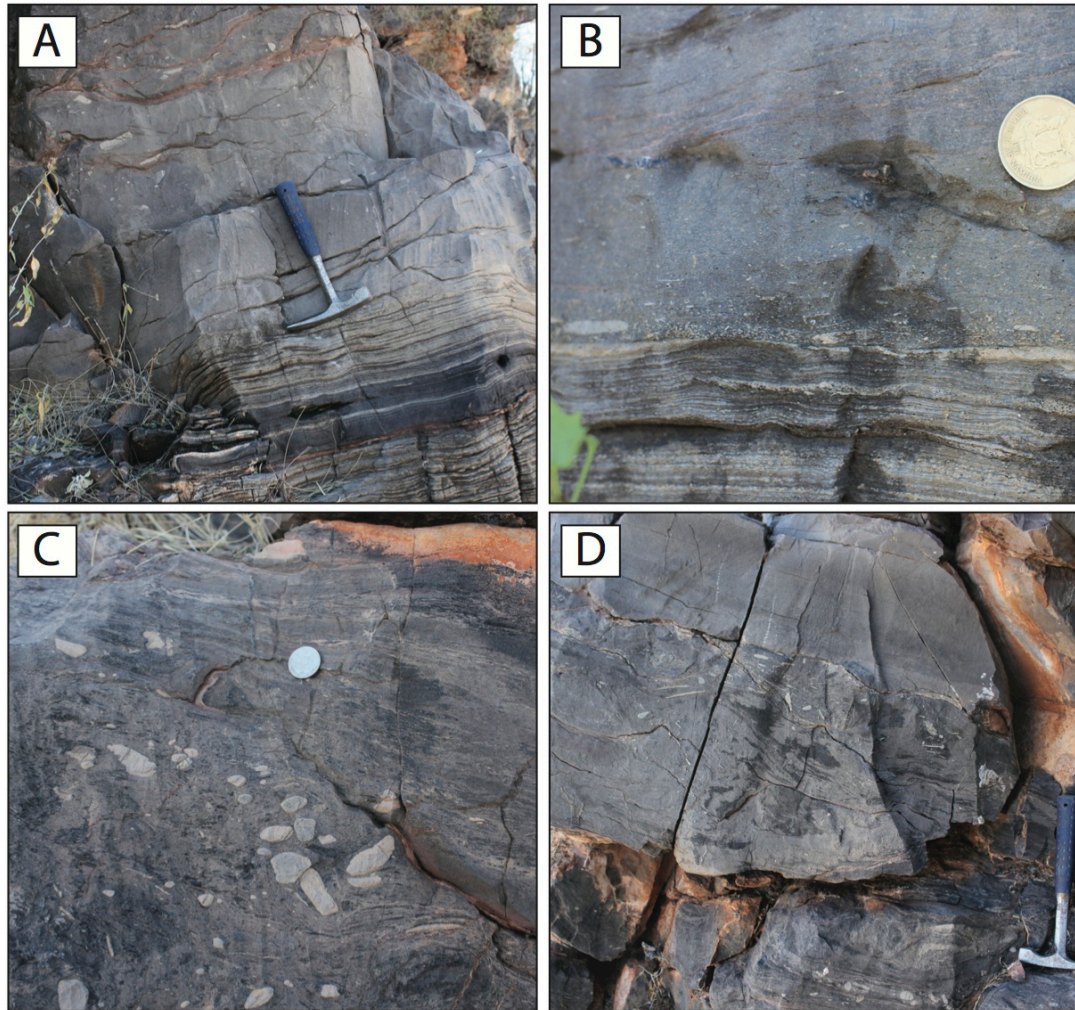
Figure 5.23: Cap dolostone, Omutirapo area (2/3). **A**. Transition from laminated to non-laminated facies. **B**. Base of the non-laminated interval, with abundant oriented clasts at the base. **C**. cm-sized mud clasts. **D**. Convolutes (darker) followed by clasts and brutal change to a fine-grained interval. Coin is 23 mm Ø.

Smooth, sub-mm-thick laminae are the dominant facies in the cap dolostone. However, this facies is punctuated by three white to grey beds, separated from each other by 0.3–0.7 m. White beds are ~30 cm-thick and non-laminated (Figure 5.24.A). No clasts are observed in these beds. Randomly spaced 1–2 cm high and large lumps rise from their top surface, the hemispheroids are made of the same material than the non-laminated beds (Figure 5.24.A). Overlying laminae drape these beds and the lumps conformably. In the top 3 m of this member, possible cross-bedding can be observed (Figure 5.24.B). Owing to the close association with unequivocal soft-sediment deformation structures, it remains possible that the putative cross-bedding is soft-sediment deformation also.

Fourteen metres above the Chuos Formation, laminae start to rise with angles > 45° and the facies changes progressively to the microbial member (Figure 5.24.C, D). Laminae can rise, form a 5 cm high cone structure and then recover a perfectly flat configuration (Figure 5.24.D). Sets of laminae finally form dm high cones, marking the arrival into MM1.
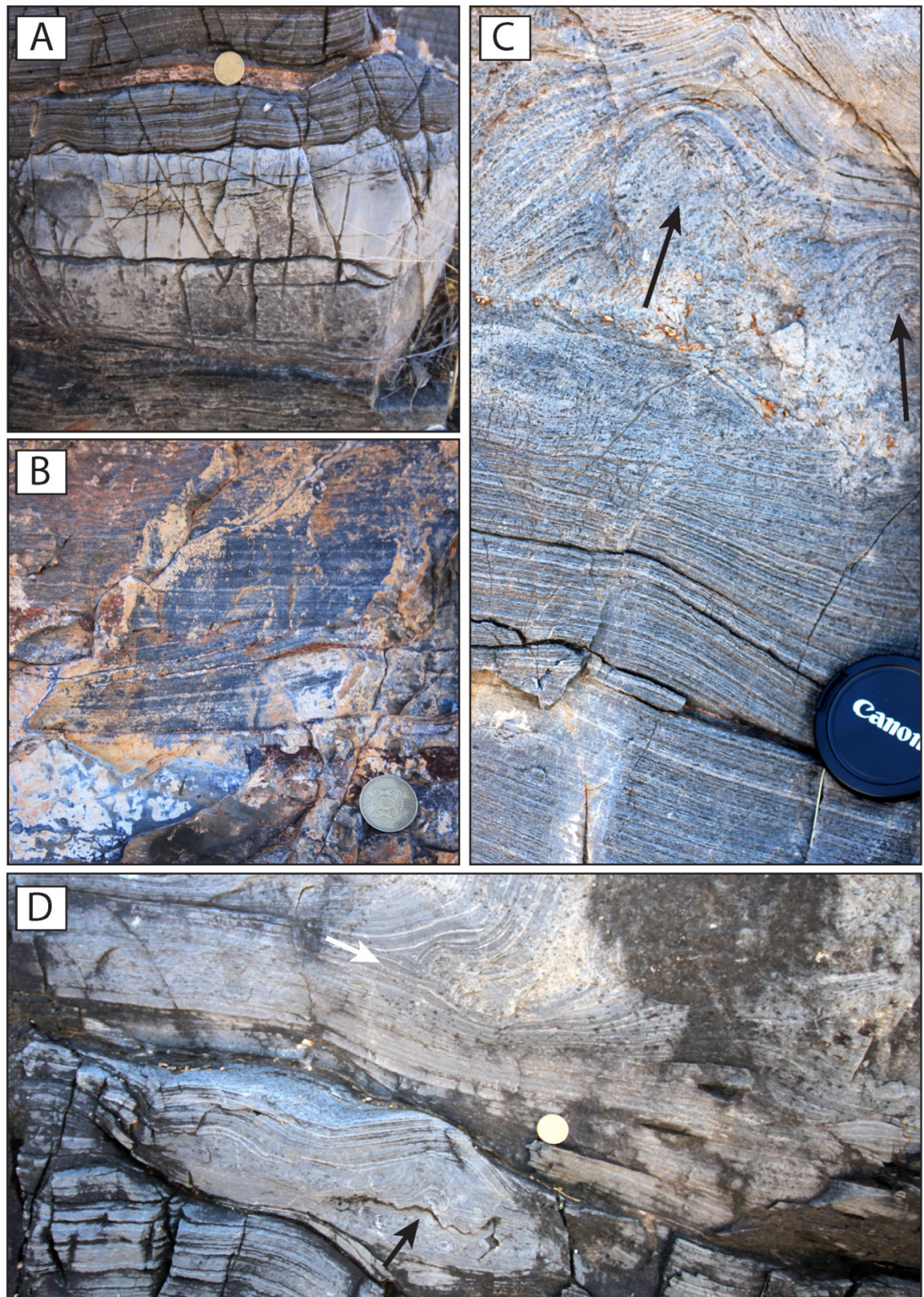
Figure 5.24: Cap dolostone, Omutirapo area (3/3). **A**. Non-laminated bed with local lumps at the top. **B**. Possible cross-bedding in the cap dolostone. **C**. Transition from flat laminae of CD to convex upward geometries of MM1 (arrows). **D**. Local convex upward (black arrow) between flat laminae of CD, then rise of the laminae indicating the arrival in MM1 (white arrow). Coin is 23 mm Ø, lens cap is 58 mm Ø.

### 3.4.2    Microbial member

The ridge formed by MM1 is approximately 30 m-thick but its exact thickness was not measured at the visited sections because it involved dangerous climbing. From afar, it is organised into 2–4 m-thick beds, as mentioned before in the general features of the Rasthof Formation. At Omutirapo, MM1 generally appears less chaotic than at Rasthof Farm. Laminae are 1–5 mm-thick, and form sets that undulate with a 10–30 cm amplitude and wavelength (Figure 5.25). Undulations are not perfect and can appear slightly contorted. Locally, sets of laminae appear to develop as concentric layers around a nucleus (Figure 5.26.A, B). Also, convex upward sets of laminae can form hemispheroid geometries with rare, cm wide chimney-like structures that can be observed (Figure 5.26.C, D).

Whilst the boundary between two beds is clear from the distance, it is more difficult to point it directly at the outcrop. Above and below putative bed boundaries, undulating sets of laminae are present, without chaotic features (Figure 5.26.E). Facies between the base and the top the beds is often fractured, making observation of a potential contact difficult. Where observed from below, the base of a bed exhibits well-defined domes that correspond to the undulations observed on a cross section.

Towards the top of the ridge, thinner, relatively flat laminae are common. Some roll-up structures were observed, interpreted as the base of MM2. However at Omutirapo, MM2 is rarely exposed because it has been eroded. It is better exposed westward, in the Ongongo area (Pruss et al., 2010). Some blocks of MM2 were still found and carried for petrographic comparisons with other areas.
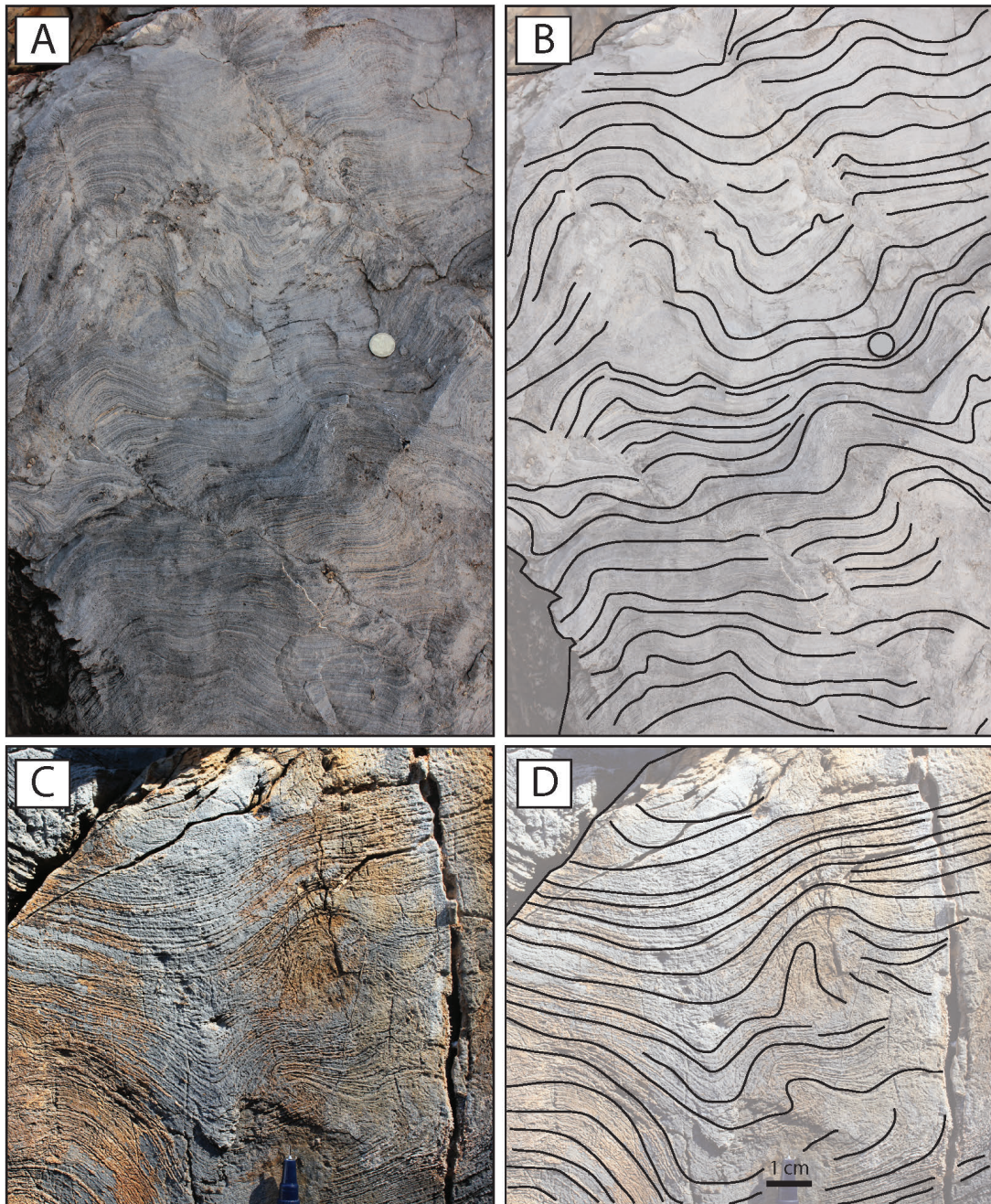
Figure 5.25: MM1, Omutirapo area (1/2). **A**. Typical deformations in MM1. **B**. Sketch, coins is 23 mm Ø. **C**. cm-scale antiform structures. **D**. Sketch.
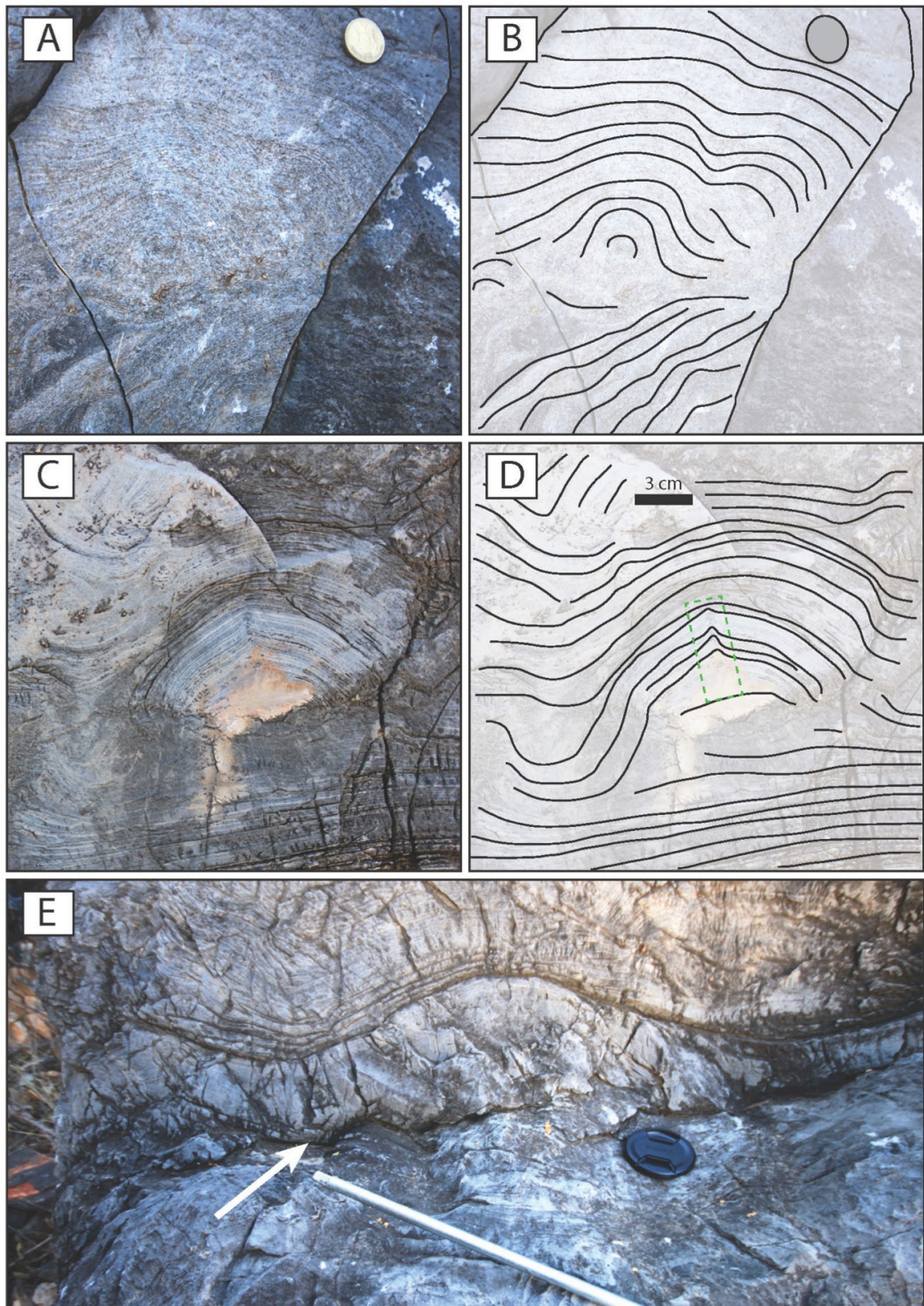
Figure 5.26: MM1, Omutirapo area (2/2). **A**. Local concentric growths. **B**. Sketch, coin is 23 mm Ø. **C**. Dome geometry with a chimney-like structure in the middle. **D**. Sketch, with the chimney in the green rectangle. **E**. Interface between two layers of MM1 (white arrow). Note the long wavelength laminae above the contact, often occurring at the base of a layer at Omutirapo. Lens cap is 72 mm Ø.

## 3.5    Okaaru area

The Rasthof Formation is exposed along the road C43, north of Sesfontein (Figure 5.27). Outcrops are accessible east of the Okaaru village, on the fringe of an eroded syncline topping a hill. The section is described east of the syncline, where the cap dolostone and the base of MM1 are exposed less than 300 m from the road C43. MM2 was observed on the western side of the syncline, where the full section is accessible and was also described by Pruss et al. (2010). Between the road and the outcrop, the slope of the small hill consists of recent sediments, blocks of the Rasthof and Chuos formations as well as exposures of the Chuos Formation.
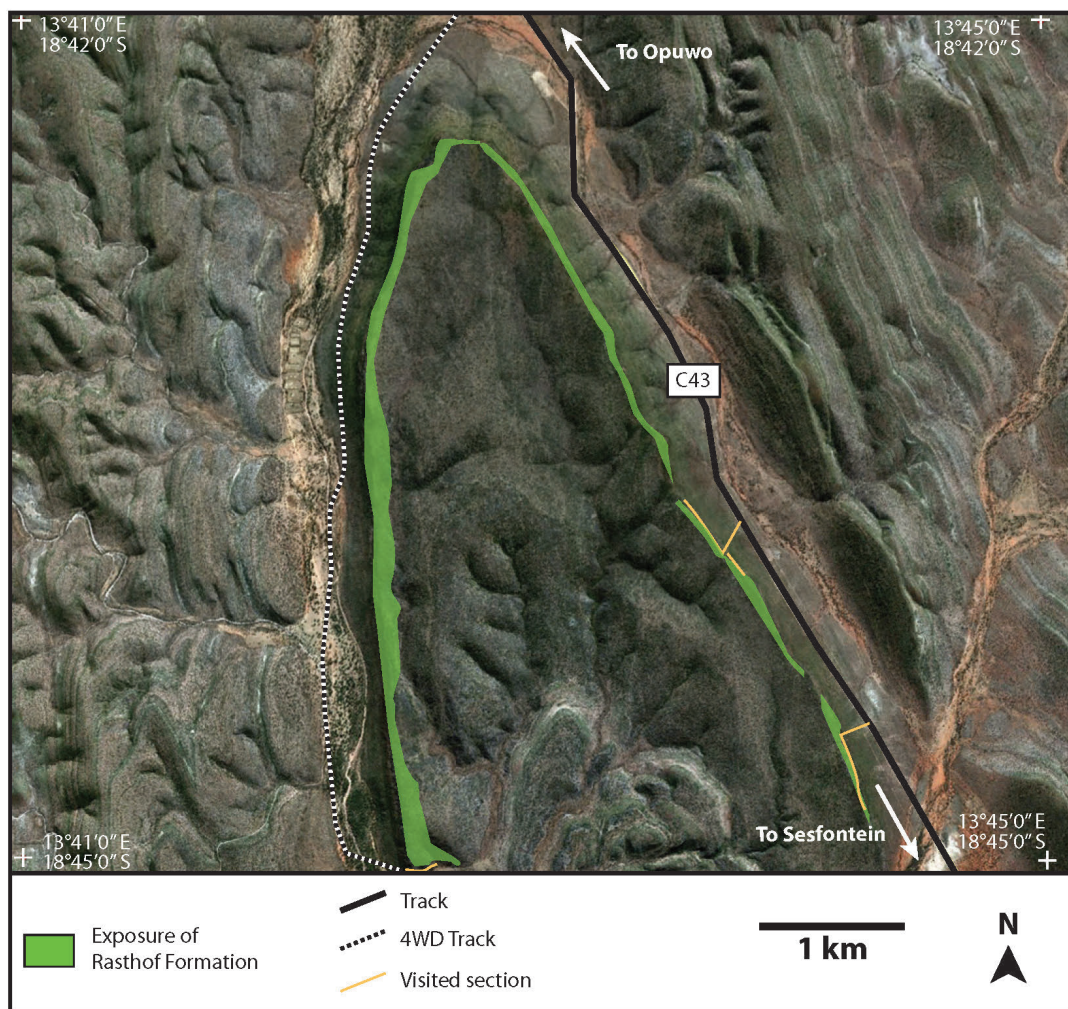


Figure 5.27: Satellite view of the Okaaru area. Outcrops are easily accessible in the southern half area of the picture (Modified from satellite image (Google Earth): © 2013 DigitalGlobe; © 2013 Google; © 2013 Cnes/Spot Image).

### 3.5.1    Cap dolostone

The cap dolostone is 3 m-thick and consists of sub-mm-thick parallel laminae. It rests in sharp contact with the underlying Chuos Formation. The base of the unit can have a salmon colour for 50 cm (Figure 5.28.A), then turns to grey upsection. Laminae are flat and perfectly parallel (Figure 5.28.B). After 2 m, laterally linked hemispheroids can rise from horizontal laminae. They are closely spaced and can stack for up to 20 cm, with a 5–10 cm wavelength and less than 5 cm amplitude (Figure 5.28.C). Above, laminae become perfectly flat again. From the top, they form equally spaced, < 5 cm diameter regular domes (Figure 5.28.D), no crests were observed. Within one hemispheroid, laminae are parallel.

The transition with the microbial member is more complex than in the Rasthof Farm or Omutirapo areas. After 3 m, laminae of the cap dolostone start to develop a sub-parallel crinkly aspect, sometimes with small laterally linked hemispheroids as described above. Above, delicately laminated facies can reappear, resting in knife-sharp contact on the crinkly laminae (Figure 5.29). The contact between crinkly laminae and cap dolostone laminae is not always perfectly flat and the cap dolostone laminae can drape a cm-scale palaeotopography (Figure 5.29.C). There are two such cycles beneath uninterrupted microbialites of MM1. However, evaluating the exact number of cycles is challenging because cap dolostone intervals become thinner upsection. Weathering can also make the distinction between the two facies problematic.
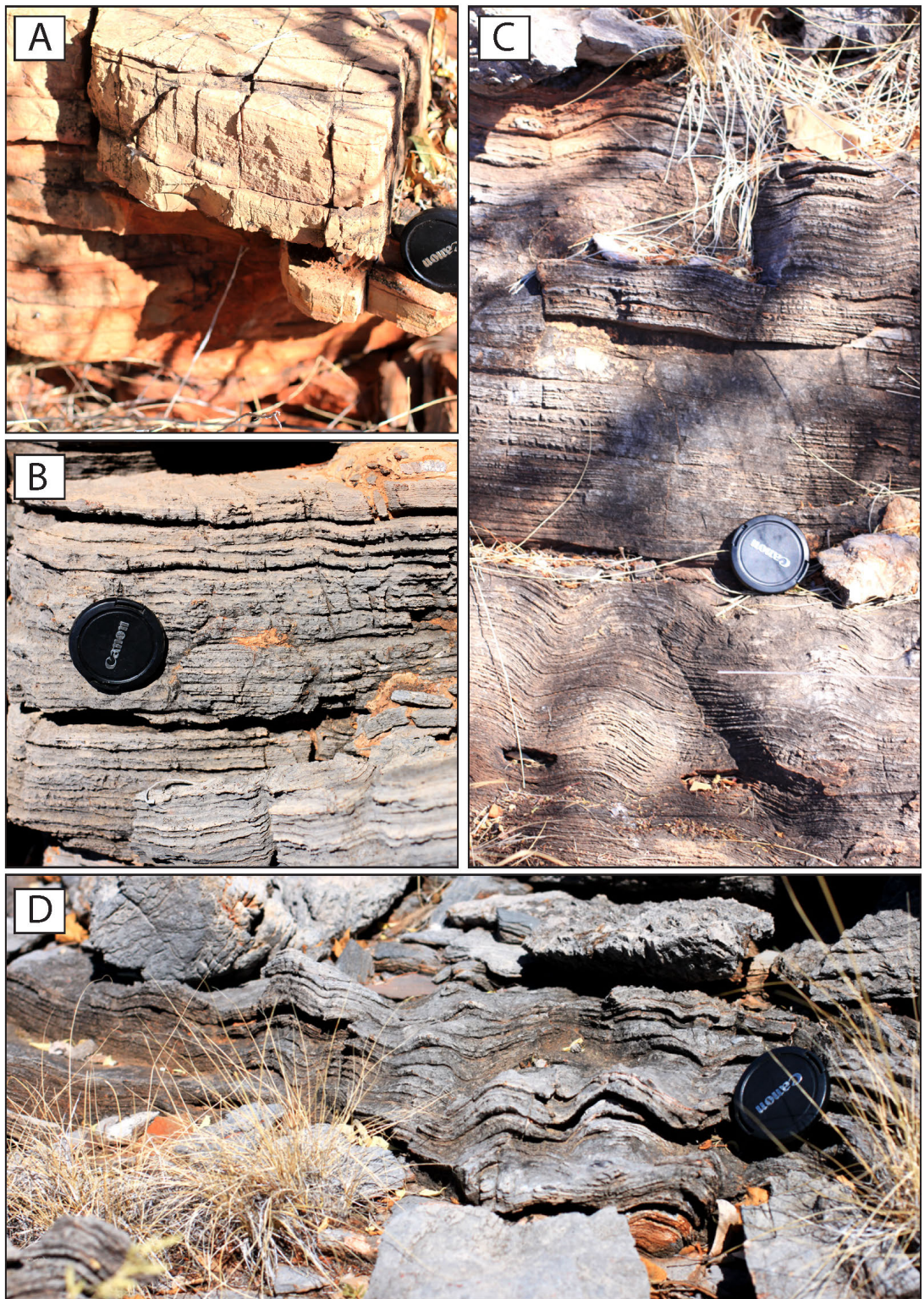
Figure 5.28: Cap dolostone, Okaaru area (1/2). **A**. Salmon laminated facies at the base of the cap dolostone. **B**. Typical flat laminated facies. **C**. Local development of laterally linked hemispheroids (below lens cap) followed by flat laminae. **D**. Laterally linked hemispheroids. Lens cap is 58 mm Ø.
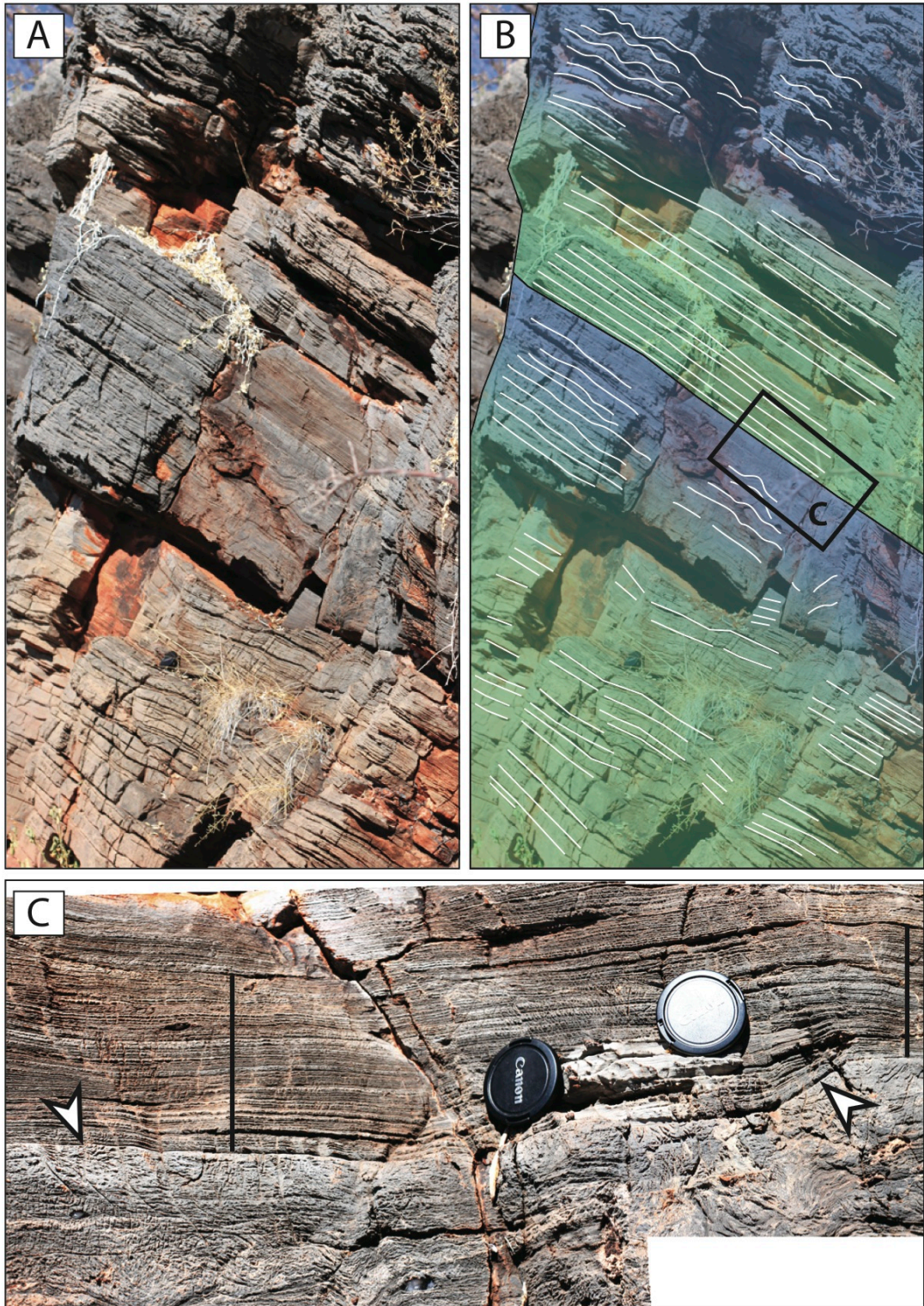
Figure 5.29: Cap dolostone, Okaaru area (2/2). **A**. Development of crinkly laminae, sharply overlain by cap dolostone laminae. **B**. Sketch. **C**. Detail of the contact (arrows) between crinkly laminae (below) and flat laminae (above). The contact is not horizontal and overlying laminae were deposited following the topography, with more accommodation to the left of the picture. Lens cap is 58 mm Ø.

### 3.5.2    Microbial member 1

MM1 consists of undulating to chaotic sets of thick laminae (1–6 mm). If mats' natural trend is to develop into crinkly horizontal laminae (Figure 5.30.A, B), they commonly form cm–dm-scale irregular domes. The folding gives a chaotic aspect. In extreme cases, deformation styles include complex folds. Dm-thick sets of laminae can appear contorted, locally rolling over the underlying set of laminae. They form dm-scale, crinkly overturned to recumbent folds (Figure 5.30.C, D).

Several oblique sedimentary dykes cut through the stromatolites (Figure 5.31), as already observed by Pruss et al. (2010, fig.3.B and 6.A, D). On both side of one dyke, laminae do not seem more disrupted than elsewhere in the formation. There is no contortion or preferential orientation of the laminae along the dykes. Sediments in the dykes include intraclasts and chaotic sets of laminae. On the other hand, deformation structures are widespread, even if no dyke is observed.
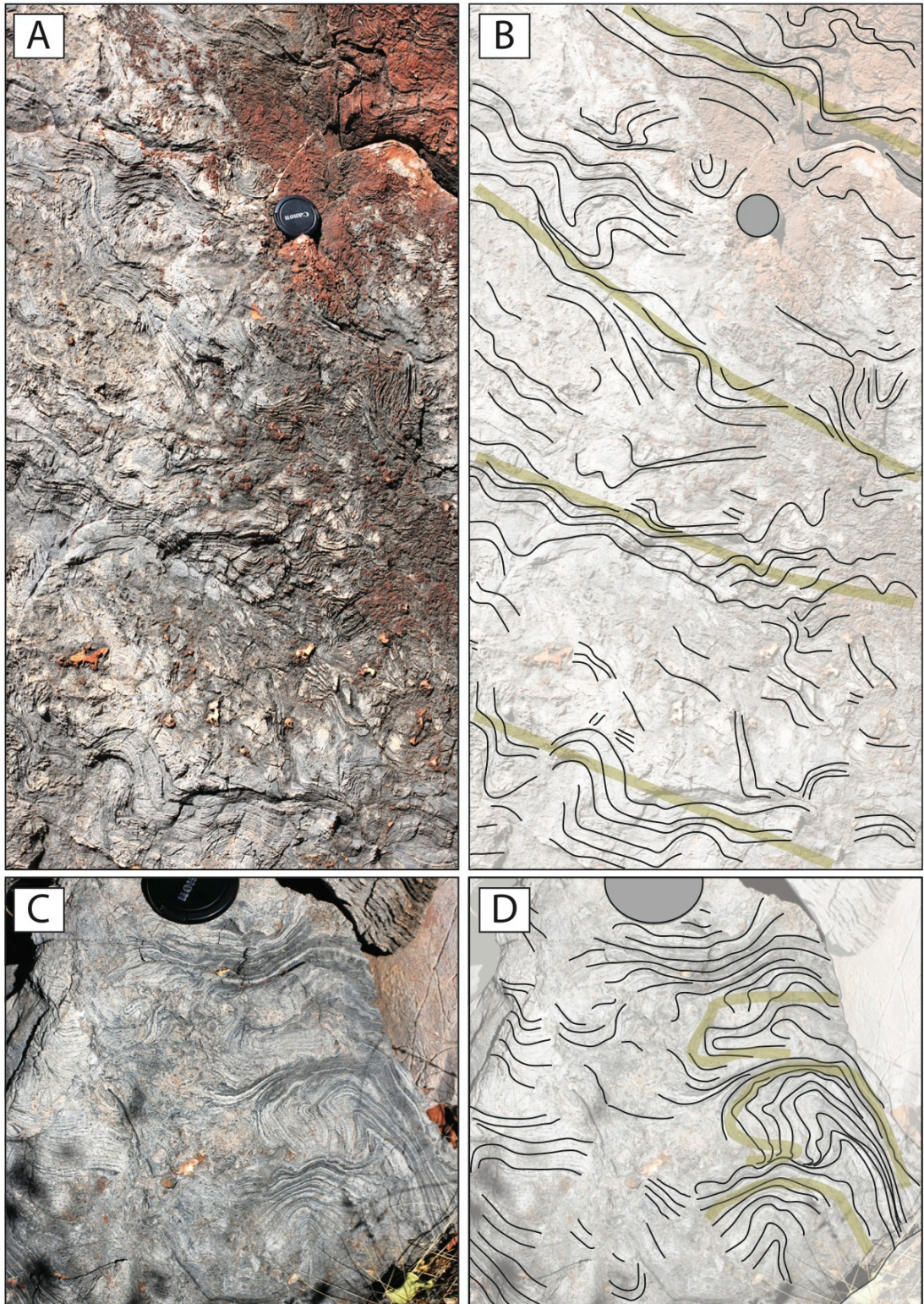
Figure 5.30: MM1, Okaaru area. **A**. Typical chaotic aspect of the outcrops. **B**. Sketch illustrating the preserved laminated trend. **C**. Rolled folds. **D**. Sketch. Lens cap is 58 mm Ø.

Figure 5.31: Sketch of a dyke (~50 cm wide) as observed in the microbial member. Dykes can be 20–100 cm wide.

### 3.5.3    Microbial member 2

MM2 is well exposed on the western side of the syncline. It is typically made of flat thinly laminated (sub-mm) dolostone. Common cm-scale roll-up structures occur (Figure 5.32). Rolled-up intervals do not appear broken and form highly deformed, cm-thick structures intercalated beween non-deformed laminae.
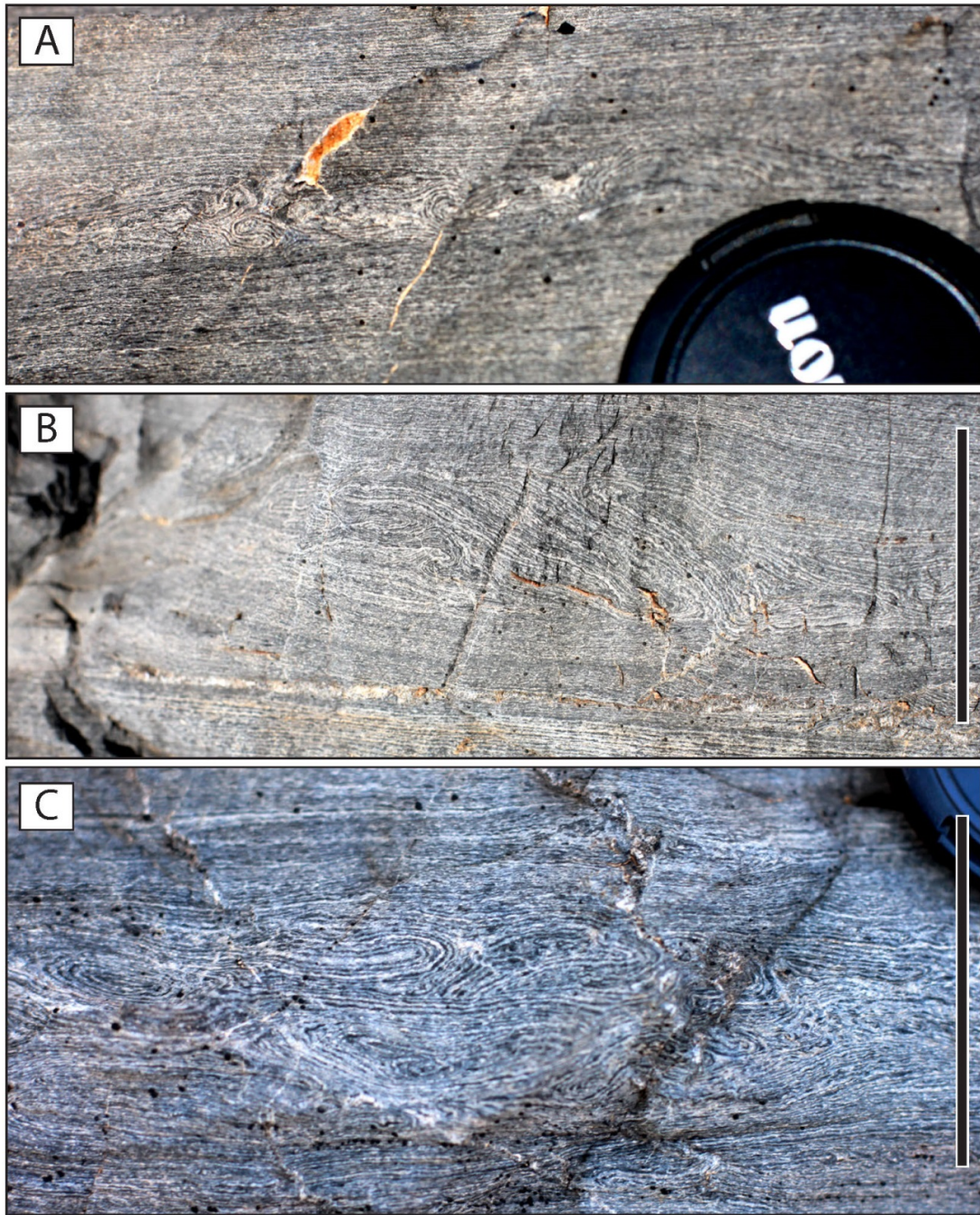
Figure 5.32: MM2, Okaaru area. **A**, **B** and **C**. Examples of roll-up structures. Lens cap is 58 mm Ø and scale bar is 50 mm long.

## 3.6    Synthesis

A synthetic log from each visited sections is presented in Figure 5.33.
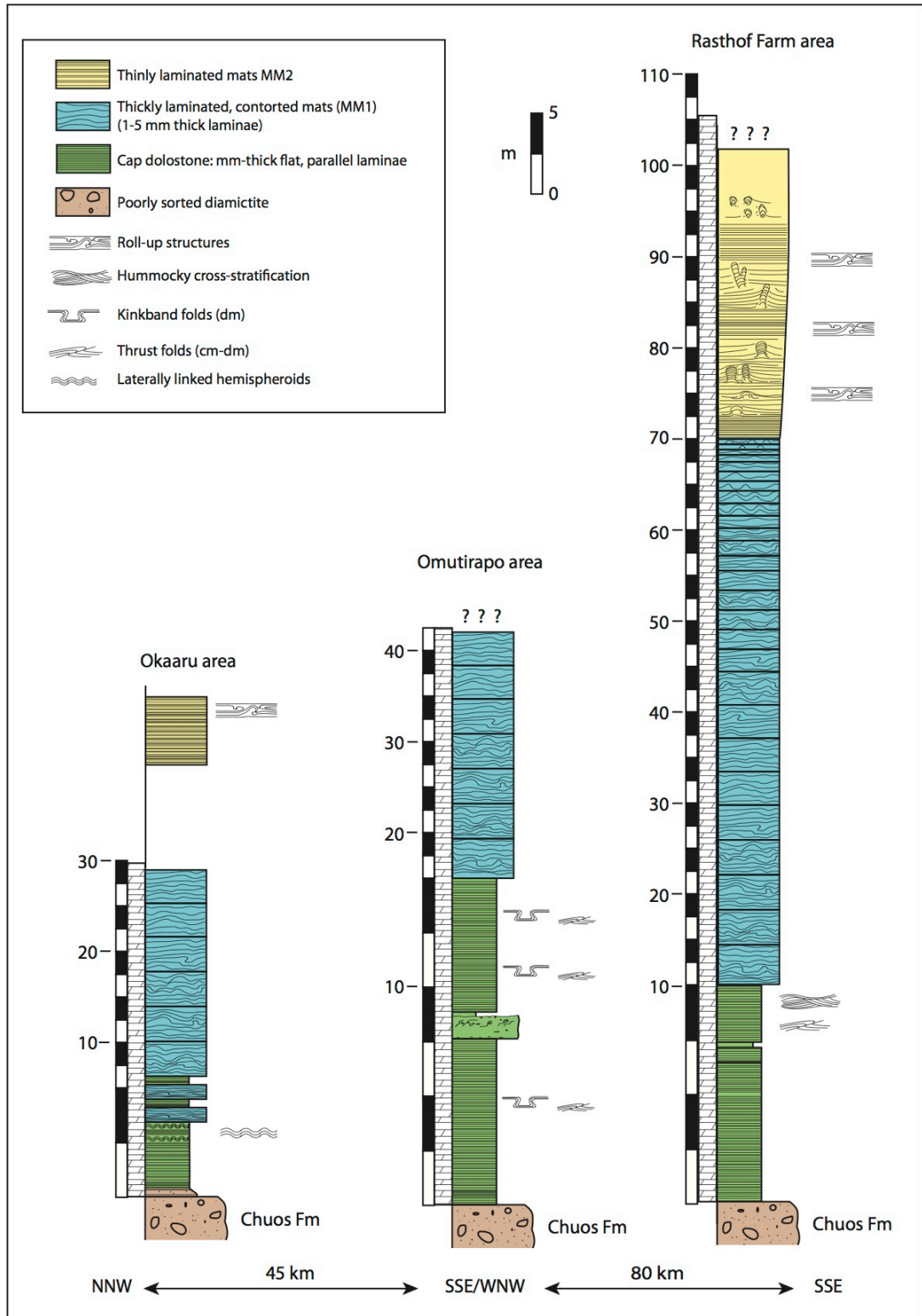


Figure 5.33: Synthetic logs, northwest Namibia. Remaining samples are referenced in Appendix D.

### 3.6.1 Cap dolostone

The cap dolostone was described above the glacigenic Chuos Formation (Hoffman and Halverson, 2008; Le Heron et al., 2013a) at the three locations. At the visited sections and apparently elsewhere on the platform, there is no obvious hiatus or major unconformity and we can expect the cap dolostone (as well as overlying microbialites) to have sedimented during the aftermath of a glacial event (Hoffman and Halverson, 2008).

The base of the member can be pink (Rasthof Farm, Okaaru) but colour changes to grey after a couple of dm–m. The cap dolostone is remarkably flat laminated, with the thickness of one lamina not exceeding 1 mm. Only one thick (< 2 m) non-laminated, clast-rich bed was described at Omutirapo. Few thinner (< 30 cm), non-laminated, light coloured beds were observed (Rasthof Farm area, Omutirapo).

The top of the member can exhibit what can tentatively be described as cross-stratification (Rasthof Farm, Omutirapo) and different transition style to the microbial member. At Okaaru, the transition consists of m-scale cycles. One cycle is recorded by laminae of the cap dolostone that progressively form well-defined laterally linked hemispheroids, then change to thicker and more chaotic laminae in turn capped by cap dolostone flat laminated facies. At Omutirapo the transition is more direct with the rise of the laminae to form < dm large cone structures. In the Rasthof Farm area, the contact with MM1 is not very well preserved and often brecciated.

### 3.6.2 Microbial member

The microbial member 1 was described above the cap dolostone in the three visited areas. It always consists of undulated to contorted laminae, giving a chaotic aspect to the outcrop. This facies and its vertical and lateral continuities are characteristic from the Rasthof Formation. Comparable facies occur at Omutirapo, Okaaru and Rasthof Farm areas. However, the style and the intensity of the undulations or deformation structures vary (Table 5.1).

Table 5.1: Facies variations in MM1.

| Area | Horizontal, undulated sets of laminae | | Style of deformations | Other | Relative chaotic aspect |
|---|---|---|---|---|---|
| | Wavelength | Amplitude | | | |
| Rasthof Farm | ~10 cm | < 5 cm | dm–m antiform to recumbent folds | Development of 20 cm high cones at the top of MM1 | ++ |
| Omutirapo | > 10 cm | 5–30 cm | dm–m antiform folds | Local < dm-scale concentric sets of laminae | + |
| Okaaru | ~10 cm | < 5 cm | dm antiform to recumbent folds | Local dykes | +++ |

If MM1 is easily distinguishable and well exposed, MM2 is more difficult to observe. At the visited sections, it is always located above MM1. But the effects of recent erosion can reduce the quality of observations, especially at Omutirapo or east of the Okaaru area where it has locally been eroded. Laminae of MM2 are much flatter than in MM1. Neither undulations nor dm–m-scale deformations were observed. The only deformations observed are cm-scale roll-up structures resulting from the contortion of only few cm-thick (e.g. < 5 cm) sets of laminae. Below and above a rolled interval, laminae are perfectly flat.

# 4     Interpretations

The unusual nature of the facies observed in the Rasthof Formation makes comparisons and analogies with other microbial sediments complicated. Although the facies are laterally continuous over hundreds of km, they have been interpreted from deep-water (Bosak et al., 2013b; Pruss et al., 2010) to relatively shallower environments (Hedberg, 1979; Le Ber et al., 2013). Below, we address the interpretation of these unusual facies that lack classic sedimentological features.

In this study, nothing but dolostone, mostly laminated, was described on the field. Before interpreting each of the members, it is worth recalling that argillites are described in the Rasthof Formation elsewhere (Hoffman and Halverson, 2008; Pruss et al., 2010). They are observed south of the Fransfontein Ridge, and west of the Kaoko Belt. Argillites with turbidites and platform-derived blocks potentially imply the most distal and deep facies known for the Rasthof Formation. On the Northern Platform, no such facies are described, probably indicating a relatively shallower setting.

## 4.1    Cap dolostone

On the platform, the cap dolostone is interpreted as the deepest facies of the cap carbonate sequence (Hoffman and Halverson, 2008), deposited below the storm wave base (Tojo et al., 2007; Yoshioka et al., 2003). Several features can be added to the general knowledge of this member, giving information about the context at the time of deposition.

### 4.1.1    Bedforms

The cap dolostone is typically flat laminated, without bedforms except locally at the top of the member of the Rasthof Farm and possibly Omutirapo. At Rasthof Farm, the recognition of hummocky cross-stratification (HCS) implies sedimentation in an energetic setting. HCS bedforms are recognised in a range of settings from outer shelf to intertidal environments (Cheel and Leckie, 1993). On the outcrop, the bases of the swales seem erosional, the absence of migrating ripples and soft-sediment deformation structures in HCS beds, coupled with the lack of massive grainstones underlying them, discounts a genesis by turbidity currents (Mulder et al., 2009). At

Rasthof Farm, the uppermost part of the cap dolostone is interpreted to record deposition from storm wave activity. The formation of bedforms indicates that sediments were mobile at the time of deposition, contrasting with the supposed cohesive nature of the overlying sediments from the microbial member.

### 4.1.2    Non-laminated intervals

In the Rasthof Farm and in Omutirapo areas, non-laminated beds record episodes of sedimentation different from background sedimentation of the cap dolostone. At Omutirapo the 1.5 m-thick clast rich bed is interpreted as an allodapic sequence (i.e. carbonate turbidite, Flügel, 2004; Meischner, 1964). This interpretation is supported by the observation of 1) clastic carbonates (pebble-sized mudclasts); 2) sharp lower contact; 3) grading; 4) local convolute lamina. Some clasts were soft during their transport and were soon deformed during early compaction. Tojo et al. (2007) also interpreted the same bed as a turbidite. It tapers and disappears ~20 km south from Omutirapo. A turbiditic origin is the best interpretation for this bed, however the facies encountered do not fulfil all the criteria to be interpreted as such, especially the lack of indistinct upper contact (Meischner, 1964). Indeed, there is a sharp contact between the top of the bed and overlying laminae. So far, comparable clast-rich beds have not been reported on the Northern Platform. In term of context, the bed was deposited in a former glacial palaeovalley (Le Heron et al., 2013a) filled by the Chuos Formation. Thus, residual accommodation space, in a former topographic low may have favoured the deposition of the turbidite. This residual accommodation in the underlying palaeovalley can also explain the relatively thicker cap dolostone compared to other visited sections.

Non-laminated, thinner (< 30 cm-thick) beds with no obvious clasts are also described above the turbidite. Similar beds are interpreted as sub-storm turbidites by Tojo et al. (2007). Microfacies analysis (Chapter 6) reveals the presence of sub-mm clasts within a muddy matrix but there is little evidence to classify them as carbonate turbidites. Characteristic features are not developed like in the more massive turbidite described in the previous paragraph. They still record the transport of detrital material and can therefore be interpreted as allochthonous. Similar (although rarer and thinner: < 10 cm) beds are also described in the Rasthof

Farm area. Grains are extremely rare yet present in thin section. Like in the turbidite of Omutirapo the non-laminated thin beds have a sharp upper contact. Overlying laminae can drape the bed (Omutirapo) or downlap onto it (Rasthof Farm).

They cannot be viewed as the result of deep-water turbidity current *sensu stricto*. It might result from the settling of fluid mud and could correspond to "mud-only" turbidite ($T_{E-2,3}$, Talling et al., 2012). Such deposits can form on very low slopes, in shallow environments (Talling et al., 2012). Resuspension of sediments across the platform may have diffused large quantity of muds and small lithoclasts in the water column, changing episodically the nature of the sedimentation. The upper half of the cap dolostone at Rasthof Farm is compatible with this interpretation. Hydrodynamic energy in the environment formed cross-bedded intervals, this energy also scattered some material in the water column that progressively settled on the seafloor. Rare discrete laminated fabric in some of these muddy beds (e.g. Figure 5.6.C) validates their formation by slow settling of material in suspension rather than by instantaneous turbidity current. Resuspension of sediments might result of destabilisation of sediments (also generating turbidity current down the slope), storms or wind blown dust.

### 4.1.3    Microbial influence

In the Okaaru area, the upper half of the cap dolostone exhibits laterally linked hemispheroids. These geometries are typical from this specific outcrop/area and different from any facies of the microbial member: they are well defined and not chaotic. In these structures, laminae can stack for tens of centimetres and suddenly recover a horizontal setting. Internally, no cross-bedding is observed, discounting them as wave-formed ripples. They bear no similarity with soft-sediment deformation structures observed at other localities, and hemispheroids are systematically pointing upward. No different sediments or grains were deposited in the depressions between the hemispheroids. Hemispheroids are likely to be the result of an influence of the sedimentation by microbial communities. The convex upward sets of laminae were probably able to bind the grains, avoiding their accumulation in the depressions. Alternatively, there was a negligible supply of sand-grade grains, as seems to be the case on the Northern Platform.

The hemispheroid structures are tentatively interpreted as stromatolites. The development of hemispheroids is closely associated with the cyclic transition to MM1. They might record episodes when the environment was favourable for microbial communities to colonise the seafloor. Microbial communities have locally influenced the sedimentation of the cap dolostone with the development of laterally linked hemispheroids. Yet this facies cannot be incorporated to the cap dolostone *sensu stricto* or "abiotic member" (Hoffman and Halverson, 2008), but as an intermediate stage between the cap dolostone and the microbial member.

This putative microbial facies alternates with classic cap dolostone laminated fabric. One of the facies changes is marked by a local disconformity (Figure 5.29.C). The surface between the two facies is not flat and the cap dolostone facies asymmetrically fills the negative topography. This surface, associated with possible microbially influenced facies can point to an extremely shallow-water environment, involving local short time subaerial exposure.

## 4.2    Microbial member

Since described as a stratotype, suggested palaeodepths at the time of deposition range from shallow (Hedberg, 1979) to shallow subtidal (Le Ber et al., 2013), sub-storm (Bosak et al., 2013b) or deep-water (Pruss et al., 2010). Several hypotheses have been addressed to explain the chaotic and contorted aspect of the microbial member (see Chapter 4). The author's field observations favour the rejection of most of these hypotheses. One or several causes still remain to be determined to understand the deformation of the microbial mats.

### 4.2.1    Microbial member 1

MM1 looks chaotic but the general horizontal trend of the laminae is preserved. Laminae recover a more undulated and horizontal setting after each dm–m-scale deformed interval. This means that the deformations result from disruption of soft-sediments. The facies looks chaotic but looking carefully allows the recognition of different degrees of deformation. Laminae formed large cohesive, undulated mats. A stress deformed them; overlying laminae recovered a horizontal setting until the next stress.

Lithification of the mats did not start before they were buried several dm below the seafloor. Such a late lithification of the microbial sediments gave them a rubbery texture, allowing their folding. In term of style, scale and extensiveness associated with supposed cohesive sediments, the deformations of MM1 bear no similarity with other soft-sediment deformation (e.g. Maltman, 1994). The lack of orientation in the deformation is incompatible with a slumping origin. The microbial member was deposited after the Sturtian glaciation; no ice movement pushed the microbial mats. Clastic dykes observed by Pruss et al. (2010) are not always present, while deformation is always observed. Whilst they seem to result from fluid escape, dykes do not seem to have caused the deformation structures (Chapter 4); they are associated with them. Deformations do not specifically point upward along the dykes. Yet, fluid escape cannot be discounted in the disruption of the mats: at Omutirapo a 20 cm large dome exhibits a central, vertical chimney-like structure (Figure 5.26.C, D). A fluid may have bent-up the laminae while escaping via the chimney. This escape is marked by an apparent perforation of the cohesive mats. This feature was observed only once on the field and does not seem to be associated with m-scale deformations. The chaotic aspect is typical from MM1 and widespread for > 100 km, a regional and recurrent stress must be invoked. Regional possibilities than can be considered are hydrodynamic energy (Le Ber et al., 2013) and seismic shocks.

On the studied part of the platform, the Rasthof Formation and especially the microbial member constantly lack obvious siliciclastic input or grains. This can be explained by the lack of clastic source. Furthermore, we can expect any grain to be trapped by the widespread microbial communities, inhibiting the creation of bedforms, even if hydrodynamic energy might have allowed their formation. Rare dm-sized clasts can be observed (e.g. Pioneer Farm), indicating fairly violent events able to break sets of cohesive mats. If episodic storms passed through the platform, waves might have hit the seafloor, affecting and deforming the non-lithified microbial mats. No scour marks would result from these waves because the mats were cohesive; therefore episodic stresses were not able to dig the sediments. One deformed interval observed in MM1 can be viewed as a surface to shallow shearing/traction of the mats due to a percussion of the water on the seafloor.

Microbial mats of MM1 are never flat for more than a couple of dm–m. Undulation is typical, developed at different degrees (Table 5.1). Dm–m-thick sets of laminae are deformed and overprint the initial undulation. The undulated facies might be due to a moderate oscillatory regime of waves. Folded intervals result from more violent, episodic events such as storms. MM1 was probably not deposited in a shallow subtidal or intertidal setting, but hydrodynamic energy cannot be discounted as a key factor to produce the facies observed.

Another possible origin for the chaotic aspect of MM1 is the effect of active tectonics along the margin of the Angola Block (Hoffman and Halverson, 2008) or of a post-glacial rebound. The Northern Platform was accumulated on the Angola Block. It means that ice deposited at Chuos time was probably partly present in a continental setting in northern Namibia. This ice applied pressure on emerged landmasses, creating subsidence. The Rasthof Formation was deposited in the aftermath of the Sturtian glaciation. The melting of the ice cover led to a flooding and an uplift of the cratonic block, accompanied by seismic shocks. These seismic shocks might then have triggered episodic soft-sediment deformations in the microbial mats of MM1. The intensity of the deformations decreases upsection. This is consistent with a return to an isostatic equilibrium. Given the context, seismic shocks cannot be discounted as a reason for soft-sediment deformations found in MM1. But diminution of the deformations upsection in the microbial member might also be due to a change in the microbial architecture, the rheology of the mats.

Other studies invoke a seismic origin in deformed microbial mats (Kahle, 2002; Martín-Chivelet et al., 2011; Nogueira et al., 2003). Deformation structures such as boudinages, pinch-and-swell structures, faults, kink-bands, microbreccias are typical features resulting from seismic shock on microbial sediments. Except from microbreccias, they are missing in MM1. But a difference in lithology, with implications for rate of lithification, rheology and cohesion may also explain the restricted range of deformation structures in the Rasthof Formation compared to analogous deformed microbial mats. Nogueira et al. (2003) also invoked earthquakes during the post-glacial rebound to explain observed soft-sediment

deformations in a Neoproterozoic cap carbonate in Brazil. However, the deformed stromatolite interval they described is much thinner than in the Rasthof Formation.

## 4.2.2 Microbial member 2

The thickness of the deformed sets implies different styles of deformations than in MM1. Roll-up structures do not exceed a couple of cm-scale, and are thus interpreted to result from an intense contortion of a thin set of laminae. The stress did not affect the two members in the same way, possibly because of a different rheology. In MM2, only the first centimetres of the seafloor were readily deformable (Figure 5.34.B), possibly snatched or peeled off from underlying sediments. It is logical to think that a few cm-thick set (MM2) is much flexible than a dm–m-thick set (MM1), in that it is easier to roll 10 sheets of paper than 500 stacked together. This results in a high degree of contortion of the sets, with several roll-up structures in a couple of centimetres. No such structures are observed in MM1, where the deformed sets are often dm–m-thick (Figure 5.34.A). The dm–m-thick beds of MM1 were deformable but less flexible. This led to the formation of larger scale fold structures.
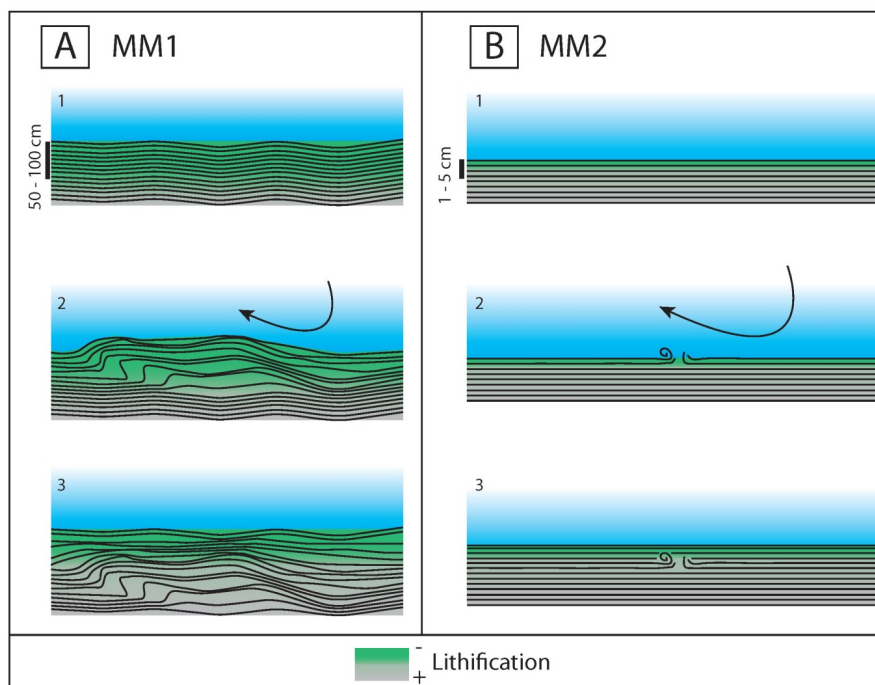


Figure 5.34: Suggested behaviours of the microbial mats. **A**. Later lithification or different rheology of the microbial mats in MM1 allowed the production of thicker deformations than in MM2. **B**. Only the first few centimetres of the seafloor were readily deformable, creating more contorted and compact intervals than in MM1.

Roll-up, or jelly-roll and similar structures are observed and interpreted in a variety of environments: shelfal marine, possibly sub-photic settings (Simonson and Carney, 1999), shallow subtidal to supratidal environments (Harwood and Sumner, 2011; Schieber et al., 2007) and in lacustrine settings where they are interpreted as slope-generated slump structures (Dean and Fouch, 1983). While their formation in inter- to supratidal settings can be observed in modern environments (Schieber et al., 2007), their formation in the subtidal zone remains problematic.

In the Rasthof Formation, different degrees of deformation are observed within MM2. In the Okaaru area, the deformed intervals contain pristine roll-up structures; at Rasthof Farm, roll-up structures can also be broken. This suggests that at Rasthof Farm, increased hydrodynamic energy levels were characteristic and locally able to break the thin sets of cohesive mats. Such rolled-up or broken intervals are generally found nearby the domes and column stromatolites, and it is widely accepted that one of the main parameter responsible for vertical growths in stromatolites is the increasing hydrodynamic energy in the environment (Bosak et al., 2013a and references therein).

On the platform, the Rasthof Formation is interpreted as a single shallowing upward succession (Halverson et al., 2005), with the deepest facies recorded by the cap dolostone and the shallowest facies recorded by grainstones and a subaerial exposure of the Northern Platform (Hoffman and Halverson, 2008). Pruss et al. (2010) logged grainstones facies at the top of the Rasthof Formation in Okaaru and Warmquelle areas (nearby Omutirapo). The shallowing upward trend is concomitant with an increasing hydrodynamic energy and input of grains (epiclastic member, Hoffman and Halverson, 2008) at the top of the Rasthof Formation. The combination of the two previous factors might have overtaken the microbial communities.

A key observation to support this increasing hydrodynamic energy is the occurrence of a variety of individual stromatolite growths (domes, columns and branching columns) in MM2, at Rasthof Farm (Le Ber et al., 2013). Growths are associated with the disturbance or destruction of surrounding laminae, leading to the formation of roll-up structures and mm–cm large intraclasts. No vertical growths

were observed in Okaaru and Omutirapo areas during the fieldwork, and this might be due to the lack of exposure. If no vertical growths are present in the Warmquelle–Okaaru area, it might be because the platform setting was relatively deeper than at Rasthof Farm.

### 4.2.2.1    Individual stromatolite growths (Rasthof Farm)

Vertical growths start at the top of MM1, with local vertically oriented, 20 cm high cones. Then in MM2, the cones change into domes, then large columns (< 40 cm Ø) and branching columns (< 20 cm Ø). Laminae are well preserved between the cones and domes but start to become rare between the columns. They almost disappear with the increasing branching, where intergrowth laminae are rolled-up and broken. Ultimately, stromatolites or laminated fabric disappear from the upper part of the outcrop.

It has been proposed that increasing hydrodynamic energy diminishes the preservation of the laminae (bridges) between the growths (Bosak et al., 2013a and references therein). It is also admitted that such energy in the environment associated with a logically more important transport of grains will favour the development of individual vertical growths. Stochastic growth simulation models suggest that partial burial by sediments is one of the main factors to drive the branching of the stromatolites (e.g. Dupraz et al., 2006). This explanation seems logical: if sediments cover microbial communities, they will have difficulty to develop. Growth will therefore occur where there is less burial, creating distinct positive relief. Moreover once positive reliefs or columns start to be well differentiated, grain input in the environment will preferentially ends-up in the depressions between the positive reliefs. This again favours the microbial communities to develop vertically rather than laterally. This model assumes that grains (intra or extraclasts) are available to locally bury the microbial mats.

At Rasthof Farm, two key observations have been made: 1) the upsection loss of laminae between the columns (bridges); and 2) the intensification of branching upsection. Regarding the statements from Dupraz et al. (2006) and Bosak et al. (2013a), the geometries of the stromatolites at Rasthof Farm are compatible with

an increasing hydrodynamic energy in the environment. The lack of direct, obvious external input of grains at Rasthof Farm suggests they were produced *in situ* as intraclasts. Vertical growths and intensification of branching upsection result from an increasing hydrodynamic energy associated logically with an increasing amount of intraclasts. Flows and currents probably forced the microbial communities to concentrate more vertically, creating different degrees of branching upsection. They ultimately did not manage to survive in the face of this changing environment and disappeared.

## 5 Discussion

### 5.1 Cap dolostone

Millimetric laminated fabric in carbonate rocks is often the result of microbial activity, or rapid sea level changes (e.g. tide) in shallow, quiet environments. The cap dolostone of the Rasthof Formation is not interpreted as such in the literature (Hoffman and Halverson, 2008; Tojo et al., 2007). No evidence for a microbial influence is observed, except locally in the Okaaru area. The flat laminae are not sufficient to interpret a very shallow-water environment (sabkhas, tidal flats, inter to supratidal) because more features would be expected (e.g. evaporites, mudcracks implying subaerial exposure). In the Okaaru area, one feature is possibly suggestive of subaerial exposure (Figure 5.29.C), but more observations are required to confirm this unusual interpretation of the cap dolostone. Other typical environments for laminated carbonate are deep-water, associated with turbidites. Hoffman and Halverson (2008) illustrate extremely common allodapic beds in the cap dolostone (abiotic member), without precision about the depth at the time of deposition, on the other hand Fox et al. (date unknown) suggest a typical shallow and warm water environment. At the visited sections, allodapic beds are rather rare and there is little evidence to support these features as deep-water turbidites. They might result from the settling of mud resuspended across the platform after storms or seismic shock. The water depth at the time of deposition is difficult to evaluate, but local bedforms that are not associated with turbidites inform that hydrodynamic energy was locally present.

After distal argillites, the cap dolostone is thought to record the deepest facies of the Rasthof Formation. Upsection, facies of the Rasthof Formation are getting shallower until the emersion of the platform (Hoffman and Halverson, 2008). If the cap dolostone records 1) some hydrodynamic energy such as storms (Rasthof Farm); 2) possible microbial activity (Okaaru area) and 3) if the non-laminated, so-called allodapic beds are the result of settling from resuspended mud instead of deep-water turbidites, there is some implication for the amplitude of the post-glacial sea level rise.

## 5.2 Microbial member

Deformation abundance, scale and style change greatly between MM1 and MM2. Deformed sets of laminae in MM1 are common and generally dm–m-thick. This thickness limits the degree of contortion. In MM2, the much rarer deformed sets of laminae are only a few cm-thick, allowing a greater contortion and rolling of the rubbery mats, sometimes leading to their break-up (Rasthof Farm). The process of deformation remains unclear: seismic shocks represent a solid candidate but the style of deformation does not compare well with other analogues (section 4.2.1). Fluid escape, as suggested by Pruss et al. (2010) and Bosak et al. (2013b), does not appear to account as a trigger for deformation (Chapter 4 and section 4.2.1). Even though wave percussion and elevated hydrodynamic energy, is preferred herein and by Le Ber et al. (2013), it should be noted that many of the features expected to be produced by such processes in mats exposed to flow (e.g. abundant fragments) are not observed (Bosak et al., 2013b and references therein). The stress that deformed the mats is still enigmatic.

The reason for different abundance and styles of deformation is uncertain. Different rheologies might be attributable to varying water content of the sediments. At the time of deposition and deformation, MM1 was probably more saturated in water than MM2, favouring deformation of thicker sets of laminae. The structure and framework of the microbial sediments was also possibly more rigid in MM2 than in MM1, allowing only the shallowest laminae to be peeled from the seafloor and limiting the overall deformations in MM2. The building of several dm-thick non-deformed growths in MM2 (Rasthof Farm) illustrates the rigidity of the facies.

At Rasthof Farm, just below MM2, distinct cones are observed in MM1. The latter indicate a greater resistance to stress (possibly hydrodynamic stress) than the underlying repetitively deformed mats, and the beginning of vertical accretion. In MM2, these more resistant facies associated with high hydrodynamic levels in the environment led to the development of the vertical growths (Figure 5.35). Roll-up structures are still present between the vertical growths. This indicates a different behaviour of the microbial communities or the cohabitation of two different types of microbial communities controlling the development of 1) individual growths; and 2) bridges with local roll-up structures.
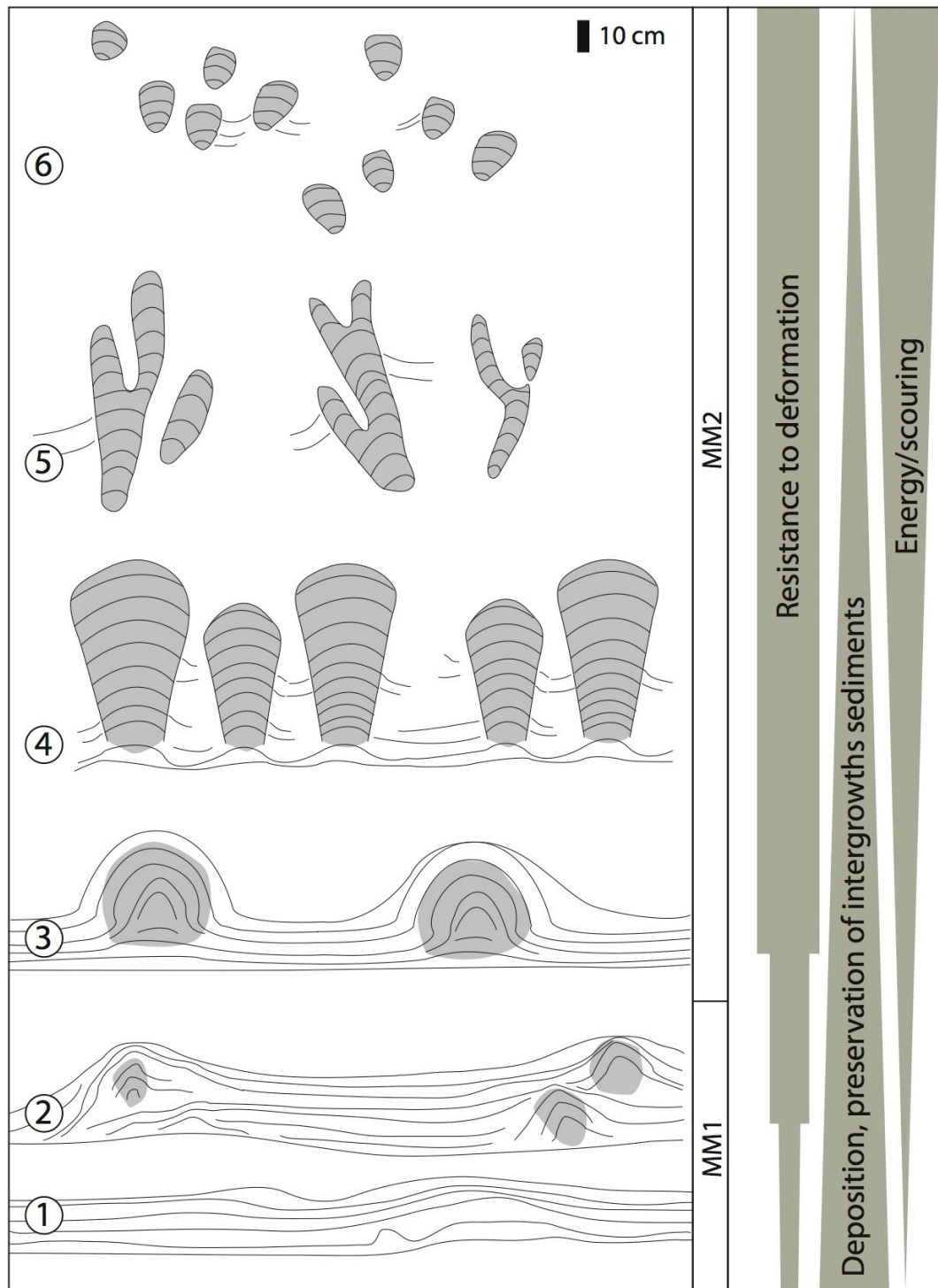
Figure 5.35: Idealised section of individual stromatolite growths, Rasthof Farm. The chaotic mats of MM1 (1) start to rise and form cones (2). Then in MM2 the supposed increasing hydrodynamic energy led to the formation of domes (3), columns (4) and different degrees of branching columns. A different rheology between MM1 and MM2 can explain why such geometries formed without being deformed. From the base to the top of the visible MM2, the bridges and laminae between the growths tend to disappear to give place to intraclasts.

The concepts of sublittoral, sub-storm or deep-water give only a poor constraint in term of water depth. The microbial facies of the Rasthof Formation seem continuous over a large area and were deposited in a platform setting. Hoffman and Halverson (2008) described the Rasthof Formation south of the Kamanjab Inlier where facies are dominated by allodapic limestones, turbidites, debris flows and argillites (Summas Mountains); coarse debris flows with intraclasts of microbialites and angular oolitic blocks (Fransfontein ridge). On the platform, the microbial member should logically be relatively shallower. The most significant facies variation observed is the diversity of individual growths found at Rasthof Farm, compatible with hydrodynamic energy in the environment. The Okaaru and Omutirapo areas may record relatively deeper settings since such vertical growths are lacking, or maybe they have not been observed. If the facies do not change a lot between the visited areas, it can be because the environments of deposition do not vary significantly across the platform or because the sections are located almost along strike of a slope.

## 5.3    Petroleum potential

In a post-glacial setting, source rocks "hot shales" can accumulate in the depressions, incisions and basins (Lüning et al., 1999, 2000) flooded by the sea level rise. Bechstädt et al. (2009) suggested that this hypothesis might apply to Neoproterozoic glaciations (and specifically to the cap carbonates of the Maieberg Formation which overlies the Ghaub glacials in northern Namibia). A problem with the Rasthof Formation is that no shales are reported at all at the base of the cap carbonate sequence on the platform. This limits analogies with well-understood Phanerozoic post-glacial settings and potential source rock deposits. Source rock potential of the cap dolostone and overlying microbial facies is fairly low with TOC values ≤ 0.1% on the collected samples. These low values might reflect the long history of these rocks that underwent diagenesis and weathering. But what if the TOC was never present at elevated levels at the time of deposition? In this scenario, no restricted basins with limited circulation were present on the platform, as envisaged by Bechstädt et al. (2009). In which case anoxia setting favourable to the accumulation of organic rich sediments was not present, explaining the global low TOC values.

The Rasthof Formation may however represent a potential reservoir, or at least an analogue to study fracture patterns in massive microbial facies. The > 100 m-thick microbial member is characterised by a dense vertical fracture pattern associated with horizontal layer-cake bedding. At the outcrop, fractures can be dm wide. Fracture network is so dense that the outcrops often consist of closely spaced blocks rather than continuous layers. This pattern is visible on satellite pictures with a good resolution.

## 5.4 An attempt to explain the layer cake aspect

Vertical continuity of the exposure at Rasthof Farm (Figure 5.36.A.B) allows the verification of a thinning-upward trend in the microbial member. The thicknesses of the beds were not measured on the field because the bedding is difficult to see on the outcrop. On a selected picture from one outcrop, 28 beds were traced and measured (arbitrary unit, Figure 5.36.C, D). The Spearman's rank correlation coefficient allows verifying if there is a trend in bed thicknesses variation (Swan and Sandilands, 1995).
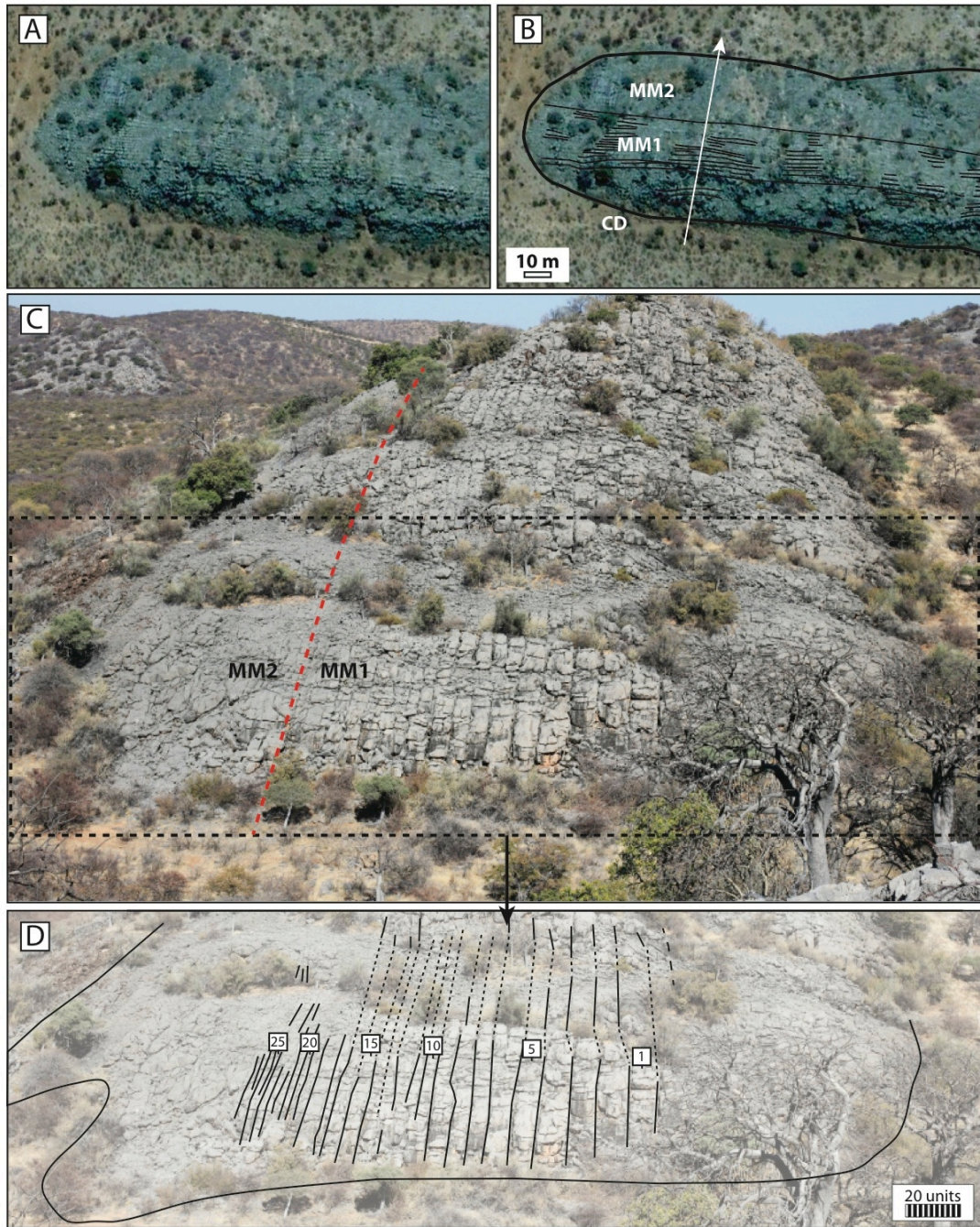
Figure 5.36: Layer cake aspect of the Rasthof Formation, Rasthof Farm. **A**. Satellite image (© 2013 DigitalGlobe; © 2013 Google; © 2013 Cnes/Spot Image). **B**. division into members. Note the thicker beds allowing the differentiation between MM1 and MM2. **C**. Photography of the outcrop (left: top, right: bottom). **D**. Numbered beds used to demonstrate there is a thinning-upward trend. Beds might be still present towards the top of the outcrop but their reduced thickness make them indistinguishable with the dense fracture pattern.

The two hypotheses are:

**H₀**: no trend of change in bed thicknesses.

**H₁**: beds become thinner/thicker.

Spearman's rank correlation coefficient **r'**:

$$r' = 1 - \frac{6\sum_{i=1}^{n}(i - R(h_i))^2}{n(n^2 - 1)}$$

Where **h$_i$** is the thickness of the **i$^{th}$** bed, and **n** is the number of beds.

The table used for the calculation is presented in Appendix B. Here, $|r'| = 0.94$. For *n*=28 and α= 5%, the theoretical R=0.33.

At Rasthof Farm, $|r'| > R$, *H₀* is rejected, beds are becoming thinner.

The origin of the layer cake aspect of the outcrops is enigmatic. No changes of lithology are observed at the interface between two beds. But sediments are fairly old carbonates, possibly limiting the preservation of all the features initially present. A different lithology at the interface between two layers might have been dissolved, removed or compacted. It is demonstrated that the beds are thinning upward. A regional phenomenon must have created such bedding. A suggestion is that these beds result from cycles of the relative sea level. Each layer represents one of these cycles, a competition between accommodation and sedimentation (Figure 5.37).

The thinning-upward trend is compatible with the accumulation of sediments in a high stand system tract. The post-glacial transgression on the craton recorded the maximum flooding surface, possibly at the very base of the cap carbonate sequence (Hoffman and Halverson, 2008). The maximum flooding is followed by the high stand system tract recorded by the Rasthof Formation. The sequence boundary is documented by shallow-water facies and a subaerial exposure of the platform (Hoffman and Halverson, 2008). The high stand system tract followed the increasing

relative sea level. Layer cake aspect results from a "catching-up" microbial member. At each rise of the relative sea level, microbial communities did not follow immediately, marking the top of one layer. The high stand system tract was aggrading during the deposition of MM1. Thinning upward of the beds in MM2 might record the progradation of the sediments.
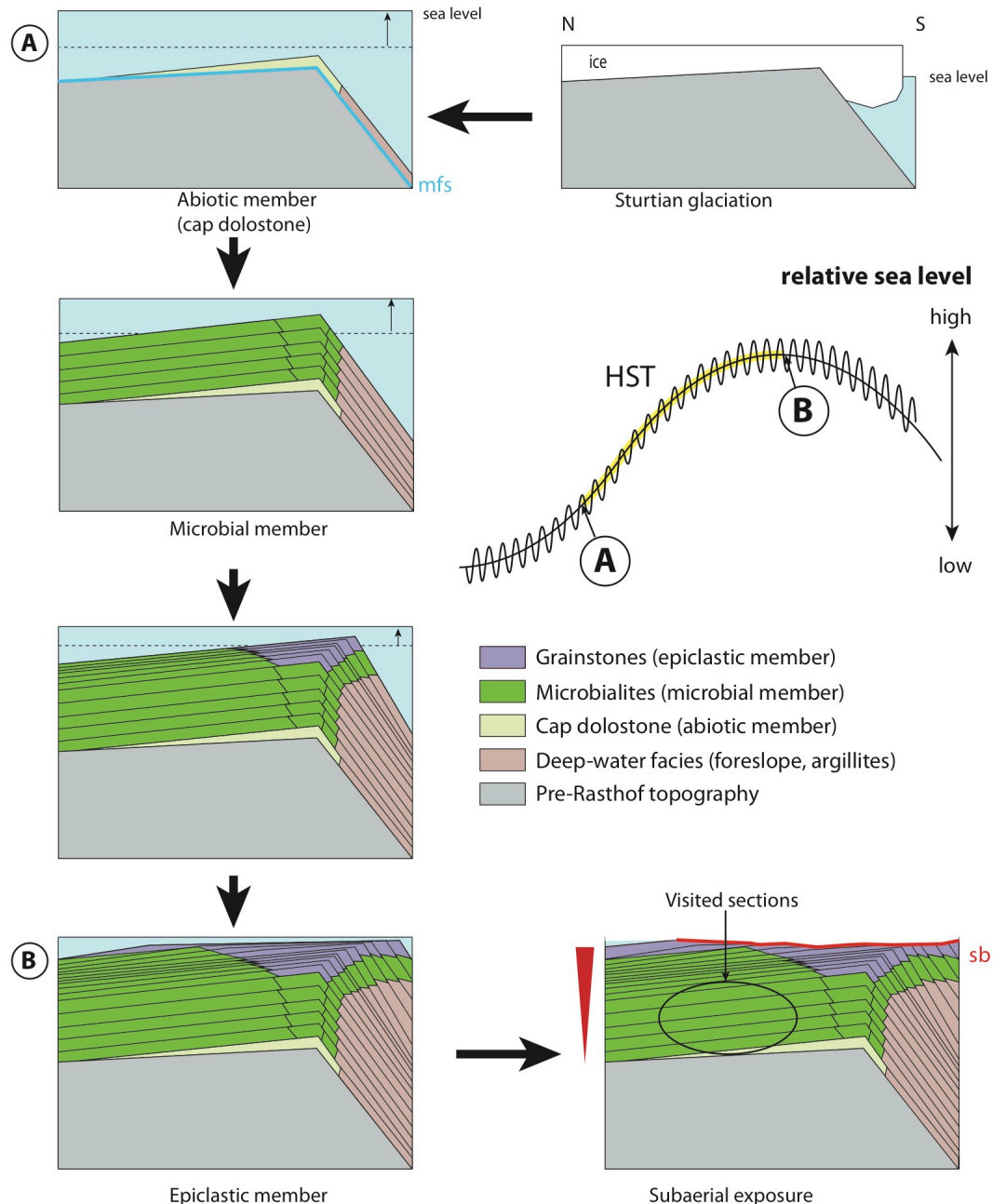


Figure 5.37: The Rasthof Formation as a highstand system tract (HST). After the glaciation, the sea level rose (A) creating the maximum flooding surface (mfs). From then, sea level continued to rise but always balanced with the cratonic rebound, creating continuously shallower facies upsection (B). The top of the HST is marked by a sequence boundary (sb) and a subaerial exposure of the platform.

# 6    Conclusion

On the Northern Platform, the global lateral continuity of the facies observed over tens/hundreds of kilometres suggests a relatively homogenous environment in the aftermath of the Sturtian glaciation. The homogeneity of the facies found in the Rasthof Formation could mean they were formed along strike of the dipslope, limiting observation of laterally deeper/shallower facies. The facies observed are likely to be subtidal. Despite the lack of classic sedimentological evidence for hydrodynamic energy in the environment, this possibility cannot be ruled out (Le Ber et al., 2013): evidence for wave action such as bedforms or scour marks are lacking, but the nature of the sediments probably inhibited their formation.

MM1 is constantly deformed, the general lack of intraclasts might be due to the thickness of deformed sets of laminae, that limited their break-up. Also, hydrodynamic stress was not constant at the time of deposition. Above MM1, the local development of individual stromatolite growths associated with intraclasts in MM2 confirms more constant energy in the environment, at least in the upper part of the microbial member of Rasthof Farm. Here, hydrodynamic stress allowed the formation of intraclasts because the disturbed sets of laminae were thin and more likely to break compared to MM1. MM2 is in turn followed by the epiclastic member and an emersion of the platform (Hoffman and Halverson, 2008). The lack of classic shallow-water facies in the microbial member reflects the complexity of the environment at that time, with no obvious grains input and continuous, cohesive microbial mats.

# Chapter 6 – Microfacies of the Rasthof Formation

## 1    Introduction

In the Rasthof Formation, field observations are limited by recrystallisation, weathering and karstification. These effects preclude the recognition of allochems, and obscure textures, and thus detailed microscopy is essential. In this chapter, a microscopic approach is adopted to shed light on microfacies. All the facies described in Chapter 5 were sampled for microscopy, including cap dolostone and both microbial members at each of the three study areas (Rasthof Farm, Omutirapo and Okaaru).

Microscopic analyses in Cryogenian carbonates are comparatively few and most of them have a micropaleobiologic or diagenetic approach. The first approach reveals poorly understood fossil types in abundance (e.g. Knoll et al., 2006). Putative eukaryotes associated with microbial mats have been described from the Rasthof Formation (Bosak et al., 2012, 2011; Dalton et al., 2013; Pruss et al., 2010). These putative life forms are typically observed with a classic microscopic (optical) approach complemented by scanning electron microscopy with associated elemental mapping to strengthen the interpretation of a biologic origin. The diagenetic approach is also a major component of petrographic analyses in Neoproterozoic carbonates. Dolomites are considered to be more common than limestones during the Precambrian (Tucker, 2001) and this is verified in the Rasthof Formation. A major interrogation is whether dolomite results from primary precipitation, and from which processes. The answer to this question remains unclear but Cryogenian examples for possible primary dolomite include the Rasthof Formation (Tojo et al., 2007) and the Oodnaminta Reef Complex in Australia (Hood and Wallace, 2012). Both suggest possible syn-sedimentary precipitation of the dolomite, directly from the seawater. Yet, the exact rationale for a primary precipitation remains speculative. Above authors invoke low sulphate concentration as well as elevated Mg/Ca ratio in Neoproterozoic seas (Hood et al., 2011; Tojo et al., 2007), or possibly microbial sulphate reduction processes (e.g. Deng et al., 2010; Wright and Wacey, 2005).

The aim of this chapter is not to demonstrate if the above processes apply, or to detail the diagenetic history of the Rasthof Formation. The aim is to use petrographic descriptions to extract pertinent textural detail of primary sedimentary origin from otherwise macroscopically monotonous facies. These details are expected to shed light on depositional processes. Samples selected in the field were prepared for microscopic descriptions. Analyses consist of petrographic study, using the "white paper" method (WP) (Delgado, 1977), plane polarised light (PPL), cross polarised light (CPL) and cathodoluminescence (CL). After basic observations under PPL and CL, some outstanding samples were examined under UV light. This technique, however, did not produce good quality images. Some samples were also analysed using the scanning electron microscope (SEM) to collect more information.

## 2    Material and method

## 2.1    Petrography

### 2.1.1    Sample preparation

First, samples were cut with a saw for thin section preparation. Cut samples were then polished on a lapping machine at 250, 125 µm (diamond plates), then with a 25 µm powder. Thin sections are ~30 µm-thick both for classic petrographic analysis and CL. Specimens are not covered to allow their study under CL, UV and SEM. To differentiate potential limestone from dolostone, the Alizarin Red staining was performed on part of each thin section, taking care to reserve a non-stained part of the slide for CL, UV and SEM analyses. Prior to analysis, it was noted that none of the samples prepared with alizarin acquired a pinkish colour, indicating a general lack of calcite.

### 2.1.2    Image acquisition

Photomicrographs were obtained using a Nikon Microphot-FX, mounted with a Nikon DS Camera Head DS-5M and a Nikon Digital Sight DS-L1. Three different techniques were used to capture and illustrate the microfacies. The most common was plane polarised light (PPL) microscopy. As initial fabric and textures are dolomitised, another technique was adopted to mitigate this problem. A sheet of

white paper (80 gsm) can be placed under the thin section (Figure 6.1) to help highlighting the texture and fabric prior to dolomitisation (Delgado, 1977). This technique is referred as "WP" for "white paper" in the rest of the chapter.
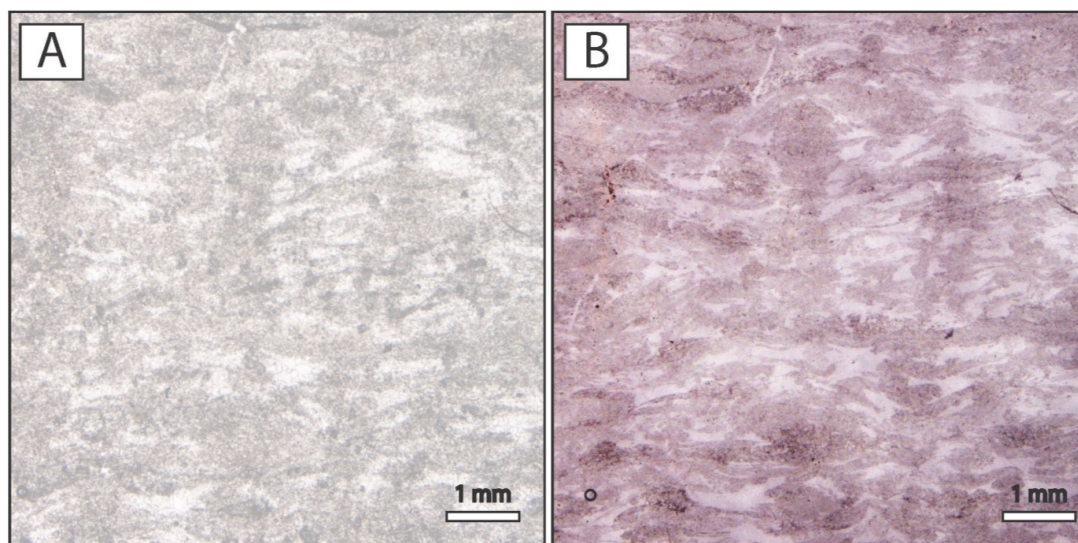


Figure 6.1: Plane polarised light vs. white paper technique. **A**. PPL picture of a thin section. **B**. Same area with a piece of white paper under the thin section.

CL image acquisition was performed with a Nikon Optiphot petrological microscope fitted with a Technosyn 8200 MkII luminoscope. For each area of interest, both CL and PPL images were captured for comparison. In this chapter, not all the members of the Rasthof Formation are equally illustrated with CL images. The cap dolostone and MM1 tend to have a poor range of luminescence, or crystals are so small that no distinction can be made. On the other hand, MM2 reveals exceptional level of details with this technique.

### 2.1.3    Image processing

The pictures were processed with Adobe Photoshop CS5. The aim of the processing was to adjust contrast, intensity and brightness to make colours and contrasts clearer. This technique applies to classic petrography but also to CL pictures where the luminescence can be extremely dull (Figure 6.2).
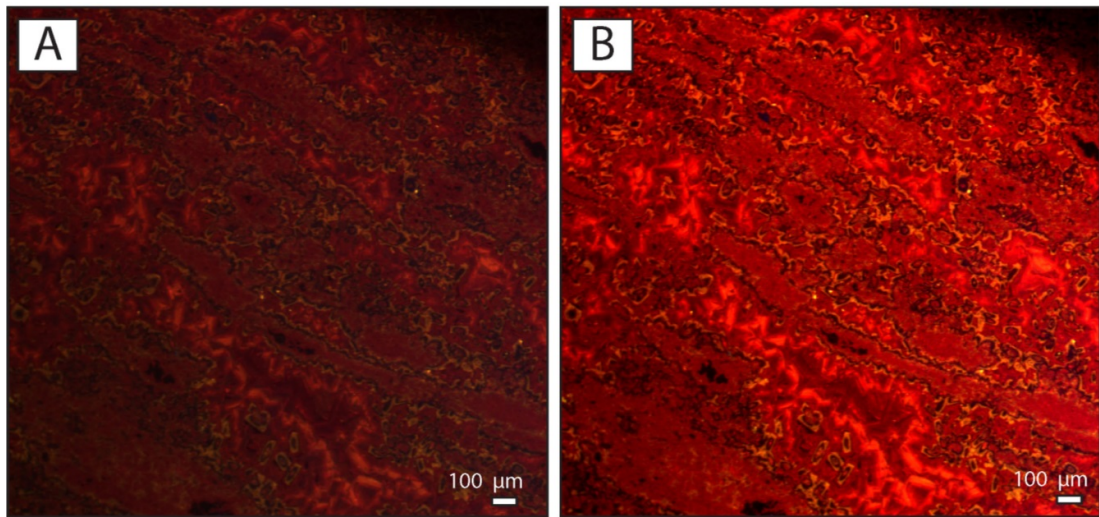
Figure 6.2: CL imaging. **A**. Before histogram equalisation. **B**. After histogram equalisation.

### 2.1.4    Description

The aim of the petrographic study is 1) to reveal primary textural characteristics and 2) to evaluate grains of possible biogenic affinity. Under a classic microscope (PPL, CPL), dolomite diagenetic textures are determined using the methodology of Sibley and Gregg (1987). If grains or intraclasts are observed; the Dunham (1962) classification can help to characterise the facies. Most facies are microbial, as explained in Chapter 5, and thus consist of "boundstones". More advanced classification exists for boundstone (Embry and Klovan, 1972) in which stromatolites of the Rasthof Formation classify as framestones or bindstones.

Multiple generations and growths of crystals are revealed with the CL technique (Boggs and Krinsley, 2006). Images allow to clearly distinguishing the boundary between the microbial framework and the primary voids; such boundaries are far less apparent using classic optical techniques where microbial laminae can appear very diffuse.

## 2.2    Scanning electron microscope

The scanning electron microscope used in this study is a Hitachi S3000N, used in back scattered electron mode operating between 10 and 20kV. Working with a SEM also allows energy-dispersive X-ray spectroscopy (EDX), which is used to have an elemental qualitative analysis of targeted grain or crystal. Analysed samples ranged from small rock fragments to uncovered thin sections.

# 3 Petrographic descriptions

## 3.1 Cap dolostone

### 3.1.1 General facies

In all three study areas, cap dolostone facies comprise alternating light crystalline laminae and dark fine-grained drapes (Figure 6.3). Light laminae can be partly micritic, sub-mm-thick and exhibit dolomitic cement. Dark laminae are much thinner (< 0.1 mm-thick) and made of a dense fine-grained material. Stylolites, with iron-rich residue, are quite common along the dark laminae. Laminated fabrics range from flat, undulating to irregular at the sub-mm-scale.

Dolomite recrystallisation has overprinted the initial facies to varying degrees. In light laminae, dolomites texture is variable. Commonly, unimodal, 10–30 µm wide planar-e crystals, forming a microsucrosic texture, are encased in a brick-shaped dolomite cement (Figure 6.4.A, B). The brick shaped cement is well illustrated in Figure 6.3.E. The concentration of euhedral rhombs in this cement varies between 20–90%. Another texture observed shows unimodal, 60–100 µm wide planar-s dolomite (Figure 6.4.C–F), with some crystals developed around cloudy, 10–40 µm diameter nuclei. In CL (Figure 6.4.E, F), the cloudy nuclei appear to be angular crystals, comparable to the rhombs observed in the microsucrosic texture (Figure 6.4.A, B). Note that both euhedral and subhedral dolomite textures can occur on the same thin section (i.e. a few centimetres apart from each other).

Clasts, ghosts of clasts (section 3.1.2), and ovoid geometries (section 3.1.3) are quite common in the cap dolostone. Their micritic aspect classifies them as peloids. More rarely, possible walled ovoid shapes are recognised: these are found alone or in small groups of 2–6. They are often concentrated towards the base of a single light lamina.
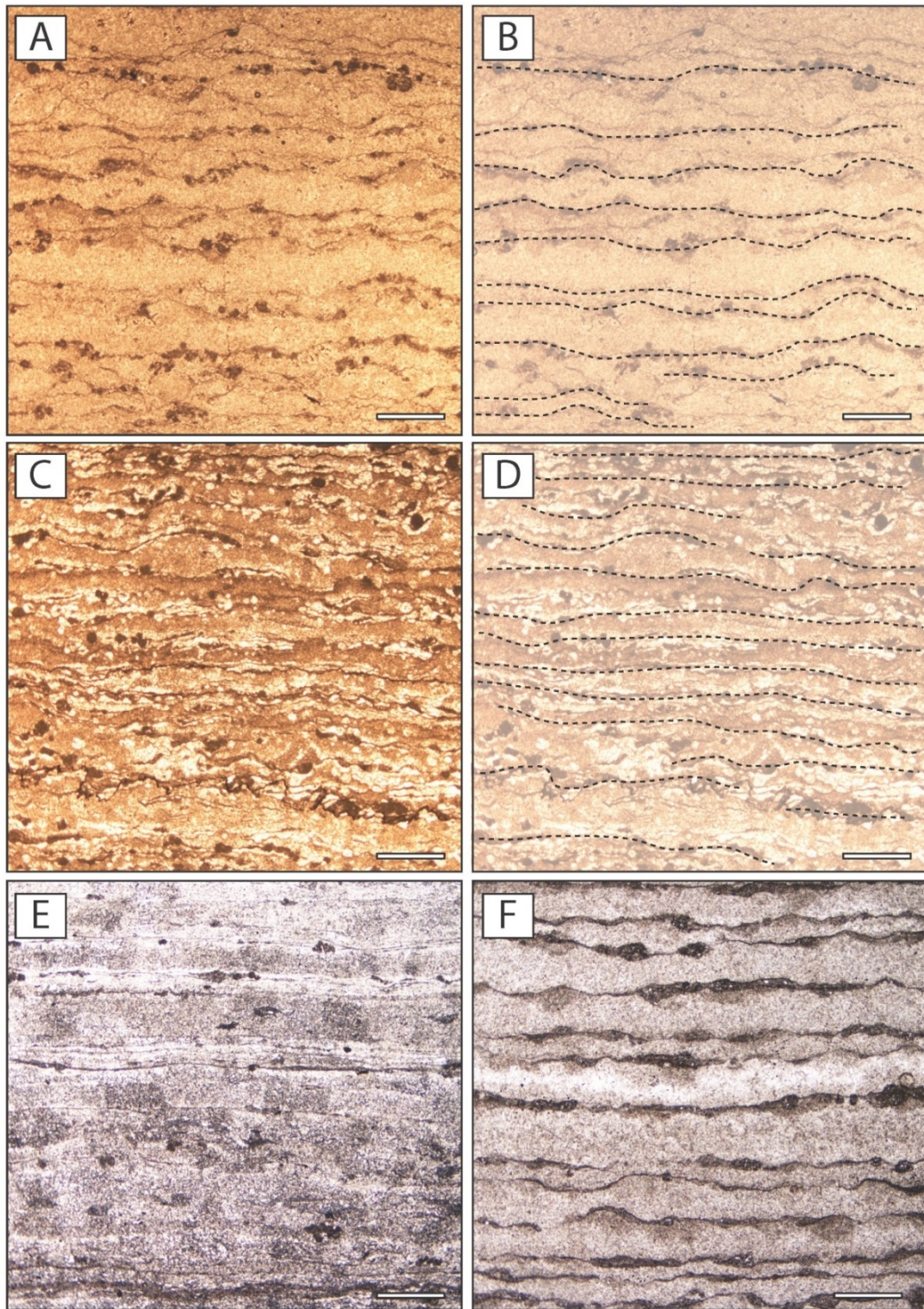
Figure 6.3: General cap dolostone microfacies. **A**. Rasthof Farm area. **B**. Laminated fabric in A, emphasised for clarity. **C**. Rasthof Farm area. **D**. Laminated fabric in C, emphasised for clarity. **E**. Omutirapo area. **F**. Okaaru area. Scale bars: 1mm.
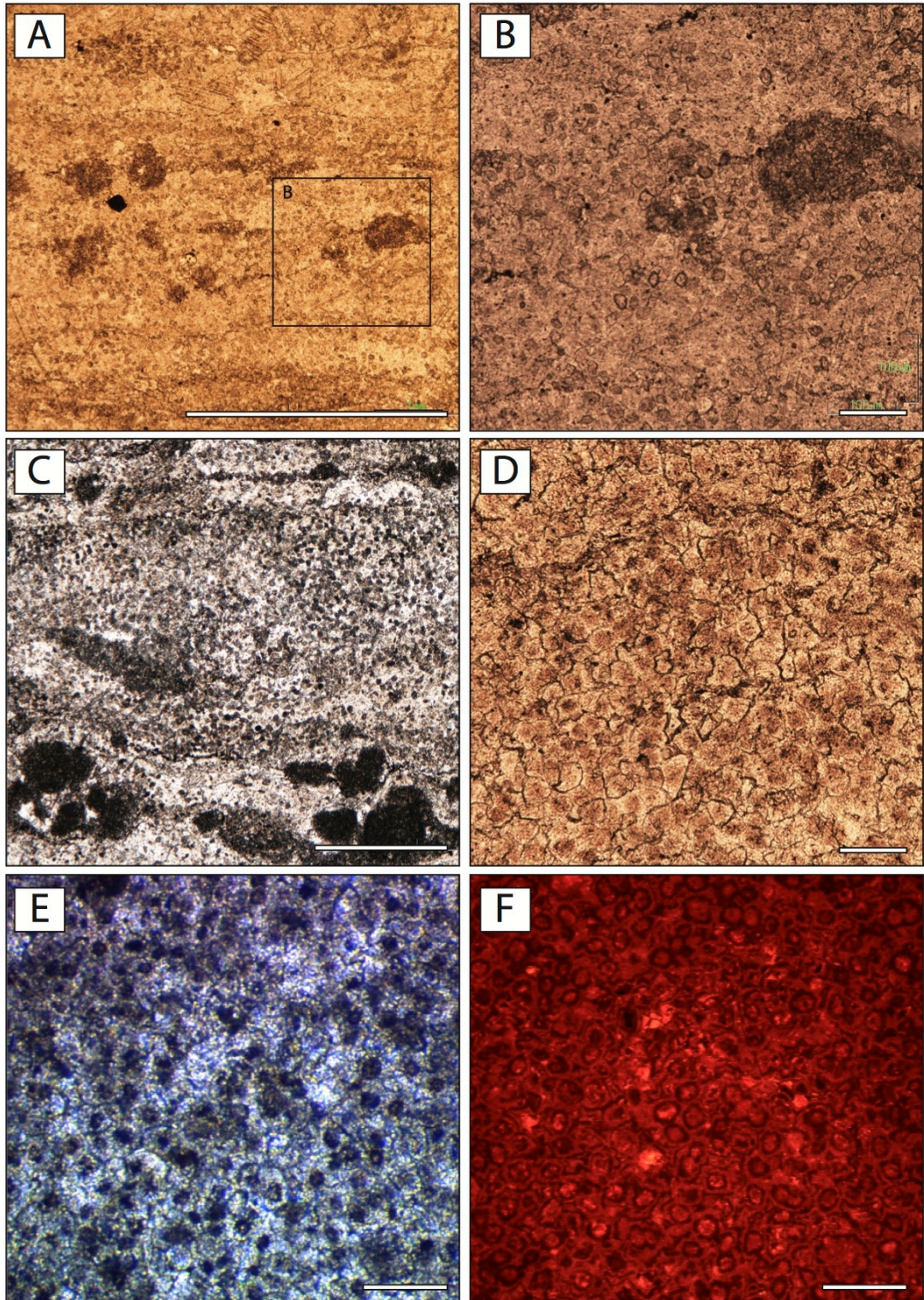
Figure 6.4: Dolomitic texture of the cap dolostone. **A**. Euhedral rhombs in a brick-shaped cement. Note the darker area corresponding to a "ghost" of a peloid, Rasthof Farm area. **B**. Detail of A. **C**. Similar to A but in the Omutirapo area. Note the peloids at the bottom. **D**. Cloudy nuclei in subhedral dolomitic texture, Rasthof Farm area. **E**. PPL and **F**. CL imaging of the dolomite texture with cloudy nuclei. Most of the nuclei have rhombic geometry. Scale bars: 1 mm (A, C) and 100 μm (B, D, E, F).

### 3.1.2    Clast-rich intervals

Several < 2 mm-thick intervals are grain rich (specifically ghost of grains), classifying them as microwackestones–packstones (Figure 6.5). These thin layers are extremely common through the cap dolostone of the Rasthof Formation. However, due to their thickness and the weathering, they are not obvious at the outcrop scale. Original aspect of the grains has been overprinted by dolomitisation. The resulting ghosts are 0.1–0.7 mm diameter and rarely exceed 1 mm.

Thicker, non-laminated intervals also occur at the visited outcrops. They appear as very fine-grained material (mudstone), typically condensed in < 10 cm-thick intervals. Petrographic analysis of these beds revealed microcrystalline dolomite, but no clasts or grains. However, thicker beds (20–50 cm), with similar muddy macrofacies observed in the Omutirapo area do preserve some lithoclasts (Figure 6.6.A, B). They have a very different texture from the thinner (mm–dm-thick) beds described above. They contain scarce, mm wide mud clasts in a muddy to crystalline matrix. These beds are sandwiched between laminites. The m-thick, clast rich turbidite observed by Tojo et al. (2007) and sampled in the Omutirapo area (Chapter 5, section 3.4.1) is similar though less muddy and with a higher grain content (Figure 6.6. C, D).
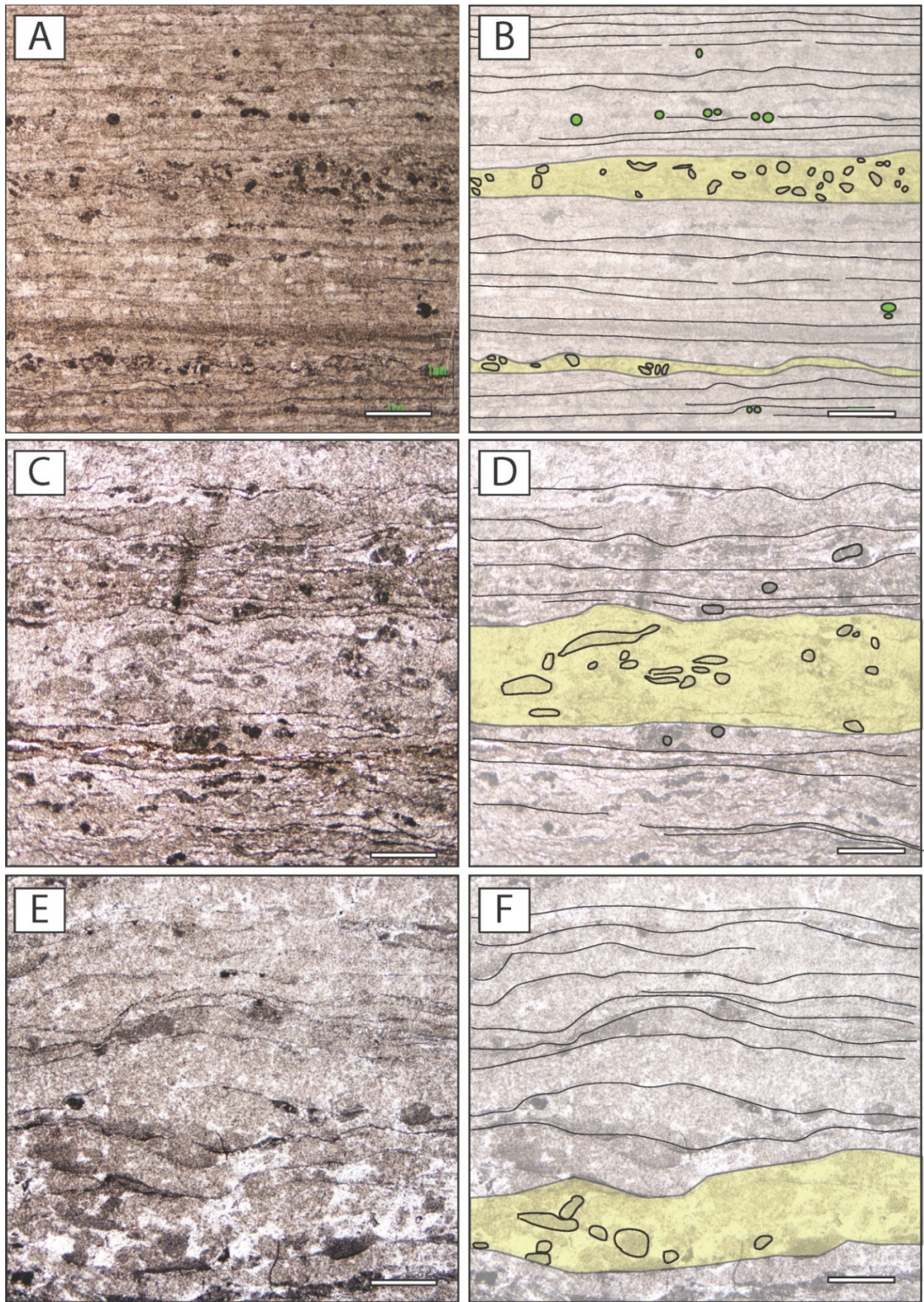
Figure 6.5: Clast rich intervals in the cap dolostone (yellow). Right column is the interpretation of the left one. **A** and **B**. Rasthof Farm area. **C** and **D**. Omutirapo area. **E** and **F**. Okaaru area. Scale bars: 1mm.
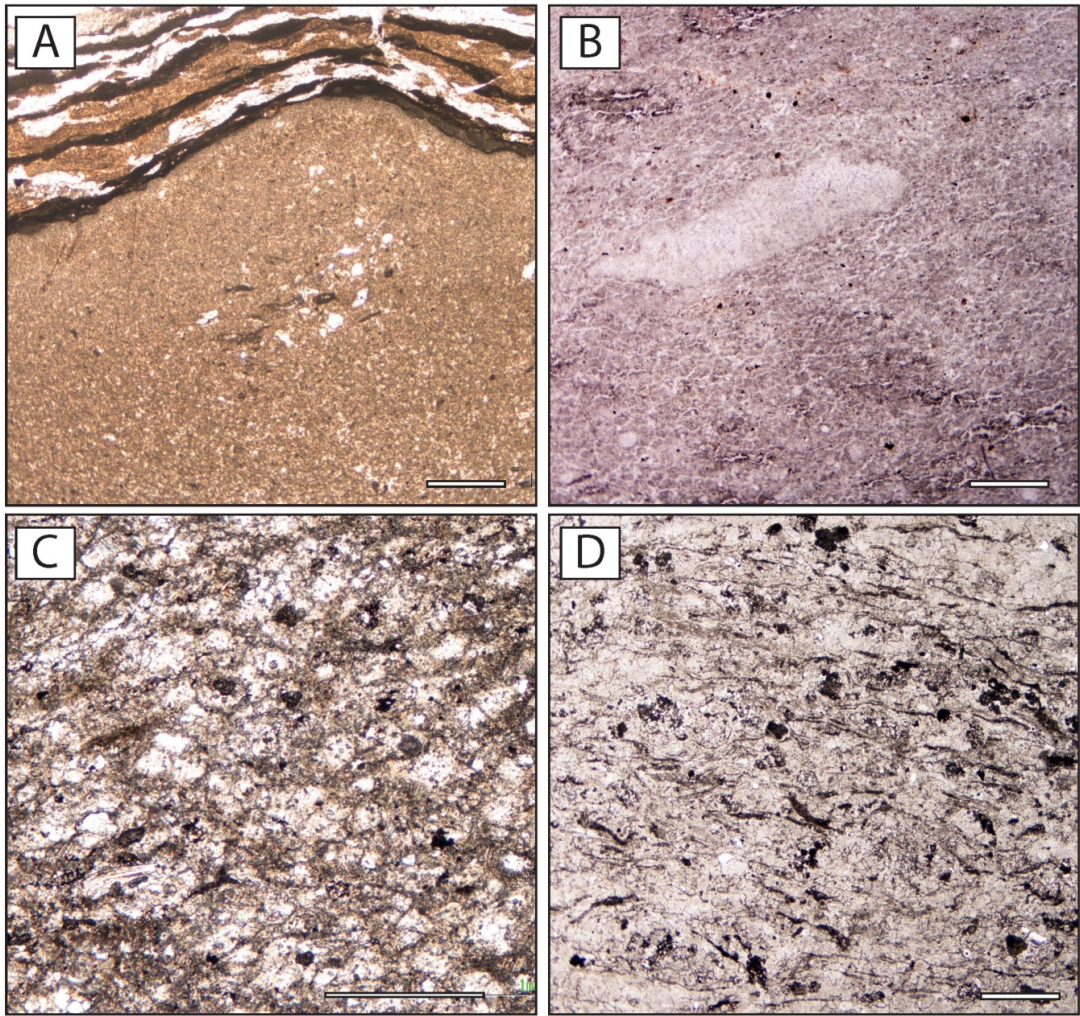
Figure 6.6: Non-laminated interval (A and B) and turbidite in the Omutirapo area (C and D). **A**. Top of a clast-poor non-laminated bed. Note the dark dolomicritic drapes at the top of the interval. **B**. Detail of one clast in the same interval. **C**. Coarse, grainy texture in the 1.5 m-thick turbidite. **D**. Clast-rich facies in the same bed as C. Scale bars: 1 mm.

### 3.1.3 Ovoid features

Scarce ovoid to well-rounded; sometimes apparently walled dolomicritic structures are observed in the cap dolostone, especially in Rasthof Farm (Figure 6.7.A–C) and Omutirapo areas (Figure 6.7.D–F). They are rarer in the thin sections from the Okaaru area but the cap dolostone is much thinner at this location (3 m) and was consequently less sampled. The peloids have an average diameter of 100 μm, but sizes vary between 60 and 140 μm. The oval to rounded peloids generally occur along one same interval, at the interface between two light laminae, they do not "float" in the cement and are often in contact with each other, in groups of 2–6. Where a wall is visible, it can be broken (Figure 6.7.E–F). Otherwise, the peloids exhibit compaction or distortion features. Tojo et al. (2007) refer to them as "clay galls" that "occur as spherical clusters". To better investigate these structures SEM analysis was attempted. Unfortunately, surface charging effects occurred almost universally inhibiting precise observations: even where no charging was apparent, no grains could be differentiated. Rock samples were also dissolved in HCl and HF but no peloids were preserved in the residue, meaning they were probably destroyed during the process.
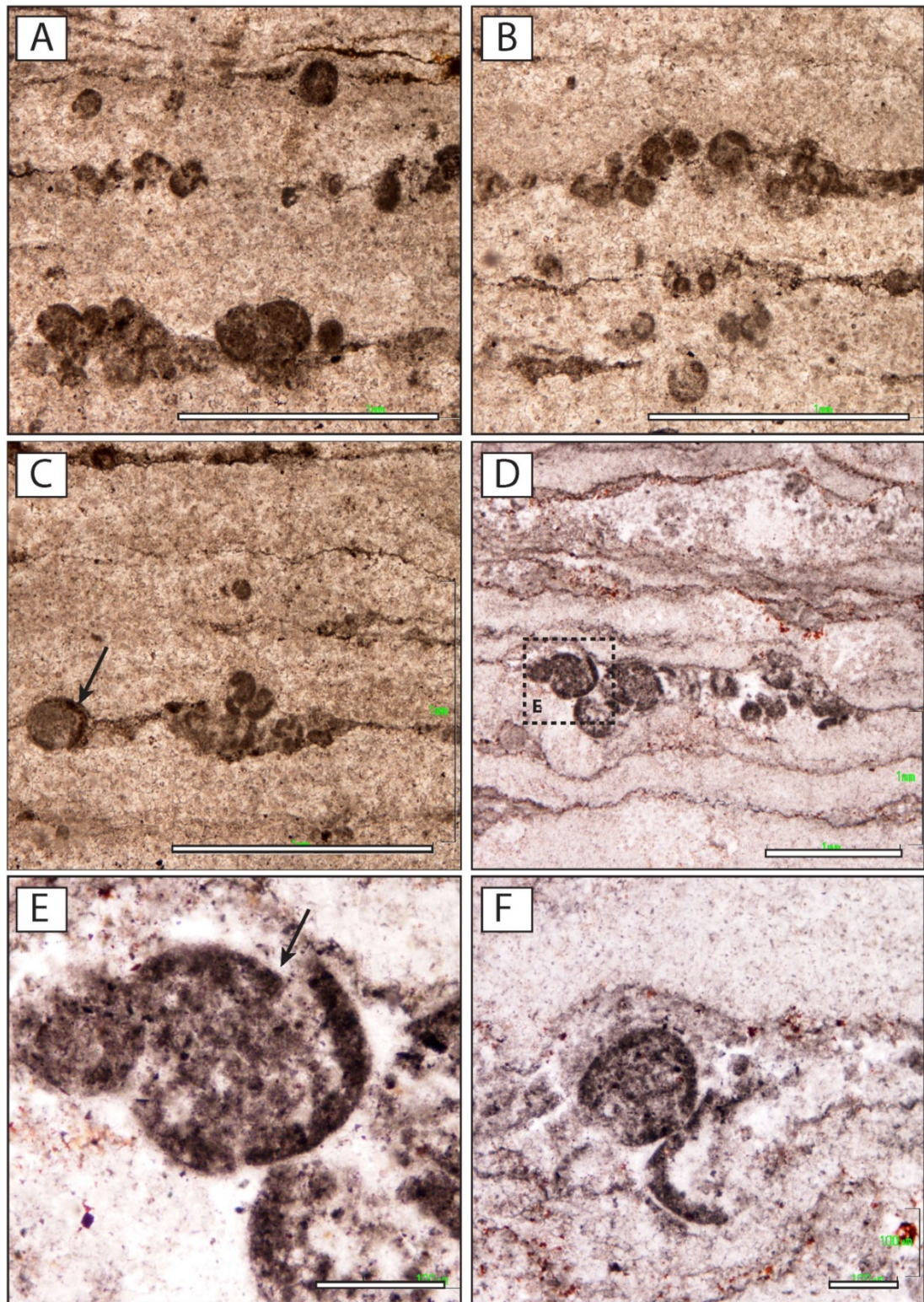
Figure 6.7: Ovoid features found in the cap dolostone. **A**, **B** and **C**. Rasthof Farm area. Note their concentration in specific intervals. **D**. Omutirapo area. **E** and **F**. Details. The arrow in E points at a broken wall. D, E and F. White paper technique. Scale bars: 1mm (A–D) and 100 μm (E and F).

## 3.2 Microbial member

### 3.2.1 Microbial member 1

The laminated fabric of the microbial member 1 consists of an alternation of relatively thick (1–5 mm) light cement laminae with thinner (< 0.5 mm) dark fine-grained laminae (Figure 6.8). In the light laminae, cloudy, < 100 μm dark rounded features are common (Figure 6.9.A, B). They are comparable to those observed in the cap dolostone (cloudy nuclei). At first inspection, some cloudy nuclei seem to have dark walls and light core. In detail, they reveal an angular light core (dolomite rhomb) with a darker fibrous overgrowth (Figure 6.9.B). Dark laminae are party clotted, creating subtle discontinuities to create a diffuse aspect. Laminae are locally broken, forming mm-sized intraclasts.

In the Omutirapo area, undeformed dome-like geometries are locally developed. The dome-like geometries are recognised as laminae that encrust a cm wide nucleus (Figure 6.8.D, E), resulting geometries appear as solid structures by contrast with the classic deformed facies of MM1. Similar apparently rigid structures developed at the top of MM1 at Rasthof Farm; the geometries point upward and do not exhibit chaotic folding. Dark fine-grained intervals in these dome-like structures of Omutirapo are often thicker, more diffuse, or more clotted than in the classic laminated facies of MM1, forming a continuous framework, both laterally and vertically. These dark laminae can also be broken and form mm large intraclasts. This microfacies is overall rare in MM1.

The effects of dolomitisation can be summarised as follows. Light laminae are now composed of subhedral dolomite crystals < 200 μm diameter, sometimes developing around the cloudy rounded features described above (Figure 6.9.A, B). The dark laminae are overprinted by a dolomicritic texture, with crystals < 10 μm. Light 100 μm long monoclinic crystals may locally occur in the dark laminae (Figure 6.9.C–E). EDX analysis performed on these crystals revealed the presence of O, Si, Al, K, Ca and Mg, by decreasing relative abundance.
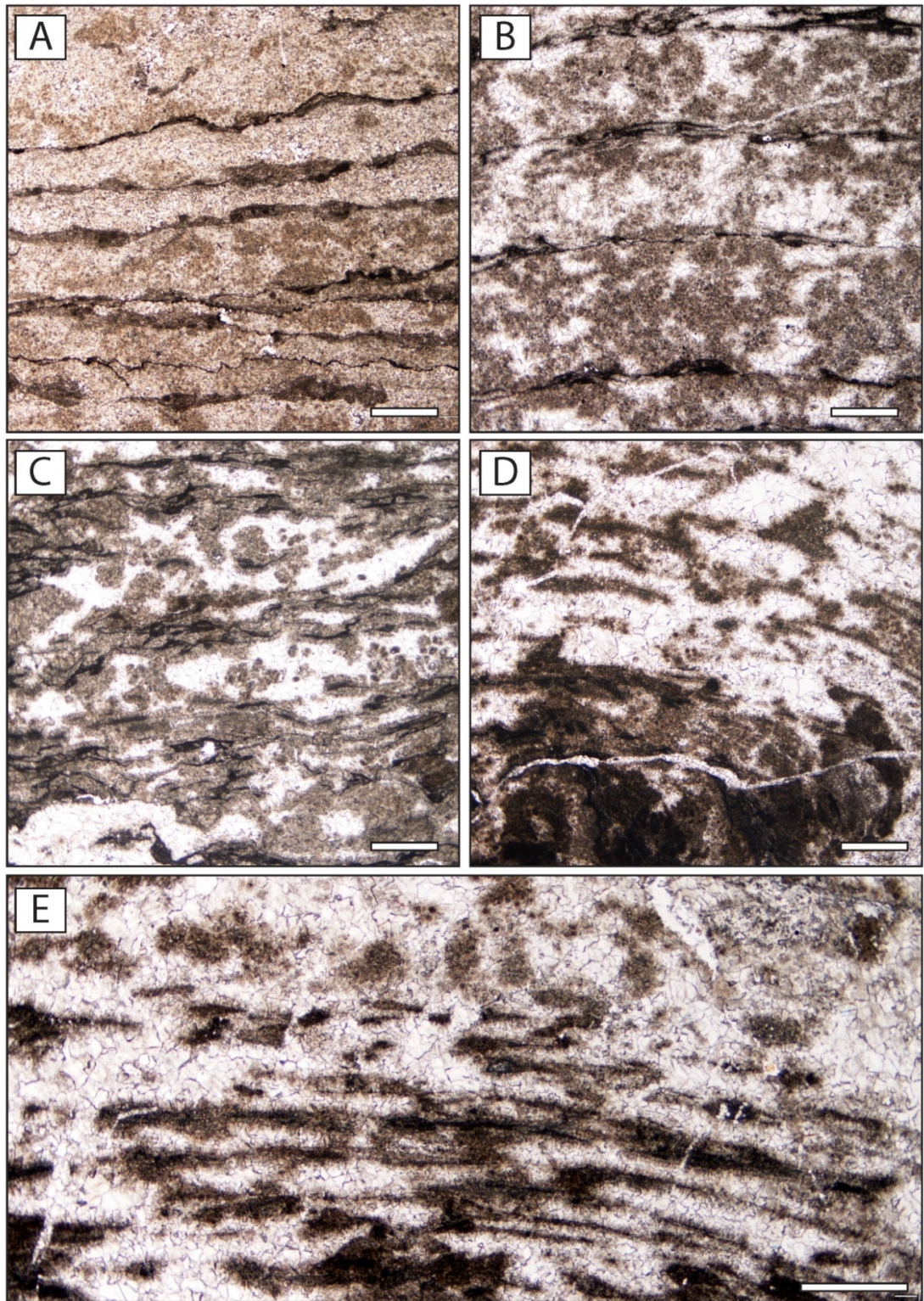
Figure 6.8: Microfacies of the microbial member 1 (1/2). **A**. Rasthof Farm area. **B**. Okaaru area. **C**, **D** and **E**. Omutirapo area. Darker laminae are partly clotted, discontinuous (C) or form a framework (D: Framework (top) developing around a nucleus (bottom), E: Lower half of the picture). Scale bars: 1 mm.
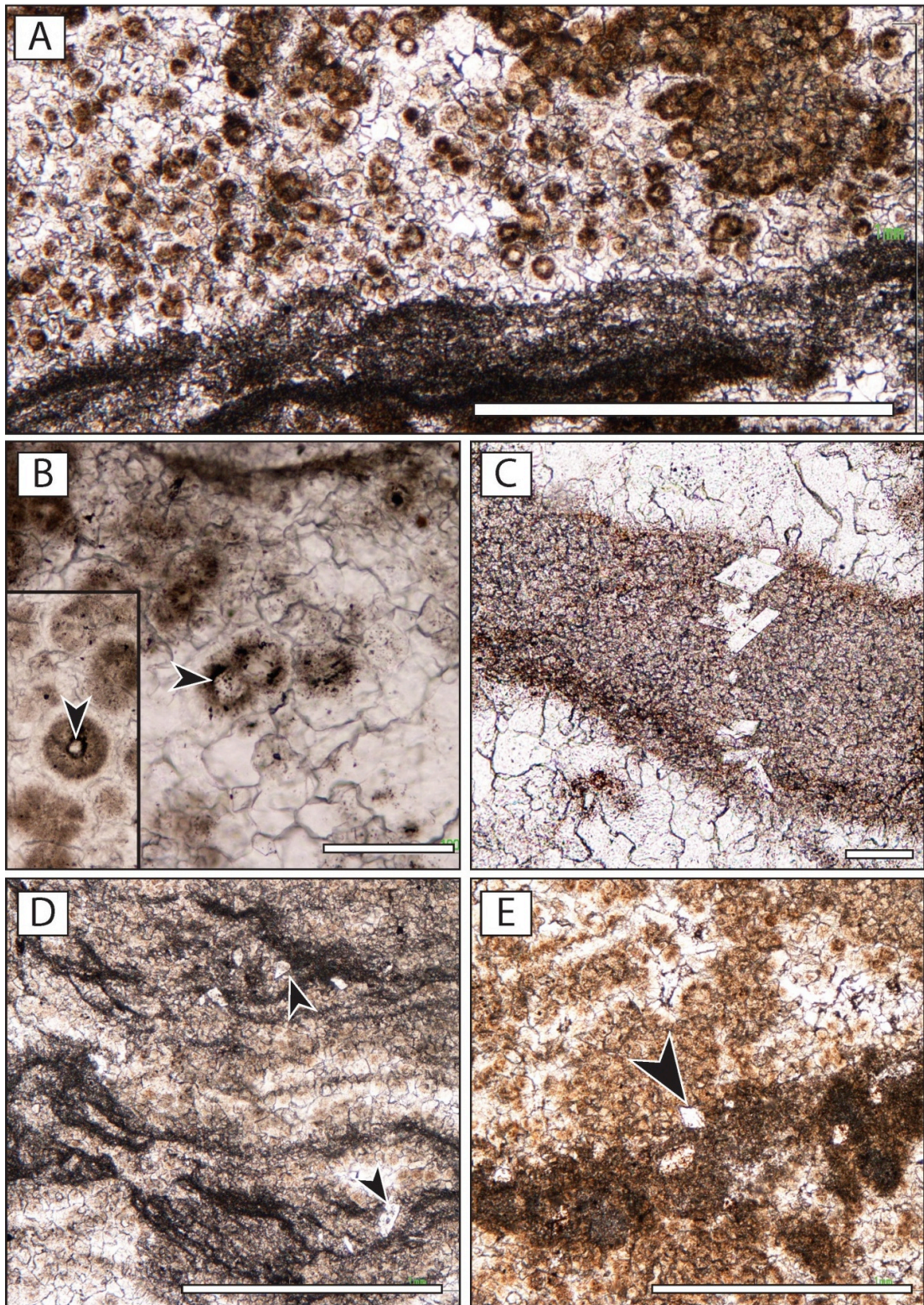
Figure 6.9: Microfacies of the microbial member 1 (2/2). **A**. Rounded features in the light laminae, Omutirapo area. **B**. Detail of a rounded feature, with euhedral rhomb in the centre. **C**, **D** and **E**. Monoclinic crystals in dark laminae, from Okaaru area (C), Omutirapo area (D), Rasthof Farm area (E). Scale bars: 1 mm (A, D and E) and 100 μm (B and C).

### 3.2.2 Microbial member 2

The macrofacies in MM2 is variable but dominated by thinly laminated microbial mats associated with roll-up structures (Hoffman and Halverson, 2008; Pruss et al., 2010). At Rasthof Farm, greater facies variations are recognised owing to the development of vertical growths. In the following, the flat-laminated and rolled-up facies are differentiated from the vertical developments of the Rasthof Farm. CL imaging is extremely useful for these facies because it emphases the sharp limits between the microbial mats and the filling of the many voids observed. Such voids were globally absent in the cap dolostone and MM1.

### *3.2.2.1 Thinly laminated facies*

The microbial member 2 is generally thinly laminated at the outcrop, and the corresponding microfacies differs greatly from MM1. The well-defined alternation of light and dark laminae is absent at this level. Instead, dark fine-grained (< 10 µm ø grains) laminae and clots are dominant, forming a dense and continuous framework (Figure 6.10.A–C), yet the laminated trend is still observable. The effects of dolomitisation occlude sedimentary textures in PPL, but the WP technique greatly emphases textural contrasts, allowing fine-grained laminae, clots and void cements to be distinguished. Voids are common throughout but are larger adjacent to roll-up structures (Figure 6.10.C, D). These textures are also clearly observable using CL images, revealing fine-grained mats/clots together with multiple phases of void-filling cements. In CL, the mats and clots comprise 60–100 µm long, agglutinated ovoid features. These are better observable in the vertical growths of MM2, where they also occur apparently isolated in the voids, not far from the mats. The table below (Table 6.1) lists the different main phases of cement observed. In detail, many sub-zonations can be distinguished (Figure 6.10.D–F).

Table 6.1: Different cementation phases observed in MM2, thinly laminated facies.

| Facies | Phase # | Cement shape | Luminescence |
|---|---|---|---|
| Fine-grained mat | 1 | Fine dolomite | Brownish/red dull |
| Edge of fine-grained mat | 2 | Syntaxial cement | Yellow |
| Void filling | 3a | Equant overgrowth, drusy | Dark red |
| | 3b | Equant overgrowth, drusy | Light red |
| | 4 | Xenomorphic cement | Dark red |
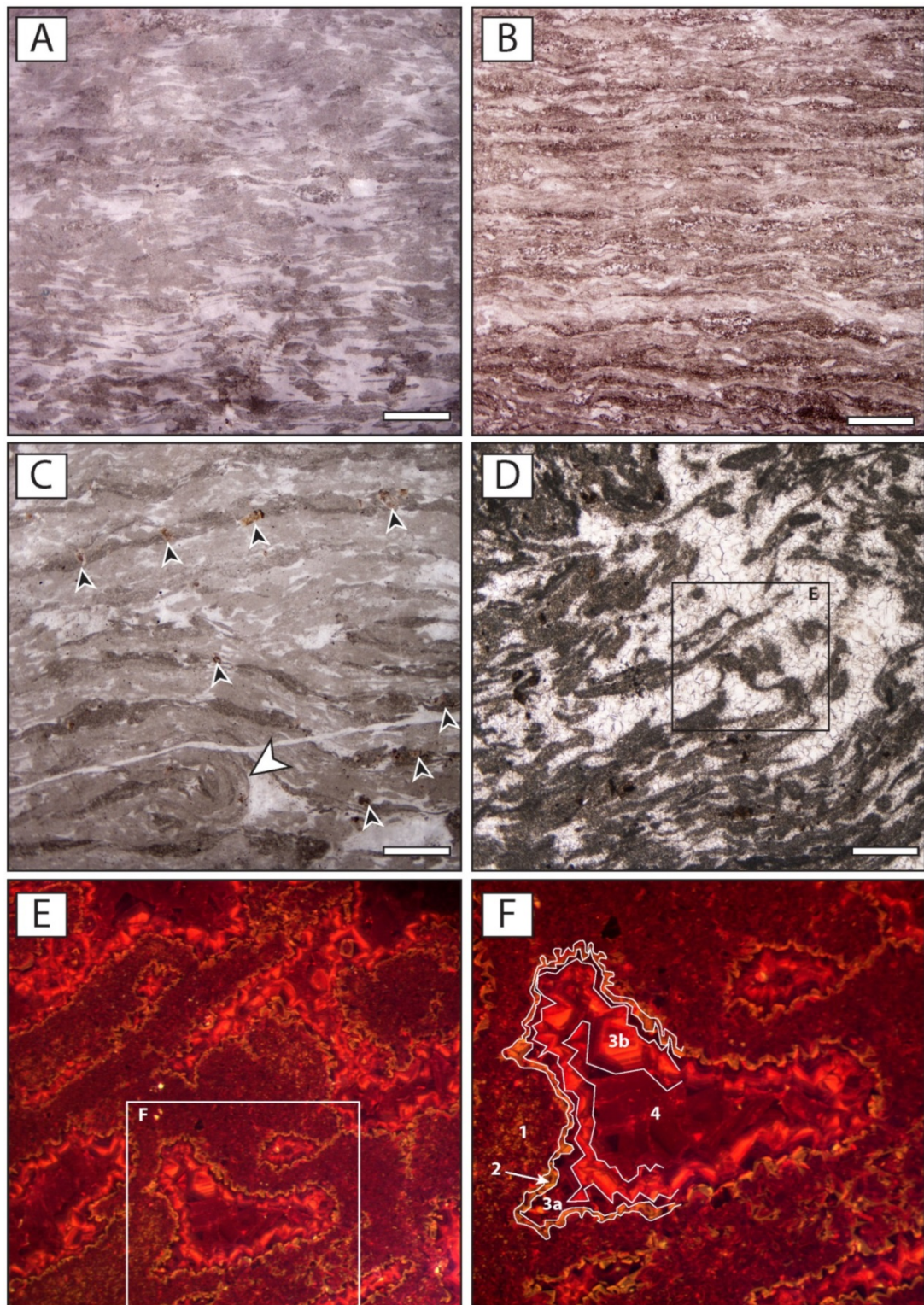
Figure 6.10: Microfacies of the microbial member 2, thinly laminated facies. **A**. Omutirapo area. **B**. Okaaru area. **C**. Rasthof Farm area. Note the rolled lamina (white arrow) and cement voids. Note also the rectangular brown crystals (black arrows, details in Figure 6.11). **D**. Broken laminae in a roll-up structure with mm wide voids. **E**. CL image of D, note the clear boundaries between the mats (dull brown) and cement-filled voids. **F**. Detail of E, with the different cements growing in the void (see Table 6.1). A, B and C: WP technique. Scale bars: 1 mm.

Polished slabs of rolled up facies from the Rasthof Farm reveal the occurrence of crystals that are white and soft, soapy. They are concentrated in the darker laminae only, and appear orange to brown (Figure 6.10.C; Figure 6.11) in petrographic study (PPL), with a low birefringence (CPL). No obvious cleavage is distinguishable and they tend to be rectangular, maximum 300 µm long and 100 µm large. Finally, they cut through the dolomite texture. EDX analysis indicates that the crystals are made of Si, O, Al, Mg, Cl, Ca, by decreasing relative abundance.
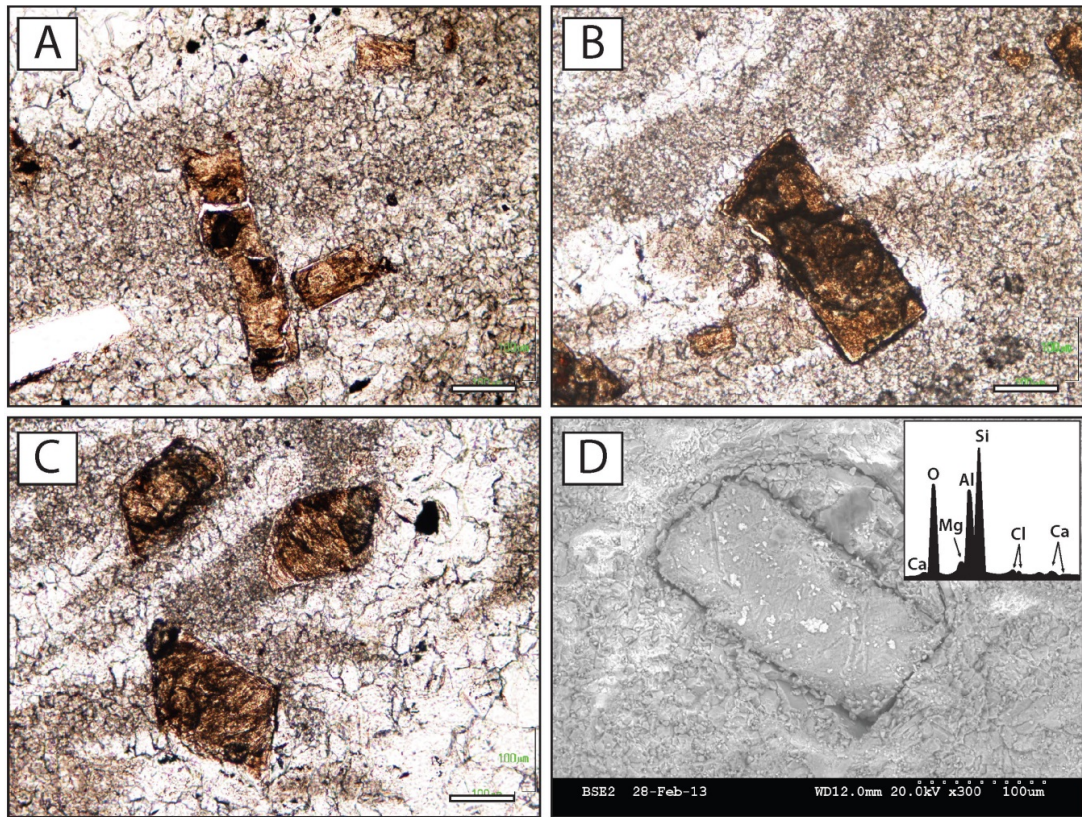


Figure 6.11: Unidentified crystals in the thinly laminated facies, Rasthof Farm area. **A** and **B**. Typical rectangular geometry of the crystals. Note in A, a rectangular white gap in the bottom left corner. The gap results from the destruction of a crystal during the preparation of the thin section, illustrating the softness of the crystals. **C**. Different sections through the crystals. **D**. SEM image and EDX of one crystal. Scale bars: 100 µm.

### 3.2.2.2 Vertical growths and intergrowth sediments.

Different degrees of branching/vertical growths were described by Le Ber et al. (2013) and detailed in Chapter 5. These include dm high domes, columns and branching columns. In thin section, several sub-mm to mm large well-rounded intraclasts form micrograinstones in contact with the vertical growths (Figure 6.12.A), creating a transition zone between the thinly laminated facies and the growths. In domes, laminated fabric is not as obvious and continuous as in the thinly laminated facies. Voids are abundant though a mixture of dark fine-grained (< 10 μm ∅ grains) laminae and micro-clots is still present (Figure 6.12.B).

With the WP technique, < 100 μm long and < 30 μm wide inclusion-rich rectangular crystals are highlighted in former voids (Figure 6.12.C). They are now encased in a dolomitic void filling cement. These brown, translucent crystals were observed under CL and are formed of a < 60 μm long, brown/red dull oval fine-grained core with a first black coating and a second yellow syntaxial growth (Figure 6.12.D–F). If these crystals are obvious in the voids they are more difficult to identify in the fine-grained mats. Similar crystals occur in the other vertical growths. The inclusion rich rectangular crystals were also observed with fluorescence microscopy, they appear rather dull, dark blue while the dolomite cement appears light blue. The resolution of this method did allow more observation of the external or internal structure of the oval cores.

Boundaries of the dark fine-grained framework tend to be difficult to trace precisely with classic petrographic methods (PPL, CPL). CL imaging offers an excellent insight into the zoning of framework boundaries and cement phases filling the voids. The fine-grained intervals are brown/red (a bit dull before image processing). They are coated with a thin black syntaxial fringe that is in turn followed by yellow syntaxial crystals: neither phase exceeds 20 μm thickness. The framework and individual ovoid cores from the previous paragraph have the same luminescence and texture, the same black then yellow syntaxial fringe; they are likely to be made of the same material. The framework results from the dense concentration of ovoid structures (Figure 6.12.F). The voids are filled with different generations of red drusy crystals

growing on the yellow syntaxial cement towards the inner part of the voids (Table 6.2).

Table 6.2: Different cement phases observed in the vertical growths of MM2.

| Facies | Phase # | Cement shape | Luminescence |
|---|---|---|---|
| Fine-grained mat | 1 | Fine dolomite | Brownish/red dull |
| Edge of fine-grained mat | 2a | Syntaxial on 1 | Black |
| | 2b | Syntaxial on 2a | Yellow |
| Void filling | 3a | Equant overgrowth, drusy | Dark red |
| | 3b | Equant overgrowth, drusy | Light red |
| | 4 | Xenomorphic cement | Dark red |

Between columnar stromatolites, concave upward laminated fabric is there in some situations, but it is absent in others. Some relatively well-laminated intervals alternate with poorly laminated (Figure 6.13.A, B), clast rich micropackstone–grainstone intervals. Laminated fabric may be completely destroyed with chaotic facies that dominate the intercolumnar intervals, forming micropackstones–grainstones (Figure 6.13.C). The variable presence of the inter-column fill reflects differential preservation, and partial destruction, of these deposits. The inner facies of the columns consist of a well-laminated concave downward fabric that is obvious in hand specimen but less evident in thin section (Figure 6.13.D). Microfacies consist, as in the domes, of a mixture of laminae and micro-clots forming a continuous framework (Figure 6.13.E, F).
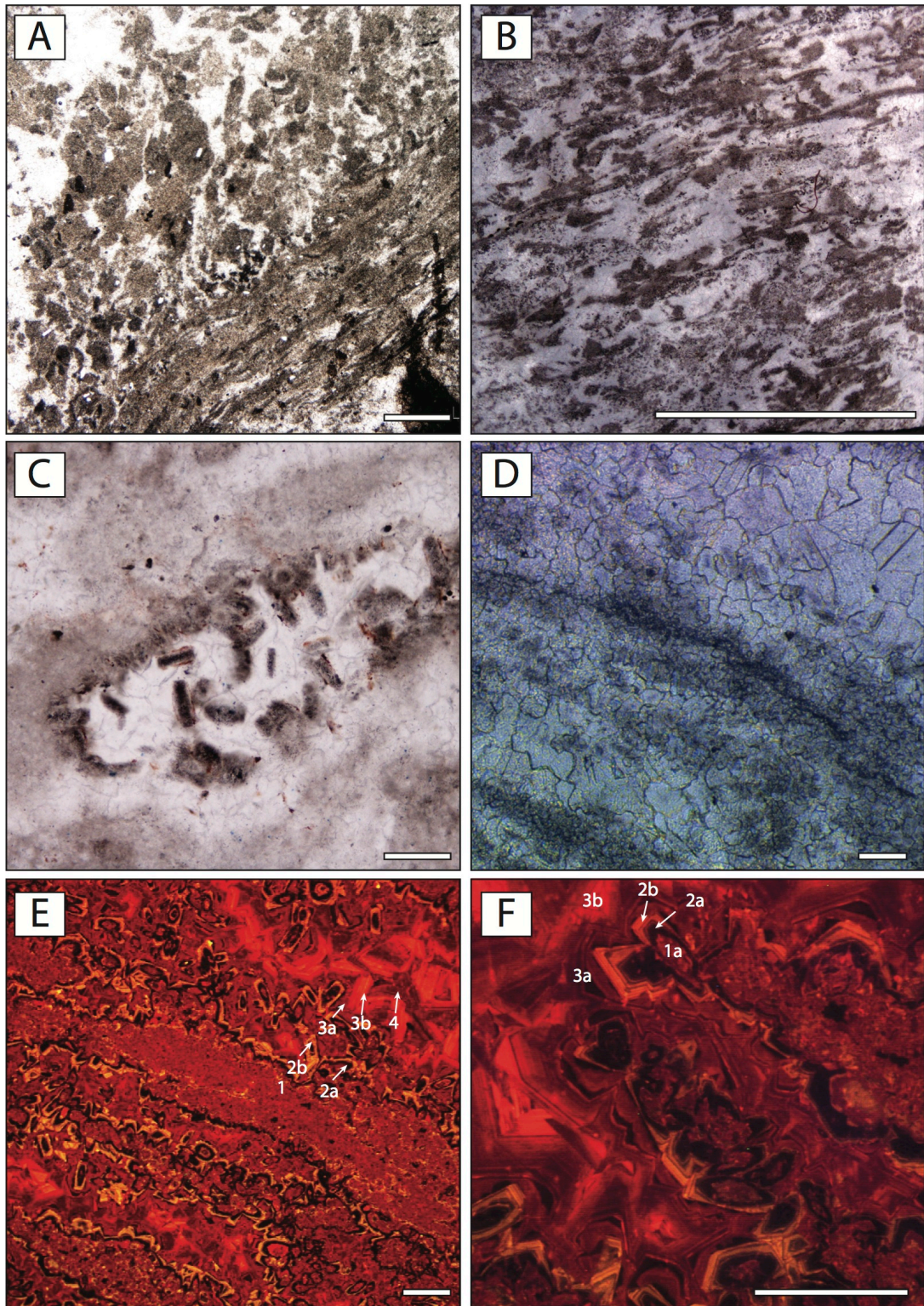
Figure 6.12: Microfacies associated with vertical growths, Rasthof Farm. **A**. Edge of a dome, with large amount of intraclasts in the upper left half, resting on the fine-grained mats. **B**. Inner facies of one dome illustrating the partly clotted microfabric. Laminated fabric is still visible. Note the widespread cement-filled voids. **C**. Rectangular inclusion rich crystals in a void (WP technique). **D** and **E**. PPL and CL images of mats with the different cements. **F**. Detail of the mats, with the dense concentration of ovoid features forming the mats. Dark rectangles in C. correspond to yellow rectangles in F. Scale bars are 1 mm (A–B) and 0.1 mm (C–F).
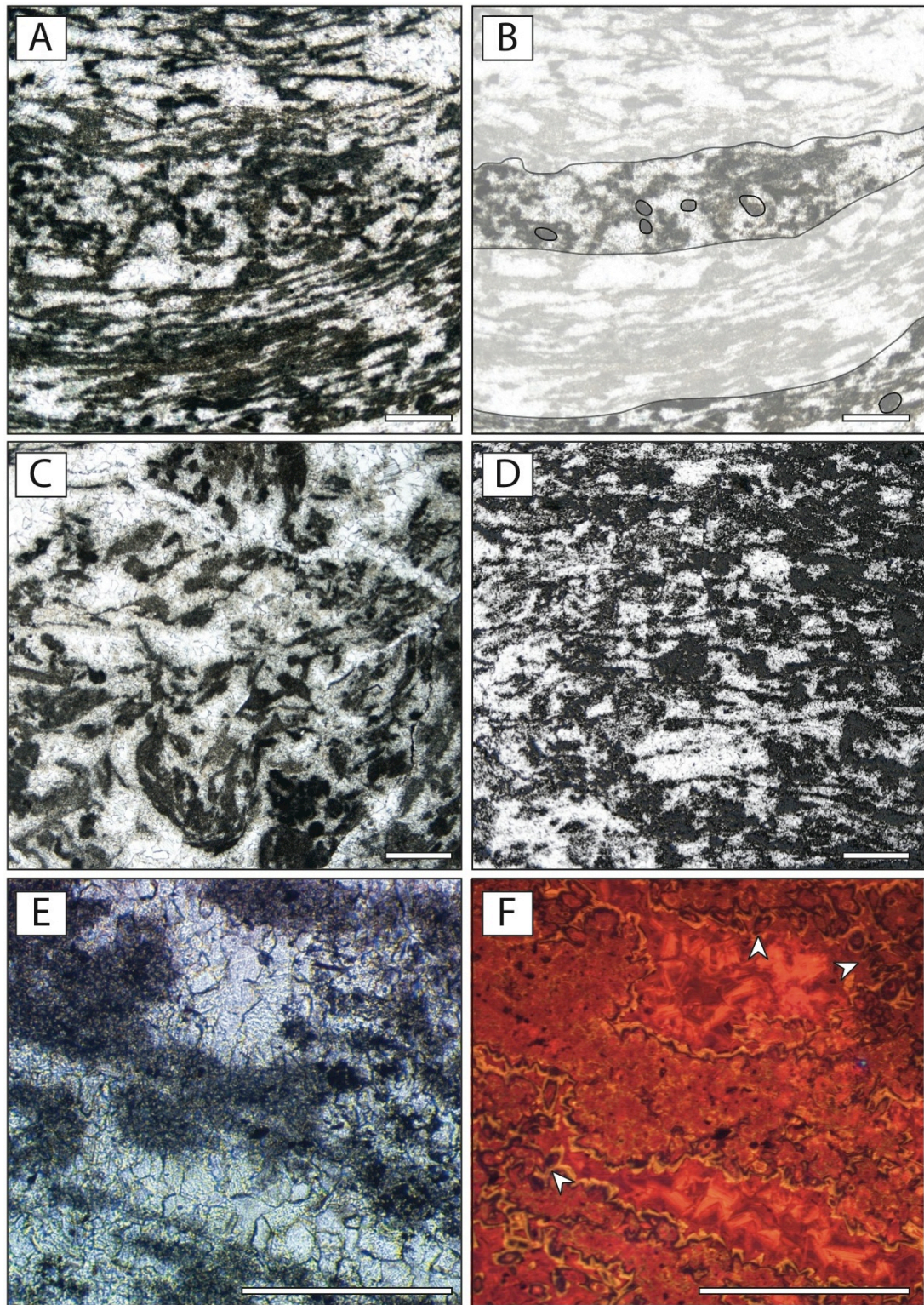
Figure 6.13: Microfacies of columns and intercolumn intervals. **A**. Intercolumnar sediments with well-laminated facies and intraclast intervals. **B**. Sketch, white areas represent the preserved laminated fabric, non-coloured areas represent intraclast rich intervals. **C**. Intraclasts between two columns, note the chaotic aspect and the lack of laminated fabric. **D**. Core of one column, with a continuous fine-grained framework. This photomicrograph illustrates how the laminated fabric is less obvious at a mm-scale. **E**. Detail of the inner part of a column and **F**. CL imaging, the white arrows illustrate areas where ovoid structures are obviously acting as building material for the fine-grained framework. Scale bars: 1 mm.

# 4    Interpretations

## 4.1    Cap dolostone

### 4.1.1    General facies

Despite dolomitisation, several features can be identified in the cap dolostone. A general observation is that it compares well between the three visited areas. Micrite or dolomicrite mud accumulated on the seafloor and relative abundance of fine-sized material created depositional couplets. Yet in this rhythmite, the timing and causes for such variation of abundance remain enigmatic. Thin dark fine-grained drapes record the low energy episodes while thicker light crystalline laminae may record relatively more energetic episodes, which bear some grains/clasts.

### 4.1.2    Millimetre-thick clast-rich intervals

Grains in these horizons are amorphous, poorly preserved peloids and have a diameter < 200 μm. Previous works suggest that the cap dolostone is a rhythmite, punctuated by several allodapic beds (Hoffman and Halverson, 2008, Tojo et al., 2007). The mm-thick horizons observed during the petrographic study are not obvious at the outcrop but are suggested to record individual event laminae and are interpreted as allodapic. In previous works, the term allodapic is widely used, referring to sub-storm deposits (e.g. Tojo et al., 2007). The allodapic intervals might result from settling of grains in suspensions after storms or other event reworking the sediments across the platform (e.g. seismic shock, wind blown dust), not necessarily implying sub-storm settings. They may compare with the background sedimentation of the cap dolostone (rhythmites), but recording punctual more intense events with transport of larger grains.

### 4.1.3    Non-laminated intervals

Thick non-laminated beds observed at Omutirapo exhibit mm–dm large grains or clasts, implying fairly energetic and almost instantaneous events of sedimentation. Like in the previous section, they are allodapic beds. They are generally capped by classic rhythmite facies. Considering the general lack of direct evidence for a shallow-water environment, transport of grains can result from derived material

due to storms or destabilisation of sediments upslope/ramp. In the Omutirapo area, the cap dolostone was deposited in a former glacial palaeovalley (Le Heron et al., 2013a), and thus local residual accommodation space may have favoured more intense reworking events than elsewhere on the platform, with allodapic beds going from the high topographies to be funnelled down the lower topography. This might also explain the overall large size of the clasts (cm–dm) observed in the 1.5 m-thick turbidite found at this location.

### 4.1.4    Peloids

The oval to rounded peloids observed in samples from the Omutirapo and Rasthof Farm areas may either have originated in the water column or on the seafloor. Their occurrence in discrete horizons is puzzling. Two hypotheses are entertained: (1) tractive reworking and (2) fallout from the water column. If the first scenario, evidence of scour and undulose lamina contacts might be expected. However, peloids are concentrated in diffusely bounded layers near the interface between two light coloured laminae, along which no obvious truncation of underlying laminae is recognised. These observations thus support a fallout mechanism, rather than a tractive reworking hypothesis. The absence of associated allochthonous grains or beds also tends to argue against tractive reworking.

The origin of the peloid fabric itself is also puzzling. Their scarcity and their age do not favour a faecal origin (Flügel, 2004; Scholle and Ulmer-Scholle, 2003). They compare well in shape and size with some of the ovoid features observed and interpreted as microfossils by Pruss et al. (2010), Bosak et al. (2012, 2011) and Dalton et al. (2013) in the microbial member of the Rasthof Formation. Thus, do the oval to rounded peloids represent dolomite-overprinted microfossils? Insights from SEM analysis were inhibited by a constant charging of the samples and the peloids were not preserved after dissolution of the samples. They occur in the cap dolostone while the previous authors observed them in the microbial member. It is stressed here that a microfossil interpretation is beyond the resolution of my dataset, and other, equally plausible interpretations exist. For example, peloids generated through the mechanical aggregation of micritic material (e.g. Tojo et al., 2007) is a possibility. In that scenario, they should probably be more common and

not only occur in concentrated intervals, unless they were produced seasonally. A third possibility is that they result from the micritisation of grains such as ooids, where some vestiges of the cortex are preserved (walls). Considering the relatively small size of the peloids (< 200 μm), they are unlikely to be the result of micritisation of ooids. Indeed, ooids tend to be larger than one millimetre (Sumner and Grotzinger, 1993). Furthermore, there is no evidence for nuclei in the peloids described herein. Thus, the origin of the ovoid grains remains, for the time being, inconclusive.

### 4.1.5    Diagenesis

CL imaging reveals little about the origins of the cap dolostone facies. Classic petrographic study suggests that laminated fabric initially consisted of an alternation of "brick shaped" muddy cement alternating with thin dark, fine-grained horizons. The precursor of the brick-shaped cement is uncertain. At an early stage, 10–30 μm dolomite euhedral rhombs developed, possibly around smaller nuclei. These may have been present at the time of deposition as authigenic "seeds" crystals (e.g. Choquette and Hiatt, 2008). Larger micritised grains, such as peloids, were also overprinted by a dense concentration of these euhedral rhombs.

The brick-shaped cement was dissolved, creating a microporous network later filled by subhedral, syntaxial crystals growing around the seeds/rhombs of sucrosic dolomite. Rhombs tend to be dark and cloudy, possibly because they came in replacement of an impure, micritic material. Dolomitic overgrowths are lighter because they developed in a porous network and do not replace mud-sized material. The final microfacies appears as a subhedral dolomitic texture, with a cloudy core in some of the crystals.

Suggested timing (Figure 6.14):

1.  Authigenic nuclei crystal in a carbonate mud. Note the peloids to the right.

2.  Development of euhedral dolomite around the nuclei. This creates a microsucrosic dolomite. Observed in (Figure 6.14.A–C).

3.  Cloudy overgrowth around the rhombs. From this stage, a change in fluid chemistry probably led to the dissolution of the brick shaped cement while rhombs were preserved.

4.  Limpid cement overgrowth around the rhombs replaces the brick shaped cement.

Stages 3 and 4 (Observed in Figure 5.14.D–G) consist of cement overgrowths around a same initial rhomb formed during phase 2. Note that more than 2 cement overgrowths may occur but size of the crystal and quality of picture acquisition do not allow more distinction.
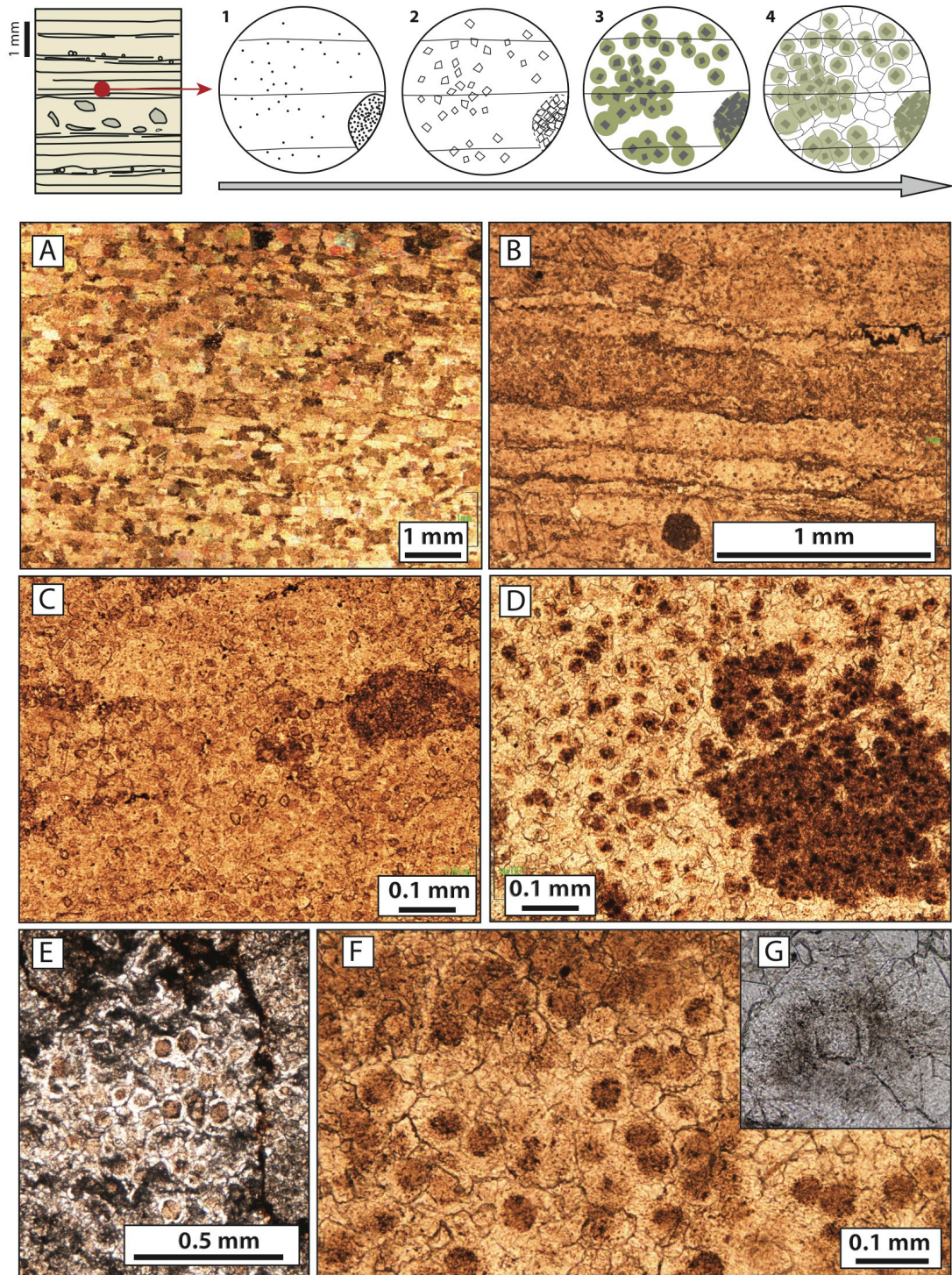
Figure 6.14: Suggested model for the microfacies found in the cap dolostone. **A**. Brick-shaped cement (CPL). **B**. Brick-shaped cement with visible rhombs (dots). **C**. Detail of the rhombs. Note the peloids to the right, itself now made of a dense concentration of rhombs. They are darker than in the cement because they replaced a relatively more micritic area. **D**. Detail of another peloid, now made of a dense concentration of dark, rounded rhombs. Each individual rhomb is now wrapped in a subhedral dolomite crystal. **E–G**. Extremely well-preserved rhombs wrapped in subhedral dolomite.

## 4.2 Microbial member

### 4.2.1 Generalities

It is widely accepted that the contorted facies of the microbial member result from the rubbery and cohesive nature of the sediments at the time of deformation, and that these properties are due to the microbial nature of the sediment (Hoffman and Halverson, 2008; Le Ber et al., 2013; Pruss et al., 2010). The darker fine-grained intervals, both in MM1 and MM2 are likely to be the result of microbial activity, even if direct evidence of cyanobacterial sheaths are presently unreported. Local occurrence of monoclinic crystals in dark laminae probably reflects a sulphate reduction process by microbial communities at the time of deposition, as suggested by Pruss et al. (2010). In MM1, microbial communities were regularly overtaken by carbonate cementation or sedimentation, illustrated by the light laminae/intervals. This is obvious in MM1 where the laminated fabric is distinct; on the other hand, MM2 is poorer in light cement and appears more dolomicritic, reflecting a relative abundance of microbial communities compared to cementation and background sedimentation.

Microbial facies of MM1 were cohesive and communities were likely to form a sticky texture, limiting both grain generation and transport. Therefore, under occasional hydrodynamic stress, disaggregation of the mats was limited by the cohesive facies, and transport of intraclasts was reduced by the binding action of the mats.

MM2 consists of an apparent, continuous, microbial framework and the geometries (domes, columns) associated with nearby intraclasts demonstrate a frequent and increasing hydrodynamic energy in the environment compared to MM1. The different degrees of disruption of the mats, from roll-up structures to broken sets of laminae bear witness of variation in flow regime. Also, the development of vertical growths in MM2 at Rasthof Farm demonstrates that microbial communities were able to buildup to a dm-scale without being deformed. Vertical developments were inhibited during deposition of MM1 where microbial communities were 1) often overtaken by carbonate cementation and/or sedimentation; 2) a continuous framework was not able to develop.

### 4.2.2    Microbial member 1

At first sight, microfacies of the cap dolostone and MM1 can be very similar. In MM1 however, dark laminae are thicker (generally 500 μm but up to 1 mm of diffuse dolomicrite) and partly clotted. The lateral thickening of one dark lamina might result from a denser local concentration of microbes. No microbial filaments were preserved in these laminae, yet this is a strong consensus that they are microbial in origin (Hedberg, 1979; Hoffman and Halverson, 2008; Le Ber et al., 2013; Pruss et al., 2010). Local monoclinic crystals may suggest sulphate reduction at the time of deposition. EDX analysis revealed that they are now replaced by silica; which is a common replacement process (Scholle and Ulmer-Scholle, 2003; Tucker et al., 1990). As it is demonstrated in several studies of sulphate-reducing bacteria (e.g. Deng et al., 2010; Wright and Wacey, 2005), microbial population can lead to a direct precipitation of dolomite from the seawater. Therefore, even if no bacteria or filaments are preserved, we can tentatively suggest that dolomite may have precipitated directly from the seawater during the deposition of the microbial member.

In the light laminae, round cloudy nuclei are observed in a dolomitic subhedral texture. They can be isolated or grouped into mm-sized structures. Pruss et al. (2010, fig.4.B, C) observed the same cloudy features. Based on Raman spectroscopy analyses, the same authors indicate that they contain organic matter. At high magnification, most of the circular features exhibit a rhombohedral core surrounded by darker overgrowths. This suggests that, similarly to the cap dolostone, a rhomb developed in the initial carbonate mud, and dark fibrous overgrowths developed around it. The dark colour of the circular features results from replacement of a micritic texture, possibly biogenic in this microbial environment (Pruss et al., 2010), replacing grumeleuse intervals (Turner et al., 2000). It is suggested that the cloudy nuclei result from a diagenetic process (central rhomb + circular overgrowth). Later, light subhedral dolomite texture developed around these circular features, in a micropore-filling stage. Note that Pruss et al. (2010), Bosak et al. (2012, 2011) and Dalton et al. (2013) observed and isolated possible eukaryotes preserved preferentially in the dark laminae of the microbial

member. Their petrographic expression in PPL differs greatly form the cloudy nuclei, which are more abundant and grouped in lighter laminae.

Dolomite texture in light laminae is much coarser (80–150 µm) than in the dark laminae (< 10 µm). It is argued that the difference in the size of dolomite crystals derives from the original texture of the sediment.

Dark laminae can be slightly discontinuous in dome-like structures (e.g. Omutirapo area). They can also form a continuous framework and several associated rounded intraclasts can be observed. The latter are interpreted to reflect hydrodynamic energy at the time of deposition, strong enough to locally break the mats into fragments. Meanwhile, the framework probably allowed the local bio-construction of solid growths compared to classic deformed mats typically found in MM1.

### 4.2.3    Microbial member 2

#### 4.2.3.1    Cathodoluminescence imaging

The different phases observed in the vertical growths (Table 6.2) are very similar to the one found in the classic MM2, thinly laminated facies (Table 6.1). The only difference is that two phases (2a and 2b) are differentiated in the vertical growths while only one seems to be present in the classic laminated facies. Note, however, that phase 2a (black coating of the microbial mats, Table 6.2) was not observed during all the session of CL. For example, a same sample from a dome was observed during two different sessions of CL, and the black phase 2a only appeared during the second session. The best explanation for this must be in the device settings during picture acquisition. Overall, both laminated/rolled facies and vertical growths exhibit the same cement phases.

#### 4.2.3.2    Framework

In MM2, the microbial communities developed a vertically and laterally continuous framework, keeping the trend of a laminated fabric as observed at the macroscopic scale. The framework that developed in MM2 prevented the development of soft-sediment deformation structures, such as the dm–m-scale examples described in MM1. This continuous framework probably limited the disruption of the facies to a

"peeling" of shallowest sediments, forming cm-scale roll-up structures to local intraclasts. Also, a more rigid structure of the sediments is likely to have favoured vertical accretion (e.g. Rasthof Farm) that could grow without being deformed. The latter are themselves a mix of microbial framework, clots and sub-mm intraclasts.

The sediments found between the growths at Rasthof Farm are in some respects similar to the classic facies from MM2, such as the thinly laminated facies observed in Okaaru and Omutirapo area with some roll-up structures. However, laminae between the growths of the Rasthof Farm area are locally completely broken and reworked, indicating intense energy and scouring. Also, at a mm-scale, laminated intervals can alternate with intraclast rich intervals, reflecting variations in flow regime (Figure 6.13.A, B).

### 4.2.3.3    Mat-building, ovoid features

Details of the inclusion rich rectangular crystals observed in the voids were captured with CL imaging. They all consist of an ovoid fine-grained (micritic) core surrounded by a yellow syntaxial crystal growth. What CL reveals is that the ovoid cores have actually the same luminescence than the mats. But also, the ovoid cores can be closely spaced and concentrated, merging and actually forming a lamina or a clot. They are the smallest elements discernible in the mats. These ovoid features are 60–40 µm long and difficult to affiliate to any bacteriomorphs, usually < 10 µm in size. Yet they could be relicts of large bacteria such as the *Chromatium* genus that can be > 40 µm long (e.g. Lindtke et al., 2011; Schulz and Jørgensen, 2001). If so, they were not the only type of bacteria present at Rasthof time, but as they are larger than classic bacteria, their relicts are more visible. Analysis of modern microbial mats demonstrates the diversity of microbial communities found in stromatolites (e.g. Khodadad and Foster, 2012; Papineau et al., 2005). Limited observations from the samples of MM2 do not permit to be conclusive for large bacteriomorphs hypothesis to explain the occurrence of abundant ovoid features. Chemical analyse and more detailed microscopic investigation could help to strengthen or reject this hypothesis. Another hypothesis is to view the ovoid features as micro-clots resulting from microbial activity or agglutination of microbes. Finally, they are very abundant, their regular size and shape may suggest

pellets produced by some form of invertebrate organism(s), which is not expected during the Cryogenian. The only possible organisms found in the Rasthof Formation so far do not seem to be associated with pellets (Bosak et al., 2012, 2011; Dalton et al., 2013).

### 4.2.3.4    *Unidentified crystals*

The composition and properties of the crystals presented in Figure 6.11 did not permit precise identification. They are likely to be a variety of talc ($Mg_3Si_4 O_{10}(OH)_2$) and result from a low-grade metamorphism. But none of the petrographic properties or chemical elements allow a definitive conclusion on these crystals. They form preferentially in the darker laminae of MM2; which were likely to be the more concentrated in clay material, containing Al and Si. During low-grade metamorphism the latter were incorporated in the unidentified crystals.

## 5    Discussion

The cap dolostone remains poorly studied compared to the microbial member. Further studies would be helpful to understand all the aspects of this member, specifically its diagenesis and initial texture. A key observation presented in this chapter and touched on by other authors is the occurrence of peloids. The localised peloids might be organic or the result of mechanical accumulation of mud-sized material. In the first case, it might mean that life was present very soon after the glaciation and prior to the development of mat building microbial communities. They are difficult to isolate or observe apart from classic PPL and CPL techniques, but some seem to have a walled structure. Each scenario must explain their occurrence in 1 mm-thick intervals, implying their generation by a short-lived event. The unsuccessful attempts to isolate and observe them more in details limit further interpretations.

Still within short-live events, the cap dolostone is punctuated with mm-thick intervals of reworked grains, intraclasts. Where observed, the cap dolostone does not consist of a rhythmite associated with common debris flows. The author has used the term allodapic to interpret clast-rich mm-thick intervals, but they do not

necessarily represent violent transport, reworking of sediments into deep-water. Such intervals could be formed in subtidal, relatively shallow water settings.

In the microbial member, soft-sediment deformation structures are far less common in MM2 than in MM1. Only cm-scale roll-up structures were observed at outcrop. A more vertically continuous microbial framework probably limited the deformations. Establishing why these frameworks developed is a complex problem: do they record a succession of slightly different microbial communities, environmental parameters, or a combination of both? This framework may have increased the lithification rate, or sediment rigidity, compared to MM1. Since the sediments were more rigid in MM2, only the first few centimetres of the seafloor were deformable, allowing only local roll-up structures and intraclasts. The two microbial members also differ in their composition: while ovoid elements are typical from the mats of MM2, none were observed in MM1 so far. These ovoid elements could be individual organisms but might as well be agglutinated colonies, themselves merging to form microbial mats.

A noteworthy observation from the CL imaging is that MM2 contained the most porous facies at the time of deposition. No large void filling cements were observed in the cap dolostone or MM1. In MM2 however, void filling cements are extremely common, both in the vertical growths and in the facies deposited around them. All the pores are now cemented but at the time of deposition MM2 probably consisted of a complex system of connected micropores. This microbial texture might therefore be used as an analogue for a microbial hydrocarbon reservoir. These pore networks are likely to have given better permeability and porosity properties than in MM1. In MM1, the water trapped in the sediments was not able to circulate as easily as in MM2, increasing water saturation, slowing lithification and favouring larger soft-sediment deformations than in MM2.

## 6    Conclusions

Microscopic descriptions are essential to understand macrofacies observed in the Rasthof Formation. Several studies have already made major observations and interpretations (Bosak et al., 2012, 2011; Dalton et al., 2013; Le Ber et al., 2013; Pruss et al., 2010; Tojo et al., 2007). However, further studies are expected to reveal

more about these unusual facies. The use of techniques such as the white paper (Delgado, 1977) or CL help to see what history is hidden behind an intense dolomite overprint. The main observations and conclusions suggest that:

- Dolomite was present at an early stage (both in the cap dolostone and microbial member) but it is not possible to confirm if it results from syn-sedimentary precipitation. The evidence for early dolomite consists in rhomb-shaped, cloudy nuclei (MM1). These are the earliest crystal type that can be traced back. Similar cloudy nuclei and microsucrosic rhombs are also found in brick-shaped carbonate mud of the cap dolostone;

- The microbial input for the formation of the microbial member is suggested by 1) the occurrence of pseudomorph after sulphate reduction crystals (MM1); 2) the apparent cohesiveness of the facies at the time of deformation and 3) possible mat building ovoid features (MM2);

- MM1 differs from MM2 with 1) a different organisation/type of microbial communities and 2) a different framework (Figure 6.15). This results in different rheologies and facies.
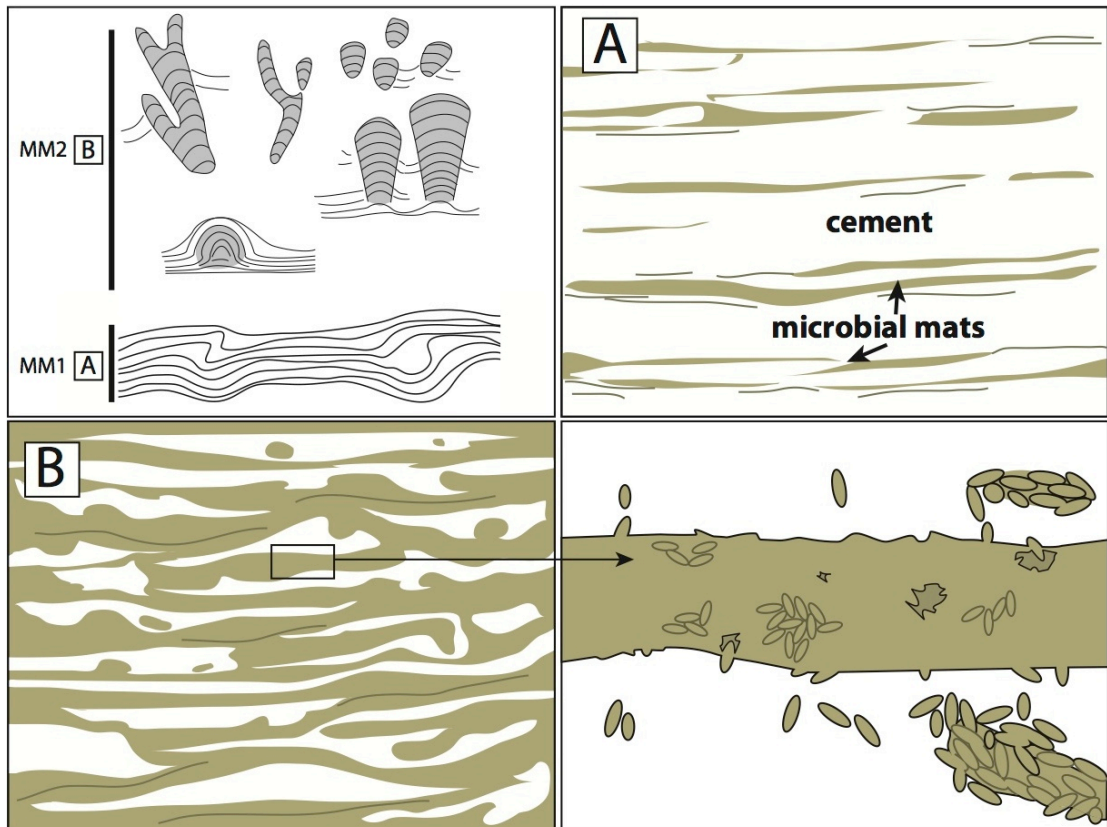
Figure 6.15: Microbial fabrics of the microbial member. **A**. MM1, Thickly laminated **B**. Dense microbial framework as found in MM2. Detail to the right illustrates how ovoid elements (observed in CL) compose microbial mats of MM2 (both in vertical growths and preserved surrounding laminae).

# Chapter 7 – The Berg Aukas Formation

## 1    Introduction

The northeast part of the Otavi Platform (Figure 7.1) is well known for its ore deposits, especially in the Tsumeb area, where Neoproterozoic carbonate sediments of the area host highly diverse assemblage of minerals (Kamona and Günzel, 2007). The entire Otavi Group is consequently of major economic importance: the ore bodies that occur in this carbonate-dominated succession have been exploited since the late 19th century. Most of the work undertaken on the Neoproterozoic rocks focuses on the mineralisation process, the genesis of the ore deposits, with a geochemical approach (e.g. Chetty and Frimmel, 2000; Schneider et al., 2008). Despite this mining interest, comparatively little has been published on the sedimentology of Neoproterozoic carbonates in this area. A few publications describe the actual facies and features on the platform (Cloud and Semikhatov, 1969; Miller, 2008; Misiewicz, 1988). The paucity of previous work motivated the author to gather new observations in the field, in order to make detailed comparisons between the Rasthof Formation in northwest Namibia and its lateral equivalent in northeast Namibia: the Berg Aukas Formation.

On the Northern Platform, the main challenges to interpret the palaeoenvironments of the post-Sturtian cap carbonate are 1) the unusual microbial facies and 2) the lack of facies variation. In Chapter 5, the occurrence of individual stromatolite growths has been reported in the vicinity of the Rasthof Farm, northwest Namibia, indicating local facies variations on the microbial dominated platform. These growths have not been fully described in the Rasthof Formation before, although passing mention has been made to them (Hedberg, 1979; Miller, 2008), and without reference to their distribution and geometries. In northeast Namibia, Cloud and Semikhatov (1969), Misiewicz (1988) and Miller (2008) works illustrate individual growths in the Berg Aukas Formation. Fieldwork in northeast Namibia was undertaken in order to 1) compare stromatolite geometries to the time equivalent ones observed in northwest Namibia (Rasthof Formation, Rasthof Farm); 2) evaluate facies variations on the platform. One week was spent focussing on the Otavi Mountain Land, SSW of Tsumeb (Figure 7.1 and Figure 7.4). The work

presented in this chapter is based on literature, map data, field observations, and description of thin sections. Details related to the organisation of the fieldwork are mentioned in Chapter 5. In the following, key literature data are synthesised, presenting the main facies found in the Berg Aukas Formation. The literature data are then integrated with field observations.
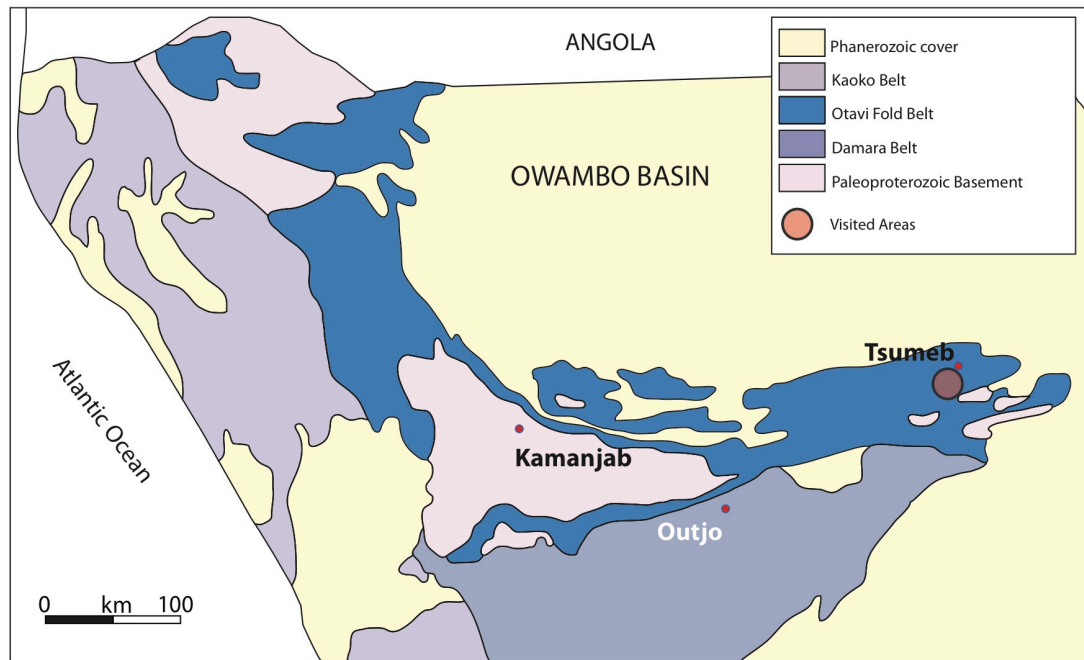


Figure 7.1: Location of Tsumeb in northern Namibia.

## 2  Methodology

### 2.1  Literature data

#### 2.1.1  Facies overview of the Berg Aukas Formation

Misiewicz (1988) and Miller (2008) described the facies of the Berg Aukas Formation in the Otavi Mountain Land. Based on Misiewicz's 1988 work, earlier publications and fieldwork, Miller (2008) compiled and illustrated key observations and facies of the formation. Misiewicz (1988) worked on his thesis prior to the snowball Earth hypothesis (Hoffman et al., 1998a, 1998b). He mentions the glacial Varianto Formation as part of the Nosib Group. But he does not refer to it as a major glacial event followed by a sea level rise and a cap carbonate sequence.

The change in the stratigraphy proposed by Hoffmann and Prave (1996) has moved the Chuos Formation from the base of the Tsumeb Subgroup to the base of the Abenab Subgroup, placing it below the Berg Aukas Formation. They differentiate the Chuos (or Varianto) Formation (base of the Abenab Subgroup) from the Ghaub Formation (base of the Tsumeb Subgroup). The Chuos Formation is interpreted as the local record of the Sturtian ice age (Chetty and Frimmel, 2000). Misiewicz (1988) described the Berg Aukas Formation as a carbonate succession resting on the Nosib Group and locally the Varianto Formation. Its context as a post-glacial cap carbonate was not considered. On the other hand, Miller's (2008) work was published one decade after Hoffman et al. (1998b) snowball Earth hypothesis; he thus described the Berg Aukas Formation as a post-glacial succession.

The Berg Aukas Formation can rest in sharp contact on the Chuos/Varianto Formation, the Nosib Group or the basement (Miller, 2008). The irregular nature of the basal contact reflects lateral variation in accommodation space, thus the sequence varies from ~100 m to more than 300 m-thick (Miller, 2008; Misiewicz, 1988). It is divisible into 3 to 4 facies. A < 25 m-thick cap dolostone consisting of finely laminated dolomicrite forms the base of the succession. It can be interbedded with arkose and conglomerates. Misiewicz (1988) interpreted it as the record of a back reef setting. A light grey dolomite follows, with stromatolitic reef facies, associated with debris and intraclasts. Finally a black laminated packstone interbedded with mass-flow and oolitic grainstones marks the last facies of the Berg Aukas Formation.

### 2.1.2 Individual stromatolite growths

Several individual stromatolite growths appear to occur in the Berg Aukas Formation. Misiewicz (1988) described distorted stromatolites (Figure 7.2) and local growths using the term *Conophyton*. He interpreted the microbial facies of the Berg Aukas Formation to have formed in a turbulent environment. This interpretation is supported by the observation of broken stromatolitic fragments and intraclasts caught in younger growths. The formation exhibits a general chaotic aspect, previously described as "contorted dolomites" during the mapping of the area (Misiewicz, 1988). "Chaotic" or "contorted" are words that can typically be used to

describe the facies of MM1 (thickly laminated microbialites) in the Rasthof Formation, northwest Namibia (Hedberg, 1979; Hoffman and Halverson, 2008; Pruss et al., 2010).
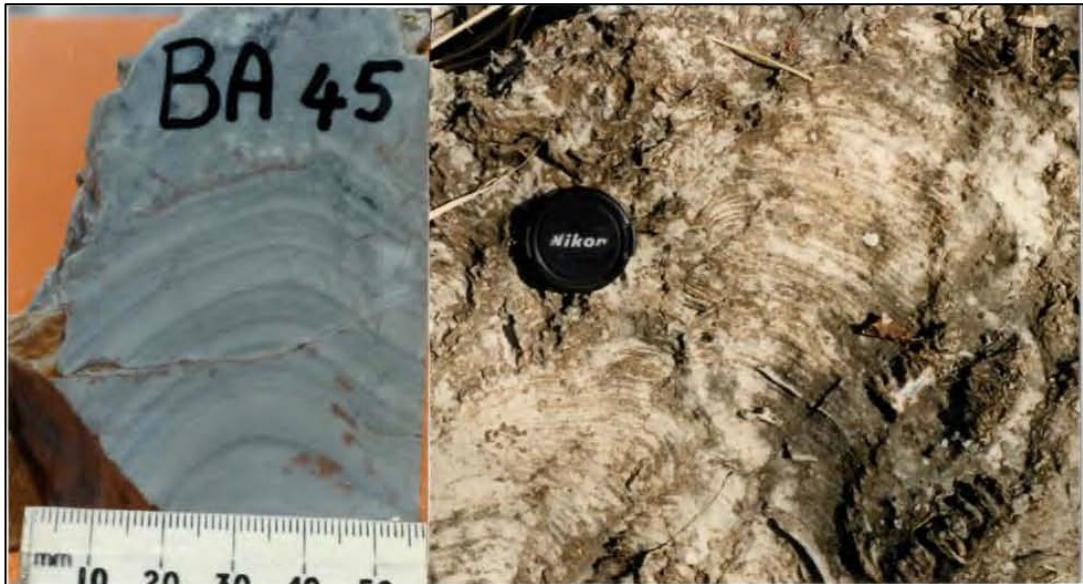


Figure 7.2: Laminated microbial sediments, Berg Aukas Formation (Misiewicz, 1988). They appear as relatively thickly laminated (2–5 mm) mats with a low degree of contortion.

Miller (2008) also described stromatolites: silicified cryptozoon in the upper part of the formation, without giving more details or interpretations. He also refers to previous work such as Cloud and Semikhatov (1969). The latter published a compilation of Proterozoic stromatolites around the world in which they refer to two different "forms" in northeast Namibia: *Baicala* (Figure 7.3. A, B) and *Conophyton*, occurring in the "Abenab Formation":

"*Baicala* aff. *B. rara* Semikhatov. Lower Abenab Formation, Cloud's locality 1 of 28/8/65, about 25 km southeast of Tsumeb and 50 m west of the main road to Grootfontein, South West Africa" (Cloud and Semikhatov, 1969, p.1056).

221
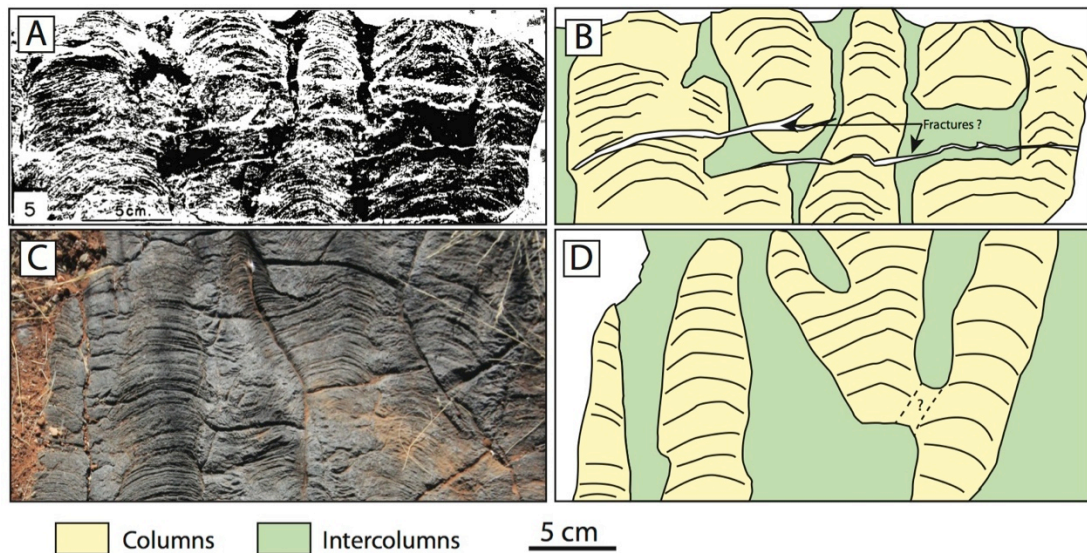
Figure 7.3: Comparison of branching columns as found in the literature and on the field. **A**. Columnar stromatolites observed by Cloud and Semikhatov (1969) in the Tsumeb area, Lower Abenab Subgroup. **B**. Sketch emphasising the morphologies. **C**. Columnar branching stromatolites observed in the Rasthof Formation, Rasthof Farm, northwest Namibia. **D**. Sketch emphasising the morphologies.

Figure 7.3.A, B shows a slab through closely spaced columnar stromatolite facies observed by Cloud and Semikhatov (1969), with a interpretive sketch by the present author emphasising the geometries. Columns are 5–10 cm wide, possibly branching. Miller's (2008) illustration of cryptozoon may correspond to the top view of similar facies. In lateral view, they have an aspect similar to the one observed at Rasthof Farm (northwest Namibia), where different degrees of branching occur, leading to different spacing between the columns. Figure 7.3 (C and D) illustrates highly comparable morphologies from the Rasthof Farm, with well-expressed branching columns.

Note that another stromatolite growth (*Conophyton resotti*) was described by Cloud and Semikhatov (1969, fig.6, plate 2). This stromatolite is illustrated by those authors in plan view, exhibiting concentric layers. However, this type of concentric geometry can be formed by any dome-like structure, such as those common in MM1 of the Rasthof Formation. The geometry does not, therefore, necessarily imply the occurrence of individual growths. More illustrations would be necessary to know if the information is relevant. Furthermore, this feature is indicated as part of the "Upper Abenab Formation" (now Abenab Subgroup), 1000 m above the

222

*Baicala* geometry from Figure 7.3.A. The precise stratigraphic position of Cloud and Semikhatov's (1969) descriptions are uncertain, but it is plausible that they derive from part of the Gruis or Ombaatjie formations.

### 2.1.3    Summary

The Berg Aukas Formation is a carbonate sequence recording the flooding of the Angola Block after the Sturtian glaciation (Miller, 2008). It often rests on the underlying glacigenic Chuos/Varianto Formation, but in some locations rests on older formations. This indicates local non-deposition or erosion of the diamictite. The Berg Aukas Formation consists first of a cap dolostone facies, followed by light to dark grey laminated dolostone, with variation in the density of the lamination. Thicknesses and lateral relationship between the facies remain poorly constrained. Overall, the Berg Aukas Formation is a succession of laminated dolostone with local individual stromatolite growths.

Misiewicz (1988) interpreted the Berg Aukas Formation as deposited in a mid-energy, backreef to forereef environment. His interpretation is supported by the observation of some clastic input (arkose), and intraclasts of microbial laminae within chaotic mats. Cloud and Semikhatov (1969) also described clear individual growths in the same formation. Local oolitic grainstones, siliciclastic input and well differentiated stromatolite growths (Cloud and Semikhatov, 1969; Miller, 2008; Misiewicz, 1988) support energetic settings at Berg Aukas times. From the few references available on this formation, it appears that facies variations are more common than on the observed western part of the Northern Platform.

The remainder of this chapter is dedicated to the description of Berg Aukas outcrops in the Otavi Mountain Land, where one week of the 2012 field campaign was used to target pre-identified outcrops. Our objective here is to describe and interpret the facies and stromatolite geometries. Comparison of the facies between the western (Rasthof) and eastern (Berg Aukas) parts of the platform represents an excellent opportunity to present a new spatially distributed dataset on the post-Sturtian carbonate platform.

## 2.2    Outcrops locations and accessibility

Neoproterozoic outcrops are present through the Otavi Mountain Land. The field area is located north of the Road D3022 (Figure 7.4). This area was selected on the basis of previous work done on the underlying Chuos Formation in the area by Busfield and Le Heron (2013) and Le Heron et al. (2013b, Appendix C), whose reconnaissance identified suitable outcrops. The author also attempted to visit the study area of Cloud and Semikhatov (1969). It is extremely important to mention that the accessibility and quality of the outcrops are limiting factors in this study. In northeast Namibia, vegetation is much denser than in northwest Namibia and outcrop can be scarce and discontinuous. Several attempts to reach outcrops were unsuccessful long drives.

### 2.2.1    Location of Cloud and Semikhatov's (1969) outcrop

Information given by Cloud and Semikhatov (1969) includes what kind of stromatolite geometry is found and their location, "about 25 km southeast of Tsumeb and 50 m west of the main road to Grootfontein". The "main road" corresponds to the road C42, however, indications about the distance remain rather vague.

Following the road for 28 km leads to what is mapped as the Berg Aukas Formation, just next to the road. However, following it for 25 km leads to a hill where rocks are mapped as the younger Elandshoek Formation (Tsumeb Subgroup); this second outcrop was not accessible at the time of the visit and is out of the scope of the study. The supposed location of *Baicala* from Cloud and Semikhatov (1969) is placed on the map with a red triangle (Figure 7.4, location ①), 28 km from Tsumeb. However, from the above, note that this location is highly uncertain.
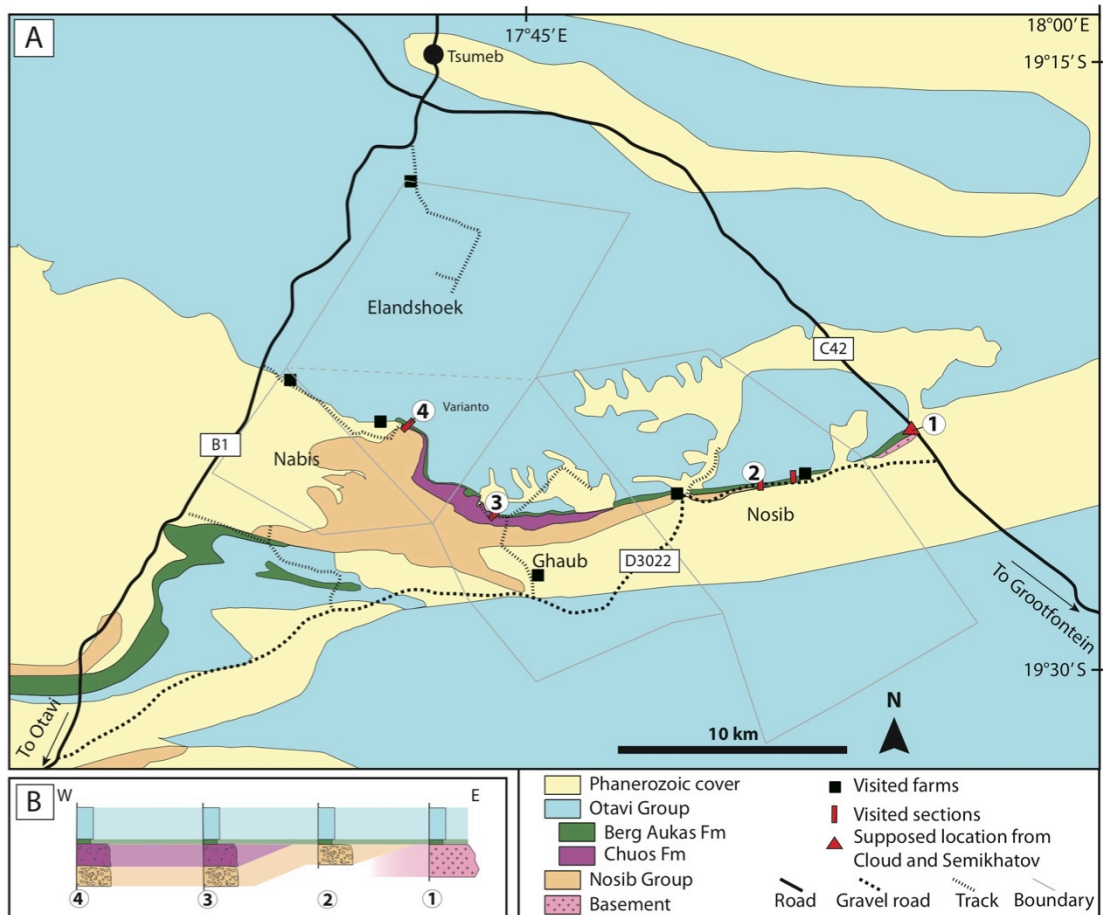
Figure 7.4: Study area, northeast Namibia. **A**. Sketch map of the area, with the main roads, visited tracks and outcrop locations, modified from Schreiber (2008). **B**. Sediment succession deduced from the map showing the Berg Aukas draping the basement, the Nosib and Chuos/Varianto formations. This sketch illustrates the discontinuous occurrence of the Chuos Formation.

## 2.3    Other Berg Aukas Formation outcrops

In addition to the supposed location from Cloud and Semikhatov (1969), several farms were visited in the view to describe the Berg Aukas Formation. They are all located inside the triangle formed by the roads C42, D3022 and B1: the Ghaub Farm, the Nosib Block, and the Elandshoek/Varianto Farm. The road D3022 follows the axis of the eroded Nosib Anticline, where pre-Tsumeb Subgroup sediments are exposed. In this area, the cap carbonate crops out on the southern flank of the hills rising north of the road D3022. It rests on the Chuos Formation to the west, and then the diamictite pinches out eastward. The Gauss Formation, mapped as a massive dolostone, overlies the Berg Aukas Formation.

The outcrops of the Berg Aukas Formation are less exposed but similar to the ones from the Rasthof Formation: extremely fractured, with random unstable blocks and razor-sharp weathering. Due to the dense vegetation and the exposure on the flanks of the hills, vertical and lateral continuity of the outcrop rarely exceed a few metres. Once on an outcrop, facies are well preserved but partly overprinted by weathering patterns.

## 3    Field Observations

In the following, field observations are presented from the east to the west of the study area. Starting at the supposed location from Cloud and Semikhatov (1969), and then at the Nosib Block, Ghaub Farm and finally the Elandshoek/Varianto Farm. The total transect is ~25 km long.

### 3.1    Location 1: Cloud and Semikhatov's outcrop, Road C42

Outcrop (Berg Aukas Formation): 19° 24.215' S – 17° 55.067' E.

Cloud and Semikhatov (1969) reported columnar stromatolites, located along the road C42 joining Tsumeb to Grootfontein. The deduced outcrop is mapped as the Berg Aukas Formation, resting on a granite but the contact was not observed during the fieldwork. Nevertheless, granite blocks are found along the road C42, close to the outcrop.

The strata comprise a thickly laminated (2–5 mm laminae) light grey dolomite (Figure 7.5.A). Undulations of the laminae are comparable to those from MM1 of the Rasthof Formation found in northwest Namibia. No obvious individual growths such as those illustrated in Figure 7.3 (A and B) were observed. The strata often exhibit a white colored enterolithic network associated with nodules. The network forms m long and cm large veins, their precise orientation compared to dolostone laminae in ambiguous because of the lack of obvious bedding. Nodules are generaly less than 5 cm large and appear both in fenestrae (Figure 7.5.C) and as more continuous phenomena (Figure 7.5.B). A chicken-wire texture is frequent but not widespread (Figure 7.5.D). These features, occurring in a light grey laminated dolostone exhibit a dark grey contour and a white core made of fibrous isopachous cement. The outcrop, with the same illustration has been attributed as part of the

Gauss Formation by Miller (2008, fig.13.31.a). He described the same outcrop as a massive dolostone, the enterolithic network as a typical stromatactis texture, associated with oolitic grainstones. Bechstädt et al. (2009, p.276) also reported the same features at the same outcrop (Annshope Farm, west of the Road C42): a network of fissures, colloform structures, filled with radial sparry carbonate. They suggest they are related as secondary, tectonic features. This latter interpretation is not fully justified by these authors: alternative interpretations by the present author are formulated in the section 4.2.3.
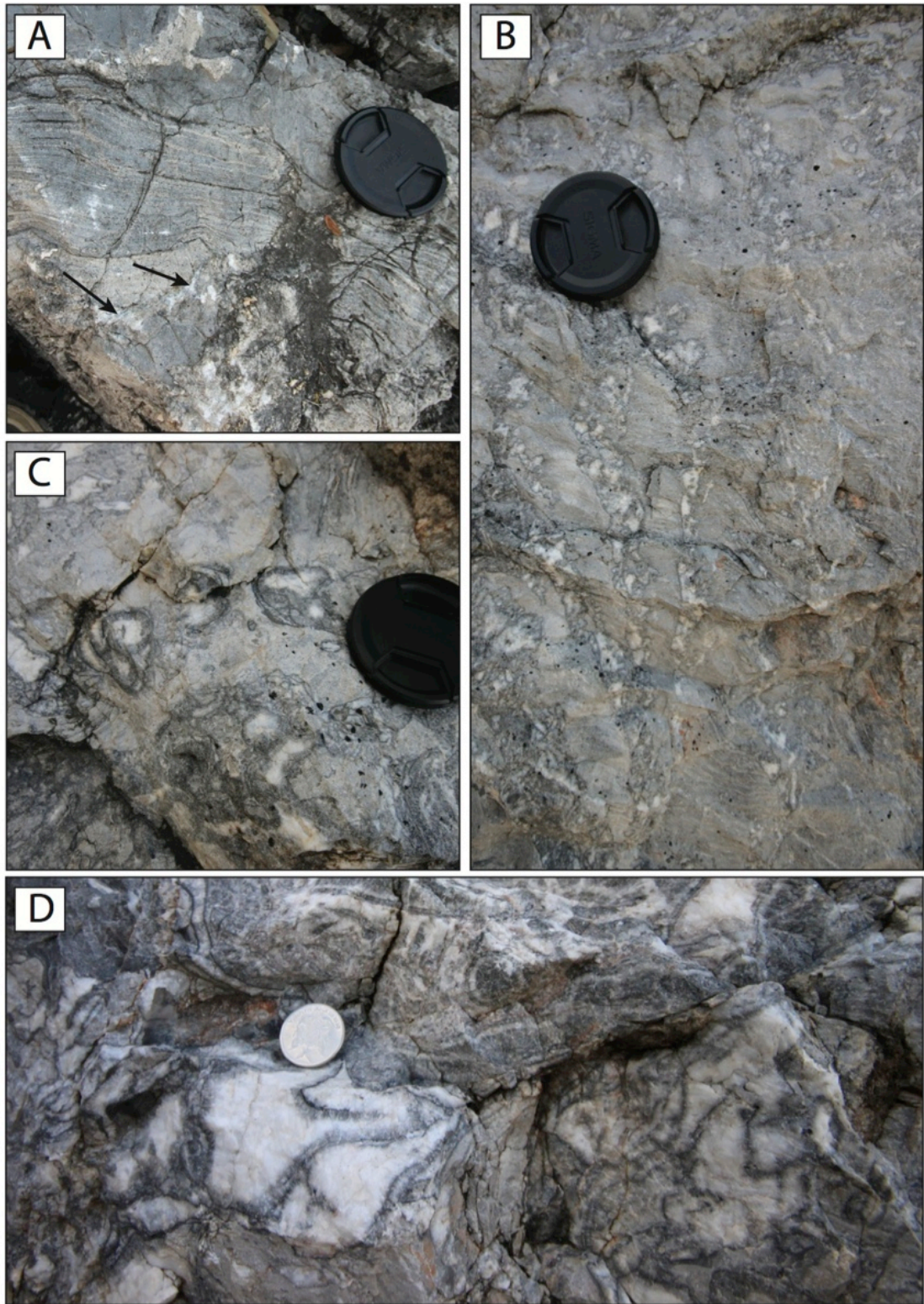
Figure 7.5: Laminated dolostone, Berg Aukas Formation. Road C42, 28 km south from Tsumeb. **A**. Thickly laminated, slightly undulated dolostone with white enterolithic network (arrows). **B**. Subvertical enterolithic structures. **C**. Section through the nodules, part of the enterolithic network. Note also white inter laminae layering (top right corner). **D**. Chicken-wire texture. Lens cap is 77 mm Ø.

## 3.2   Location 2: Nosib Farm

Outcrop 1 (Berg Aukas Formation): 19° 25.261' S – 17° 51.791' E.

Outcrop 2 (Nabis Formation): 19° 25.553' S – 17° 50.689' E.

The outcrop 1 is located 150 metres northwest from a family farm. The Berg Aukas Formation forms a small hill and consists of thickly laminated dolostone. The facies is again slightly undulated (Figure 7.6.A), comparable to MM1 in northwest Namibia. Razor sharp weathering is also similar to the one observed in MM1, creating a pattern than overprints the facies and limits observations. No outstanding observations were made at this outcrop. However, Miller also described oolitic grainstones in the Berg Aukas Formation in the same area (Miller, 2008, fig.13.31.d).

Two km WSW from this farm (outcrop 2), a river bed/path used by the game and livestock cuts through a massive conglomerate. Pebbles are well- to sub-rounded, 5 to 30 cm large and contained in a fine to coarse-grained to sandy matrix (Figure 7.6.B). The Berg Aukas Formation was not accessible at the location 2, but mapping of the region indicates that at Nosib Farm, it rests directly on the Nosib Group, while westward, it rests on the Chuos/Varianto Formation.

Figure 7.6: Outcrops observed at Nosib Farm. **A**. Berg Aukas thickly laminated, undulated dolostone. **B**. Well-rounded pebbles within a mid- to coarse-grained matrix. Lens cap is 77 mm Ø.

## 3.3    Location 3: Ghaub Farm

Outcrop 1 (Nabis Formation): 19° 26.888' S – 17° 44.246' E.

Outcrop 2 (Varianto/Chuos Formation): 19° 26.460' S – 17° 44.330' E.

Outcrop 3 (Varianto/Chuos Formation): 19° 26.356' S – 17° 44.034' E.

Outcrop 4 (Berg Aukas/Gauss formations?): from 19° 26.337' S – 17° 44.026' E to 19° 26.064' S – 17° 44.175' E.

The track following the outcrops 1 to 4 cuts through the Nosib Group, Varianto/Chuos and Berg Aukas formations. At the outcrop 1, the sediments of the Nabis Formation (Figure 7.7.A) consist of several cycles of 1) > 1 m-thick

conglomerate with well-rounded pebbles built in a sandy matrix alternating with 2) m-thick cross-bedded sandstones. In the conglomerate, clasts are 5–20 cm large, occasionally larger. Upsection, blocks of ironstone poorly arise from the ground at the outcrop 2 (Figure 7.7.B). The ironstone corresponds to the Varianto Formation, a local iron-rich variant of the Chuos Formation. The last facies before the cap carbonate is found at the outcrop 3, where the Chuos Formation is again poorly exposed. Observed blocks (Figure 7.7.C) show a sandy matrix with poorly sorted, angular to well-rounded clasts that do not exceed 5 cm in size.

The contact between the Chuos and the Berg Aukas formations was not observed due to low-lying topography and the dense ground vegetation cover. It is however visible at the Varianto Farm (Figure 7.7.D, northwest from Ghaub Farm). The outcrop 4 is found on the slope of a hill; exposure is very poor due to the weathering and the vegetation. Observations are consequently scarce and establishing the thicknesses and facies variations is complicated. From the base to the near-top of the hills, the Berg Aukas Formation exhibits 3 different facies. The first is a dark to light grey, perfectly flat and thinly (mm to sub-mm-thick laminae) laminated dolostone (Figure 7.8.A). Rare cross-bedding can occur as shown on Figure 7.8.B. The exact thickness was not measurable but this facies occurs for less than 30 m.

Several local, 1–10 m large exposures were found upsection, corresponding to the second facies, another laminated dolostone. Laminae appear thicker (2–5 mm) than at the base of the hill (Figure 7.8.C), more crinkly, with local dm-scale folding (Figure 7.8.D) intercalated between non-deformed intervals. This facies is comparable to that found at the outcrop 1 of the Nosib Block and in MM1 in the Rasthof Formation, northwest Namibia.

In the upper part of the hills, a third dolostone facies is characterised by thin (sub-mm), dark and flat laminae, in which cm-thick sets of laminae can be deformed (Figure 7.8.E). Deformed intervals are contorted and tend to occur between non-deformed laminae, for a thickness not exceeding 5 cm. This kind of contorted interval is described as a roll-up feature and is common in MM2 of the Rasthof Formation (Hoffman and Halverson, 2008; Pruss et al., 2010, Chapter 5).
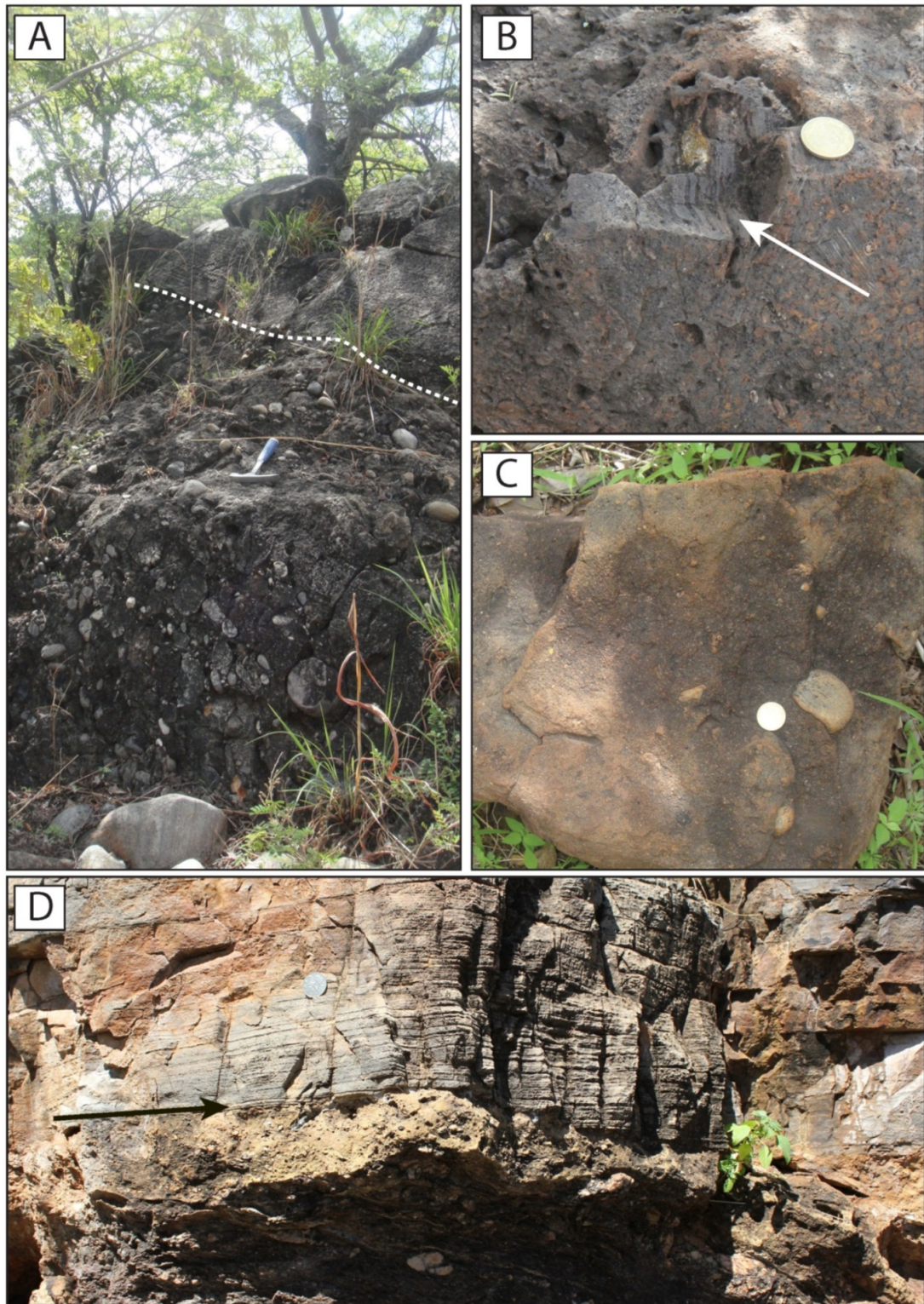
Figure 7.7: Facies from the Ghaub Farm (1/2). **A**. A cycle of well-sorted and rounded conglomerate and coarse sandstone, Nabis Formation (outcrop 1). **B**. Clast of stromatolite in the Varianto Formation ironstone (outcrop 2). **C**. A block of Chuos Formation, with poorly sorted pebbles (outcrop 3). **D**. Contact between the Chuos Formation and the Berg Aukas Formation (Varianto Farm, photo credit D.P. Le Heron).
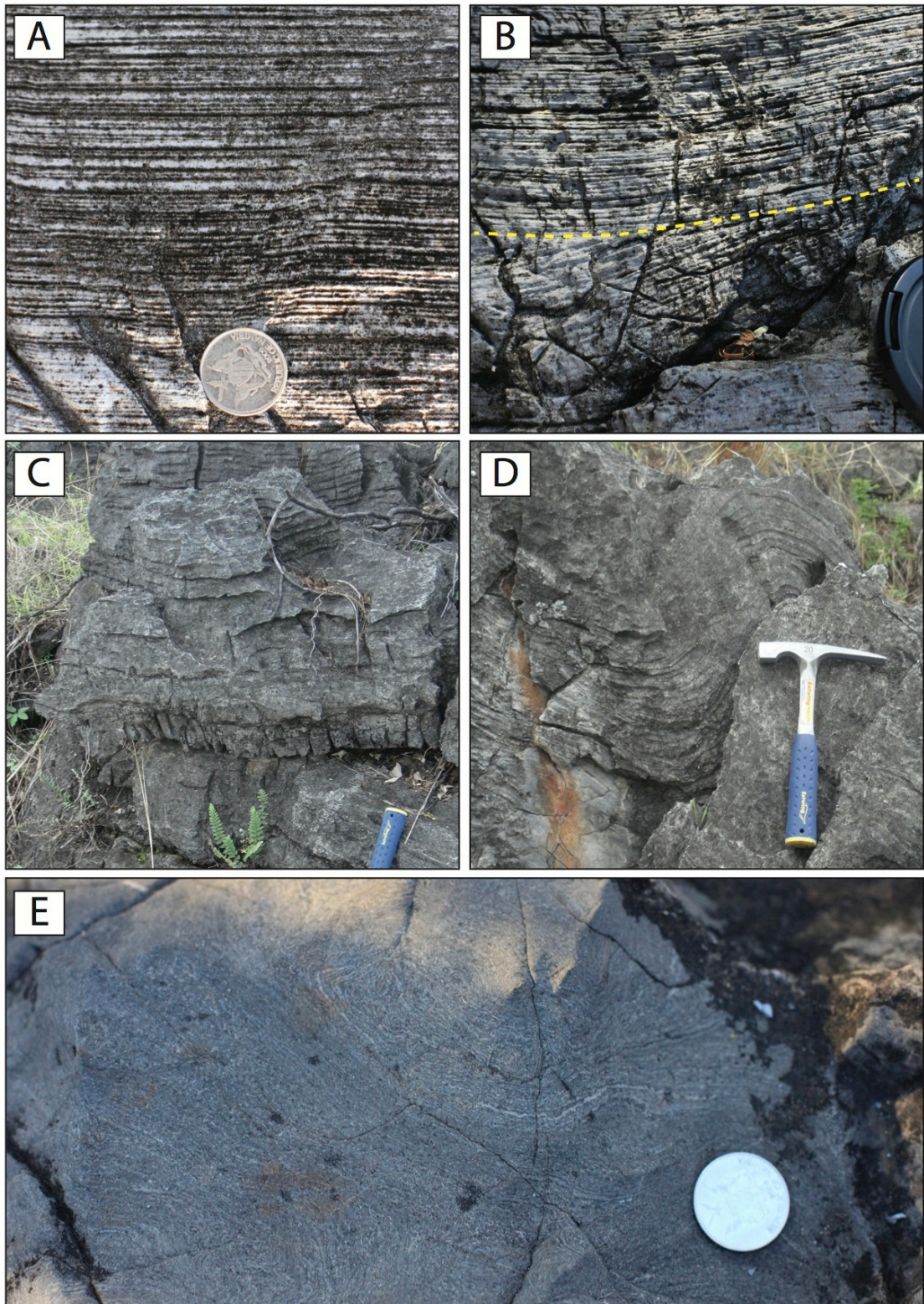
Figure 7.8: Facies from the Ghaub Farm (2/2). **A**. Flat, smooth laminae at the base of the succession. **B**. Local occurrence of cross-bedding. **C** and **D**. Thickly laminated (1–5 mm) crinkly dolostone with local deformations. **E**. Finely laminated (sub-mm) dolostone with occurrence of roll-up structures.

## 3.4 Location 4: Varianto Farm

Outcrops (Berg Aukas/Gauss formations?): from 19° 24.031' S – 17° 41.705' E to 19° 23.873' S – 17° 42.007' E.

The last farm visited, the Varianto Farm, is enclosed at the southern end of the Elandshoek Farm. The base of the section is only accessible by car from the west via the Nabis Farm. As with the other locations, the Berg Aukas Formation is exposed on the southern flank of a hill. At the base of the hill, the Chuos Formation is locally exposed but the contact with the Berg Aukas Formation was not observed. The contact was observed by Busfield and Le Heron (2013, location: 19° 24.415' S, 17° 42.443' E – see Figure 7.7.D), between locations 3 and 4.

The first cap carbonate facies occurs at the base of the hill and carbonates are still visible at the top of the hill, where they are mapped as the Gauss Formation. From the base to the top of the hill, the total thickness of the sediment succession is approximately 250 m. Exposure and accessibility to outcrops are poor. The first facies consists of a 20 m high cliff of very dark, finely laminated dolostone (Figure 7.9.A), and then vegetation and recent rockslides cover a more recessive facies. Many loose blocks occur in this second facies. They consist of breccia made of light grey, perfectly flat, mm-thick laminated dolostone clasts (Figure 7.9.B). Clasts found in these blocks are the same facies than the basal dolostone from Ghaub Farm (see Figure 7.8.A).

Above the first recessive facies, a second exposure of laminated dolostone is revealed, with crinkly and thick laminae (2–5 mm), similar to the second dolostone facies found at Ghaub Farm. Laminae are slightly undulating and the rock is razor-sharp weathered. The lateral extent of this exposure is less than 20 m. These rocks are followed by recessive strata that locally expose thickly laminated dolostones. Several blocks are found and these are nodular (Figure 7.9.C). The blocks are not *in situ* but are likely derived from the strata at the top of the hill.

This last laminated dolostone facies, exposed for more than 50 m, is characterised by thick and slightly undulose subhorizontal laminae. They locally form 3–5 cm wide, 2–3 cm amplitude reversed hemispheroids also named cuspate structures

(Sumner, 1997) (Figure 7.9.D). Enterolithic networks and < 5 cm large nodules commonly occur. These nodules exhibit bladed to fibrous crystals (Figure 7.10.A, B). Observation of polished slabs of sample reveals a regular alternation of white and grey laminae (Figure 7.10.C) that is not obvious at the outcrop.

Carbonate facies do not change considerably from the base to the top of the hill: they consist of laminated dolostone. Only the first cliff and recessive unit are mapped as the Berg Aukas Formation while the overlying sediments appear as the Gauss Formation on the geological map of the area (Schreiber, 2008).
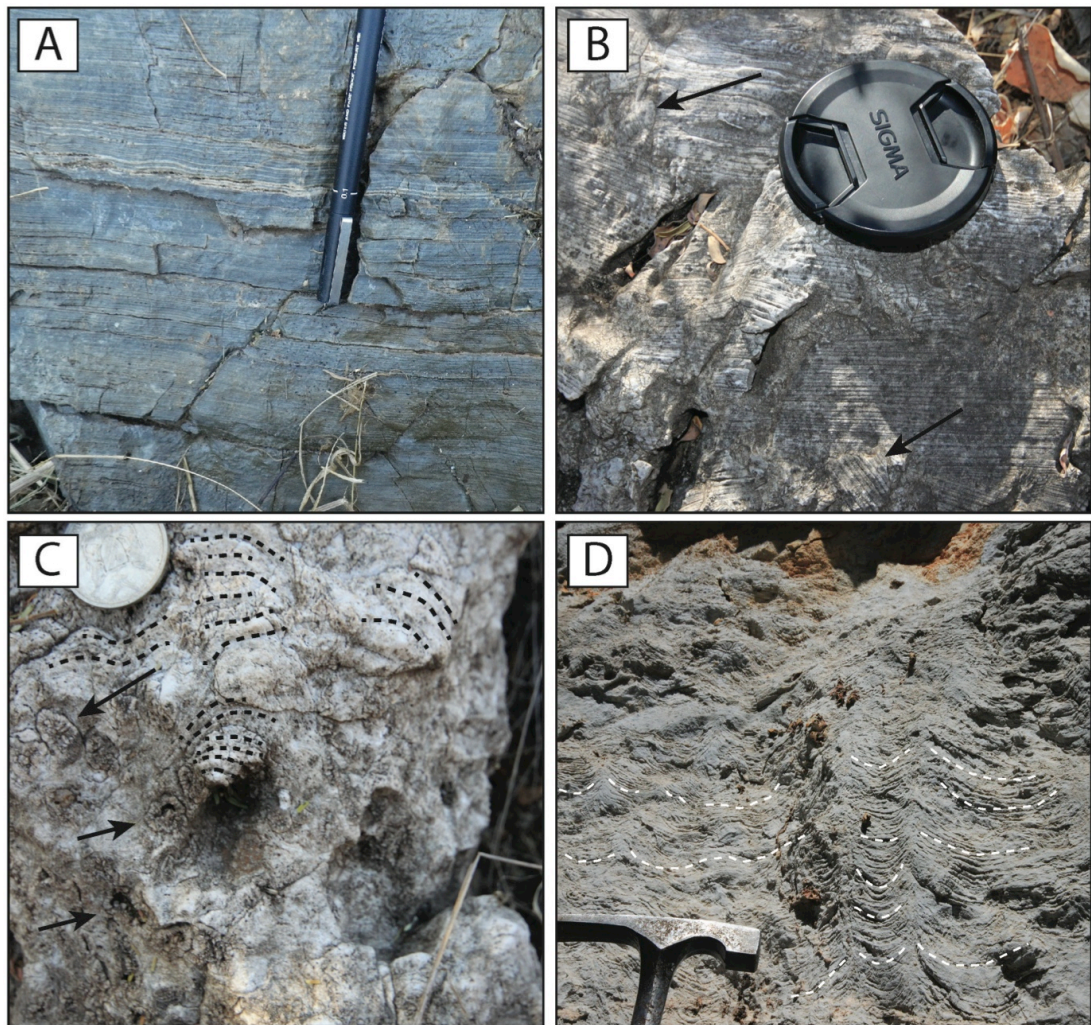


Figure 7.9: Facies from the Varianto Farm. **A**. Flat, dark, thinly laminated dolostone observed at the base of the succession. **B**. Breccia of finely, flat, laminated dolostone. Two clasts are shown with arrows. **C**. Thickly laminated stromatolites with occurrence of nodules (arrows). **D**. Topping hill outcrop, with laminae forming cuspate structures (outlines with white dashed lines).
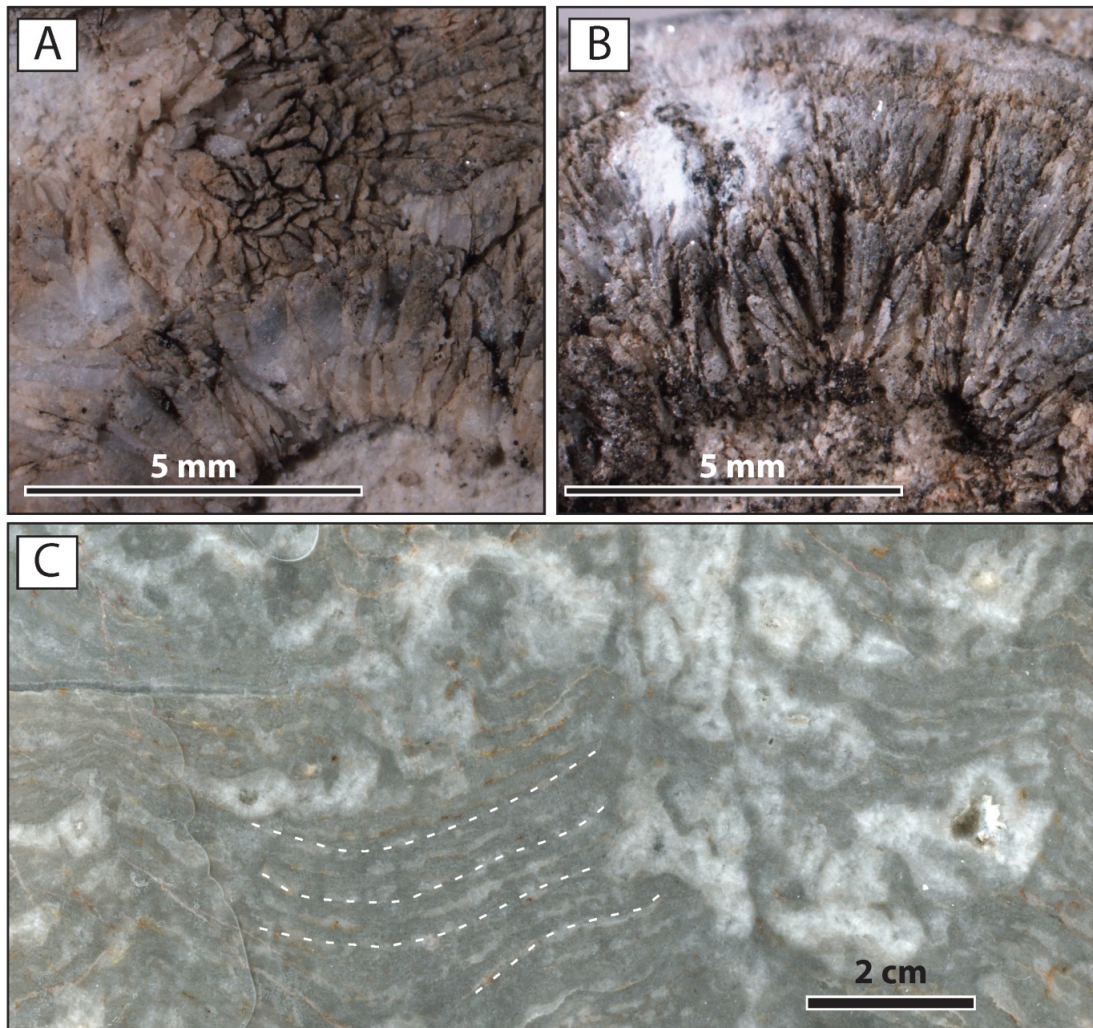
Figure 7.10: Detail of the nodules and enterolithic network found in the thickly laminated dolomites, Varianto Farm. **A** and **B**. Bladed fans fringing the nodules. In top view (upper part of photography (A) and lateral view (B). **C**. Polished slab of the cuspate structure with grey laminae alternating with white, recrystallised and discontinuous layers. The thin white intervals are connected to the nodules, forming an extensive lateral network.

## 4 Interpretations of the cap carbonate facies

At all the visited locations, carbonate outcrops are characterised by laminated dolostone, with different degrees of undulation and different thicknesses of laminated fabric. No obvious bedforms or oolitic intervals were observed; yet they are described in the literature in the same area (Miller, 2008). The visited sections are sometimes mapped or considered as the Gauss Formation (Miller, 2008; Schreiber, 2008). A problem is that on the map and in the literature, the Gauss Formation is described as a massive dolomite and the Berg Aukas Formation as a laminated dolomite. Thus, the constant observation of laminated facies at all the

visited sections tends to designate the observed dolostone as the Berg Aukas Formation. The four sections, ranging from 250 m (Varianto Farm) to less than 100 m-thick (Road C42) are synthesised in Figure 7.11.

## 4.1  Cap dolostone

Typical cap dolostone facies were observed at the base of the succession at the Ghaub Farm (Figure 7.8.A). They are similar to those observed elsewhere on the northwestern part of the platform, at the base of the Rasthof Formation. They are apparently non-biologically accumulated, smooth, and perfectly flat when not deformed, with a consistent mm-thick layering. Rare cross-bedding occurs, indicating locally elevated hydrodynamic energy levels of sufficient magnitude to produce tractive bedforms. At Ghaub Farm, it is less than 30 m-thick, which is consistent with observations made by Miller (2008) on this facies. The previous author and Misiewicz (1988) also mentioned the occurrence of interbedded arkose or conglomerate in nearby areas. Few sedimentological features have been observed but the occurrence of cross-bedding and clastic bedforms in the cap dolostone indicate some energy as well as fairly proximal detrital input.

Similar but darker, slightly wavy facies are characteristic from the basal outcrop of the cap carbonate sequence at the Varianto Farm (Figure 7.9.A). They may represent the deepest observed facies of the cap carbonate, possibly deposited in an anoxic setting by analogy to similar facies recognised by Bechstädt (2009) from the Maieberg cap carbonate. Laminae are relatively smooth and flat with a mm-thick laminated fabric. Upsection, exhumed brecciated blocks of lighter cap dolostone appear on the slope of the hill (Figure 7.9.B). This second cap dolostone facies is more comparable to that observed at Ghaub Farm (i.e. regular, thin light millimetric fabric, Figure 7.8.A). The exact thickness of the cap dolostone was not measured at Varianto Farm but it is around 60 m-thick, exceeding the < 30 m from the Ghaub Farm and probably indicating more accommodation at the time of deposition.
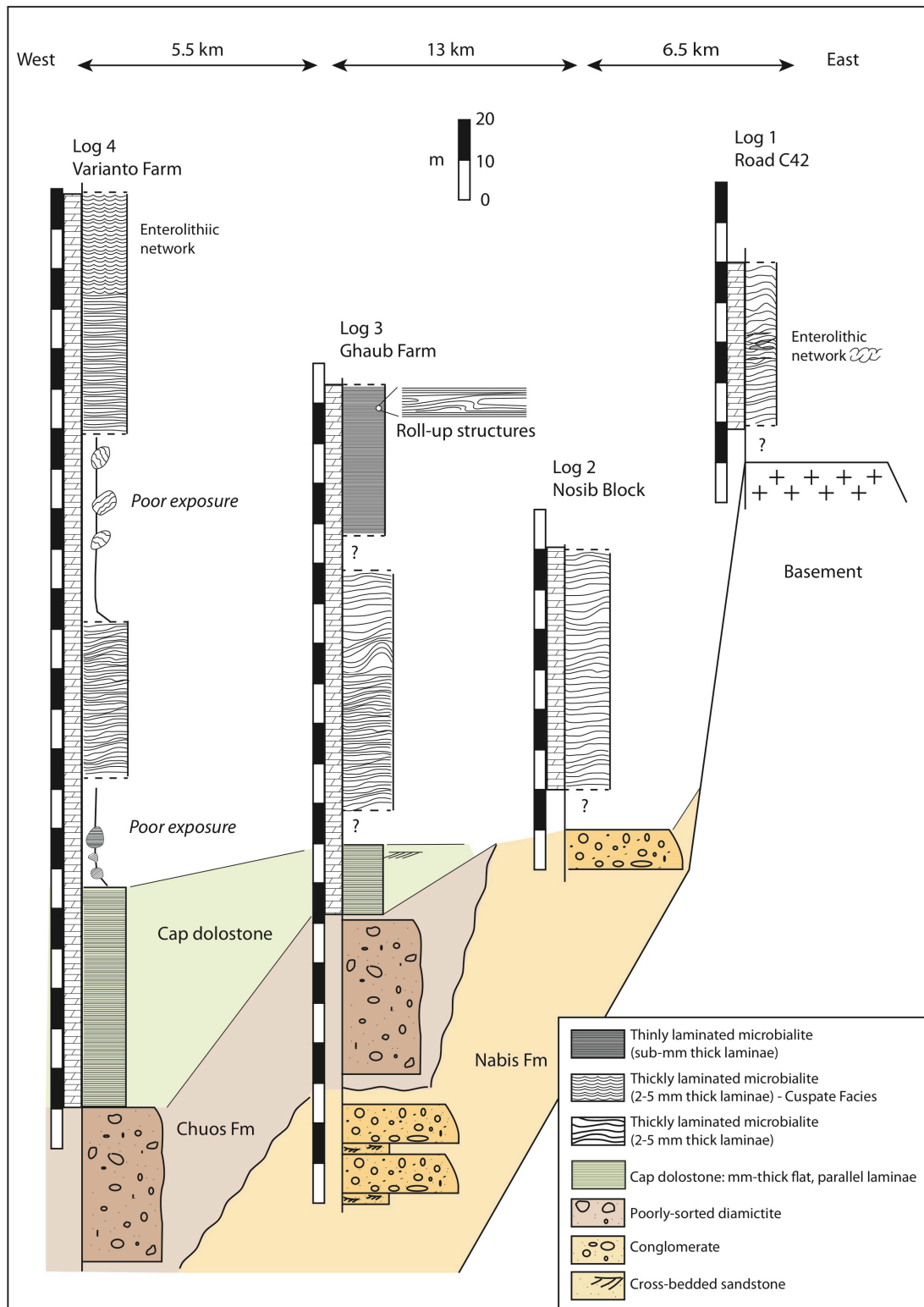
Figure 7.11: Correlation panel of the four studied locations in the Otavi Mountain Land. The 4 logs transect is ~25 km long. Lithostratigraphy is easy to correlate for the cap dolostone (green), Chuos Formation (red) or Nabis Formation (yellow). However, laminated microbialite deposited after the cap dolostone are more complicated to correlate from one outcrop to another. Remaining samples are referenced in Appendix D.

238

## 4.2 Microbial Facies

Like in northwest Namibia, the Abenab Subgroup records extensive, undulated and laminated dolostone. Though microfacies analysis did not reveal any preservation of microbial communities, a microbial origin is generally accepted (Miller, 2008; Misiewicz, 1988). At the Ghaub Farm, the undulated, crinkly laminated dolostone can be differentiated into two facies. The first, thickly laminated facies is characterised by relatively thick (2–5 mm) crinkly and undulated laminae while the second is thinly laminated (sub-mm-thick laminae).

### 4.2.1 Thickly laminated facies

At the Ghaub Farm, the second facies, encountered after the cap dolostone, is very similar to the one observed in MM1 in northwest Namibia. Laminae are thick and crinkly, 10–50 cm-thick sets of laminae can locally be deformed (Figure 7.8.C, D). Because the deformations tend to occur between non-deformed intervals, they probably occurred prior to lithification. Similar facies are observed at the first location of the Nosib Farm (Figure 7.6.A). At the supposed location from Cloud and Semikhatov (1969), the sediments mapped as the Berg Aukas Formation (Schreiber, 2008) and described as the Gauss Formation by Miller (2008) exhibit a complex arrangement of MM1 type facies associated with enterolithic networks (Figure 7.5). The facies topping the hill at Varianto Farm is similar, with thick (2–5 mm) grey laminae interbedded with white thin (< 2 mm) vertical and horizontal discontinuous recrystallised network. This facies also includes 2–4 cm large recrystallised nodules. Miller (2008) and Misiewicz (1988) described and illustrated, elsewhere in the Otavi Mountain Land (e.g. Farm Schonbrunn 344, Berg Aukas Anticline) similar structures in shape and size, naming them "colloform structures". The nature of the above features will be detailed in section 4.2.3.

In Misiewicz's (1988) illustration (Figure 7.2), the stromatolites are comparable to thickly laminated facies from MM1: they consist of relatively thickly laminated microbial laminae, forming laterally continuous and undulated mats. The same author also described them as distorted, once again reminiscent of the facies of MM1 in northwest Namibia. This facies occurs at several farms in northeast Namibia but is rarely as chaotic as in northwest Namibia.

No individual observations point definitively to an exact depositional setting. However, Miller (2008) described oolites associated with the same facies, in the same area (Nosib Block). We can expect this facies to have formed in or nearby a relatively agitated environment, shallow subtidal to intertidal. Undulated to slightly chaotic nature of the laminae indicates they were probably cohesive, limiting their break-up under a wave energy setting. Yet Misiewicz (1988) described intraclasts associated with the distorted microbial laminae of the Berg Aukas, indicating they can break under intense hydrodynamic stress.

### 4.2.2    Thinly laminated facies

Dark grey, thinly laminated facies with local roll-up structures are typical from MM2 (Rasthof Formation) in northwest Namibia (Chapter 5, Hoffman and Halverson, 2008; Pruss et al., 2010). It can also be associated with columnar and branching stromatolites (Chapter 5). In northeast Namibia, this facies was only observed at the Ghaub Farm, not associated with any vertical stromatolite growths. The rare observation of rolled-up facies along the transect is possibly due to the general poor exposure in the area.

Similarly to MM2 in northwest Namibia laminae are mostly flat and thin (sub-mm). They possibly record a quiet setting with local high-energy events that shape roll-up structures. The occurrence of these structures between non-deformed laminae indicates they are soft-sediment deformations. The supposed microbial and cohesive nature of the sediments prevented the sets of laminae to break during potential hydrodynamic energy events.

### 4.2.3    Enterolithic networks

Laminated dolostones associated with enterolithic networks and nodules occur at two visited outcrops. These are 1) along the road C42 where the sediments are mapped as the Berg Aukas Formation (Schreiber, 2008) and described as the Gauss Formation (Miller, 2008), and 2) at the top the hill at Varianto Farm, > 200 m above the underlying diamictite, where they are mapped as the Gauss Formation. The stratigraphic relationship will be discussed in section 5.3.

### 4.2.3.1    Stromatactis?

Miller (2008) described this facies as stromatactis, a poorly understood, rare feature in the sedimentological record (Aubrecht et al., 2009 and references therein) and extremely uncommon in the Precambrian (Hladil, 2005).

Five criteria are required to identify stromatactis (Bathurst, 1982): masses of spar, smooth base, digitate roof, occurrence in swarms and reticulate distribution. South of Tsumeb, the enterolithic networks have an uncertain orientation. They can appear flat and well interbedded with dolomite laminae. Most of the criteria are present but digitate tops are globally absent. Thus, according to the criteria of Bathurst (1982), enterolithic networks fulfil most but not all of the criteria to be interpreted as stromatactis.

Aubrecht et al. (2009) summarised the different hypotheses to explain the origin of stromatactis features. They explain that the most common explanation invoked is that "they are cavities which remained after decomposition of an unknown soft-bodied organism or by neomorphism of carbonate-secreting organism". During the Cryogenian, apart from microbial colonies, other forms of life have been reported (Bosak et al., 2012; Brain et al., 2012; Dalton et al., 2013; Maloof et al., 2010; Porter et al., 2003) but not in form of extensive lateral colonies. Known Cryogenian forms of life do not compare in form and abundance with the observed enterolithic networks. However, the occurrence of soft material during and soon after deposition can still explain the features observed at the outcrop. A possibility in a microbial dominated setting, is the extracellular polymeric substance (EPS, e.g. Decho et al., 2005) generated by the microbial communities. Such material gives a soft, gelatinous texture to the sediments.

The features observed are unlikely to be qualified as stromatactis because they do not fulfil all the criteria (Bathurst, 1982). Also, Precambrian features interpreted as stromatactis are rare and uncertain (Hladil, 2005). However, as the previous authors pointed out, the initial material in stromatactis was soft, which is compatible with the production and preservation of EPS at the time of sedimentation. In the following parts, very different interpretations are suggested: 1) another possible initial occurrence of soft material is illustrated, where the features are also

compared to possible evaporites; 2) the enterolithic networks and veins result from later fluid circulation (brines).

### 4.2.3.2    Evaporites?

The enterolithic networks (Figure 7.5.B), nodules (Figure 7.5.C) and chicken-wire textures (Figure 7.5.D) observed share common features with old evaporites as found in the literature (El Tabakh et al., 1999; Gandin and Wright, 2007). Gandin and Wright (2007) published a detailed analogy between Neoarchaean carbonate sediments, modern sabkhas environments and Messinian evaporites.

Meso- to microscopic observations undertaken on the samples collected along the road C42 (location 1) and at Varianto Farm (location 4) reveal mm-thick folded intervals, similar in shape but not in scale (Figure 7.12) to the one used as an analogue by Gandin and Wright (2007). The folding of these thin layers interlaminated with grey dolomite indicates they were probably soft material, deformed before lithification. Different degrees of deformation can be identified (Figure 7.13.A, B). This material was maybe present at an early stage as primary evaporites. The cuspate structures from Varianto Farm might as well represent primary gypsum associated with microbial facies.

### 4.2.3.3    Fluid flowing through veins?

The above section suggests that interlaminated, recrystallised enterolithic facies and possibly nodules and chicken-wire textures may correspond to primary evaporites. When observed, enterolithic network also exhibits vertical structures, apparently cutting through laminae (Figure 7.5.B). Those may also result from a completely different, non-syn-sedimentary process. After the lithification of the laminated dolostone, fluids circulation created or filled veins cutting through the sediments. A likely scenario in the Otavi Mountain Land, where similar mineralisation processes are extremely common. The timing of such fluid circulation is difficult to evaluate with current data (Kamona and Günzel, 2007). However, the observation of clearly folded features suggests a deformation prior to lithification of the veins (Figure 7.13.C–E). Interlaminated folds and subvertical veins

result from two different processes, at different timing, as suggested in the following section.

### *4.2.3.4    Interpretation*

Bechstädt et al. (2009), Miller (2008) and Misiewicz (1988) works mention and/or illustrate, both in the Gauss and Berg Aukas formations, colloform structures that compare well with observed nodules, enterolithic networks or veins. Yet their suggested origin remains vague. They can be interpreted as stromatactis (presumably syn-sedimentary features) (Miller, 2008), diagenetic features that formed in a subaerial environment (Misiewicz, 1988), or fissures resulting from tensional tectonics (Bechstädt et al., 2009).

It is suggested here that the material found in the enterolithic network (veins, laminae and nodules) was deformed at some point (Figure 7.13. A, B); possibly due to volume changes, expansion of that material. Figure 7.13.C illustrates veins cutting through the outcrop. In the detail each sparry vein has an intensely folded texture, with folds similar to the one observed in Figure 7.12.A, and local development of mm–cm-scale nodule or chicken-wire texture (Figure 7.13.D, E). From meso- to microscopic scale observations, it is possible to suggest an initially soft material that was deformed during or shortly after its formation. The origin and chronology of these features is, however, difficult to evaluate.

Given the supposed relatively shallow water setting in which accumulated the Berg Auks Formation (Miller, 2008; Misiewicz, 1988) and additional observations presented in this chapter, it is possible to consider local development of evaporites at the time of deposition. Interlaminated, folded intervals, cuspate structures, cm large nodules and dm large chicken-wire texture then support this interpretation. Evaporites first started to develop as mm–cm-thick layers interlaminated or interbedded with laminated microbial carbonate. Before lithification, migrations and volumes changes due to early compaction probably led to the deformation of the soft material, forming small-scale folding (Figure 7.12). At the most advanced stage of deformation, individual nodules (Figure 7.5.C; Figure 7.13.B) and chicken-wire textures (Figure 7.5.D) started to form.

However the subvertical veins most probably result from a later process, with dissolution, transport and precipitation of soft material in the veins. This kind of model was already suggested in evaporitic successions, where initial, stratified evaporites were dissolved, transported in solution through fractures, and then precipitated as secondary gypsum (Gustavson et al., 1994; Philipp and Gudmundsson, 2006; Testa and Lugli, 2000). The mineralisation of the Berg Aukas Formation can follow comparable chimney like features ("sparry veins", Kamona and Günzel, 2007). With the observation gathered on the field, it is not possible to establish how the veins formed and at which stage their filling occurred.
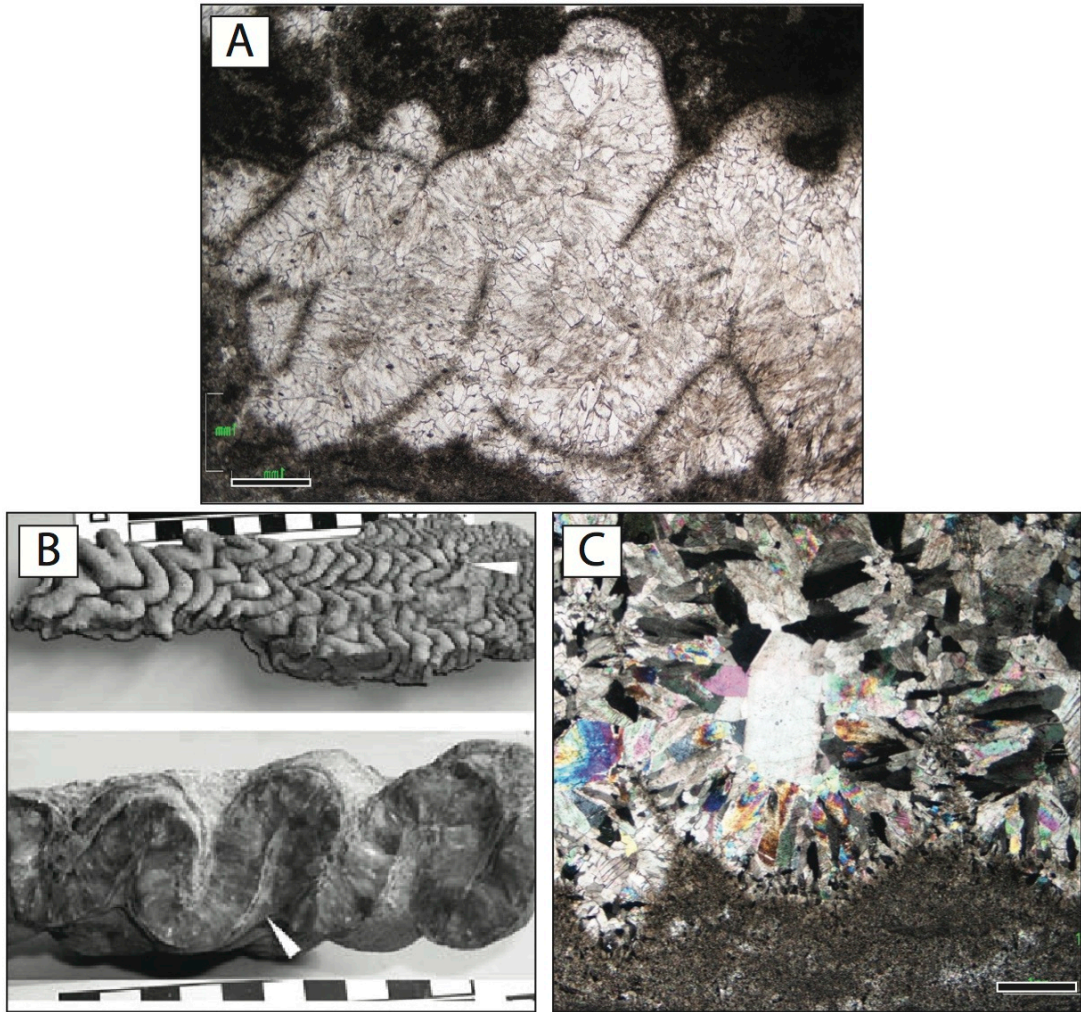
Figure 7.12: Folds interlaminated with dolomicrite. **A**. Thin section through a folded interval in a laminated dolostone. Sample from road C42 (scale bar is 1 mm). **B**. Comparable enterolithic folds formed by expansion of evaporites (from Gandin and Wright, 2007, fig. 11.b,c). **C**. Detail of A: cross polarised microphotograph of an enterolithic fold. Sample from Road C42 (scale bar is 1 mm).
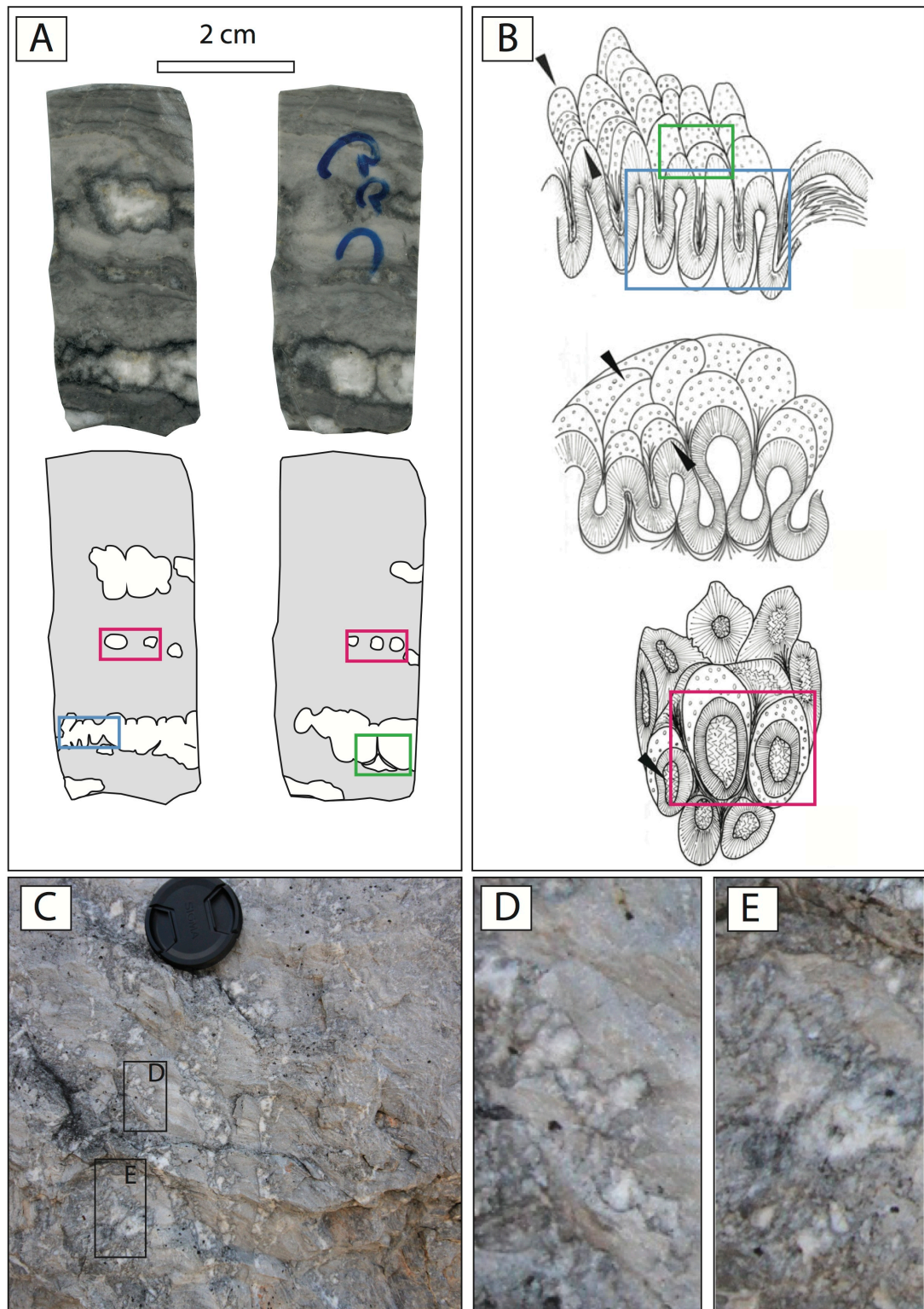
Figure 7.13: Different degrees of deformation of soft material. **A**. Slab sample from the Road C42, with deformed material (white) interbedded with microbial mats (grey). Coloured rectangles are used to compare with different degrees of deformations with **B**. Suggested stages of deformation from folds (blue, green rectangles) to nodules (red rectangle) (Gandin and Wright, 1997). The blue rectangle is detailed in Figure 7.12.A. Note that large nodules are also observed at the location 1 (Figure 7.5.C). **C**. Location 1, subvertical veins viewed at the outcrop scale (lens cap is 72 mm ∅). **D** and **E**. Details showing they are not stromatactis or fissure but intensely deformed intervals forming folds and nodules comparable to phases shown in B.

# 5    Discussion

## 5.1    Rifting and glaciation

Where observed, the Nosib Group is characterised by conglomerate and sandstone sediments; logically interpreted as continental deposits in the area (Misiewicz, 1988). In a more regional setting, the area is located to the north of the Northern Nosib Rift. Rifting has stopped before any continental crust rupture (Frimmel et al., 2011; Miller, 2008; Miller et al., 2009); therefore to the south and to the north of the area, continental to very proximal, settings are expected. The glacigenic Chuos/Varianto Formation was deposited after the Nosib Group, probably in an intra- or epicratonic setting. The mapping of the area (Schreiber, 2008) suggets that the diamictite does not occur as a continuous sedimentary unit: it tends to pinch out laterally on a 10s of km-scale. On the map, these discontinuities are indicated by a direct contact between the Berg Aukas Formation and the Nosib Group or the basement. The patchy occurrence of the diamictite might be due to its deposition and preservation either in the palaeotopographic depressions or in the incisions created by ice, or a combination of both. Another possibility is that the diamictites was deposited everywhere but locally eroded before the deposition of the Berg Aukas Formation. In this second scenario, the post-glacial transgression was minor and allowed erosion of emerged lands. Critically, no lag deposits are present, and the cap carbonate sits in sharp contact on underlying glaciogenic strata (Figure 7.7.D).

What was the basin polarity during the Chuos glaciation, and was this inherited by Rasthof/Berg Aukas time? Busfield and Le Heron (2013) demonstrated that in the studied area, ice movement was from south (proximal) to north (distal). Their model suggests that there was a depocenter towards the north. This model assumes an intra- or epicratonic setting, with basins located on the Angola Block. As suggested in a previous model (Misiewicz, 1988), a part of the sedimentation was also probably oriented towards the south in the Northern Nosib Rift (Figure 7.14.1) but corresponding sediments must then be preserved south of the study area. It also means that high topography (rift shoulder, horst) probably separated one or several intracratonic depocenter(s) to the north from the Northern Nosib Rift to the

south. In this setting ice moved from the high topography, moving into depressions and/or incising valleys (Figure 7.14.2). The combination of the reduction of the extensional regime associated with the end of the ice age led to 1) a more stable tectonic system, with a diminution of massive continental, detrital input, and 2) a melt of the ice which initiated flooding. Both of these conditions allowed the accumulation of the extensive Otavi platform (Figure 7.14.3).

## 5.2 Cap carbonate

In the study area, the post-glacial cap carbonate sequence is recorded by the Berg Aukas Formation. The cap carbonate drapes the Chuos/Varianto and Nabis formations as well as the basement. The fact that the cap carbonate appears to rest not only on the diamictite, but also on older non-glacial facies indicates that the ice was possibly not present everywhere during the Sturtian Glaciation, or that ice was locally cold-based.

Facies associations and interactions in the cap carbonate remain obscure. In the studied area, the Berg Aukas Formation is exposed along a 25 km east–west transect. Facies are exposed virtually all along the south slope of several hills. Dense acacia vegetation and weathering limit observations. The cap carbonate exhibits various degrees of laminated dolostone, ranging from smooth, flat and thin, clearly non-biologically accumulated to crinkly, undulated to contorted and biologically influenced. No typical facies succession can be established from the field observations but it is possible to differentiate:

- the typical cap dolostone facies observed in the lower part of the cap carbonate sequence (Ghaub Farm, Varianto Farm), which is very similar to its lateral equivalent in the Rasthof Formation;

- thicker, more crinkly and disturbed/distorted laminae. This second category can be interpreted as mainly microbial in origin, like on the northwestern part of the platform (Hedberg, 1979; Hoffman and Halverson, 2008; Pruss et al., 2010; chapters 5, 6).

In the western half of the transect, cap dolostone rests in direct contact on the Chuos/Varianto Formation. In the eastern half, the cap dolostone was not observed,

and nor was the diamictite. Cap dolostone facies were probably deposited in the relatively deepest environment, to the west of the transect, such as the depressions created and used by ice streams. At the westernmost outcrop (Varianto Farm), the very base of the cap dolostone is characterised by dark laminated dolostone lying directly on the diamictite. They possibly represent the deepest observed facies for the cap dolostone, it is at this location that the cap dolostone is the thicker (~60 m). The cap dolostone is overlain by thicker microbial laminae, observed at all the locations. These facies include thickly laminated microbialites and local thinly laminated microbialites, characterised by typical roll-up structures.

Interpretation of all the above facies is complicated because analogues are rare in the sedimentological record. The cap dolostone is likely to have accumulated preferentially in depressions. The nature of these depressions in unknown and may correspond to incisions made by ice or local small intracratonic basins. Overlying microbial facies are more laterally continuous and may have accumulated once the depressions were filled by the cap dolostone facies. Previous interpretations found in the literature promote a relatively shallow-water, possibly lagoonal environment for the Berg Aukas Formation. An interpretation based on the observation of stromatolite facies associated with local debrite, breccias and siliciclastic input (Misiewicz, 1988). No such features were observed in the field but local cross-bedding in the cap dolostone and possible evaporites may indicate a relatively shallow setting. Also, observations found in the literature of the same sections such as oolite rich intervals (Miller, 2008) help to interpret microbialites as deposited in a relatively shallow, subtidal to intertidal environment.

Evaporitic environments may explain the occurrence of sparry nodules and folded intervals interbedded with laminated dolomite. A later fluid circulation filled the subvertical veins observed at the location 1. Each vein exhibits an intense folding compatible with the expansion of the filling material prior to its lithification. Evaporites at the time of deposition are a possibility, but their stratigraphic occurrence remains uncertain. Where described (locations 1 and 4), evidence for evaporites occur in ambiguous strata, sometimes designed as the Gauss Formation.

## 5.3  Berg Aukas and Gauss formations

Several inconsistencies are identified when comparing field observations, publications and geological map. The location 1 along the road C42 (19° 24.215' S – 17° 55.067' E) consists of thickly laminated microbialites associated with nodules and veins. It is mapped as the Berg Aukas Formation (Schreiber, 2008) but described as the Gauss Formation by Miller (2008). If this outcrop corresponds to the Gauss Formation, it means that the Berg Aukas is absent at this specific location, with the Gauss Formation lying directly on the basement. Interestingly, a comparable facies occurs at the top of the hill at Varianto Farm (location 4), mapped as the Gauss Formation.

Laminated facies are not typical from the Gauss Formation (Misiewicz, 1988; Miller, 2008), indeed the previous authors use "massive" to qualify the Gauss Formation while they use "laminated" for the Berg Aukas Formation. Thus all the observed facies are very likely to belong to the Berg Aukas Formation. Its thickness can range from 0 to up to 750 m, with an average of 300 m (Misiewicz, 1988), or according to Miller (2008), between 100 and 200 m. At the Varianto Farm, thickest carbonate outcrop observed, the succession is approximately 250 m, meaning that it could be qualified as the Berg Aukas Formation. If all the facies described belong to the Berg Aukas Formation, it has major implications for the palaeodepths in the aftermath of the Sturtian Glaciation in northeast Namibia, particularly with the occurrence of possible evaporites.
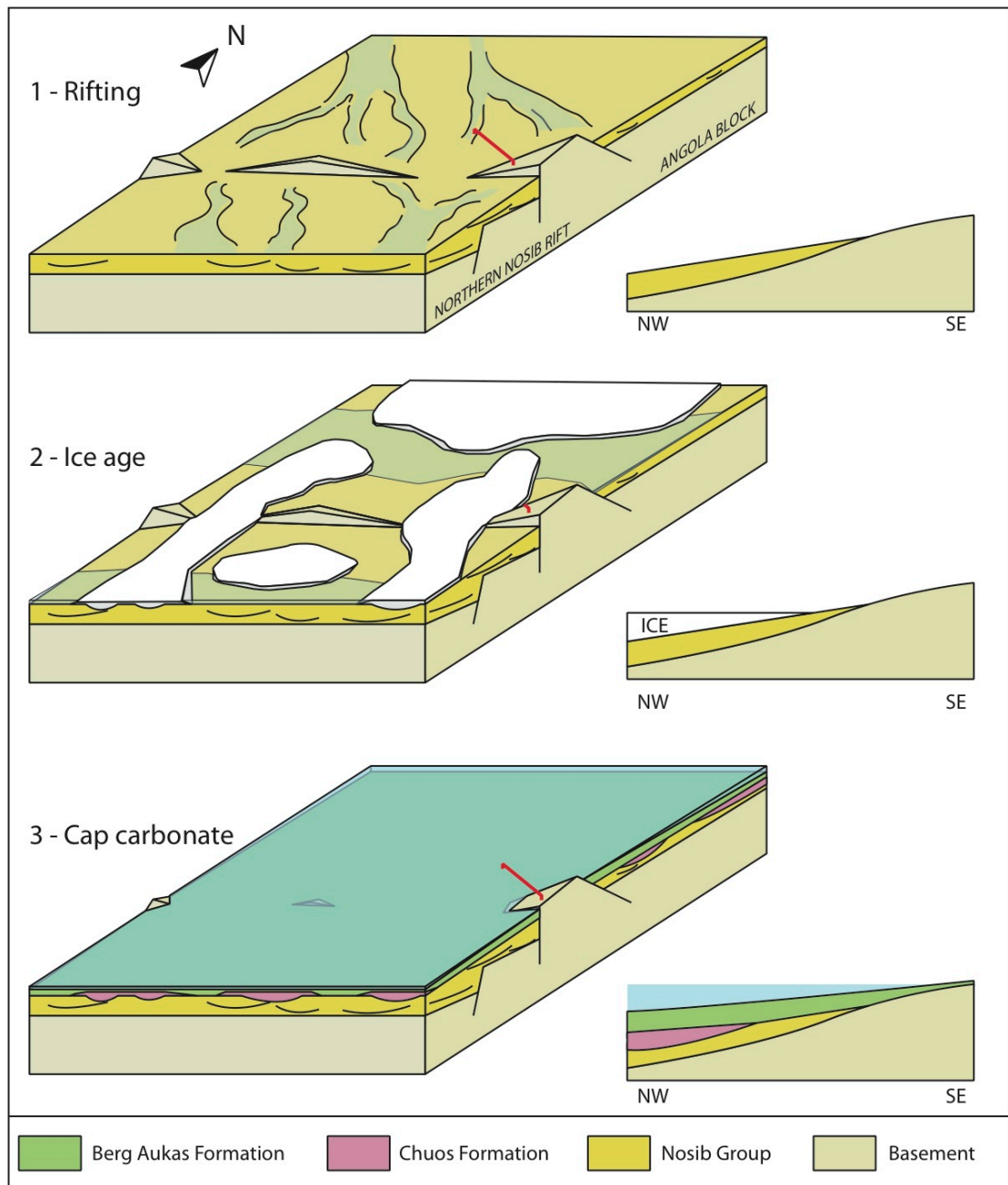
Figure 7.14: Model for the interpretation of the studied transect. The top sketch illustrates the general morphology of the southern edge of the Congo Craton during the late Tonian – Cryogenian. The study area is located north of the Northern Nosib Rift (red line and corresponding transect to the right). During the rifting (1), extensional regime led to the creation of an intra- or epicratonic basin. Silisiclastics of the Nosib Group were deposited in this setting. During the Sturtian ice age (2), ice sheets moved towards the depocenters, using palaeodepressions or incising previous sediments. At the end of the ice age, melting of the ice led to a flooding of the craton and the deposition of the Berg Aukas Formation (3).

251

# 6    Conclusion

The fieldwork in northeast Namibia was initially planned to 1) observe and compare individual stromatolite growths with the one found at Rasthof Farm in northwest Namibia; 2) evaluate facies variation on the Northern Platform. No individual stromatolites were observed although key observations have been gathered in the visited area.

- The siliciclastic and glacigenic facies were deposited north of the Northern Nosib Rift, in an intra- or epicratonic setting that was flooded after the Sturtian glaciation.

- The cap carbonate sequence following the glaciation is composed of one cap dolostone, non-biologically influenced followed by crinkly laminated dolostone, interpreted as microbially influenced. Unusual facies within the crinkly laminated dolostone include microfolds, nodules and veins, interpreted as former soft material (evaporites and secondary gypsum?). The cap dolostone is likely to have accumulated in the relatively deepest settings, then above sediments record a shallowing of the platform, possibly ending with evaporitic intervals.

- Facies variations in the crinkly laminated dolostones are difficult to evaluate due to the overall poor exposure in the area. Resulting from this, literature, mapping and field observations point at confusing designations of the stratigraphy. Differentiation of Berg Aukas Formation and the Gauss Formation can change from one author to the other, from one facies to another.

# Chapter 8 – Synthesis

## 1    Introduction

Many aspects of the Neoproterozoic have been touched upon in this thesis, at different levels of detail and depths of investigation. As each chapter contains a focussed discussion section, this chapter attempts to provide an overarching synthesis of the project and more holistic discussion.

This thesis has involved the study of three different areas on the edges of the Congo Craton: in the DRC, Zambia and Namibia. A specific stratigraphic interval has been investigated in each area, all of Neoproterozoic age, but not necessarily time equivalent from one area to the other. Based on the same global Neoproterozoic background, each area reveals different elements of the story and raises different problems, yet several observations and properties of the studied intervals are valid in each area. In this chapter, megaregional to regional scale observations such as geotectonic setting and their relationship to glaciation and development of carbonate platforms will be summarised, before synthesising more local observations on the genesis of the stromatolites.

## 2    The geotectonic setting

The break-up of the supercontinent Rodinia took place during the earlier part of the Neoproterozoic. Each of the three study areas was affected by this event. The timing is diachronous (Figure 8.1), with the oldest evidence of rifting dated at 999 ± 7 Ma in the WCB (DRC) by Tack et al. (2001), then around 883 ± 10 in the Lufilian Belt (Zambia) by Armstrong et al. (2005) and finally before 750 Ma (759 ± 1 Ma, 752 ± 7 Ma) in northern Namibia (Frimmel and Miller, 2009; Frimmel et al., 2011; Miller, 2008). Similarly, the late Neoproterozoic – early Cambrian Pan-African collisions are not perfectly synchronous but occured roughly between 600 and 500 Ma (Figure 8.1). The collisions are dated between 580 and 530 Ma in northern Namibia (Frimmel et al., 2011; Goscombe et al., 2005; Gray et al., 2008, 2006), around 566 ± 42 Ma in the WCB (Frimmel et al., 2006; Tack et al., 2001) and between ca. 590 and 512 Ma in the Lufilian Belt (Master and Wendorff, 2011).
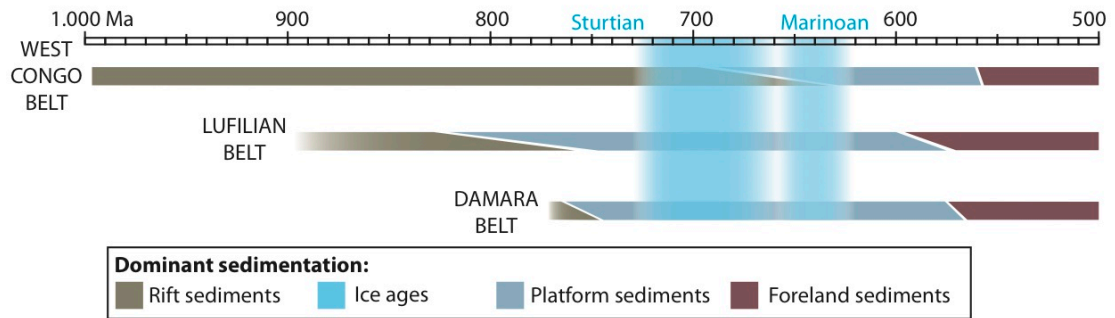
Figure 8.1: Synthesis of the main type of sedimentation in the three study areas: WCB (Frimmel et al., 2011, 2006; Tack et al., 2001), Lufilian Belt (Armstrong et al., 2005; Frimmel et al., 2011; Master and Wendorff, 2011) and Damara Belt (Frimmel et al., 2011; Gray et al., 2008, 2006; Miller, 2008). Ice ages are from Hoffman and Li, 2009.

As a result of the rifting, common palaeotopographic features are mentioned (or at least illustrated in previous literature) in Zambia and Namibia and can tentatively be suggested for the DRC. In northern Namibia, the Otavi Platform accumulated on high topographies (Figure 8.2.A), SSW of the Congo Craton. These rims (Halverson et al., 2005) or ridges (Hoffman and Halverson, 2008) comprise uplifted rift shoulders (Miller et al., 2009). Note that such topography is a key motivator for Eyles and Januszczak (2004) to criticise the idea of global glaciations during the Neoproterozoic: ice was present but probably only on these palaeohighs. Snowball Earth or not, an uplifted shoulder was present along the southern edge of the Congo Craton, now located in northern Namibia. During the Cryogenian (ca. 765 Ma) in Zambia, the uplift of a rift shoulder (Figure 8.2.B) was suggested by Wendorff and Key (2009). The uplift occurred south of the Congo Craton. The same authors suggest that the uplifted area was a source for glacial sediments, pointing at the occurrence of glacial sediments found in low elevation settings. Little is known on the role of this uplifted shoulder on the development of a Cryogenian – Ediacaran Neoproterozoic platform in the Zambian part of the Lufilian Belt. Nevertheless the break-up of Rodinia was accompanied by the development of palaeohighs, not far from the edges of the Congo Craton.
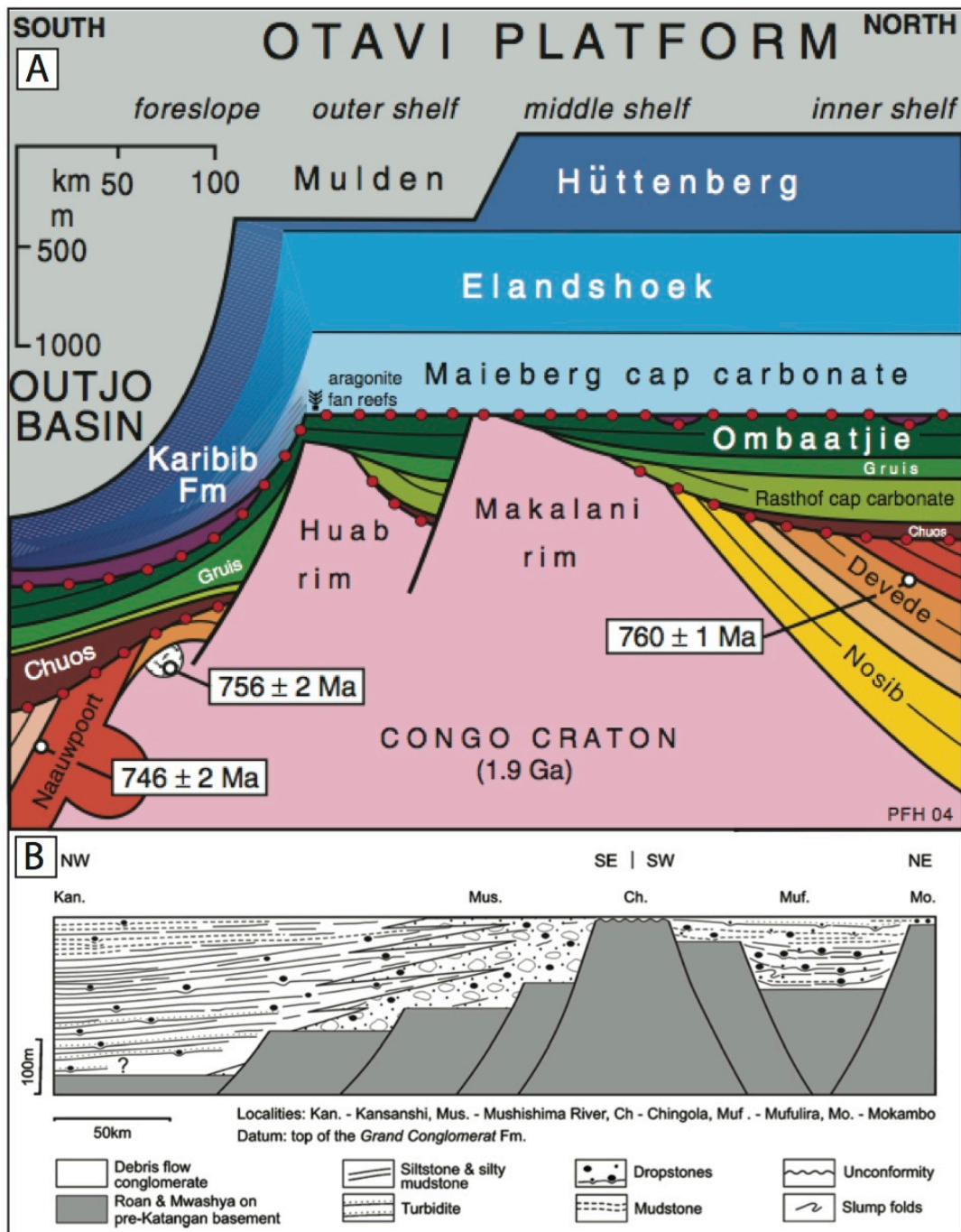
Figure 8.2: Illustration of high topographies on the edges of the Congo Craton. **A**. Namibia (Halverson et al., 2005). **B**. Zambia (Wendorff and Key, 2009). The high topographies are horst - half graben geometries.

Geotectonic models of the West Congo Belt have evolved considerably due to different interpretations of the Mayumbian Group (see Chapter 2). The latter has been interpreted as the result of a Meso-Neoproterozoic orogen for decades but more recent models suggest it results from a rifting between the Congo and the São

Francisco cratons at the very beginning of the Neoproterozoic, the Mayumbian Group has been bracketed between 920 ± 8 and 912 ± 7 Ma (Tack et al., 2001). A palaeohigh located west of the Congo Craton has often been considered, sediments were shed from this palaeohigh towards the Congo Craton, in a basin (foreland basin? failed rift basin?) following the modern coast from Gabon to Angola (e.g. Alvarez, 1995; Boudzoumou and Trompette, 1988; Vellutini et al., 1983). Note that the tectonic timing is not compatible with a Meso-Neoproterozoic orogen. Yet, Frimmel et al. (2006) found that some siliciclastic from the West Congo Group are of Mesoproterozoic age and infer that an island arc was possibly present in the vicinity of the West Congo Belt area, probably west from the rifted margin. This suggestion again raises the idea of a high topography along the rifted margin. An island arc is a possibility but considering observations from northern Namibia and Zambia, a high rift shoulder might also be considered. This would explain the high topography west of the West Congo Belt area and that component of the sedimentation were directed towards the craton (eastward). This hypothesis is compatible with a Tonian rifting setting (Pedrosa-Soares et al., 2008; Tack et al., 2001) and the solicitation of an epicontinental basin ("geosyncline", e.g. Schermerhorn and Stanton, 1963; Vellutini and Vicat, 1983; Vellutini et al., 1983) or an failed rift basin ("aulacogen", e.g. Alvarez, 1999; Boudzoumou and Trompette, 1988) east of the uplifted area. Boudzoumou and Trompette (1988) already suggested that a horst was present west of the WCB.

Whilst they are probably difficult to locate or to demonstrate owing to the long, complex geotectonic history of each area, horst and/or rift shoulders must be considered when studying strata accumulated along the edges of the Congo Craton. Their presence or absence has major implications for the direction of sediment supply and basin orientation. They were probably accompanied by the development of epicratonic basins, lagoons, opened or closed to the sea (Figure 8.3). Note that the uplift of a high topography may have occurred at various stages during the break-up of Rodinia. In northern Namibia, the high topography had first a palaeoslope oriented towards the open ocean (southward), a progressive change in the slope direction occurred, ending with a slope in the opposite direction (northward) (Hoffman and Halverson, 2008). In Zambia, the palaeohigh that created

an epicratonic basin occurred during the second rifting stage (Nguba rift) (Wendorff and Key, 2009).
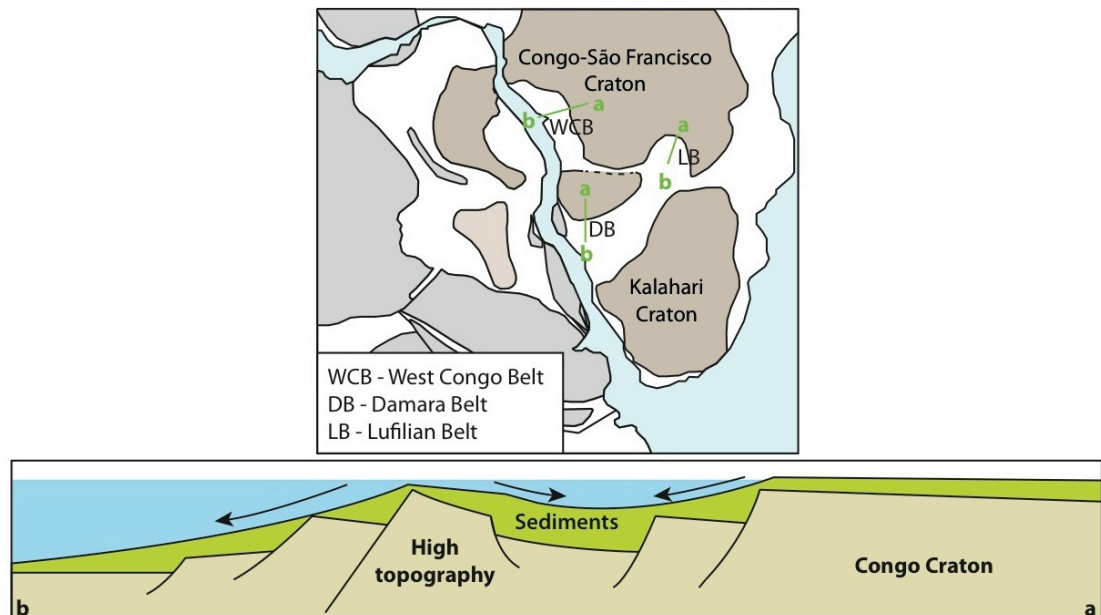


Figure 8.3: Topography and sedimentation along the Congo Craton. Idealised transect of the basement and resulting sedimentation during the rifting in the three study areas.

# 3    Ice ages

The Neoproterozoic is well known for its diamictites (Arnaud et al., 2011; Hoffman and Li, 2009), often interpreted as deposited in glacial to periglacial settings. Whilst the diamictites have not been specifically studied in this project the nature of the glaciations that may have produced them provides essential context in each study area, notably Namibia. The literature reveals long-lived vigorous debates. Authors can question the global tectonic setting (e.g. Eyles and Januszczak, 2004) as well as the facies of the diamictites to consider the degree of glacial influence on the diamictites (e.g. Eyles and Januszczak, 2007; Schermerhorn and Stanton, 1963), given that similar poorly-sorted rocks can form through gravitational instability. It is widely accepted that hard snowball Earth periods were unlikely to happen during the Neoproterozoic, various degrees and models of glaciations have been suggested (e.g. Allen and Etienne, 2008; Fairchild and Kennedy, 2007; Le Heron et al., 2013a, 2011; Wendorff and Key, 2009) to moderate the extreme, initial snowball Earth hypothesis (Hoffman et al., 1998).

Evidence for high topography along the rifted margins of the Congo Craton has been discussed in the previous section. The same kind of topography, uplifts has been invoked by Eyles and Januszczcak (2004) and also specifically in Namibia by Bechstädt et al. (2009) to explain the deposition of glacial to non-glacial Marinoan aged (terminal Cryogenian) diamictites. Uplift of some blocks or rift shoulders along the margins led to tectonic activity and the deposition of debrites both towards epicratonic basins and the open ocean (Figure 8.3). The same uplifted blocks had then a relatively high topography, favouring the development of ice bodies at high altitude. In northeast Namibia for example, Busfield and Le Heron (2013) demonstrate that the diamictites of the Chuos Formation record subglacial deformation beneath a northward flowing ice sheet. This implies a source to the south, compatible with a high palaeotopography. Wendorff and Key (2009) discuss that in Zambia a part of the sediments of the Grand Conglomérat Formation comes from a source area located to the south of the basin (highly uplifted block). In the West Congo Belt, little is known about source areas for the mixtites of the Bas Congo but they both thicken towards the south (Vellutini and Vicat, 1983) while the main rift basin (the open ocean) is located to the west of the WCB. This area has a complex basement structure with several intracratonic basins (Alvarez, 1999), and hence many sources can be expected for the diamictites of the Bas Congo. In the three study areas, the break-up of Rodinia seems to have created intra- or epicratonic basins and local uplifts while open oceans were opened in more distal settings. Epicratonic basins favoured a part of the sedimentation to be directed towards the craton, both in icehouse and greenhouse periods (Figure 8.4).
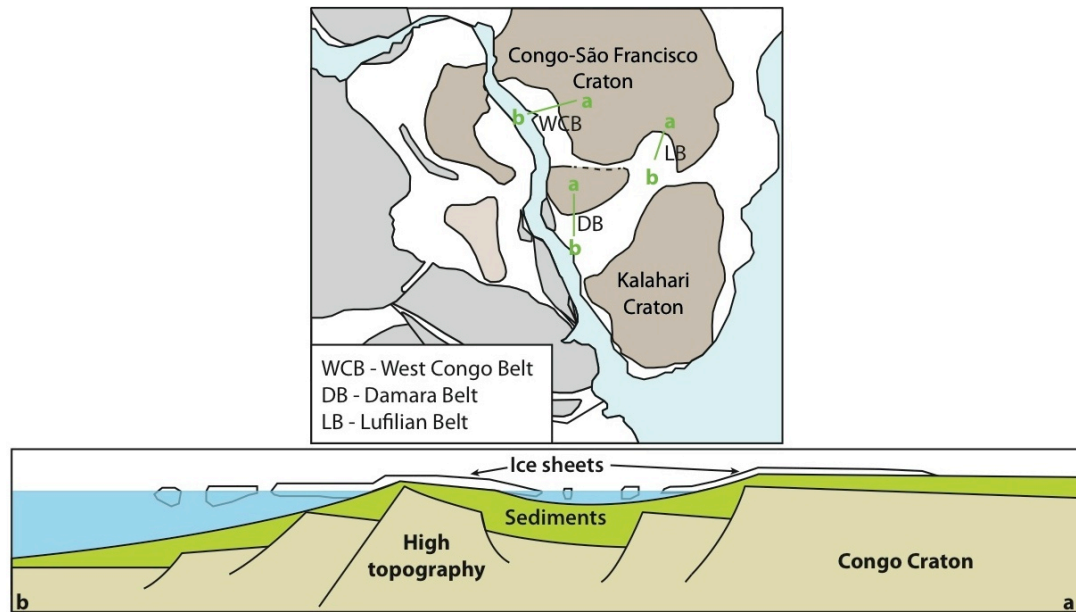
Figure 8.4: Ice ages. Idealised transect of the topography and its influence on ice ages in the three study areas.

## 4    Carbonate platforms

The diamictites from each study area are generally followed by a cap carbonate sequence and platform deposits. Following ice ages, meltdown of the ice bodies must have been accompanied by both eustatic sea level rise and isostatic rebound of the landmasses. Postglacial cap carbonates accumulated in this setting.

During the Neoproterozoic, carbonate platforms were widespread along the edges of the Congo Craton. They developed soon after the break-up of Rodinia, when siliciclastic input diminished. The structure of the basement favoured the growth of carbonate platforms. Basement highs created during the rifting defined the edges of epicratonic basins and platforms.

Local carbonate-dominated environments were present before the glaciations in Zambia, with the Roan Group (see Chapter 3) or in Namibia with the Ombombo Subgroup (Hoffman and Halverson, 2008). The platform of the Roan Group is well understood due to its important economic interest in the Copperbelt. Younger strata and platform environments are better preserved on the Congolian side of the Lufilian Belt and have not been studied in this project.

259

In the West Congo Belt, only the upper part of the Haut Shiloango and the Schisto-Calcaire subgroups record platform settings, while previous sediments are continental to proximal siliciclastics. This late platform setting in the West Congo Belt probably reflects a long-lived tectonic history with important siliciclastic supplies that inhibited the development of the carbonate platform. Frimmel et al. (2006) estimated the maximum age of sedimentation for the Haut Shiloango Subgroup at 650 Ma, Delpomdor et al. (2014) suggested it was deposited between 694 ± 4 Ma and 635 Ma, whilst the earliest rifting stage was dated at 999 ± 7 Ma by Tack et al. (2001). According to the ages above, it took more than 300 millions years for a carbonate platform to develop in the West Congo Belt area. As discussed in Chapter 2, the orientation of this platform seems to be opposite to the main rifted basin, with part of the sediments shed towards the east (Alvarez, 1999) whilst the main basin opened west of this area. A high topography/uplifted block is thus a credible hypothesis to explain a source area west of the platform. This setting can be compared to the ridges and dipslope of the Northern Platform in northern Namibia.

In northern Namibia, the rifting started before ~750 Ma and carbonate facies were deposited soon after in the Ombombo Subgroup, prior to the glaciogenic Chuos Formation (dated by underlying volcanics at 747 ± 2 Ma) (Hoffman et al., 1996). From then, the Otavi Platform developed for more than 100 million years on the Congo Craton, north of the aborted Northern Nosib Rift. Deposition of the Otavi Group continued until the Pan-African collisions that occurred between 580 and 530 Ma. Hoffman and Halverson (2008) suggest that in this setting, some sediments were delivered down the north dipping dipslope, towards the Congo Craton. Deeper facies (shales, turbidites) are found along and down the foreslope of the platform (Hoffman and Halverson, 2008; Pruss et al., 2010).

The interpretation of the facies found in the Rasthof Formation is extremely challenging owing to the lack of analogues. From a stratigraphic approach, the formation has been interpreted on the Northern Platform as a single 200–400 m-thick shoaling upward sequence (Halverson et al., 2005). The deepest platform facies are generally represented by cap dolostone (abiotic member), followed by

microbial facies association (microbial member), and finally the epiclastic member (Hoffman and Halverson, 2008). On the platform, the top of the formation is marked by a regional subaerial exposure surface. Field observations from this thesis have focussed on the cap dolostone and the microbial member. On the platform, considering 1) the structural context in which the platform accumulated (high topographies formed north of the aborted Northern Nosib Rift), and 2) interpretations of possible elevated hydrodynamic energy (chapters 5, 6 and Le Ber et al., 2013), the author suggests that the cap dolostone and microbial facies of the Rasthof Formation may have deposited in a mid to shallow subtidal setting. This interpretation seems to run contrary to other studies (Bosak et al., 2013b; Pruss et al., 2010; Tojo et al., 2007) which suggest subtidal deep-water facies. However, note that the latter authors studied outcrops from the Kaoko Belt only, where recorded facies are likely to be deeper than at the stratotype in the Rasthof Farm area. The observations presented in this thesis are limited due to the difficulty to access a larger set of outcrops during the project and due to the overall puzzling facies. The geology of the western part of the Northern Platform at Rasthof time is (and will remain) problematic since the majority of the succession is probably preserved beneath the Owambo Basin. The key to unlock the conundrum of the Rasthof Formation are 1) to collect further extremely detailed facies observations and 2) to be able to correlate precisely the formation through the platform. This is possible along the edge of the Owambo Basin as Hoffman and Halverson (2008) already illustrated. With the current knowledge on the Rasthof Formation, it is extremely speculative to place any given section with precision on a carbonate platform model. The microbial member 2 at Rasthof Farm exhibits a significant facies variation compared to the Okaaru or Omutirapo areas: the presence of clear individual vertical growths. These geometries and their associated intraclast-rich facies are a robust evidence for elevated hydrodynamic conditions in the Rasthof Farm area.

# 5    Stromatolites

Stromatolites result from complex interactions between microbial communities and their physical and chemical environment. In northern Namibia, the microbial member of the Rasthof Formation was originally interpreted as microbial in origin by Hedberg (1979). The interpretation was principally based on their apparent cohesive nature at the time of deposition. Successive authors (Bosak et al., 2013b; Hoffman and Halverson, 2008; Le Ber et al., 2013; Pruss et al., 2010) have agreed with this interpretation.

Two facies types are recognised in the microbial member. Vertical accretion is extremely localised in MM1 with most of the unit characterised by contorted, thickly laminated microbialites (1–5 mm-thick sparry crust alternating with sub-mm micritic biogenic layers). MM2 is characterised by thinly laminated (sub-mm-thick lamina) microbialites and local cm-scale roll-up structures (soft-sediment deformation). Both MM1 and MM2 may develop non-deformed vertical growths (see chapters 5 and 6). The origin of the deformation structures is uncertain (Bosak et al., 2013b; Le Ber et al., 2013; Pruss et al., 2010), both MM1 and MM2 result from microbial activity and are macroscopically-laminated sediments. The degree of deformation and local solid accretion are associated with variation of microbial microscopic scale framework and environmental controls:

- In MM1 the sparry intervals are much thicker (1–5 mm) than the supposed biogenic, dolomicritic mats (< 1 mm). These correspond to what Riding (2011, 2008) refers to as hybrid crust. MM1 is organised into a regular alternation of abiogenic sparry intervals with biogenic dolomicritic mats. One dolomicritic mat is laterally extremely continuous and probably acted as a sill between what are now two sparry intervals. This setting limited vertical water circulation through the microbial facies, increasing water saturation and slowing lithification. A late lithification favoured the deformation of dm–m-thick sets of lamina. At the time of deposition, microbial communities of MM1 did not produce rigid structures. They principally increased the cohesion of the sediments, allowing soft-sediment deformation without

break-up of the lamina. The thickness of the deformed sets of lamina limited the degree of contortion and the production of intraclasts.

- In MM2, the biogenic mats/intervals are more abundant than the abiogenic sparry intervals. If the biogenic mats appear to be independent from each other at the macroscopic scale they show connections when observed at the microscopic scale, forming a structure made of lamina, clots and bridges. They create a complex, laterally and vertically continuous framework. CL imaging shows that the abiogenic sparry intervals formed after the development of the biogenic levels, filling the voids of the microbial framework. Such a microbial framework probably favoured the creation of a pore network that allowed good fluid circulation. MM2 is a microbially-built framework, which was less susceptible to deformation than MM1. The only deformation features observed are roll-up structures. The present author suggests that these structures result from extreme hydrodynamic stress, peeling a few laminae beneath of the sediment surface. The reduced thickness of deformed lamina (compared to MM1) favoured intense contortion (roll-up structures) and local formation of intraclasts. In settings exposed to more constant hydrodynamic stress, the flows/currents forced the microbial communities to develop vertically. By contrast with MM1, the continuity of the microbial framework created rigid structures that favoured accretion instead of deformation.

Note that in MM1, rare cm-dm large cones and domes are associated with vertical connection of the microbial framework. This probably provided the rigidity necessary to facilitate local vertical accretion. It is difficult to interpret if the development of continuous microbial framework (Figure 8.5) results from environmental controls, from a specific microbial strategy or a combination of both. The framework is common to MM2, even when no evidence for flow or current is found, suggesting that microbial communities developed the framework regardless of currents and flows in the environment. The hydrodynamic regime favoured scouring and slightly modified the framework structure, allowing vertical growths to develop (e.g. Rasthof Farm).

At Rasthof Farm, the idealised section through the microbial member (Figure 8.5) points to a trend starting with typical chaotic, cohesive mats (MM1) unable to develop vertical growths. Just beneath MM2 some solid cones develop, followed upsection in MM2 by domes, columns and various degrees of branching until the apparent disappearance of laminated sediments. The strategy of the microbial communities or the effect of the environmental controls on microbial communities created a progressive transition from flat/undulating mats to vertical growths, ultimately branching then vanishing upsection. So far, these facies variations have only been reported and illustrated at the type section and it would be interesting to see if similar features can be observed at other sections, or if different geometries can be observed. Vertical growths can be lined, surrounded by mm–cm wide intraclasts: the growths seem to be associated with hydrodynamic energy, currents, and scouring in the environment.

The various geometries and new observations presented in this study are not sufficient to determine precise water depths at the time of deposition. Yet the observations from the Rasthof Farm point towards facies variations on the western part of the Northern Platform. They have to be considered with the facies variations allowing the differentiation foreslope/platform (Hoffman and Halverson, 2008). In northeast Namibia, the Berg Aukas Formation, lateral equivalent of the Rasthof Formation, can exhibit shallow-water facies (e.g. oolites, bedforms: Miller, 2008; Misiewicz, 1988) associated with microbial mats. The present study also reports possible evaporitic facies. Those facies variations also have to be considered on the whole Northern Platform. Facies observed on the eastern part of the platform are likely to be shallower, or more proximal than the one observed on the western part of the platform.
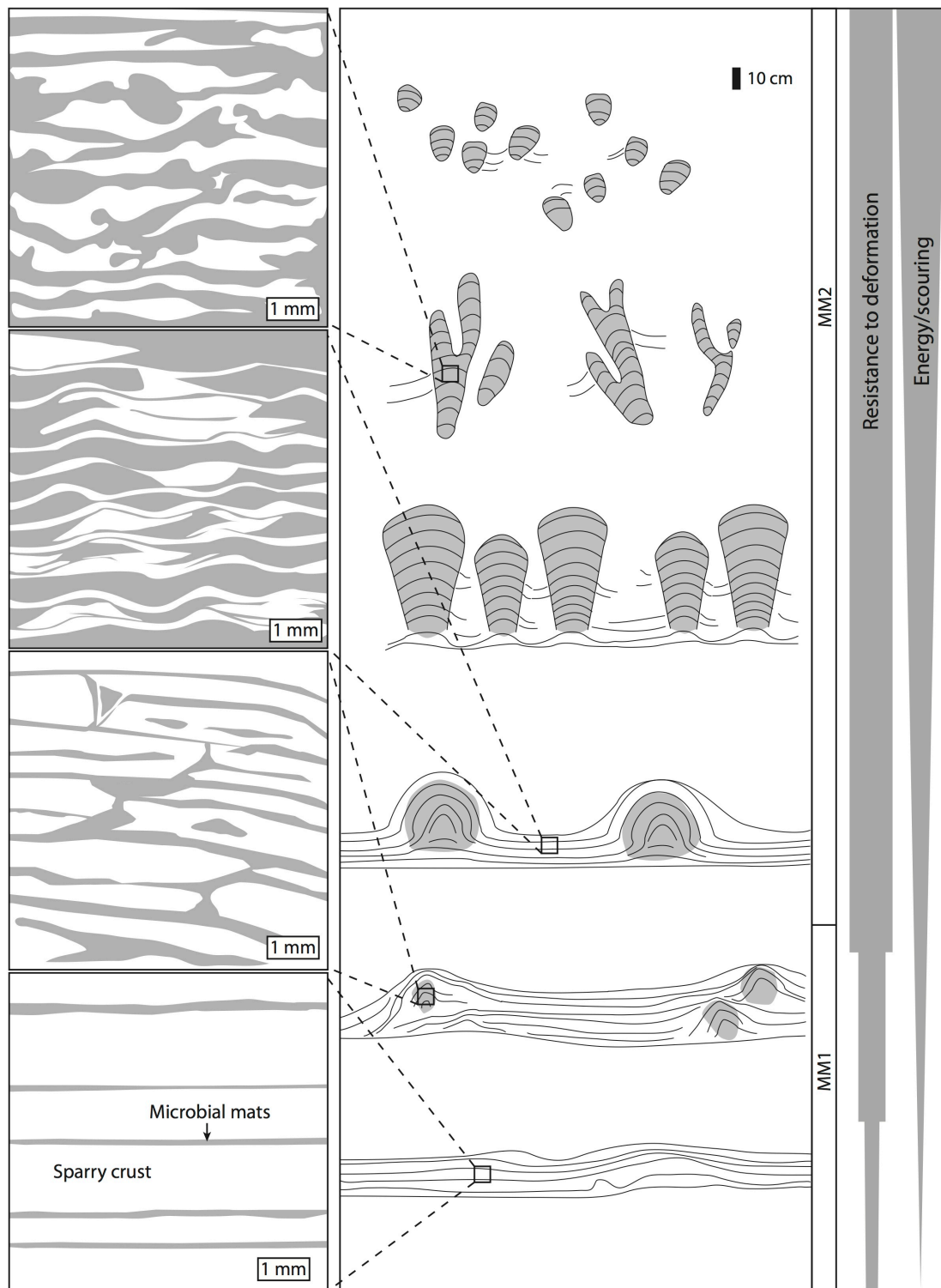
Figure 8.5: Microfacies, micro-framework and macroscopic expression.

# 6    Petroleum potential

Neoproterozoic strata and their glacial/post-glacial systems are experiencing increasing interest from the Petroleum industry (Craig et al., 2013, 2009). Microbial strata of this age have an underestimated potential, particularly as supposed icehouse/greenhouse transitions may have favoured the deposition of potential source rocks (Bechstädt et al., 2009; Le Heron and Craig, 2012; Lüning et al., 2000, 1999), such as Ordovician – Silurian icehouse/greenhouse transition zone of north Africa. The settings in which the sediments studied in this thesis accumulated appear to be epicratonic. The strata deposited along the edges of the Congo Craton have been deformed and uplifted during the Pan-African orogen. The craton seems to be fairly stable since then. In the case of Namibia, the Neoproterozoic sediments preserved under the Owambo Basin have almost not been deformed during the orogeny, except along the edges of the basin. Thus, if favourable elements and configurations for a petroleum system were present in one of the study area after the Pan-African orogen, they remain in place.

This project has gathered data from previous works and adds new observations to the study areas; it is a first critical step towards the evaluation of potential or analogue petroleum systems. By looking at sediments, it is possible to investigate the first key element of a petroleum system and perhaps the more complex for Neoproterozoic strata: the source rock. None of the studied areas revealed outstanding results. TOC levels are almost universally low (< 0.1 %); the rare higher values (2–3 %, Roan Group, Zambia) produced disappointing Rock-Eval results. Some low TOC samples from Namibia were dissolved for other isotopic analyses (not presented in this thesis), the microbial member of the Rasthof Formation clearly contains organic matter after dissolution of all the dolomite (Figure 8.6).
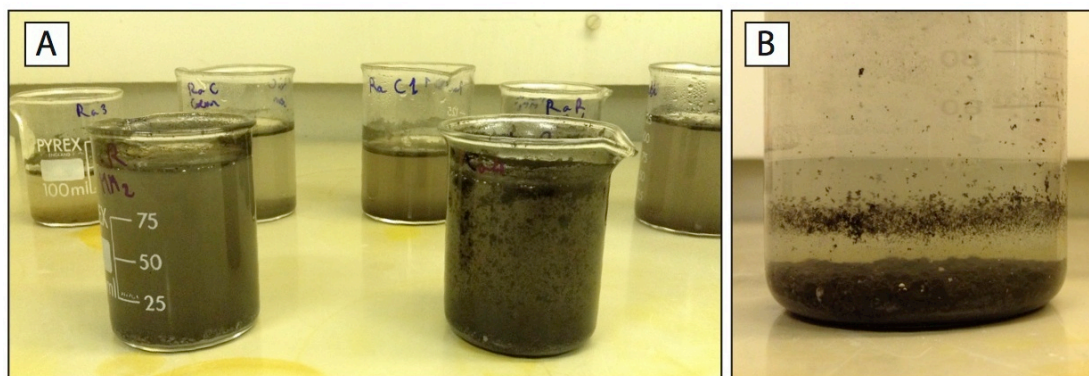
Figure 8.6: Organic matter in the microbial member. **A**. Samples (10–20 g) in 20% HCl. **B**. Sample after partial settling.

Poor results from the samples do not mean that source rocks are or were not present. Little has been sampled compared to the size of the platforms. A better understanding of the platforms may allow the location of environments/settings favourable to the deposition of organic rich facies and potential source rocks. Strata from the Lufilian Belt represent a good analogue for the deposition of organic rich shales associated with microbial carbonates. But they have undergone considerable metamorphism and despite high TOC values, they are now unable to generate hydrocarbons.

Other data would be essential to evaluate hydrocarbon potential of Neoproterozoic strata from the Owambo Basin (Namibia) or the Central Cuvette (Democratic Republic of Congo). Field data are not enough and seismic, gravity and magnetic datasets would be helpful. They all exist to some extent but are generally old (e.g. 1970's for the 2D seismic of the Owambo Basin), scarce with a poor resolution and incomplete. Acquiring such datasets is expensive and extremely complicated, notably in the vast, remote and tropical Central Cuvette.

Field observations in northern Namibia suggest that the microbial member of the Rasthof Formation is a potential analogue for microbial reservoirs. It is highly and continuously fractured, creating a network of fracture. Also, microscopic scale observations of biogenic facies reveal a continuous network of pores in MM2. These pores are now cemented.

# 7    Conclusion

The West Congo Belt (DRC), the Lufilian Belt (Zambia-DRC) and the northern Damara Belt-Northern Platform (Namibia) share common features and debates. They are not easy to highlight because different authors do not express the same questions and approach for each area. This thesis has critically appraised literature and emphasised comparable facts between each geographic area. Understanding the geotectonic history and associated palaeohighs and basins is essential for further sedimentological studies. It is emphasised that more work would be necessary to evaluate hydrocarbon potential of such settings.

The sedimentology of microbial carbonates is receiving increasing attention from the scientific and industrial communities. The structures and geometries of microbial carbonate result from a complex interaction between microbial communities and their environment. This thesis focuses on a very unusual series of microbial facies. Classic sedimentological study with macro- to microscopic descriptions seems to be the best way to tackle this kind of facies. The geometries and morphodiversity are unlikely to give precise ideas about the sedimentary depositional environment or the age of the strata. However, microbial sediments and associated facies may highlight at some of the environmental stresses at work at the time of deposition (e.g. hydrodynamic energy, sediment supply).

Beyond data acquisition and interpretations, this project gave to the author the challenge to evaluate and synthesise literature of different vintage and from different challenging field areas. The literature-based aspect of this study highlights the difficulty of evaluating the geological history of this region and of interpreting Precambrian strata. Much more field and subsurface data would be necessary to better understand the Neoproterozoic sediments that accumulated on the west, southwest and south edges of the Congo Craton.

## Conclusion

This project has dealt with strata of Neoproterozoic age encompassing large-scale concepts and regional to microscopic observations. The author has 1) looked at the Neoproterozoic Earth system; 2) compared existing literature with other subjects not limited to the Neoproterozoic (e.g. microbialites); and 3) focussed on specific areas. These three approaches have constantly been interconnected during the project to allow progression.

At the megaregional scale, the three study areas (West Congo Belt, Lufilian Belt and Otavi Platform), share many uncertainties. The uncertainties are related to the interpretations of the geotectonic configuration and their resulting sedimentary systems. This work points at analogies that can be made between each area, demonstrating common features:

- During the Tonian – mid-Cryogenian, the break-up of Rodinia led to the accumulation of rift sediments on the west, southwest and south edges of the Congo Craton. The rifting was accompanied by the development of palaeohighs along the edges of the craton;

- Once siliciclastic input diminished, platforms accumulated from the palaeohighs to the craton. The sedimentation of these carbonate platforms was interrupted by the deposition of diamictites, locally interpreted as glacially influenced;

- By the end of the Neoproterozoic, all the sedimentary strata that accumulated along the edges of the Congo Craton were uplifted, forming Pan-African orogens.

At the regional scale, issues of accessibility to the data from the West Congo and Lufilian belts were deemed incompatible with the three years period of this project. Nevertheless, information gathered from the Neoproterozoic strata preserved in these Pan-African belts offered an useful background, with concepts to be compared with the Neoproterozoic strata from northern Namibia. There, most of

the thesis focuses on the post-Sturtian cap carbonate (Rasthof and Berg Aukas formations).

In the post-Sturtian cap carbonate sequence of northern Namibia, new observations have been presented suggesting new sedimentological interpretations. Identification of local facies variations compatible with relatively shallow-water settings (e.g. stromatolites from the Rasthof Farm) may question the amplitude of sea level rise in the aftermath of the Sturtian glaciation. Moreover, connections between the nature and rheology of microbial facies have been formulated, and a relationship between microscopic and macroscopic microbial facies has been suggested.

The author looks forward to new research on the post-Sturtian cap carbonate sequence, and hopes that whilst new studies may modify and possibly overturn some of his interpretations, that the observations will stand the test of time.

# Bibliography

Alkmim, F.F., Marshak, S., Pedrosa-Soares, A.C., Peres, G.G., Cruz, S.C.P., Whittington, A., 2006. Kinematic evolution of the Araçuaí-West Congo orogen in Brazil and Africa: Nutcracker tectonics during the Neoproterozoic assembly of Gondwana. Precambrian Res. 149, 43–64.

Allen, P.A., Etienne, J.L., 2008. Sedimentary challenge to Snowball Earth. Nat. Geosci. 1, 817–825.

Allen, P.A., Hoffman, P.F., 2005. Extreme winds and waves in the aftermath of a Neoproterozoic glaciation. Nature 433, 123–127.

Allwood, A.C., Grotzinger, J.P., Knoll, A.H., Burch, I.W., Anderson, M.S., Coleman, M.L., Kanik, I., 2009. Controls on development and diversity of Early Archean stromatolites. Proc. Natl. Acad. Sci. U. S. A. 106, 9548–9555.

Allwood, A.C., Walter, M.R., Kamber, B.S., Marshall, C.P., Burch, I.W., 2006. Stromatolite reef from the Early Archaean era of Australia. Nature 441, 714–718.

Altermann, W., Kazmierczak, J., 2003. Archean microfossils: a reappraisal of early life on Earth. Res. Microbiol. 154, 611–617.

Alvarez, P., 1992. Répartition de la sédimentation dans le golfe Protérozoique supérieur du Schisto-calcaire au Congo et Gabon. Implications en Afrique centrale. Palaeogeogr. Palaeoclimatol. Palaeoecol. 96, 281–297.

Alvarez, P., 1995. Evidence for a Neoproterozoic carbonate ramp on the northern edge of the Central African craton: relations with Late Proterozoic intracratonic troughs. Geol Rundsch 84, 636–648.

Alvarez, P., 1999. La transition Précambrien-Cambrien en Afrique centrale. Approche intégrée : paléoenvironnements et données paléontologiques. Université de Poitiers.

Alvarez, P., Chauvel, J.J., Van Viet-Lanöe, B., 1995. Obruchevella, cyanobactérie fossile du Protérozoïque supérieur du Congo. Implications sur l'âge du groupe Schisto-calcaire et de la glaciation fini-Protérozoïque. Comptes Rendus Académie des Sci. Paris 320, 639–646.

Alvarez, P., Maurin, J.-C., 1991. Evolution sédimentaire et tectonique du bassin Protérozoïque Supérieur de Comba (Congo): stratigraphie séquentielle du Supergroupe Ouest-Congolien et modéle d'amortissement sur décrochements dans le contexte de la tectogénése panafricaine. Precambrian Res. 50, 137–171.

Andres, M.S., Reid, R.P., 2006. Growth morphologies of modern marine stromatolites: A case study from Highborne Cay, Bahamas. Sediment. Geol. 185, 319–328.

Annels, A.E., 1984. The geotectonic environment of Zambian copper-cobalt mineralization. J. Geol. Soc. London 141, 279–289.

Armstrong, R.A., Master, S., Robb, L.J., 2005. Geochronology of the Nchanga Granite, and constraints on the maximum age of the Katanga Supergroup, Zambian Copperbelt. J. African Earth Sci. 42, 32–40.

Arnaud, E., Halverson, G.P., Shields-Zhou, G., 2011. Chapter 1 The geological record of Neoproterozoic ice ages, in: Arnaud, E., Halverson, G.P., Shields-Zhou, G. (Eds.), The Geological Record of Neoproterozoic Glaciations. Geological Society, London, Memoirs, 1–16.

Aubrecht, R., Schlögl, J., Krobicki, M., Wierzbowski, H., Matyja, B.A., Wierzbowski, A., 2009. Middle Jurassic stromatactis mud-mounds in the Pieniny Klippen Belt (Carpathians) — A possible clue to the origin of stromatactis. Sediment. Geol. 213, 97–112.

Awramik, S.M., Sprinkle, J., 1999. Proterozoic stromatolites: the first marine evolutionary biota. Hist. Biol. 13, 241–253.

Babinski, M., Pedrosa-Soares, A.C., Trindade, R.I.F., Martins, M., Noce, C.M., Liu, D., 2012. Neoproterozoic glacial deposits from the Araçuaí orogen, Brazil: Age, provenance and correlations with the São Francisco craton and West Congo belt. Gondwana Res. 21, 451–465.

Bathurst, R.G.C., 1982. Genesis of stromatactis cavities between submarine crusts in Palaeozoic carbonate mud buildups. J. Geol. Soc. London 139, 165–181.

Batumike, M.J., Cailteux, J.L.H., Kampunzu, A.B., 2007. Lithostratigraphy, basin development, base metal deposits, and regional correlations of the Neoproterozoic Nguba and Kundelungu rock successions, central African Copperbelt. Gondwana Res. 11, 432–447.

Bechstädt, T., Jäger, H., Spence, G., Werner, G., 2009. Late Cryogenian (Neoproterozoic) glacial and post-glacial successions at the southern margin of the Congo craton, northern Namibia: facies, palaeogeography and hydrocarbon perspective, in: Craig, J., Thurow, J., Thusu, B., Whitham, A., Abutarruma, Y. (Eds.), Global Neoproterozoic Petroleum Systems: The Emerging Potential in North Africa. Geological Society, London, Special Publications, 255–287.

Bertrand-Sarfati, J., 1972. Stromatolites columnaires de certaines formations carbonatées du Précambrien Supérieur du Bassin Congolais. Ann. du Musée R. l'Afrique Cent. Tervuren, Belgique, Sci. Géologiques 74, 45p.

Bertrand-Sarfati, J., Walter, M.R., 1981. Stromatolites biostratigraphy. Precambrian Res. 15, 353–371.

Boggs, S., Krinsley, D., 2006. Application of cathodoluminescence imaging to the study of sedimentary rocks. Cambridge University Press, 176p.

Borring, J.W., Broughton, D.W., Armstrong, R.A., Hitzman, M.W., 2003. Petrology, geochemistry and age of gabbroic bodies in the Solwezi area, northwestern Zambia, in: Contributions Presented at the 3rd IGCP-450 Conference, Proterozoic Sediment-Hosted Base Metal Deposits of Western Gondwana; Conference and Field Workshop Lubumbashi 2003, Lubumbashi, D.R. Congo. pp. 75–77.

Bosak, T., Knoll, A.H., Petroff, A.P., 2013a. The Meaning of Stromatolites. Annu. Rev. Earth Planet. Sci. 41, 3.1–3.24.

Bosak, T., Lahr, D.J.G., Pruss, S.B., Macdonald, F.A., Dalton, L.A., Matys, E., 2011. Agglutinated tests in post-Sturtian cap carbonates of Namibia and Mongolia. Earth Planet. Sci. Lett. 308, 29–40.

Bosak, T., Lahr, D.J.G., Pruss, S.B., Macdonald, F.A., Gooday, A.J., Dalton, L.A., Matys, E.D., 2012. Possible early foraminiferans in post-Sturtian (716–635 Ma) cap carbonates. Geology 40, 67–70.

Bosak, T., Mariotti, G., Macdonald, F.A., Perron, J.T., Pruss, S.B., 2013b. Microbial sedimentology of stromatolites in Neoproterozoic cap carbonates, in: Bush, A.M., Pruss, S.B., Payne, J.L. (Eds.), The Paleontological Society Papers. The Paleontological Society, 1–25.

Boudzoumou, F., Trompette, R., 1988. La chaîne panafricaine ouest-congolienne au Congo (Afrique Equatoriale) : un socle polycyclique charrié sur un domaine subauchtone fermé par l'aulacogène du Mayombe et la basin de l'Ouest-Congo. Bull. la Société Géologique Fr. 8, 889–896.

Braga, J.C., Martin, J.M., Riding, R., 1995. Controls on microbial dome fabric development along a transect , Miocene , SE Spain. Palaios 10, 347–361.

Brain, C.K., Prave, A.R., Hoffmann, K.H., Fallick, A.E., Botha, A., Herd, D.A., Sturrock, C., Young, I., Condon, D.J., Allison, S.G., 2012. The first animals : ca . 760-million-year-old sponge-like fossils from Namibia. S. Afr. J. Sci. 108, 1–8.

Brasier, M., McLoughlin, N., Green, O., Wacey, D., 2006. A fresh look at the fossil evidence for early Archaean cellular life. Philos. Trans. R. Soc. Lond. B. Biol. Sci. 361, 887–902.

Brookfield, M.E., Martini, I.P., 1999. Facies architecture and sequence stratigraphy in glacially influenced basins : basic problems and water-level/glacier input-point controls (with an example from the Quaternary of Ontario , Canada). Sediment. Geol. 123, 183–197.

Burne, R. V, Moore, L.S., 1987. Microbialites : organosedimentary deposits of benthic microbial communities. Palaios 2, 241–254.

Busfield, M.E., Le Heron, D.P., 2013. Glacitectonic deformation in the Chuos Formation of northern Namibia: implications for Neoproterozoic ice dynamics. Proc. Geol. Assoc. 124, 778–789.

Butterfield, N.J., 2005. Probable Proterozoic fungi. Paleobiology 31, 165–182.

Butterfield, N.J., 2009. Modes of pre-Ediacaran multicellularity. Precambrian Res. 173, 201–211.

Cahen, L., 1947. Les glaciations pré-Karoo du bassin du Congo et de l'Afrique Australe. Bull. la société belge géologie 56, 109–152.

Cahen, L., 1950. Le Calcaire de Sekelolo, le Complexe tillitique et la Dolomie rose C1 dans l'Anticlinal de Congo dia Kati (Bas-Congo). Ann. du Musée du Congo Belge Tervuren (Belgique), Série 8$^o$, Sci. Géologiques 7, 55p.

Cahen, L., 1954. Géologie du Congo Belge. Imprimerie H. Vaillant-Carmanne, S.A, Liège, 577p.

Cahen, L., 1978a. La stratigraphie et la tectonique du supergroupe Ouest-Congolien dans les zones médianes et externes de l'orogène Ouest-Congolien (Pan-africain) au Bas Zaïre et dans les régions voisines. Ann. du Musée R. l'Afrique Cent. Tervuren, Belgique, Sci. Géologiques 83, 150p.

Cahen, L., 1978b. Les mixtites anté-cambriennes de l'Est du Zaïre : Mise au point intérimaire. Rapp. Annu. pour l'année 1977 du département géologie minéralogie du Musée R. l'Afrique Cent. Tervuren, Belgique 33–64.

Cahen, L., Lepersonne, J., 1976. Les mixtites du Bas-Zaïre: Mise au point intérimaire. Musée royal de l'Afrique centrale. Rapp. Annu. pour l'année 1975 du département géologie minéralogie du Musée R. l'Afrique Cent. Tervuren, Belgique 33–57.

Cailteux, J.L.H., Kampunzu, A.B., Lerouge, C., 2007. The Neoproterozoic Mwashya–Kansuki sedimentary rock succession in the central African Copperbelt, its Cu–Co mineralisation, and regional correlations. Gondwana Res. 11, 414–431.

Canfield, D.E., Poulton, S.W., Narbonne, G.M., 2007. Late-Neoproterozoic deep-ocean oxygenation and the rise of animal life. Science (80-. ). 315, 92–95.

Cheel, R.J., Leckie, D.A., 1993. Hummocky cross-stratification. Sedimentol. Rev. 1, 103–121.

Chetty, D., Frimmel, H.E., 2000. The role of evaporites in the genesis of base metal sulphide mineralisation in the Northern Platform of the Pan-African Damara

Belt , Namibia: geochemical and fluid inclusion evidence from carbonate wall rock alteration. Miner. Depos. 35, 364–376.

Choquette, P.W., Hiatt, E.E., 2008. Shallow-burial dolomite cement: a major component of many ancient sucrosic dolomites. Sedimentology 55, 423–460.

Cloud, P.E., Semikhatov, M.A., 1969. Proterozoic stromatolite zonation. Am. J. Sci. 267, 1017–1061.

Cloud, P.E., Wright, I.A., Williams, E.G., Diehl, P., Walter, M.R., 1974. Giant stromatolites and associated vertical tubes from the Upper Proterozoic Noonday Dolomite, Death Valley Region, eastern California. Geol. Soc. Am. Bull. 85, 1867–1882.

Corkeron, M., 2007. "Cap carbonates" and Neoproterozoic glacigenic successions from the Kimberley region, north-west Australia. Sedimentology 54, 871–903.

Corsetti, F.A., Awramik, S.M., Pierce, D., 2003. A complex microbiota from snowball Earth times: microfossils from the Neoproterozoic Kingston Peak Formation, Death Valley, USA. Proc. Natl. Acad. Sci. U. S. A. 100, 4399–404.

Corsetti, F.A., Grotzinger, J.P., 2005. Origin and significance of tube structures in neoproterozoic post-glacial cap carbonates: example from Noonday Dolomite, Death Valley, United States. Palaios 20, 348–362.

Corsetti, F.A., Olcott, A.N., Bakermans, C., 2006. The biotic response to Neoproterozoic snowball Earth. Palaeogeogr. Palaeoclimatol. Palaeoecol. 232, 114–130.

Craig, J., Biffi, U., Galimberti, R.F., Ghori, K.A.R., Gorter, J.D., Hakhoo, N., Le Heron, D.P., Thurow, J., Vecoli, M., 2013. The palaeobiology and geochemistry of Precambrian hydrocarbon source rocks. Mar. Pet. Geol. 40, 1–47.

Craig, J., Thurow, J., Thusu, B., Whitham, A., Abutarruma, Y., 2009. Global Neoproterozoic petroleum systems: the emerging potential in North Africa, in: Craig, J., Thurow, J., Thusu, B., Whitham, A., Abutarruma, Y. (Eds.), Global Neoproterozoic Petroleum Systems: The Emerging Potential in North Africa. Geological Society, London, Special Publications, 1–25.

Da Silva, L.C., Armstrong, R.A., Noce, C.M., Carneiro, M.A., Pimentel, M.M., Pedrosa-Soares, A.C., Leite, C.A., Vieira, V.S., Silva, M.A., Paes, V.J.C., Cardoso Filho, J.M., 2002. Reavaliação da evolução geológica em terrenos pré-cambrianos brasileiros, com base em novos dados U–Pb SHRIMP, Parte II: Orógeno Araçuaí, Cinturão Mineiro e Cráton São Francisco Meridional. Rev. Bras. Geociências 32, 513–528.

Da Silva, L.C., McNaughton, N.J., Armstrong, R.A., Hartmann, L.A., Fletcher, I.R., 2005. The neoproterozoic Mantiqueira Province and its African connections: a

zircon-based U–Pb geochronologic subdivision for the Brasiliano/Pan-African systems of orogens. Precambrian Res. 136, 203–240.

Da Silva, L.C., Pedrosa-Soares, A.C., Teixeira, L.R., Armstrong, R.A., 2008. Tonian rift-related, A-type continental plutonism in the Araçuaí Orogen, eastern Brazil: New evidence for the breakup stage of the São Francisco–Congo Paleocontinent. Gondwana Res. 13, 527–537.

Dalton, L.A., Bosak, T., Macdonald, F.A., Lahr, D.J.G., Pruss, S.B., 2013. Preservational and Morphological Variability of Assemblages of Agglutinated Eukaryotes in Cryogenian Cap Carbonates of Northern Namibia. Palaios 28, 67–79.

De Waele, B., Johnson, S.P., Pisarevsky, S.A., 2008. Palaeoproterozoic to Neoproterozoic growth and evolution of the eastern Congo Craton: Its role in the Rodinia puzzle. Precambrian Res. 160, 127–141.

Dean, W.E., Fouch, T.D., 1983. Lacustrine environment, in: Scholle, P.A., Bedout, D.G., Moore, C.H. (Eds.), Carbonate Depositional Environments. AAPG Memoir, 97–130.

Decho, A.W., Visscher, P.T., Reid, R.P., 2005. Production and cycling of natural microbial exopolymers (EPS) within a marine stromatolite. Palaeogeogr. Palaeoclimatol. Palaeoecol. 219, 71–86.

Delgado, F., 1977. Primary Textures in Dolostones and Recrystallized Limestones: A Technique for their Microscopic Study. J. Sediment. Petrol. 47, 1339–1341.

Delmoitié-Nicolaï, J., Ladmirant, H., Lepersonne, J., 1972. Carte géologique du Zaïre – Feuille Ngungu (S6/14). 1/200.000.

Delpomdor, F., Kant, F., Préat, A., 2014. Neoproterozoic Uppermost Haut-Shiloango Subgroup (West Congo Supergroup, Democratic Republic of Congo): Misinterpreted stromatolites and implications for sea-level fluctuations before the onset of the Marinoan glaciation. J. African Earth Sci. 90, 49–63.

Delpomdor, F., Préat, A., 2013. Early and late Neoproterozoic C, O and Sr isotope chemostratigraphy in the carbonates of West Congo and Mbuji-Mayi supergroups: A preserved marine signature? Palaeogeogr. Palaeoclimatol. Palaeoecol. 389, 35–47.

Deng, S., Dong, H., Lv, G., Jiang, H., Yu, B., Bishop, M.E., 2010. Microbial dolomite precipitation using sulfate reducing and halophilic bacteria: Results from Qinghai Lake, Tibetan Plateau, NW China. Chem. Geol. 278, 151–159.

Derry, L.A., 2010. On the significance of δ13C correlations in ancient sediments. Earth Planet. Sci. Lett. 296, 497–501.

Dewaele, S., Muchez, P., Vets, J., Fernandez-Alonso, M., Tack, L., 2006. Multiphase origin of the Cu–Co ore deposits in the western part of the Lufilian fold-and-thrust belt, Katanga (Democratic Republic of Congo). J. African Earth Sci. 46, 455–469.

Domack, E.W., Hoffman, P.F., 2011. An ice grounding-line wedge from the Ghaub glaciation (635 Ma) on the distal foreslope of the Otavi carbonate platform, Namibia, and its bearing on the snowball Earth hypothesis. Geol. Soc. Am. Bull. 123, 1448–1477.

Dunham, R.J., 1962. Classification of carbonate rocks according to depositional texture, in: Classification of Carbonate Rocks: AAPG. pp. 108–121.

Dupraz, C., Pattisina, R., Verrecchia, E.P., 2006. Translation of energy into morphology: Simulation of stromatolite morphospace using a stochastic model. Sediment. Geol. 185, 185–203.

El Desouky, H.A., Muchez, P., Dewaele, S., Boutwood, A., Tyler, R., 2008. Postorogenic Origin of the Stratiform Cu Mineralization at Lufukwe, Lufilian Foreland, Democratic Republic of Congo. Econ. Geol. 103, 555–582.

El Tabakh, M., Grey, K., Pirajno, F., Schreiber, B.C., 1999. Pseudomorphs after evaporitic minerals interbedded with 2.2 Ga stromatolites of the Yerrida basin, Western Australia: Origin and significance. Geology 27, 871–874.

Embry, B.F., Klovan, J., 1972. Absolute Water Depth Limits of Late Devonian Paleoeeologieal Zones. Geol. Rundschau 61, 672–686.

Eyles, N., 2008. Glacio-epochs and the supercontinent cycle after ~3.0 Ga: Tectonic boundary conditions for glaciation. Palaeogeogr. Palaeoclimatol. Palaeoecol. 258, 89–129.

Eyles, N., Januszczak, N., 2004. "Zipper-rift": a tectonic model for the Neoproterozoic glaciations during the breakup of Rodinia after 750 Ma. Earth-Science Rev. 65, 1–73.

Eyles, N., Januszczak, N., 2007. Syntectonic subaqueous mass flows of the Neoproterozoic Otavi Group, Namibia: where is the evidence of global glaciation? Basin Res. 19, 179–198.

Fairchild, I.J., Kennedy, M.J., 2007. Neoproterozoic glaciation in the Earth System. J. Geol. Soc. London 164, 895–921.

Flint, R.F., Sanders, J.E., Rodgers, J., 1969a. Symmictite: a name for nonsorted terrigenous sedimentary rocks that contain wide range of particle sizes. Bull. Geol. Soc. Am. 71, 507–510.

Flint, R.F., Sanders, J.E., Rodgers, J., 1969b. Diamictite, a substitute term for symmictite. Bull. Geol. Soc. Am. 71, 1809–1810.

Flügel, E., 2004. Microfacies of carbonate rocks. Analysis, interpretation and application. Springer-Verlag Berlin Heidelberg, 984p.

Font, E., Nédélec, A., Trindade, R.I.F., Moreau, C., 2010. Fast or slow melting of the Marinoan snowball Earth? The cap dolostone record. Palaeogeogr. Palaeoclimatol. Palaeoecol. 295, 215–225.

Fox, T., Domack, E.W., Hoffman, P.F., n.d. A Neoproterozoic Rock Sample Suite: Evidence for the Snowball Earth.

Frimmel, H.E., 2010. On the reliability of stable carbon isotopes for Neoproterozoic chemostratigraphic correlation. Precambrian Res. 182, 239–253.

Frimmel, H.E., Basei, M.S., Gaucher, C., 2011. Neoproterozoic geodynamic evolution of SW-Gondwana: a southern African perspective. Int. J. Earth Sci. 100, 323–354.

Frimmel, H.E., Fölling, P.G., Eriksson, P.G., 2002. Neoproterozoic tectonic and climatic evolution recorded in the Gariep Belt, Namibia and South Africa. Basin Res. 14, 55–67.

Frimmel, H.E., Miller, R.M., 2009. Chapter 5.2 Continental Rifting, in: Gaucher, C., Sial, A.N., Frimmel, H.E., Halverson, G.P. (Eds.), Neoproterozoic-Cambrian Tectonics, Global Change And Evolution: A Focus On South Western Gondwana. Elsevier, 153–159.

Frimmel, H.E., Tack, L., Basei, M.S., Nutman, A.P., Boven, A., 2006. Provenance and chemostratigraphy of the Neoproterozoic West Congolian Group in the Democratic Republic of Congo. J. African Earth Sci. 46, 221–239.

Frolov, S. V., Akhmanov, G.G., Kozlova, E. V., Krylov, O. V., Sitar, K. a., Galushkin, Y.I., 2011. Riphean basins of the central and western Siberian Platform. Mar. Pet. Geol. 28, 906–920.

Gandin, A., Wright, D.T., 2007. Evidence of vanished evaporites in Neoarchaean carbonates of South Africa, in: Schreiber, B.C., Lugli, S., Babel, M. (Eds.), Evaporites Through Space and Time. Geological Society, London, Special Publications, 285–308.

Garlick, W.G., 1964. Association of mineralization and algal reef structures on northern Rhodesian copperbelt, Katanga, and Australia. Econ. Geol. 59, 416–427.

Garlick, W.G., Fleischer, V.D., 1972. Sedimentary environment of Zambian copper deposits. J. R. Geol. Min. Netherlands 51, 277–298.

Gaucher, C., Frimmel, H.E., Germs, G.J.B., 2009. Chapter 8 Tectonic Events and Palaeogeographic Evolution of Southwestern Gondwana in the Neoproterozoic and Cambrian, in: Gaucher, C., Sial, A.N., Frimmel, H.E., Halverson, G.P. (Eds.),

Neoproterozoic-Cambrian Tectonics, Global Change And Evolution: A Focus On South Western Gondwana. Elsevier, 295–316.

Germs, G.J.B., Miller, R.M., Frimmel, H.E., Gaucher, C., 2009. Chapter 5.4 Syn- to Late-Orogenic Sedimentary Basins of Southwestern Africa, in: Gaucher, C., Sial, A.N., Frimmel, H.E., Halverson, G.P. (Eds.), Neoproterozoic-Cambrian Tectonics, Global Change And Evolution: A Focus On South Western Gondwana. Elsevier, pp. 183–203.

Ghori, K.A.R., Craig, J., Thusu, B., Luning, S., Geiger, M., 2009. Global Infracambrian petroleum systems: a review, in: Craig, J., Thurow, J., Thusu, B., Whitham, A., Abutarruma, Y. (Eds.), Global Neoproterozoic Petroleum Systems: The Emerging Potential in North Africa. Geological Society, London, Special Publications, 109–136.

Giddings, J.A., Wallace, M.W., 2009a. Sedimentology and C-isotope geochemistry of the "Sturtian" cap carbonate, South Australia. Sediment. Geol. 216, 1–14.

Giddings, J.A., Wallace, M.W., 2009b. Facies-dependent δ13C variation from a Cryogenian platform margin, South Australia: Evidence for stratified Neoproterozoic oceans? Palaeogeogr. Palaeoclimatol. Palaeoecol. 271, 196–214.

Goscombe, B.D., Gray, D.R., Armstrong, R.A., Foster, D.A., Vogl, J., 2005. Event geochronology of the Pan-African Kaoko Belt, Namibia. Precambrian Res. 140, 103.e1–103.e41.

Grantham, G.H., Maboko, M., Eglington, B.M., 2003. A review of the evolution of the Mozambique Belt and implications for the amalgamation and dispersal of Rodinia and Gondwana, in: Yoshida, M., Windley, B.F., Dasgupta, S. (Eds.), Proterozoic East Gondwana: Supercontinent Assembly and Breakup. Geological Society, London, Special Publications, 401–425.

Gray, D.R., Foster, D.A., Goscombe, B.D., Passchier, C.W., Trouw, R.A.J., 2006. 40Ar/39Ar thermochronology of the Pan-African Damara Orogen, Namibia, with implications for tectonothermal and geodynamic evolution. Precambrian Res. 150, 49–72.

Gray, D.R., Foster, D.A., Meert, J.G., Goscombe, B.D., Armstrong, R.A., Trouw, R.A.J., Passchier, C.W., 2008. A Damara orogen perspective on the assembly of southwestern Gondwana, in: Pankhurst, R.J., Trouw, R.A.J., Brito Neves, B.B., De Wit, M.J. (Eds.), West Gondwana: Pre-Cenozoic Correlations Across the South Atlantic Region. Geological Society, London, Special Publications, 257–278.

Grey, K., Hill, A.C., Calver, C., 2011. Chapter 8 Biostratigraphy and stratigraphic subdivision of Cryogenian successions of Australia in a global context, in:

Arnaud, E., Halverson, G.P., Shields-Zhou, G. (Eds.), The Geological Record of Neoproterozoic Glaciations. Geological Society, London, Memoirs, 113–134.

Grosjean, E., Love, G.D., Stalvies, C., Fike, D.A., Summons, R.E., 2009. Origin of petroleum in the Neoproterozoic–Cambrian South Oman Salt Basin. Org. Geochem. 40, 87–110.

Grotzinger, J.P., 1990. Geochemical model for Proterozoic stromatolite decline. Am. J. Sci. 290, 80–103.

Grotzinger, J.P., Knoll, A.H., 1999. Stromatolites in Precambrian carbonates: evolutionary mileposts or environmental dipsticks? Annu. Rev. Earth Planet. Sci. 27, 313–358.

Gustavson, T.C., Hovorka, S.D., Dutton, A.R., 1994. Origin of satin spar veins in evaporite basins. J. Sediment. Res. A64, 88–94.

Halverson, G.P., Hoffman, P.F., Schrag, D.P., Maloof, A.C., Rice, A.H.N., 2005. Toward a Neoproterozoic composite carbon-isotope record. GSA Bull. 117, 1181–1207.

Halverson, G.P., Hurtgen, M.T., Porter, S.M., Collins, A.S., 2009. Chapter 10 Neoproterozoic-Cambrian Biogeochemical Evolution, in: Gaucher, C., Sial, A.N., Frimmel, H.E., Halverson, G.P. (Eds.), Neoproterozoic-Cambrian Tectonics, Global Change And Evolution: A Focus On South Western Gondwana. Elsevier, 351–365.

Halverson, G.P., Wade, B.P., Hurtgen, M.T., Barovich, K.M., 2010. Neoproterozoic chemostratigraphy. Precambrian Res. 182, 337–350.

Harwood, C.L., Sumner, D.Y., 2011. Microbialites of the Neoproterozoic Beck Spring Dolomite, Southern California. Sedimentology 58, 1648–1673.

Hedberg, R.M., 1979. Stratigraphy of the Ovamboland Basin South West Africa. Chamb. Mines Precambrian Res. Unit. Bull. 24, 325p.

Heijlen, W., Banks, D.A., Muchez, P., Stensgard, B.M., Yardley, B.W.D., 2008. The Nature of Mineralizing Fluids of the Kipushi Zn-Cu Deposit, Katanga, Democratic Repubic of Congo: Quantitative Fluid Inclusion Analysis using Laser Ablation ICP-MS and Bulk Crush-Leach Methods. Econ. Geol. 103, 1459–1482.

Hill, A.C., Cotter, K.L., Grey, K., 2000. Mid-Neoproterozoic biostratigraphy and isotope stratigraphy in Australia. Precambrian Res. 100, 281–298.

Hladil, J., 2005. The formation of stromatactis-type fenestral structures during the sedimentation of experimental slurries – a possible clue to a 120-year-old puzzle about stromatactis. Bull. Geosci. 80, 193–211.

Hoffman, P.F., Halverson, G.P., 2008. Otavi Group of the western Northern Platform, the eastern Kaoko Zone and western Northern Margin Zone, in: Miller, R.M. (Ed.), The Geology of Namibia, Vol 2. Ministry of Mines and Energy, Geological Survey, 13.69–13.134.

Hoffman, P.F., Halverson, G.P., Domack, E.W., Husson, J.M., Higgins, J.A., Schrag, D.P., 2007. Are basal Ediacaran (635 Ma) post-glacial "cap dolostones" diachronous? Earth Planet. Sci. Lett. 258, 114–131.

Hoffman, P.F., Hawkins, D.P., Isachsen, C.E., Bowring, S.A., 1996. Precise U-Pb zircon ages for early Damaran magmatism in the Summas Mountains and Welwitschia inlier, northern Damara belt, Namibia. Commun. Geol. Surv. Namibia 11, 47–52.

Hoffman, P.F., Kaufman, A.J., Halverson, G.P., 1998a. Comings and goings of global glaciations on a Neoproterozoic tropical platform in Namibia. GSA Today 8, 1–9.

Hoffman, P.F., Kaufman, A.J., Halverson, G.P., Schrag, D.P., 1998b. A Neoproterozoic Snowball Earth. Science (80-. ). 281, 1342–1346.

Hoffman, P.F., Li, Z.X., 2009. A palaeogeographic context for Neoproterozoic glaciation. Palaeogeogr. Palaeoclimatol. Palaeoecol. 277, 158–172.

Hoffman, P.F., Macdonald, F.A., 2010. Sheet-crack cements and early regression in Marinoan (635Ma) cap dolostones: Regional benchmarks of vanishing ice-sheets? Earth Planet. Sci. Lett. 300, 374–384.

Hoffman, P.F., Schrag, D.P., 2002. The snowball Earth hypothesis: testing the limits of global change. Terra Nov. 14, 129–155.

Hoffmann, K.H., Prave, A.R., 1996. A preliminary note on revised subdivision and regional correlation of the Otavi Group based on glaciogenic diamctites and associated cap dolostones. Commun. Geol. Surv. Namibia 11, 77–82.

Hofmann, H.J., 1973. Stromatolites: Characteristics and utility. Earth-Science Rev. 9, 339–373.

Hofmann, H.J., 1994. Quantitative Stromatolitology. J. Paleontol. 68, 704–709.

Hood, A.V.S., Wallace, M.W., 2012. Synsedimentary diagenesis in a Cryogenian reef complex: Ubiquitous marine dolomite precipitation. Sediment. Geol. 255-256, 56–71.

Hood, A.V.S., Wallace, M.W., Drysdale, R.N., 2011. Neoproterozoic aragonite-dolomite seas? Widespread marine dolomite precipitation in Cryogenian reef complexes. Geology 39, 871–874.

Howard, J.P., Bogolepova, O.K., Gubanov, A.P., Gomez-Perez, M., 2012. The petroleum potential of the Riphean-Vendian succession of southern East Siberia, in: Bhat, G.M., Craig, J., Thurow, J., Thusu, B., Cozzi, A. (Eds.), Geology and Hydrocarbon Potential of Neoproterozoic–Cambrian Basins in Asia. Geological Society, London, Special Publications, 177–198.

Huuse, M., Le Heron, D.P., Dixon, R., Redfern, J., Moscariello, A., Craig, J., 2012. Glaciogenic reservoirs and hydrocarbon systems: an introduction, in: Huuse, M., Redfern, J., Le Heron, D.P., Dixon, R.J., Moscariello, A., Craig, J. (Eds.), Glaciogenic Reservoirs and Hydrocarbon Systems. Geological Society, London, Special Publications, 1–28.

Jahnert, R.J., Collins, L.B., 2011. Significance of subtidal microbial deposits in Shark Bay, Australia. Mar. Geol. 286, 106–111.

Jiang, G., Kennedy, M.J., Christie-Blick, N., 2003. Stable isotopic evidence for methane seeps in Neoproterozoic postglacial cap carbonates. Nature 426, 822–826.

Johnson, J., Grotzinger, J.P., 2006. Affect of Sedimentation on Stromatolite Reef Growth and Morphology, Ediacaran Omkyk Member (Nama Group), Namibia. South African J. Geol. 109, 87–96.

Kadima, E., Delvaux, D., Sebagenzi, S.N., Tack, L., Kabeya, S.M., 2011a. Structure and geological history of the Congo Basin: an integrated interpretation of gravity, magnetic and reflection seismic data. Basin Res. 23, 499–527.

Kadima, E., Ntabwoba, S.S.M., Lucazeau, F., 2011b. A Proterozoic-rift origin for the structure and the evolution of the cratonic Congo basin. Earth Planet. Sci. Lett. 304, 240–250.

Kahle, C.F., 2002. Seismogenic deformation structures in microbialites and mudstones, Silurian Lockport Dolomite, northwestern Ohio, U.S.A. J. Sediment. Res. 72, 201–216.

Kamona, F., Günzel, A., 2007. Stratigraphy and base metal mineralization in the Otavi Mountain Land, Northern Namibia—a review and regional interpretation. Gondwana Res. 11, 396–413.

Kasaona, M.K., 2012. Patch-Mosaic Burn in Etosha National Park [WWW Document]. African Monit. Environ. Sustain. Dev. – South. African Dev. Community. URL http://www.amesdsadc.org/patch-mosaic-burn-in-etosha-national-park-05-15-june-2012

Kaufman, A.J., Knoll, A.H., 1995. Neoproterozoic variations in the C-isotopic composition of seawater: stratigraphic and biogeochemical implications. Precambrian Res. 73, 27–49.

Kennedy, M.J., 1996. Stratigraphy, sedimentology, and isotopic geochemistry of Australian Neoproterozoic postglacial cap dolostones: deglaciation, δ13C excursions, and carbonates precipitation. J. Sediment. Res. 66, 1050–1064.

Kennedy, M.J., Christie-Blick, N., 2011. Condensation origin for Neoproterozoic cap carbonates during deglaciation. Geology 39, 319–322.

Kennedy, M.J., Christie-Blick, N., Sohl, L.E., 2001. Are Proterozoic cap carbonates and isotopic excursions a record of gas hydrate destabilization following Earth's coldest intervals? Geology 29, 443–446.

Key, R.M., Liyungu, A.K., Njamu, F.M., Somwe, V., Banda, J., Mosley, P.N., Armstrong, R.A., 2001. The western arm of the Lufilian Arc in NW Zambia and its potential for copper mineralization. J. African Earth Sci. 33, 503–528.

Khodadad, C.L.M., Foster, J.S., 2012. Metagenomic and metabolic profiling of nonlithifying and lithifying stromatolitic mats of Highborne Cay, The Bahamas. PLoS One 7, 1–13.

Kirschvink, J.L., 1992. Late Proterozoic Low-Latitude Global Glaciation: the Snowball Earth, in: Schopf, J.W., Klein, C. (Eds.), The Proterozoic Biosphere: A Multidisciplinary Study. Cambridge University Press, pp. 51–52.

Knoll, A.H., Javaux, E.J., Hewitt, D., Cohen, P., 2006. Eukaryotic organisms in Proterozoic oceans. Philos. Trans. R. Soc. Lond. B. Biol. Sci. 361, 1023–1038.

Konopásek, J., Košler, J., Tajčmanová, L., Ulrich, S., Kitt, S.L., 2008. Neoproterozoic igneous complex emplaced along major tectonic boundary in the Kaoko Belt ( NW Namibia ): ion probe and LA-ICP-MS dating of magmatic and metamorphic zircons. J. Geol. Soc. London 165, 153–165.

Lacasta, A.M., Cantalapiedra, I.R., Auguet, C.E., Peñaranda, A., Ramírez-Piscina, L., 1999. Modeling of spatiotemporal patterns in bacterial colonies. Phys. Rev. E 59, 7036–7041.

Le Ber, E., Le Heron, D.P., Winterleitner, G., Bosence, D.W.J., Vining, B.A., Kamona, F., 2013. Microbialite recovery in the aftermath of the Sturtian glaciation: Insights from the Rasthof Formation, Namibia. Sediment. Geol. 294, 1–12.

Le Guerroué, E., Cozzi, A., 2010. Veracity of Neoproterozoic negative C-isotope values: The termination of the Shuram negative excursion. Gondwana Res. 17, 653–661.

Le Heron, D.P., 2012. The Location and Styles of Ice-Free "Oases" during Neoproterozoic Glaciations with Evolutionary Implications. Geosciences 2, 90–108.

Le Heron, D.P., Busfield, M.E., Kamona, F., 2013a. An interglacial on snowball Earth? Dynamic ice behaviour revealed in the Chuos Formation, Namibia. Sedimentology 60, 411–427.

Le Heron, D.P., Busfield, M.E., Le Ber, E., Kamona, F., 2013b. Ironstone stromatolites and diamictites in the Chuos Formation of Namibia: implications for Cryogenian glaciation. Palaeogeogr. Palaeoclimatol. Palaeoecol. 369, 48–57.

Le Heron, D.P., Cox, G., Trundley, A., Collins, A.S., 2011. Sea ice-free conditions during the Sturtian glaciation (early Cryogenian), South Australia. Geology 39, 31–34.

Le Heron, D.P., Craig, J., 2012. Neoproterozoic deglacial sediments and their hydrocarbon source rock potential, in: Huuse, M., Redfern, J., Le Heron, D.P., Dixon, R.J., Moscariello, A., Craig, J. (Eds.), Glaciogenic Reservoirs and Hydrocarbon Systems. Geological Society, London, Special Publications, 381–393.

Le Heron, D.P., Craig, J., Etienne, J.L., 2009. Ancient glaciations and hydrocarbon accumulations in North Africa and the Middle East. Earth-Science Rev. 93, 47–76.

Li, Z.X., Bogdanova, S. V, Collins, A.S., Davidson, A., De Waele, B., Ernst, R.E., Fitzsimons, I.C.W., Fuck, R.A., Gladkochub, D.P., Jacobs, J., Karlstrom, K.E., Lu, S., Natapov, L.M., Pease, V., Pisarevsky, S.A., Thrane, K., Vernikovsky, V., 2008. Assembly, configuration, and break-up history of Rodinia: A synthesis. Precambrian Res. 160, 179–210.

Lindtke, J., Ziegenbalg, S.B., Brunner, B., Rouchy, J.M., Pierre, C., Peckmann, J., 2011. Authigenesis of native sulphur and dolomite in a lacustrine evaporitic setting (Hellín basin, Late Miocene, SE Spain). Geol. Mag. 148, 655–669.

Logan, B.W., Rezak, R., Ginsburg, R.N., 1964. Classification and environmental significance of algal stromatolites. J. Geol. 72, 68–83.

Lottaroli, F., Craig, J., Thusu, B., 2009. Neoproterozoic-Early Cambrian (Infracambrian) hydrocarbon prospectivity of North Africa: a synthesis, in: Craig, J., Thurow, J., Thusu, B., Whitham, A., Abutarruma, Y. (Eds.), Global Neoproterozoic Petroleum Systems: The Emerging Potential in North Africa. Geological Society, London, Special Publications, 137–156.

Lüning, S., Craig, J., Fitches, B., Mayouf, J., Busrewil, A., El Dieb, M., Gammudi, A., Loydell, D., McIlroy, D., 1999. Re-evaluation of the petroleum potential of the Kufra Basin (SE Libya, NE Chad): does the source rock barrier fall? Mar. Pet. Geol. 16, 693–718.

Lüning, S., Craig, J., Loydell, D.K., Štorch, P., Fitches, B., 2000. Lower Silurian " hot shales " in North Africa and Arabia : regional distribution and depositional model. Earth-Science Rev. 49, 121–200.

Macdonald, F.A., Schmitz, M.D., Crowley, J.L., Roots, C.F., Jones, D.S., Maloof, A.C., Strauss, J. V, Cohen, P.A., Johnston, D.T., Schrag, D.P., 2010. Calibrating the Cryogenian. Science (80-. ). 327, 1241–1243.

MacGabhann, B.A., 2014. There is no such thing as the "Ediacara Biota". Geosci. Front. 5, 53–62.

Malan, S.P., 1964. Stromatolites and other algal structures at Mufulira, northern Rhodesia. Econ. Geol. 59, 397–415.

Maloof, A.C., Rose, C. V, Beach, R., Samuels, B.M., Calmet, C.C., Erwin, D.H., Poirier, G.R., Yao, N., Simons, F.J., 2010. Possible animal-body fossils in pre-Marinoan limestones from South Australia. Nat. Geosci. 3, 653–659.

Maltman, A., 1994. The Geological Deformation of Sediments. Springer Netherlands, 362p.

Marshall, C.R., 2006. Explaining the Cambrian "Explosion" of Animals. Annu. Rev. Earth Planet. Sci. 34, 355–384.

Martín-Chivelet, J., Palma, R.M., López-Gómez, J., Kietzmann, D.A., 2011. Earthquake-induced soft-sediment deformation structures in Upper Jurassic open-marine microbialites (Neuquén Basin, Argentina). Sediment. Geol. 235, 210–221.

Master, S., Rainaud, C., Armstrong, R.A., Phillips, D., Robb, L.J., 2005. Provenance ages of the Neoproterozoic Katanga Supergroup (Central African Copperbelt), with implications for basin evolution. J. African Earth Sci. 42, 41–60.

Master, S., Wendorff, M., 2011. Chapter 12 Neoproterozoic glaciogenic diamictites of the Katanga Supergroup, Central Africa, in: Arnaud, E., Halverson, G.P., Shields-Zhou, G. (Eds.), The Geological Record of Neoproterozoic Glaciations. Geological Society, London, Memoirs, 173–184.

Matsushita, M., Wakita, J., Itoh, H., Ràfols, I., Matsuyama, T., Sakaguchi, H., Mimura, M., 1998. Interface growth and pattern formation in bacterial colonies. Phys. A Stat. Mech. its Appl. 249, 517–524.

McCall, G.J.H., 2006. The Vendian (Ediacaran) in the geological record: Enigmas in geology's prelude to the Cambrian explosion. Earth-Science Rev. 77, 1–229.

McGowan, R.R., Roberts, S., Boyce, A.J., 2006. Origin of the Nchanga copper–cobalt deposits of the Zambian Copperbelt. Miner. Depos. 40, 617–638.

McGowan, R.R., Roberts, S., Foster, R.P., Boyce, A.J., Coller, D., 2003. Origin of the copper-cobalt deposits of the Zambian Copperbelt : An epigenetic view from Nchanga. Geology 31, 497–500.

Meert, J.G., Lieberman, B.S., 2008. The Neoproterozoic assembly of Gondwana and its relationship to the Ediacaran–Cambrian radiation. Gondwana Res. 14, 5–21.

Meischner, K.D., 1964. Allodapische kalke, turbidite in riff-nahen sedimentations-becken, in: Bouma, A.H., Brouwer, A. (Eds.), Turbidites. Development in Sedimentology, Vol 3. pp. 156–191.

Miller, R.M., 2008. The Geology of Namibia. Volume 2. Neoproterozoic to Lower Palaeozoic. Ministry of mines and energy, Windhoek, Namibia.

Miller, R.M., Frimmel, H.E., Halverson, G.P., 2009. Chapter 5.3 Passive Continental Margin Evolution, in: Gaucher, C., Sial, A.N., Frimmel, H.E., Halverson, G.P. (Eds.), Neoproterozoic-Cambrian Tectonics, Global Change And Evolution: A Focus On South Western Gondwana. Elsevier, pp. 161–181.

Miller, R.M., Pickford, M., Senut, B., 2010. The geology, palaeontology and evolution of the Etosha Pan, Namibia: Implications for terminal Kalahari deposition. South African J. Geol. 113, 307–334.

Misiewicz, J.E., 1988. The geology and metallogeny of the Otavi Mountain Land, Damara Orogen, SWA/Namibia, with particular reference to the Berg Aukas Zn-Pb-V deposit - a model of ore genesis. Rhodes University, Grahamstown.

Mojzsis, S.J., Arrhenius, G., McKeegan, K.D., Harrison, T.M., Nutman, A.P., Friend, C.R.L., 1996. Evidence for life on Earth before 3,800 million years ago. Nature 384, 55–59.

Muchez, P., Brems, D., Clara, E., De Cleyn, A., Lammens, L., Boyce, A.J., De Muynck, D., Mukumba, W., Sikazwe, O., 2010. Evolution of Cu–Co mineralizing fluids at Nkana Mine, Central African Copperbelt, Zambia. J. African Earth Sci. 58, 457–474.

Muchez, P., Corbella, M., 2012. Factors controlling the precipitation of copper and cobalt minerals in sediment-hosted ore deposits: Advances and restrictions. J. Geochemical Explor. 118, 38–46.

Mulder, T., Razin, P., Faugeres, J.-C., 2009. Hummocky cross-stratification-like structures in deep-sea turbidites: Upper Cretaceous Basque basins (Western Pyrenees, France). Sedimentology 56, 997–1015.

Murphy, J.B., Nance, R.D., Cawood, P.A., 2009. Contrasting modes of supercontinent formation and the conundrum of Pangea. Gondwana Res. 15, 408–420.

Narbonne, G.M., 2005. The Ediacara biota: Neoproterozoic origin of animals and their ecosystems. Annu. Rev. Earth Planet. Sci. 33, 421–442.

Nogueira, A.C.R., Riccomini, C., Sial, A.N., Moura, C.A. V, Fairchild, T.R., 2003. Soft-sediment deformation at the base of the Neoproterozoic Puga cap carbonate

(southwestern Amazon craton , Brazil): Confirmation of rapid icehouse to greenhouse transition in snowball Earth. Geology 31, 613–616.

Ogg, G., 2009. International Stratigraphic Chart.

Papineau, D., Walker, J.J., Mojzsis, S.J., Pace, N.R., 2005. Composition and structure of microbial communities from stromatolites of Hamelin Pool in Shark Bay, Western Australia. Appl. Environ. Microbiol. 71, 4822–4832.

Pedrosa-Soares, A.C., Alkmim, F.F., Tack, L., Noce, C.M., Babinski, M., Silva, L.C., Martins-Neto, M.A., 2008. Similarities and differences between the Brazilian and African counterparts of the Neoproterozoic Aracuai-West Congo orogen, in: Pankhurst, R.J., Trouw, R.A.J., Brito Neves, B.B., De Wit, M.J. (Eds.), West Gondwana: Pre-Cenozoic Correlations Across the South Atlantic Region. Geological Society, London, Special Publications, 153–172.

Pedrosa-Soares, A.C., Noce, C.M., Vidal, P., Monteiro, R.L.B.P., Leonardos, O.H., 1992. Toward a new tectonic model for the Late Proterozoic Araçuaí (SE Brazil)-West Congolian (SW Africa) Belt. J. South Am. Earth Sci. 6, 33–47.

Pedrosa-Soares, A.C., Noce, C.M., Wiedemann, C.M., Pinto, C.P., 2001. The Araçuaí-West-Congo Orogen in Brazil: an overview of a confined orogen formed during Gondwanaland assembly. Precambrian Res. 110, 307–323.

Peterson, K.J., Butterfield, N.J., 2005. Origin of the Eumetazoa: testing ecological predictions of molecular clocks against the Proterozoic fossil record. Proc. Natl. Acad. Sci. U. S. A. 102, 9547–9552.

Peterson, K.J., Cotton, J.A., Gehling, J.G., Pisani, D., 2008. The Ediacaran emergence of bilaterians: congruence between the genetic and the geological fossil records. Philos. Trans. R. Soc. Lond. B. Biol. Sci. 363, 1435–1443.

Philipp, S.L., Gudmundsson, A., 2006. Gypsum veins as hydrofrac- tures in layered and faulted mudstones : implications for reservoir permeability (Poster), in: Göttingen 2006. 3p.

Pisarevsky, S.A., Murphy, J.B., Cawood, P.A., Collins, A.S., 2008. Late Neoproterozoic and Early Cambrian palaeogeography: models and problems, in: Pankhurst, R.J., Trouw, R.A.J., Brito Neves, B.B., De Wit, M.J. (Eds.), West Gondwana: Pre-Cenozoic Correlations Across the South Atlantic Region. Geological Society, London, Special Publications, 9–31.

Pisarevsky, S.A., Wingate, M.T.D., Powell, C.M., Johnson, S., Evans, D.A.D., 2003. Models of Rodinia assembly and fragmentation, in: Yoshida, M., Windley, B.F., Dasgupta, S. (Eds.), Proterozoic East Gondwana: Supercontinent Assembly and Breakup. Geological Society, London, Special Publications, 35–55.

Planavsky, N., Grey, K., 2008. Stromatolite branching in the Neoproterozoic of the Centralian Superbasin, Australia: an investigation into sedimentary and microbial control of stromatolite morphology. Geobiology 6, 33–45.

Poidevin, J.-L., 2007. Stratigraphie isotopique du strontium et datation des formations carbonatées et glaciogéniques néoprotérozoiques du Nord et de l'Ouest du craton du Congo. Comptes Rendus Geosci. 339, 259–273.

Porada, H., 1989. Pan-African rifting and orogenesis in southern to equatorial Africa and eastern Brazil. Precambrian Res. 44, 103–136.

Porada, H., Berhorst, V., 2000. Towards a new understanding of the Neoproterozoic-Early Palaeozoic Lufilian and northern Zambezi Belts in Zambia and the Democratic Republic of Congo. J. African Earth Sci. 30, 727–771.

Porada, H., Druschel, G., 2010. Evidence for participation of microbial mats in the deposition of the siliciclastic "ore formation" in the Copperbelt of Zambia. J. African Earth Sci. 58, 427–444.

Porter, S.M., Meisterfeld, R., Knoll, A.H., 2003. Vase-shaped microfossils from the Neoproterozoic Chuar Group, Grand Canyon: a classification guided by modern testate amoebae. J. Paleontol. 77, 409–429.

Préat, A.R., Delpomdor, F., Kolo, K., Gillan, D.C., Prian, J.-P., 2011. Stromatolites and cyanobacterial mats in peritidal evaporites environments in the Neoproterozoic of Bas-Congo (Democratic Republic of Congo) and south Gabon, in: Tewari, V.C., Seckbach, J. (Eds.), STROMATOLITES: Interaction of Microbes with Sediments. Springer, 44–63.

Préat, A.R., Kolo, K., Prian, J.-P., Delpomdor, F., 2010. A peritidal evaporite environment in the Neoproterozoic of South Gabon (Schisto-Calcaire Subgroup, Nyanga Basin). Precambrian Res. 177, 253–265.

Pruss, S.B., Bosak, T., Macdonald, F.A., McLane, M., Hoffman, P.F., 2010. Microbial facies in a Sturtian cap carbonate, the Rasthof Formation, Otavi Group, northern Namibia. Precambrian Res. 181, 187–198.

Riding, R., 1991. Classification of microbial carbonates, in: Riding, R. (Ed.), Calcareous Algae and Stromatolites. Springer-Verlag, 21–51.

Riding, R., 1999. The term stromatolite: towards an essential definition. Lethaia 32, 321–330.

Riding, R., 2000. Microbial carbonates: the geological record of calcified bacterial-algal mats and biofilms. Sedimentology 47, 179–214.

Riding, R., 2006. Microbial carbonate abundance compared with fluctuations in metazoan diversity over geological time. Sediment. Geol. 185, 229–238.

Riding, R., 2008. Abiogenic, microbial and hybrid authigenic carbonate crusts: components of Precambrian stromatolites. Geol. Croat. 61, 73–103.

Riding, R., 2011a. Microbialites, stromatolites, and thrombolites, in: Reitner, J., Thiel, V. (Eds.), Encyclopedia of Geobiology. Springer, 635–654.

Riding, R., 2011b. The nature of stromatolites: 3,500 million years of history and a century of research, in: Reitner, J., Quéric, N.-V., Arp, G. (Eds.), Advances in Stromatolite Geobiology. Springer, 29–74.

Robb, L.J., Master, S., Rainaud, C., Greyling, L.N., Yao, Y., 2003. Recent developments in the Central African Copperbelt: geological, geochronological and metallogenic perspectives, in: Geological Society of South Africa Annual Meeting, Johannesburg, South Africa. pp. 25–27.

Rose, C. V, Maloof, A.C., 2010. Testing models for post-glacial "cap dolostone" deposition: Nuccaleena Formation, South Australia. Earth Planet. Sci. Lett. 296, 165–180.

Rothman, D.H., Hayes, J.M., Summons, R.E., 2003. Dynamic of the Neoproterozoic carbon cycle. Proc. Natl. Acad. Sci. U. S. A. 100, 8124–8129.

Santosh, M., 2010. Supercontinent tectonics and biogeochemical cycle: A matter of "life and death". Geosci. Front. 21–30.

Schermerhorn, L.J.G., 1974. No evidence for glacial origin of late Precambrian tilloids in Angola. Nature 252, 114–115.

Schermerhorn, L.J.G., 1981. Late Precambrian tilloids of northwest Angola, in: Hambrey, M.J., Hardland, W.B. (Eds.), Earth's Pre-Pleistocene Glacial Record. Cambridge University Press, 158–161.

Schermerhorn, L.J.G., Stanton, W.I., 1963. Tilloids in the West Congo geosyncline. Q. J. Geol. Soc. 119, 201–241.

Schieber, J., Bose, P.K., Eriksson, P.G., Banerjee, S., Sarkar, S., Altermann, W., Catuneanu, O., 2007. Atlas of Microbial Mat Features Preserved within the Siliciclastic Rock Record. Elsevier, 324p.

Schneider, J., Boni, M., Laukamp, C., Bechstädt, T., Petzel, V., 2008. Willemite (Zn2SiO4) as a possible Rb–Sr geochronometer for dating nonsulfide Zn–Pb mineralization: Examples from the Otavi Mountainland (Namibia). Ore Geol. Rev. 33, 152–167.

Scholle, P.A., Ulmer-Scholle, D.S., 2003. A color guide to the petrography of carbonate rocks: grains, textures, porosity, diagenesis. AAPG Memoir, vol 77.

Schopf, J.W., Kudryavtsev, A.B., Agresti, D.G., Wdowiak, T.J., Czaja, A.D., 2002. Laser-Raman imagery of Earth's earliest fossils. Nature 416, 73–76.

Schreiber, U.M., 2008. Geological map of Namibia. 1:250 000 Geological series. Sheet 1916 – Tsumeb.

Schulz, H.N., Jørgensen, B.B., 2001. Big Bacteria. Annu. Rev. Microbiol. 55, 105–137.

Scotese, C.R., 2009. Late Proterozoic plate tectonics and palaeogeography: a tale of two supercontinents, Rodinia and Pannotia, in: Craig, J., Thurow, J., Thusu, B., Whitham, A., Abutarruma, Y. (Eds.), Global Neoproterozoic Petroleum Systems: The Emerging Potential in North Africa. Geological Society, London, Special Publications, 67–83.

Scott, R.J., Selley, D., Bull, S., Broughton, D., Hitzman, M., Cooke, D., Large, R., McGoldrick, P., 2006. A hydrocarbon replacement model for the Zambian Copperbelt deposits, in: AESC 2006, Melbourne, Australia. p. 6.

Seilacher, A., Grazhdankin, D., Legouta, A., 2003. Ediacaran biota: the dawn of animal life in the shadow of giant protists. Paleontol. Res. 7, 43–54.

Selley, D., Broughton, D., Scott, R., Hitzman, M., Bull, S., Large, R., McGoldrick, P., Coraker, M., Pollington, N., Barra, F., 2005. A New Look at the Geology of the Zambian Copperbelt. Econ. Geol. 100th anni, 965–1000.

Shields, G.A., 2005. Neoproterozoic cap carbonates: a critical appraisal of existing models and the plumeworld hypothesis. Terra Nov. 17, 299–310.

Sibley, D.F., Gregg, J.M., 1987. Classification of Dolomite Rock Textures. J. Sediment. Petrol. 57, 967–975.

Simonson, B.M., Carney, K.E., 1999. Roll-up structures: Evidence of in situ microbial Late Archean deep shelf environments. Palaios 14, 13–24.

Smith, A.G., 2009. Neoproterozoic timescales and stratigraphy, in: Craig, J., Thurow, J., Thusu, B., Whitham, A., Abutarruma, Y. (Eds.), Global Neoproterozoic Petroleum Systems: The Emerging Potential in North Africa. Geological Society, London, Special Publications, 27–54.

Stanton, R.L., 1972. Ore petrology. International series in the Earth and planetary sciences.

Stern, R.J., 1994. Arc assembly and continental collision in the Neoproterozoic east African orogen: Implications for the Consolidation of Gondwanaland. Annu. Rev. Earth Planet. Sci. 22, 319–351.

Sumner, D.Y., 1997. Late Archean calcite-microbe interactions: two morphologically distinct microbial communities that affected calcite nucleation differently. Palaios 12, 302–318.

Sumner, D.Y., Grotzinger, J.P., 1993. Numerical modeling of ooid size and the problem of Neoproterozoic giant ooids. J. Sediment. Petrol. 63, 974–982.

Swan, A.R.H., Sandilands, M., 1995. Introduction to Geological Data Analysis. Wiley-Blackwell Science, 464p.

Tack, L., Fernandez-Alonso, M., Kanda Nkula, V., Mpoyi, J., Delvaux, D., Trefois, P., Baudet, D., 2006. Neoproterozoic diamictites around the Congo River basin: a critical reappraisal of their origin, in: 21st Colloquium of African Geology, Maputo, Mozambique. pp. 152–154.

Tack, L., Wingate, M.T.D., Liégeois, J.-P., Fernandez-Alonso, M., Deblond, A., 2001. Early Neoproterozoic magmatism (1000–910 Ma) of the Zadinian and Mayumbian Groups (Bas-Congo): onset of Rodinia rifting at the western edge of the Congo craton. Precambrian Res. 110, 277–306.

Tait, J., Delpomdor, F., Preat, A., Tack, L., Straathof, G., Nkula, V.K., 2011. Chapter 13 Neoproterozoic sequences of the West Congo and Lindi/Ubangi Supergroups in the Congo Craton, Central Africa, in: Arnaud, E., Halverson, G.P., Shields-Zhou, G. (Eds.), The Geological Record of Neoproterozoic Glaciations. Geological Society, London, Memoirs, 185–194.

Talling, P.J., Masson, D.G., Sumner, E.J., Malgesini, G., 2012. Subaqueous sediment density flows: Depositional processes and deposit types. Sedimentology 59, 1937–2003.

Testa, G., Lugli, S., 2000. Gypsum–anhydrite transformations in Messinian evaporites of central Tuscany (Italy). Sediment. Geol. 130, 249–268.

Tojo, B., Katsuta, N., Takano, M., Kawakami, S., Ohno, T., 2007. Calcite dolomite cycles in the Neoproterozoic Cap carbonates, Otavi Group, Namibia, in: Vickers-Rich, P., Komarower, P. (Eds.), The Rise and Fall of the Ediacaran Biota. Geological Society, London, Special Publications, 103–113.

Tucker, M.E., 1977. Stromatolite biostromes and associated facies in the Late Precambrian Porsanger Dolomite Formation of finnmark, Arctic Norway. Palaeogeogr. Palaeoclimatol. Palaeoecol. 21, 55–83.

Tucker, M.E., 2001. Sedimentary Petrology: An introduction to the origin of sedimentary rocks. Blackwell Science, 272p.

Tucker, M.E., Wright, V.P., Dickson, J.A.D., 1990. Carbonate sedimentology. Blackwell Science, Wiley, 496p.

Turner, E.C., James, N.P., Narbonne, G.M., 2000. Taphonomic control on microstructure in Early Neoproterozoic reefal stromatolites and thrombolites. Palaios 15, 87–111.

Vellutini, P., Rocci, G., Vicat, J.-P., Gioan, P., 1983. Mise en évidence de complexes ophiolitiques dans la chaîne du Mayombe (Gabon-Angola) et nouvelle interprétation géotectonique. Precambrian Res. 22, 1–21.

Vellutini, P., Vicat, J.-P., 1983. Sur l'origine des formations conglomératiques de base du géosynclinal ouest-congolien (Gabon, Congo, Zaïre, Angola). Precambrian Res. 23, 87–101.

Vieira, L.C., Trindade, R.I.F., Nogueira, A.C.R., Ader, M., 2007. Identification of a Sturtian cap carbonate in the Neoproterozoic Sete Lagoas carbonate platform, Bambuí Group, Brazil. Comptes Rendus Geosci. 339, 240–258.

Walter, M.R., Heys, G.R., 1985. Links between the rise of the metazoa and the decline of stromatolites. Precambrian Res. 29, 149–174.

Wendorff, M., 2003. Stratigraphy of the Fungurume Group - evolving foreland basin succession in the Lufilian fold-thrust belt , Neoproterozoic-Lower Palaeozoic , Democratic Republic of Congo. South African J. Geol. 106, 17–34.

Wendorff, M., 2005. Evolution of Neoproterozoic-Lower Palaeozoic Lufilian arc, Central Africa: a new model based on syntectonic conglomerates. J. Geol. Soc. London 162, 5–8.

Wendorff, M., Key, R.M., 2009. The relevance of the sedimentary history of the Grand Conglomerat Formation (Central Africa) to the interpretation of the climate during a major Cryogenian glacial event. Precambrian Res. 172, 127–142.

Wimpenny, J.W.T., Colasanti, R., 1997. A unifying hypothesis for the structure of microbial biofilms based on cellular automaton models. Fems Micriobiology Ecol. 22, 1–16.

Wright, D.T., Wacey, D., 2005. Precipitation of dolomite using sulphate-reducing bacteria from the Coorong Region, South Australia: significance and implications. Sedimentology 52, 987–1008.

Xiao, S., 2004. Neoproterozoic glaciations and the fossil record. Extrem. Proterozoic Geol. Geochemistry, Clim. 146, 199–214.

Yoshioka, H., Asahara, Y., Tojo, B., Kawakami, S., 2003. Systematic variations in C, O, and Sr isotopes and elemental concentrations in Neoproterozoic carbonates in Namibia: implications for a glacial to interglacial transition. Precambrian Res. 124, 69–85.

# Appendices

**Appendix A**

Le Ber, E., Le Heron, D.P., Winterleitner, G., Bosence, D.W.J., Vining, B.A., Kamona, F., 2013. Microbialite recovery in the aftermath of the Sturtian glaciation: Insights from the Rasthof Formation, Namibia. Sediment. Geol. 294, 1–12.

**Appendix B**

Material for Chapter 5, section 5.4: Spearman's rank correlation coefficient.

**Appendix C**

Le Heron, D.P., Busfield, M.E., Le Ber, E., Kamona, F., 2013b. Ironstone stromatolites and diamictites in the Chuos Formation of Namibia: implications for Cryogenian glaciation. Palaeogeogr. Palaeoclimatol. Palaeoecol. 369, 48–57.
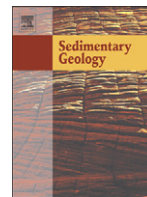
**Appendix D**

Stratigraphic position of the remaining samples collected in northern Namibia.

# APPENDIX A

# Microbialite recovery in the aftermath of the Sturtian glaciation: Insights from the Rasthof Formation, Namibia

Erwan Le Ber [a,*], Daniel P. Le Heron [a], Gerd Winterleitner [a], Dan W.J. Bosence [a], Bernie A. Vining [a,b], Fred Kamona [c]

[a] Earth Sciences Department, Queen's Building, Royal Holloway University of London, Egham, Surrey TW20 0EX, UK
[b] Baker Hughes, Bentley Hall, Blacknest, Alton, Hampshire GU34 4PU, UK
[c] Geology Department, University of Namibia, Windhoek, Namibia

## ARTICLE INFO

## ABSTRACT

Ice sheet meltback in the aftermath of the Sturtian (mid Cryogenian) glaciation was accompanied or followed by deposition of thick carbonate successions. In northern Namibia, the Rasthof Formation is a 200–400 m thick cap carbonate sequence divided into (1) a basal cap dolostone, (2) a microbial member and (3) an epiclastic member. This subdivision applies for >100 km along strike at the southern and western edges of the Owambo Basin. In this paper we focus essentially on macrofacies of the cap dolostone and the microbial member. Cap dolostones are commonly interpreted as subtidal to deep water deposits, with delicate mm thick laminae. We describe well-preserved, ungraded hummocky cross-stratification in the cap dolostone, expected to occur no deeper than the offshore transition zone. The overlying microbial member contains thickly laminated microbialites with folded and contorted intervals interpreted as soft-sediment deformation structures. The thickly laminated microbialites are followed by more thinly laminated microbialites, with "roll-up" structures and more unusual individual, vertical stromatolite morphologies. We interpret the vertical growths in the microbial member as a direct response to the changing environment. The new observations and interpretations presented in this paper contrast with previous work on the Rasthof Formation. We recognise a relatively shallower setting associated with a trend in the geometries of the microbial member.

© 2013 Elsevier B.V. All rights reserved.

## 1. Introduction

The style and intensity of glaciation, together with the nature of post-glacial climatic recovery, from the Sturtian icehouse event remain vigorously debated (e.g. Eyles and Januszcak, 2004, 2007; Fairchild and Kennedy, 2007; Allen and Etienne, 2008; Eyles, 2008; Le Heron et al., 2011; Le Heron, 2012). At least two glacial events punctuated the Neoproterozoic, the older Sturtian (750 Ma) and the younger Marinoan (635 Ma) event, sediments from which are preserved worldwide, including northern Namibia. The glaciogenic sediments are sharply overlain by a ~10 m cap dolostone unit, with mm thick laminae (Hoffman and Schrag, 2002; Shields, 2005; Hoffman et al., 2007). The cap dolostones deposited after the Marinoan glacial event have unusual features such as sheet-crack cements, low angle cross stratification, tube structures, tepee-like structures, giant wave ripples and seafloor crystal fans (Corsetti and Grotzinger, 2005; Corkeron, 2007; Hoffman et al., 2007; Hoffman and MacDonald, 2010; Rose and Maloof, 2010). They are more widely studied than the post Sturtian cap dolostones, in which these features are absent. Cap dolostones represent a real challenge in terms of interpreting

sedimentation processes, timing of deposition and paleoenvironment interpretation (Hoffman et al., 2007; Loyd and Corsetti, 2010; Rose and Maloof, 2010; Kennedy and Christie-Blick, 2011). The cap dolostones often represent the base of what is termed the "cap carbonate sequence" (Hoffman and Schrag, 2002); sediments overlying the cap dolostone can include massive carbonates, transgressive shales or siltstones (Shields, 2005). In this study, we describe and interpret a cap carbonate sequence – the Rasthof Formation – preserved above a Sturtian glacial succession in Namibia. The scope of our study includes both the cap dolostone and its overlying microbialites.

Several recent studies focused on the Rasthof Formation in north-west Namibia with observations made on the cap dolostone and the microbialites. Publications cover several disciplines, encompassing outcrop studies (Hedberg, 1979; Hoffman and Halverson, 2008; Pruss et al., 2010), isotopic analyses (Yoshioka et al., 2003; Tojo et al., 2007; Pruss et al., 2010) and microscopic investigation (Pruss et al., 2010; Bosak et al., 2011, 2012). The Rasthof Formation was initially named the Rasthof Member (Hedberg, 1979). It is interpreted as a shoaling-upward succession, with the cap dolostone deposited in the deepest environment followed by sublittoral stromatolites (Halverson et al., 2005). An abundance of soft sediment deformation structures has been described (Hoffman and Halverson, 2008; Pruss et al., 2010), creating a chaotic aspect despite continuous laminae. Most recently the

* Corresponding author.
E-mail addresses: e.leber@es.rhul.ac.uk, leber.erwan@gmail.com (E. Le Ber).

microbial member has been interpreted as a deep-water microbial ecosystem in the Warmquelle–Okaaru area (Fig. 1A) (Pruss et al., 2010), on account of the lack of bedforms, scour marks and intraclasts. Petrographic studies have revealed the occurrence of possible early agglutinated foraminifera in the microbial member (Bosak et al., 2012; Dalton et al., 2013). The aim of the present paper is to describe the Rasthof Formation at the Rasthof Farm locality. New sedimentological observations from the type area are presented, they suggest that the cap carbonate was deposited in substantially shallower water than suggested elsewhere. This interpretation has major implications both for facies models on the post-Sturtian carbonate platform and, potentially, for the interpreted magnitude of postglacial sea level rise.

## 2. Study area and stratigraphy

The Rasthof Formation was deposited on the Northern Platform and is well exposed along the edges of the Kamanjab Inlier, north-west Namibia (Fig. 1A). A regional model suggests that the Kamanjab Inlier is a basement high that created ridges separating platform facies to the north from slope facies to the south (Hoffman and Halverson, 2008). This paper presents data from the type section at Rasthof Farm, north of the Kamanjab Inlier and, therefore, on the platform.

Detailed previous studies of the platform were focused more than 50–100 km to the north-west and west. The cap dolostone and/or the microbial member were examined in the vicinity of Warmquelle, Okaaru and Ongongo localities (Yoshioka et al., 2003; Tojo et al., 2007; Hoffman and Halverson, 2008; Pruss et al., 2010; Bosak et al., 2011, 2012; Dalton et al., 2013). Hoffman and Halverson, 2008 also described the Rasthof Formation in the Northern Margin Zone, south of the Kamanjab Inlier. The type area of the unit ("Rasthof Member": Hedberg, 1979) in Rasthof Farm has, surprisingly, not been subject to detailed investigations.

In northern Namibia the Otavi Group (Fig. 1B) was deposited after the break-up of Rodinia (recorded by syn-rift sediments of the Nosib Group) and prior to the Pan African Orogen (recorded by molasse deposits of the Mulden Group) (Frimmel et al., 2011). The Otavi Group accumulated on an extensive carbonate platform lining the southern edge of the Congo Craton. It starts with the Ombombo Subgroup, consisting of mixed carbonate and siliciclastic sediments. These deposits are overlain by glacial sediments of the Chuos Formation, which are in turn followed by the Rasthof, Gruis and Ombaatjie formations; forming the Abenab Subgroup. A second glacial succession, the Ghaub Formation, is overlain by carbonate sediments, forming the Tsumeb Subgroup (Hoffmann and Prave, 1996).

On the Northern Platform, the Chuos Formation bears evidence of direct ice contact (subglacial shear zones, dropstones, ice-contact fans) with two glacial cycles preserved (Le Heron et al., 2013). The overlying 200–400 m thick Rasthof Formation rests in sharp contact,
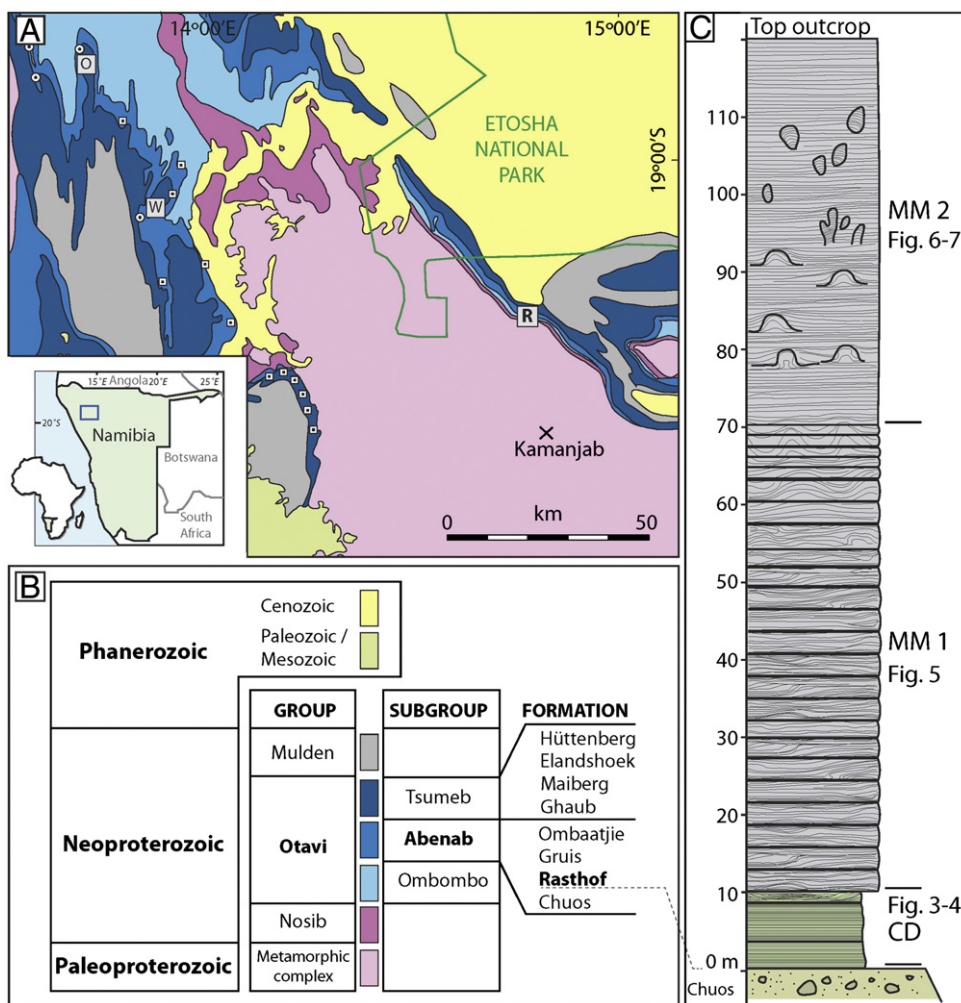


**Fig. 1.** Outcrop location and lithostratigraphy of the Otavi Group. A. Simplified geological map of the area (modified from Hoffman and Halverson, 2008), "R" is the location of the Rasthof Farm, □ are the sections described by Hoffman and Halverson, 2008, ⊙ are sections described by Pruss et al. (2010). "O" and "W" indicate Okaaru and Warmquelle areas. B. Stratigraphy of the Otavi Group, from Hoffman and Halverson, 2008. C. Idealized log of the section at Rasthof Farm, with references to others figures: Figs. 3–4 (deformation and hummocky cross-stratification, top cap dolostone); Fig. 5 (facies of MM1); and Figs. 6 and 7 (facies of MM2).

but without any evident unconformity, on the Chuos Formation. It starts with a "cap dolostone" also locally termed "rhythmite" or "abiotic member" (Hoffman and Halverson, 2008; Pruss et al., 2010), in which cm to dm thick allodapic beds alternate with m thick delicately laminated dolostone (Yoshioka et al., 2003; Tojo et al., 2007; Hoffman and Halverson, 2008). The cap dolostone is concordantly overlain by the microbial member (Hoffman and Halverson, 2008). Pruss et al. (2010) differentiated two types of facies in the microbial member: thickly and thinly laminated microbial mats, both exhibiting unusual styles of deformations interpreted as synsedimentary. Thickly laminated mats are characterised by several dm to m wide folds/dome like structures and more chaotic intervals. The thinly laminated mats are generally flat but still exhibit cm scale roll-up structures (Pruss et al., 2010).

In the Warmquelle–Khowarib area, the cap dolostone has previously been interpreted to record sub-storm wave base deposition (Yoshioka et al., 2003; Tojo et al., 2007). The microbial member was first interpreted by Hedberg (1979), on the northern flank of the Kamanjab Inlier, as a shallow water formation. This hypothesis is supported by the observation of microbial mats, oolites and intraformational breccias. The precise locations of Hedberg's observations are, however, unclear. Our study is located in the vicinity of where Hedberg first described the Rasthof Formation. The microbial member has more recently been recognised in the Warmquelle–Okaaru area (Fig. 1A, "W" and "O") of Pruss et al. (2010). There, it is interpreted as a deep water sub-storm wave base microbialite where fluid escape generated sedimentary dykes associated with soft-sediment deformation. Formation of the dykes may have been facilitated by tectonic activity.

## 3. Field observations

### 3.1. Outcrop overview

The Rasthof Formation is described at Rasthof Farm, where it is subvertical, dipping steeply north-east into the Owambo Basin. The log presented in Fig. 1C is idealized and represents observations compiled from along the outcrop. Lateral variability of the observed facies is still to be established. The contact with the underlying Chuos Formation is not apparent at this section, with the cap dolostone occupying low terrain and the microbial member present as a hill-forming unit. From afar (Fig. 2) the lower part of the outcrop exhibits a layer cake character; overlying strata are more massive in character with a less bedded aspect. Careful examination reveals that the layer cake character corresponds to the thickly laminated microbialites and the most continuous succession to the thinly laminated microbialites. We will refer to the thickly and thinly laminated microbialites respectively as the microbial member 1 (MM1) and microbial member 2 (MM2). In the following, we describe the cap dolostone, and both microbial members (Fig. 1C).
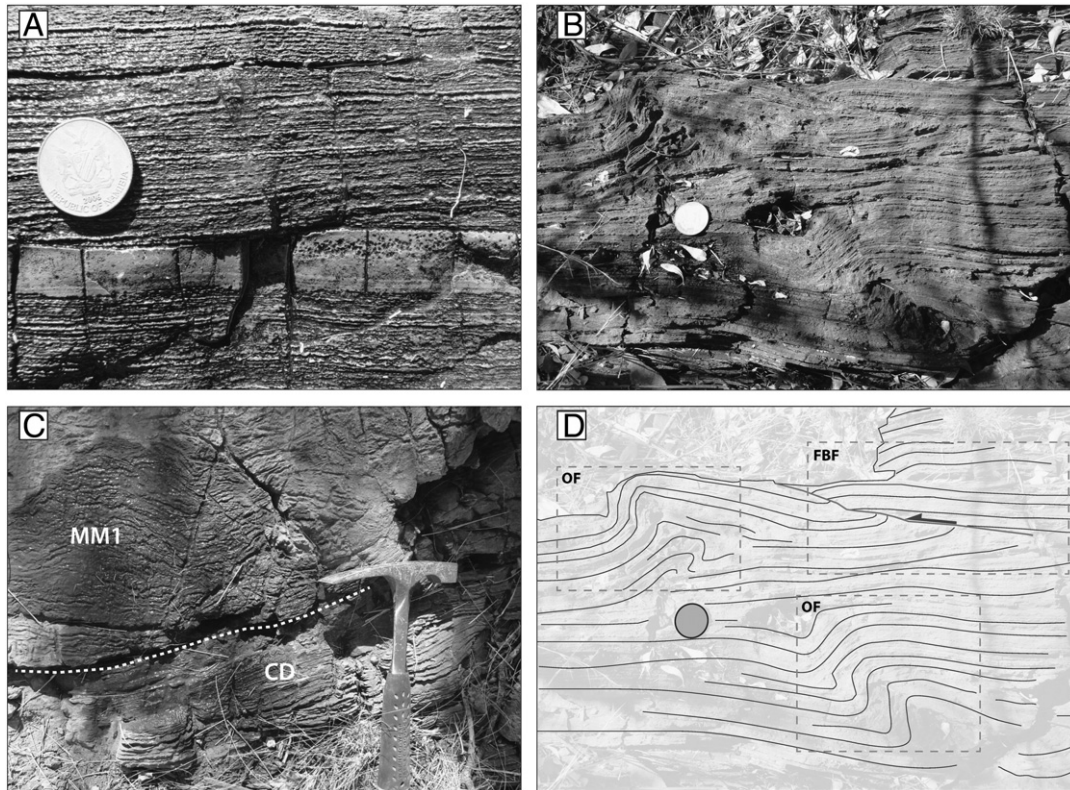
### 3.2. Cap dolostone

The contact with the Chuos Formation is concealed, but exposure quality improves upsection. The ~10 m thick unit is dominated by delicate, mm scale horizontal parallel laminae. However, rare 1–10 cm thick beds of non-laminated, white to grey beds punctuate this facies. These beds pinch out laterally over 100 m and probably correspond to the allodapic beds described by Hoffman and Halverson, 2008. Overlying laminae show subtle downlap relationships onto the top surface of these beds (Fig. 3A). The latter deposits also exhibit deformation structures. These include 1) dm scale overturned folds, with wavelengths <20 cm and short limbs dipping at 45–90° and 2) 10 cm wide fault-bend folds, with a low angle thrust ramp (Fig. 3B, D). An undeformed, hummocky cross-stratified interval occurs in the upper 2 m of the cap dolostone (Fig. 4), forming low angle, concave and convex bounding surfaces. Laminae in these bedforms are approximately parallel to the bounding surfaces, with subtle lateral variation in dip angles and lamina thicknesses. Dip directions are scattered.

At Rasthof Farm, the contact with the overlying deposits (which we describe as microbial member 1) is locally abrupt (Fig. 3C). Cap
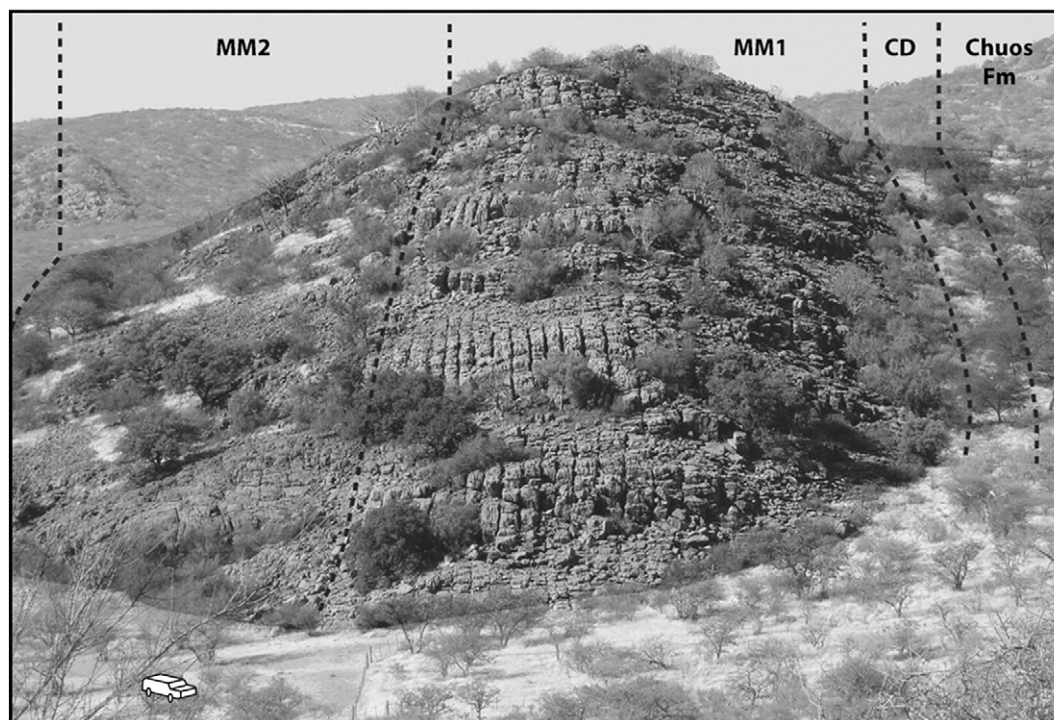


**Fig. 2.** A. View of the outcrop, looking southeast. Note the distinctions between the cap dolostone (CD), the microbial member 1 (MM1) and the microbial member 2 (MM2). MM1 is organised into 2–4 m thick beds and MM2 is more continuous. The white car is approximately 5 m long.

**Fig. 3.** Cap dolostone facies. Panel A shows thin and flat laminae, downlapping onto a white, non-laminated interval. Panels B and D show soft-sediment deformation structures in the cap dolostone. Two types of folds are observed: overturned folds (OF) and fault-bend folds (FBF). Note that the folds have the same orientation and probably represent different stages of deformation. Panel C shows sharp contact between the cap dolostone and MM1.
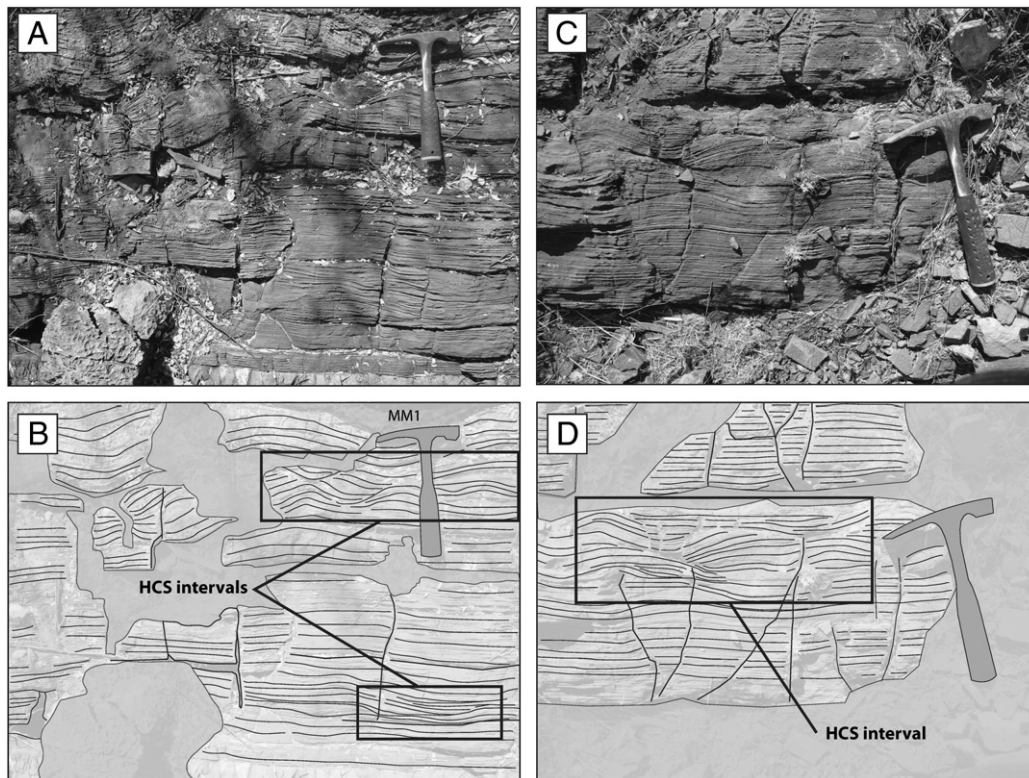


**Fig. 4.** Hummocky cross stratification (HCS): panels A, C (photos) and panels B, D (sketches), in the upper 2 m of the cap dolostone. The squares in panels B and D indicate the HCS intervals. Grey areas denote parts of the outcrop where facies are obscure as a result of weathering etc. On B, note the base of MM1 immediately above the HCS interval.

dolostone laminae generally change in thickness and become more crinkly and undulated. Recent weathering can lend a brecciated aspect to the upper few centimetres of the cap dolostone.

### 3.3. Microbial member 1 (MM1)

The microbial member 1 (MM1) is a ~60 m thick succession of thickly laminated microbialites. The facies consists of thin, sub-mm thick dark laminae, alternating with thicker (1–5 mm), crystalline laminae (Fig. 5A). Dolomitization of the formation makes observation of the primary textures complicated. Dark laminae consist of dolomicrite: these are generally continuous with local cloth-like thickenings. The light laminae are represented by an equigranular mosaic of subhedral dolomite. A similar type of crinkly laminae was described and analysed by Pruss et al. (2010) in the Rasthof Formation: they interpret thick light coloured laminae to record intervals of carbonate sedimentation outpacing the growth of microbial mats, whilst darker laminae result from microbially-induced precipitation. However, the same authors explain that no individual filaments are preserved.

The very base of this unit is characterised by crinkly laminae that grow on the top of the cap dolostone, sometime rising vertically with respect to bedding. When horizontal, undulation of the sets of laminae creates a series of weakly defined, laterally linked hemispheroids. The hemispheroids do not exceed 10 cm amplitude and wavelength. Laminae tend generally to form these undulating sets but are commonly deformed (Fig. 5B, C). Deformation consists of complex dm to m scale folds or contorted structures that do not show any preferential orientation. Rare break-up of sets can be observed at a dm scale (Fig. 5B), whilst discontinuities and thinning out of the laminae can be observed at a mm scale. These deformation structures are restricted to MM1 and are contained within individual intervals, with microbial laminae that recover a more horizontal aspect upsection. After 50 m, laminae tend to be less chaotic and flatter. They locally start to develop clear, 10 to 20 cm amplitude cone structures (Fig. 5D) indicating the arrival into microbial member 2 (MM2).
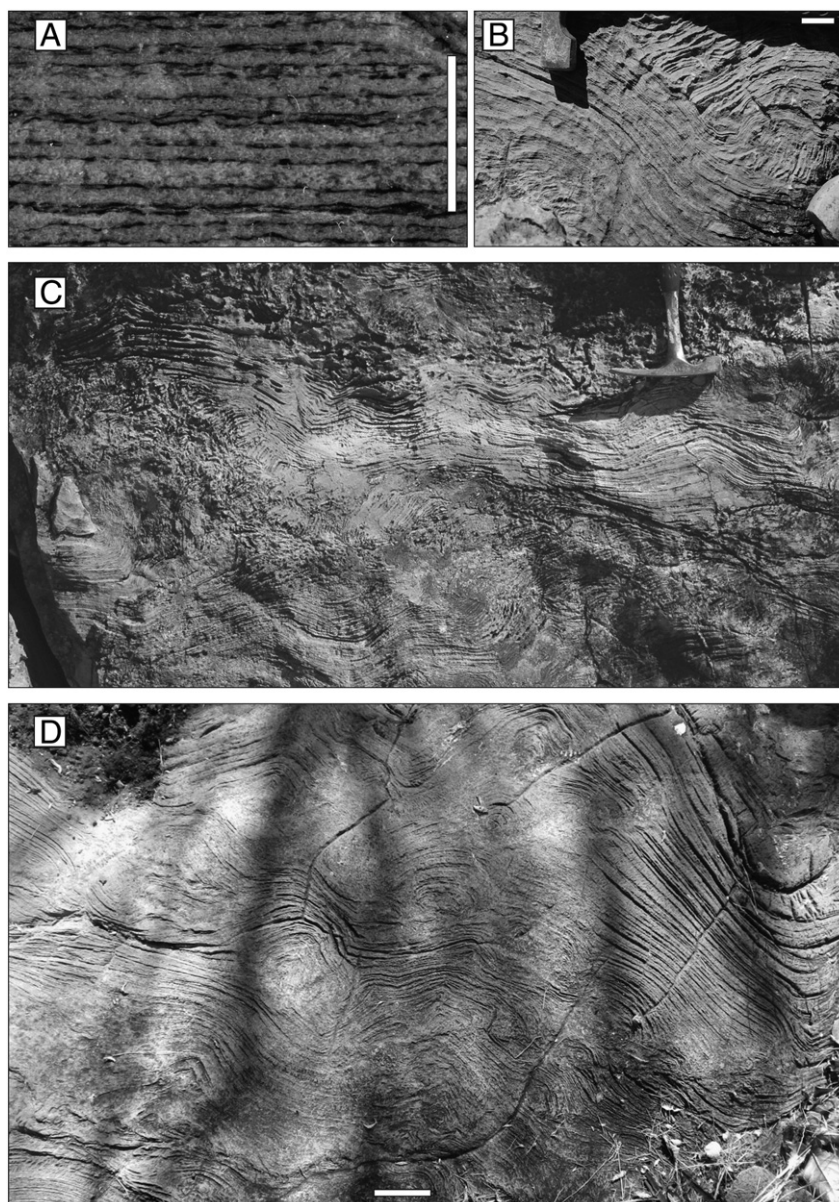


**Fig. 5.** MM1 facies. A. Mesoscale, showing thickly laminated microbialites. Thick, white equigranular mosaic of subhedral dolomite alternating with thin micritic laminae. Dark laminae are interpreted as microbial in origin (scale is 1 cm). B. Folded set of laminae (half bottom left) with angular contact with another set of laminae (top right corner). C. Typical MM1 facies with undulated bedsets. D. Upper facies found in MM1, with clearly differentiated, 10–20 cm high cones (scale is 10 cm).

### 3.4. Microbial member 2 (MM2)

The thinly laminated microbial mats of MM2 are organised differently to underlying deposits: light laminae are thinner (<1 mm), generally flat and parallel (i.e. no undulation). Locally, structures akin to roll-ups are recognised (Fig. 6): these consist of cm scale contorted intervals and can be fragmented. They lack a preferred orientation within beds, and occur adjacent to individual growths described below. Laminae above and below the contorted structures are perfectly flat and parallel.

In the lower part of MM2, horizontal laminae gradually increase in dip angle upward, approaching subvertical angles to form the flanks of 20–40 cm wide/high symmetrical dome structure (Fig. 7A and B). Above the domes, laminae recover a horizontal organisation, passing upward and gradationally into an overlying set of domes. These can be closely spaced laterally and vertically (<1 m). In other intervals upsection, very different structures occur: including up to 30 cm large columns, 10 cm large branching columns (Fig. 7C and D) or 10–20 cm wide individual morphologies probably part of a dense branching network (Fig. 7E and F). The laminae in these geometries are convex upward, whilst laminae between (where present) are concave upward (Fig. 7F) or almost horizontal. Local roll-up structures are observed close to the interface with the growth (Fig. 6B). In the geometries described above, laminated facies is obvious to a dm scale but more difficult to observe to a cm scale. This is due to an alternation of partly micro-clotted and discontinuous dark laminae with more continuous light laminae.

Sediments deposited between the columns and branching columns range between undisturbed, and different degrees of rolled-up and broken laminae. Where intergrowth laminae are broken, they form mm to cm diameter intraclasts and cm diameter void cement. Sedimentation around the individual growths can be complex and heterogeneous, with laminae on one side and intraclastic facies on the other side of the growth (Fig. 7F).

The thickness of the exposed microbial member 2 is ~50 m. A few metres from the top of the exposed section, individual microbial geometries disappear. The overlying facies of the Rasthof Formation

are not exposed in the area. Previous studies done elsewhere on the Northern Platform mention a regional transition to grainstones and cross-bedded facies, with local tepee structures (Hoffman and Halverson, 2008; Pruss et al., 2010).

## 4. Petrographic description

Examination of thin sections in the cap dolostone, MM1 and MM2 have been undertaken to assess and compare grain sizes, with the aim to deduce variations in depositional energy between the different facies. Dolomitization occludes the detail of thin sections that we examined under a standard petrographic microscope. To resolve this, we placed a sheet of paper (80 gsm) under the thin sections to reveal the primary texture (Delgado, 1977). Photomicrographs were captured with a Nikon DS-5M camera. This approach reveals that sediments are laminated from the base to top, with lamina thicknesses in the range of <1 mm and <8 mm. Sub-mm thick, dark, fine grained laminae alternate with thicker light laminae. The latter contains grains and intraclasts.

In the cap dolostone (Fig. 8A, B), tens of μm thick, micritic dark laminae alternate with mm thick wackestone textures. Perfect rhombohedral crystals growing around or replacing initial grains are <20 μm. In the cap dolostone, several relatively large ovoid to circular morphologies occur (up to 100 μm, Fig. 8A), similar to those initially observed by Pruss et al. (2010). Non-laminated intervals found in the cap dolostone usually do not show any grain texture, yet infrequently reveal a packstone texture, with 20 to 100 μm "ghosts" of grains.

Upsection, grains size increases (Fig. 8B) to reach a size <75 μm. These grains probably consist of rolled material derived from the dark, fine-grained laminae, forming wackestone–packstone textures. In the deformed microbialites of MM1 (Fig. 8C, D), grains are slightly larger than in the cap dolostone. Textures vary between wackestone and grainstone and sporadic, mm scale intraclasts of well-preserved dark laminae can be found in the light laminae (Fig. 8D). Finally, in MM2 (Fig. 8E, F), facies found between the columns and branching columns exhibit large intraclasts (>100 μm).

## 5. Interpretations

### 5.1. Cap dolostone

The mm scale laminae in the cap dolostone compare well with that described from the basal Rasthof Formation elsewhere in Namibia (Yoshioka et al., 2003; Tojo et al., 2007; Hoffman and Halverson, 2008; Pruss et al., 2010), and more broadly to cap dolostones of different ages worldwide (Hoffman and Schrag, 2002; Shields, 2005). The fault-bend folds and monoclinal folds encountered in the upper part of this unit are interpreted as soft sediment deformation structures. This interpretation is supported by their intra-bed occurrence. We tentatively invoke a seismic origin for these soft-sediment deformations, possibly triggered by a post-glacial rebound after ice-melting (cf. Nogueira et al., 2003).

Allodapic beds are reported from elsewhere in the cap dolostone: a 1 m thick interval is recorded in the Warmquelle–Omutirapo area (Tojo et al., 2007 and personal observations). This turbidite contains dm-sized rip-up clasts, mud clasts, grading, and convolute bedding. On the foreslope of the platform, south of the Kamanjab Inlier, Hoffman and Halverson, 2008 report rhythmite facies associated with debris flows derived from the Northern Platform. No such facies are observed at Rasthof Farm. The non-laminated <10 cm layers are rare and do not exhibit any typical turbidite or allodapic sequence (Flügel, 2004). The packstone–wackestone textures imply comparatively energetic transport of sand-sized particles as bedload at intervals. Such energy levels might be attributable to 1) currents or more proximal storms events or 2) transport of material during seismic shocks.
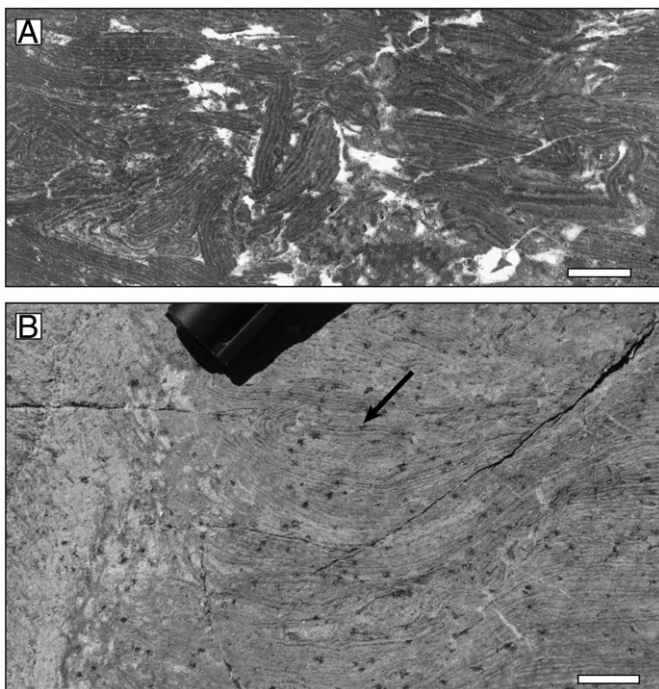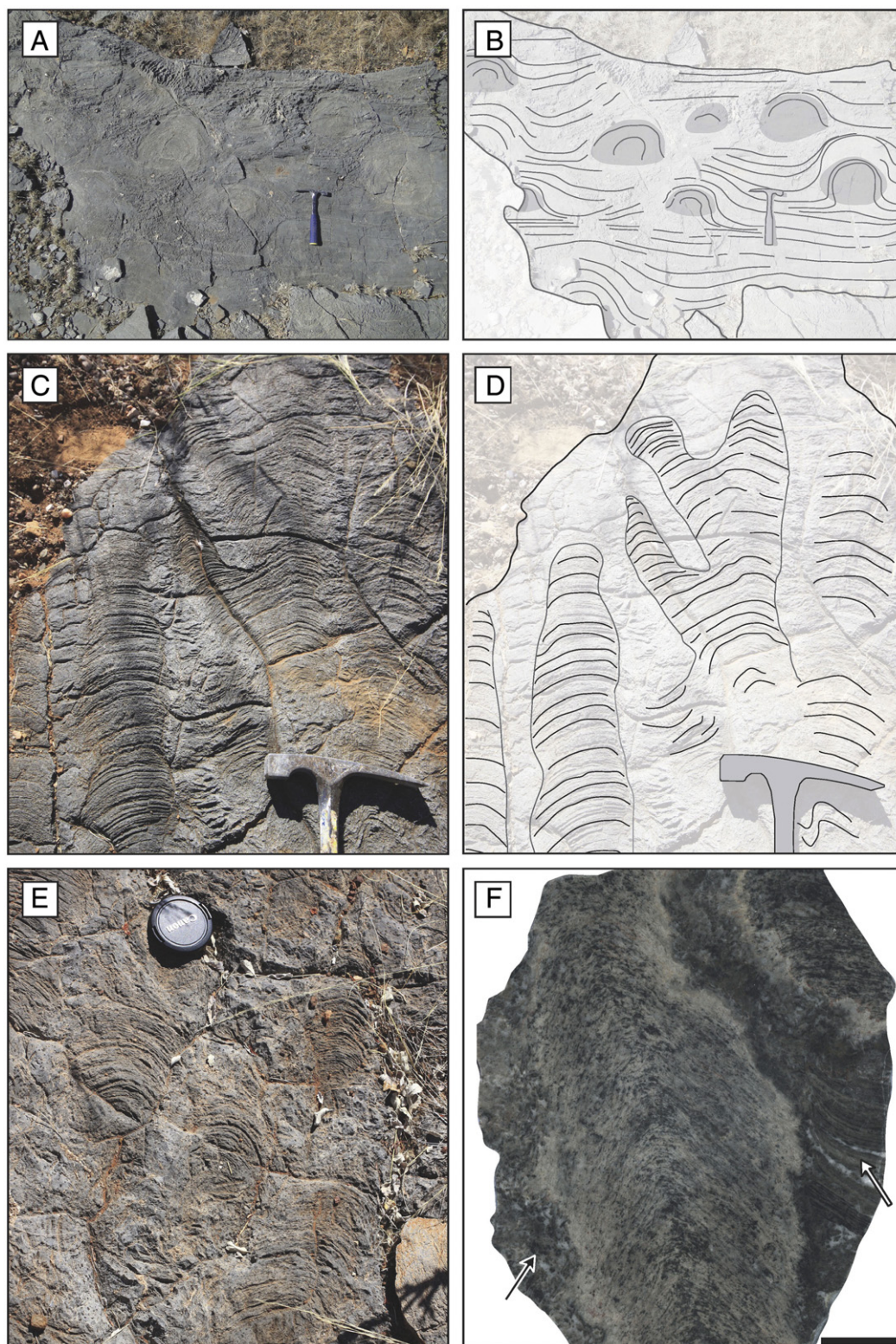


Fig. 6. Roll-up structures in MM2. A. Mix of rolled-up facies (left, right) and broken sets in the centre (scale is 1 cm). B. Rolled-up facies (arrow) sitting to the right side of a column formed of convex upward laminae (scale is 1 cm).

**Fig. 7.** Individual stromatolites morphologies in MM2. In panels A (photo) and B (sketch), thin laminae rise up to 90° to form individual dome geometries. Grey areas represent what was probably the "core" of these individual morphologies. Panels C (photo) and D (sketch) show branching columns. Another example of branching columns can also be observed as shown in panel E. Panel F is a polished sample from panel E, note the grainy facies (black arrow) and the laminated facies (white arrow) around the same growth. Scale is 2 cm.

At Rasthof Farm, the recognition of hummocky cross-stratification (HCS) is important because this structure confirms sedimentation in an energetic, comparatively shallow setting. HCS bedforms are recognised in a range of settings from outer shelf to intertidal environments (Cheel and Leckie, 1993), forming from the interaction of oscillatory gravity waves and possibly "combined" flows with geostrophic component superimposed (e.g. Dumas and Arnott, 2006). On the outcrop, the bases of the swales seem erosional, the absence of migrating ripples and soft-sediment deformation structures in HCS beds, coupled with the lack of massive grainstones underlying them, discounts a genesis
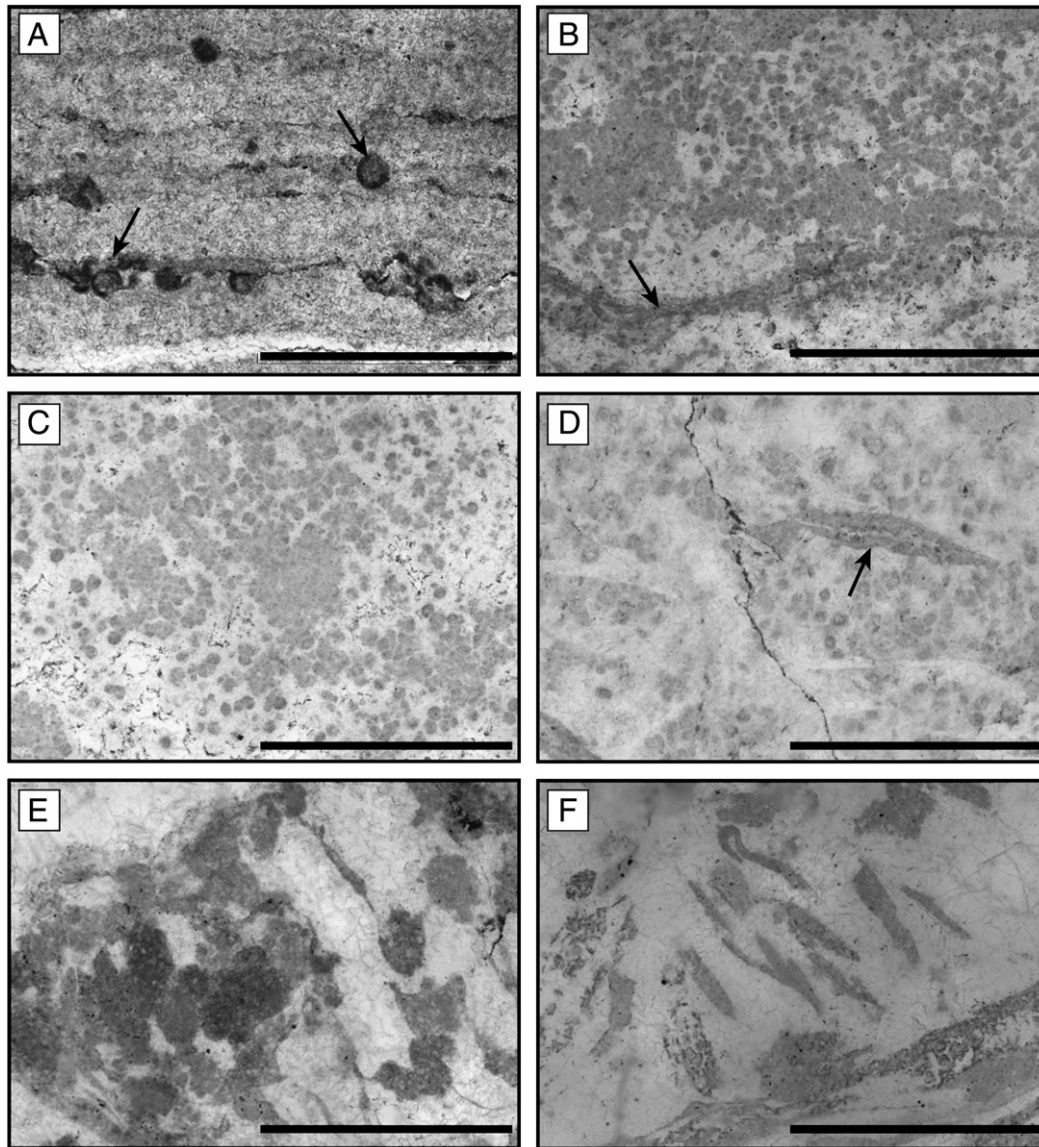
**Fig. 8.** Microfacies of the Rasthof Formation. Scale bar is 1 mm. A. Fine-grained cap dolostone facies and walled structures (arrows). B. Packstone–grainstone above a thin dark lamination (arrow). C Packstone–grainstone in MM1. D Packstone–grainstone in MM1, with an intraclast of dark lamination (arrow). E and F. Inter-columnar facies consisting of coarse intraclasts.

by turbidity currents (Mulder et al., 2009). The accumulation of at least the uppermost part of the cap dolostone, therefore, is interpreted to record deposition from storm wave activity.

The cap dolostone is described as the "abiotic member" by Hoffman and Halverson, 2008, meaning it is not biologically influenced and we agree. Occurrence of HCS at Rasthof Farm indicates that grains are not bound or trapped by microbial mats. Facies from the cap dolostone are only influenced by physical and chemical factors. Biogenic grains might be present as reworked material, but their incorporation does not imply a biogenic accumulation mechanism for the cap dolostone itself. For example, rounded and sometimes walled elements are observed (Fig. 8A). They compare in size and shape to those described and interpreted as putative eukaryotes by Pruss et al. (2010), Bosak et al. (2011, 2012) and Dalton et al. (2013) in the microbial member (80–100 km WNW from Rasthof Farm). The crinkly appearance of laminae less than 1 m above the HCS beds (basal MM1) marks the onset of microbial precipitation. We thus suggest that storm events and sea floor currents might have stimulated microbial colonization, distributing and seeding microbial communities with nutrients.

### 5.2. Microbial member 1 (MM1)

A microbial origin for MM1 is consistent with previously published interpretations (Hoffman and Halverson, 2008; Pruss et al., 2010), though no microbial filaments are preserved. Specifically, the recognition of "macroscopically layered authigenic microbial sediments with or without interlayered abiogenic precipitates" (Riding, 2011, p31) classifies them as stromatolites. The microbial origin of the unit coupled with 1) folds and contorted intervals and 2) the lack of thrust structures indicate that the stromatolites were cohesive but not lithified at the time of deformation. Under a stress regime, their rheology is more likely to be compared to a textile fabric or a rubbery material than a paper sheet.

At Rasthof Farm, no preferential orientation of the folds and no slump structures were observed, indicating a very low angle slope. Deformation styles range from gentle dm to m scale folds, contorted laminae and occasional break-up of the lamina sets (Fig. 5B). The scale of the structures and their occurrence between non deformed intervals, may suggest recurrent episodes of deformation. Cycles of quiescence to moderate energy (deposition of flat to undulated

laminae) punctuated by deformation episodes (folded and contorted strata) are thus recognised.

In previously studied outcrops (Fig. 1A), the deformation is assigned to early fluid escape during the sediment compaction, which also produced 0.5–1 m wide sedimentary dykes (Pruss et al., 2010). At Rasthof Farm, no such sedimentary dykes are observed; another process must have deformed the mats at this location. Sediments of the Rasthof Farm were also probably isolated from siliciclastic input and dominated by microbial mats. We can expect most of the grains to be trapped on the seafloor by these mats. Wave action can then shape and deform the cohesive mats with no resultant bedform. Deformed sets are >dm thick, limiting their breaking up. Furthermore, given the supposed cohesive nature of the mats upon deposition, no scour marks would be expected. To support this hypothesis at Rasthof Farm, we emphasise the occurrence of hummocky cross stratification in the underlying cap dolostone. HCS was formed in granular, non-biologically influenced sediments. In MM1, cohesive mats and trapping of grains prevented the generation of bedforms.

Thin section analysis demonstrates that grain size increases from the base to the top of the formation, consistent with a shoaling upward sequence as suggested by Halverson et al. (2005). Therefore, these data strongly imply that MM1 was deposited above the storm wave base. Furthermore, sedimentological evidence such as oolites (Hedberg, 1979) suggests that a shallow, high energy environment was present during Rasthof time in the area. At Rasthof Farm, the sediments might have been deposited between the storm wave base and an intertidal environment.

Whilst recurrent intervals of soft sediment deformation are inferred, pinpointing the trigger mechanism is challenging (e.g. Owen et al., 2011). Below, we consider two factors for the deformation in MM: storm wave impact and seismic shocks. Facies comparable to those of MM1 are unusual in the sedimentological record. The absence of sedimentary dykes excludes a fluid escape origin, whilst the lack of consistent orientation to the deformation structures likely excludes slope or gravity movements. However, since MM1 was deposited above the storm wave base, we argue that storm activity deformed the microbial mats. Also, given the depositional context of the Rasthof cap carbonate in the aftermath of the Chuos glacial event, fault re-activation during postglacial rebound cannot be excluded. For example, Nogueira et al. (2003) observed soft-sediment deformation in equivalent cap carbonates in Brazil, with rebound-induced earthquakes suggested. Soft-sediment deformation in microbial beds is commonly interpreted as a product of seismic activity (Kahle, 2002; Nogueira et al., 2003; Martín-Chivelet et al., 2011). However, a characteristic suite of deformation structures described in those papers (boudinages, pinch-and-swell structures, faults, kink bands, microbreccias) is missing from MM1. Note that a difference in lithology, with implications for rheology and cohesion, may also explain the restricted range of deformation structures and facies in the Rasthof Formation, compared to analogous deformed microbial mats from elsewhere.

Toward the top of MM1, laminae appear less chaotic and rise as dm high conical structures (Fig. 5D). Cones point upward and we do not interpret these structures as soft sediment deformations: rather, we interpret them as a stage of vertical microbial growth. Such a change compared to the underlying facies can be explained by overall increase in energy levels.

### 5.3. Microbial member 2 (MM2)

MM2 consists of thinly laminated microbialites (<1 mm) with local, cm scale, roll-up structures. Pruss et al. (2010) interpreted these geometries as the result of fluid escape perforating the sets of laminae. In the Rasthof Farm area, no dykes were observed below or nearby the roll-up structures; another process must be invoked at this location. Similar structures are described and interpreted in

shelfal marine, possibly sub-photic settings (Simonson and Carney, 1999), in supra- to shallow subtidal environments (Schieber et al., 2007; Harwood and Sumner, 2011), and in lacustrine settings where they are interpreted as slope-generated slump structures (Dean and Fouch, 1983). Roll-up structures are not restricted to a single depositional environment. The occasionally broken sets of laminae in the roll-up structures form cm-sized intraclasts, and thus result from a relatively high energy event, strong enough to break the laminae.

The size of the rolled-up intervals (<dm) differs from the deformations in MM1 (>dm to m scale. To explain the different deformation styles and scales between MM1 and MM2, we can invoke: 1) different rheologies; 2) different rates of lithification of the sediments; 3) influence of solid vertical stromatolites (columns, domes) on water movement in MM2; 4) lack of seismic shock during the deposition of MM2. The second point is important: in MM1 sediments might not be lithified as quickly as in MM2. As a result, thick (>10 cm) sets of laminae can be deformed in MM1. In MM2, a more rapid lithification only allowed the deformation of the first few centimetres (e.g. 1–2 cm) of the seafloor. Thicknesses of deformed sets have a direct result on the rheology and deformation style, with large folds in MM1 and much smaller roll-up structures in MM2. Thinner deformed intervals also allowed easier breaking up of the sediments in MM2 (Fig. 6A). A more rapid lithification in MM2 is also supported by the occurrence of vertical growths. Laminae were locally able to stack for tens of centimetres and form solid geometries. Water energy (current, waves, storms) and paths were influenced by these growths, possibly also influencing abrasion power of water.

MM2 exhibits microbial morphologies not hitherto described from the Rasthof Formation in north-west Namibia. Other stromatolite morphologies occur (Cloud and Semikhatov, 1969; Miller, 2008) in the Berg Aukas Formations: lateral equivalent of the Rasthof Formation in north-east Namibia. Hedberg (1979) may have observed what we describe as dome structures: reference to "a peculiar algal growth which resembles the structure found in pillow lava" is made in his description of facies variations along the northern flank of the Kamanjab Inlier. Also, void-filling thrombolites are noted by Hoffman et al. (1998) on the Northern Platform.

The domes, column and branching column geometries are interpreted as individual stromatolite forms. Analysis of MM2 clearly demonstrates the co-occurrence of individual stromatolite geometries and inter-stromatolite sediments (non-laminated coarse material, thinly laminated facies with roll-up structures). Between the depositions of MM1 and MM2, a change in environmental parameters and lithification rate may have stimulated the development of well-established stromatolite geometries. In MM2, some microbial communities were able to develop into vertical and solid-structured stromatolites. Meanwhile, microbial communities between individual growths also flourished, producing flat horizontal laminae. At least the topmost of these in the succession were poorly lithified, readily deformable and fragmented shortly after deposition (producing roll-up structures, intraclasts).

It is often suggested that local vertical development of microbial laminae is related to increasing wave energy (Wright, 1990; Flügel, 2004). However, stromatolite geometries are influenced by many parameters (Grotzinger and Knoll, 1999; Dupraz et al., 2006), and there is no unequivocal correlation between morphologies and paleodepth or paleoenvironment. Thus, whilst using analogue stromatolite geometries from the literature may be problematic, analysis of inter-microbialite sediments (grain size, bedforms) may be more revealing. At Rasthof Farm, we observe intraclasts between or next to individual stromatolite mounds (Fig. 7F). Intraclasts record syndepositional events that were sufficiently energetic to break and rework non-lithified and cohesive sediments. Interestingly, we have observed completely reworked sediments on one side and preserved laminae on the other side of a vertical same growth (Fig. 7F). This means that energy in the environment is highly influenced by the relief of the stromatolites. Laminae deposited between the vertical growths can not only be well protected from current energy, but can also be destroyed and reworked.

## 6. Depositional model

A regional view of the carbonate platform during deposition of the Rasthof Formation was proposed by Hoffman and Halverson, 2008 and is adapted in Fig. 9A. In this model, the Rasthof Farm facies belong to the Northern Platform. Sediments possibly accumulated in a large lagoon or intra-shelf basin setting, not far from the ridges separating the platform from the foreslope, located southward (Fig. 9A). Observations of in situ oolites intervals by Hedberg (1979) indicate a high energy, shallow, probably intertidal environment in quite close proximity to Rasthof Farm, north of the Kamanjab Inlier. South of the same Inlier, Hoffman and Halverson, 2008 also described oolitic blocks derived from the Northern Platform at Rasthof time. No oolites were observed at Rasthof Farm, indicating a relatively deeper, quieter environment of possible upper subtidal character. A simple proximal to distal facies model (Fig. 9B) places MM2 as the most shoreward microbialite assemblage. The observation of intraclasts around the individual growths of MM2 and break-up of the laminae within the roll-up structures suggests a relatively constant high energy setting, associated to the rise of individual geometries. The setting was probably quiescent during deposition of MM1: no individual growths developed, and sedimentation was dominated by (initially) slightly undulating microbial beds. Occasional high energy events across the platform locally stimulated the soft-sediment deformation of stromatolites. Note that we interpret MM1, MM2 and the cap dolostone to be laterally adjacent, as well as stratigraphically transitional deposits. At Rasthof Farm, MM1 is characterised by folded sets of laminae and rare cone structures toward the top, whilst MM2 exhibits a variety of individual growths as well as roll-up structures. Changing environmental controls, associated with different rheologies and faster lithification in MM2, probably led to the formation of individual microbial geometries.

Intercalated siliciclastic deposits are notably absent at every level at Rasthof Farm. Their absence may be attributable to either protection of the studied area from siliciclastic dilution, or an absence of siliciclastic input altogether. This might explain the generally rare occurrence of bedforms, even if favourable water depths might have allowed their formation during Rasthof time. In the microbial member, the microbial nature of the sediments implies trapping of carbonate grains, which inhibits the genesis of bedforms.

At Rasthof Farm, the deformation structures in MM1 do not appear to be associated with sedimentary dykes. Whilst early compaction probably played a part in determining the final geometry of soft-sediment deformation structures, we emphasise the likely role of storm wave activity and possible seismic shocks. The microbial laminae were formed on a very low angle slope, isolated from siliciclastic input, forming extensive cohesive mats.

## 7. Discussion: stromatolite patterns

Several approaches have been used to describe and understand stromatolite geometries (Bosak et al., 2013 and references therein). It is widely accepted that, stromatolites and more generally microbialites are the result of an interaction between microbial communities and external, environmental factors (e.g. sediment input, wave energy). From these interactions, microbial communities can create different patterns, with some examples from the Cryogenian (Tucker, 1977; Planavsky and Grey, 2008).

Few publications focus on the sedimentology of post-Sturtian cap carbonate sequences and stromatolite descriptions from this specific interval are rare. Considering microbial sediments as the result of an interaction between environmental and microbial controls, we suggest that the different morphologies observed at the Rasthof Farm follow a trend. The succession can be idealized, with 6 different geometries distinguished (Fig. 10). The first half of the microbial member is characterised by undulating to chaotic laminae (1). In the middle of the microbial member local solid cores are formed, creating dm high cones (2). This might imply increasing energy levels. The following forms are considered to result from this increasing energy, with concomitant intraclastic input. In MM2, a differing rheology allied to changing environmental controls allowed the development of greatly diversified geometries. Upsection, cone geometries are succeeded by
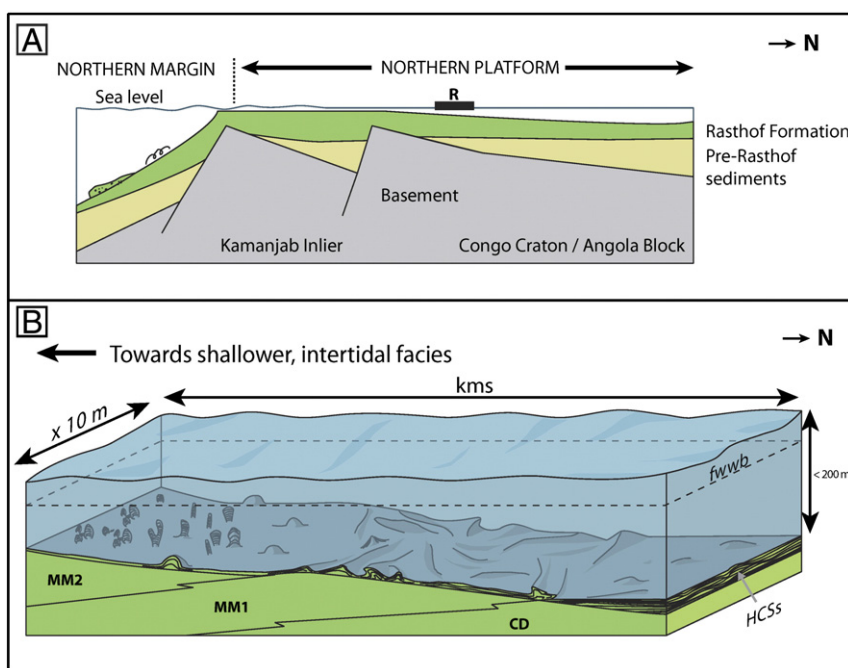


Fig. 9. Model for the Rasthof Formation, Rasthof Farm. Panel A represents a transect of the platform, "R" is the location of the Rasthof Farm. Panels B shows that the cap dolostone (CD) records the deepest facies of the Rasthof Formation (Hoffman and Halverson, 2008) but HCS indicates that it was deposited above the storm wave base. The microbial member 1 (MM1) was deposited on a very low slope and deformed by seismic shocks and/or waves. The microbial member 2 (MM2) was deposited when tectonic activity stopped and/or in a shallower setting. Increasing energy levels present in this environment led to the development of vertical growth.
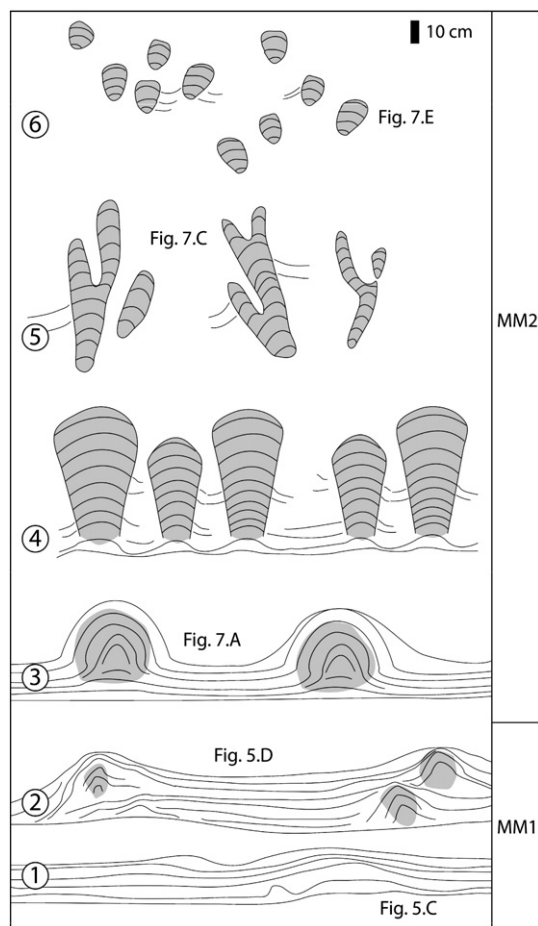
**Fig. 10.** Idealized vertical succession of stromatolite geometries observed at Rasthof Farm. The succession charts the responses of the microbial communities to a changing postglacial environment. 1. Crinkly and undulating stromatolites. 2. Crinkly and undulating stromatolites with local development of cones. 3. Domes. 4. Large columns. 5. Branching columns. 6. Extreme degree of branching.

rounded domes (3), followed by large columns (4). Inter-growth laminae tend to disappear, possibly as a result of destruction and reworking by wave processes. Nevertheless, these intergrowth laminae are preserved where they are protected in the lee of vertical growths (Fig. 7F). Throughout MM2, geometries continue to change to branching columns (5), a geometry that is developed to the extreme at the top of the succession (6).

Upsection, stromatolites become rarer to absent. We suggest that microbial communities lost their competition versus the environment. The top the Rasthof Formation is not exposed at Rasthof Farm but Hoffman and Halverson, 2008 note that, to a regional scale, the top of the formation is characterised by shallow water facies and local subaerial exposure on the Northern Platform. This is consistent with the trend observed in the microbial member at Rasthof Farm. Increasing energy in the environment led to the arrival of high energy, very shallow water facies. Microbial communities were overtaken by these facies.

## 8. Conclusions

- The cap dolostone and microbial member of Rasthof Formation were collectively interpreted to record sub-storm wave base deposition by previous authors (Tojo et al., 2007; Pruss et al., 2010). At Rasthof Farm, a shallower setting is recognised from a new dataset;
- The Rasthof Farm succession commences with a non microbially-influenced, cap dolostone unit, comprising laminites punctuated by hummocky cross stratification (HCS) intervals at the top. Formation

of HCS indicates that grains were not cohesive during the deposition of the cap dolostone. HCS records storm wave agitation of the carbonate platform;
- A locally sharp contact marks the juncture between the cap dolostone and overlying microbialites. The microbial laminae of MM1 were modified by a possible association of storm wave agitation and seismic shocks. Above, well differentiated stromatolite (columns and domes morphologies) of MM2 may record deposition in a shallower high energy setting;
- Facies models for Cryogenian carbonate platforms, and in particular those on which the post-Sturtian cap carbonates were deposited, are comparatively few. By proposing a simple depositional model for the facies from the Rasthof Farm, a trend in the organisation of microbial communities can be highlighted. This has major implications for understanding the recovery patterns of microbial communities in the aftermath of the Sturtian snowball Earth event, and possibly in other stromatolitic outcrops.

## References

Allen, P.A., Etienne, J.L., 2008. Sedimentary challenge to Snowball Earth. Nature Geoscience 1, 817–825.

Bosak, T., Lahr, D.J.G., Pruss, S.B., MacDonald, F.A., Dalton, L., Matys, E.D., 2011. Agglutinated tests in post-Sturtian cap carbonates of Namibia and Mongolia. Earth and Planetary Science Letters 308, 28–40.

Bosak, T., Lahr, J.G., Pruss, S.B., MacDonald, F.A., Gooday, A.J., Dalton, L., Matys, E.D., 2012. Possible early foraminiferans in post-Sturtian (713–636 Ma) cap carbonates. Geology 40, 67–70.

Bosak, T., Knoll, A.H., Petroff, A.P., 2013. The meaning of stromatolites. Annual Review of Earth and Planetary Sciences 41, 3.1–3.24.

Cheel, R.J., Leckie, D.A., 1993. Hummocky cross-stratification. In: Wright, V.P. (Ed.), Sedimentary Review. Wiley Blackwell, London, pp. 103–122.

Cloud, P.E., Semikhatov, M.A., 1969. Proterozoic stromatolite zonation. American Journal of Science 267, 1017–1061.

Corkeron, M., 2007. 'Cap carbonates' and Neoproterozoic glacigenic successions from the Kimberley region, north-west Australia. Sedimentology 54, 871–903.

Corsetti, F.A., Grotzinger, J.P., 2005. Origin and Significance of tube structures in Neoproterozoic post-glacial cap carbonates. Example from noonday dolomite, Death Valley, United States. Palaios 20, 348–362.

Dalton, L.A., Bosak, T., Macdonald, F.A., Lahr, D.J.G., Pruss, S.B., 2013. Preservational and morphological variability of assemblages of agglutinated eukaryotes in Cryogenian cap carbonates of northern Namibia. Palaios 28, 67–79.

Dean, W.E., Fouch, T.D., 1983. Lacustrine environment. In: Scholle, P.A., Bedout, D.G., Moore, C.H. (Eds.), Carbonate Depositional Environments: AAPG Memoir, 33, pp. 97–130.

Delgado, F., 1977. Primary textures in dolostones and recrystallized limestones: a technique for their microscopic study. Journal of Sedimentary Petrology 47, 1339–1341.

Dumas, S., Arnott, R.W.C., 2006. Origin of hummocky and swaley cross-stratification-The controlling influence of unidirectional current strength and aggradation rate. Geology 34, 1073–1076.

Dupraz, C., Pattisina, R., Verrecchia, E.P., 2006. Translation of energy into morphology: simulation of stromatolites morphospace using a stochastic model. Sedimentary Geology 185, 185–203.

Eyles, N., 2008. Glacio-epochs and the supercontinent cycle after 3.0 Ga: tectonic boundary conditions for glaciation. Palaeogeography, Palaeoclimatology, Palaeoecology 258, 89–129.

Eyles, N., Januszczak, N., 2004. 'Zipper-rift': a tectonic model for Neoproterozoic glaciations during the breakup of Rodinia after 750 Ma. Earth-Science Reviews 65, 1–73.

Eyles, N., Januszczak, N., 2007. Syntectonic subaqueous mass flows of the Neoproterozoic Otavi Group, Namibia: where is the evidence of global glaciation? Basin Research 19, 179–198.

Fairchild, I.J., Kennedy, M.J., 2007. Neoproterozoic glaciation in the Earth System. Journal of the Geological Society of London 164, 895–921.

Flügel, E., 2004. Microfacies of Carbonate Rocks: Analysis, Interpretation and Application. Springer (976 pp.).

Frimmel, H.E., Basei, M.S., Gaucher, C., 2011. Neoproterozoic geodynamic evolution of SW-Gondwana: a southern African perspective. International Journal of Earth Sciences 100, 323–354.

Grotzinger, J.P., Knoll, A.H., 1999. Stromatolites in Precambrian: evolutionary mileposts or environmental dipsticks? Annual Review of Earth and Planetary Science 27, 313–358.

Halverson, G.P., Hoffman, P.F., Schrag, D.P., Maloof, A.C., Rice, A.H.N., 2005. Toward a Neoproterozoic composite carbon-isotope record. GSA Bulletin 117, 1181–1207.

Harwood, C.L., Sumner, D.Y., 2011. Microbialites of the Neoproterozoic Beck Spring Dolomite, Southern California. Sedimentology 58, 1648–1673.

Hedberg, R.M., 1979. Stratigraphy of the Ovamboland Basin South West Africa. Chamber of Mines Precambrian Research Unit. : Bulletin, 24 (325 pp.).

Hoffmann, K.H., Prave, A.R., 1996. A preliminary note on a revised subdivision and regional correlation of the Otavi Group based on glaciogenic diamictites and associated cap dolostones. Communications of the Geological Survey of Namibia 11, 77–82.

Hoffman, P.F., Halverson, G.P., 2008. Otavi Group of the western Northern Platform, the Eastern Kaoko Zone and the western Northern Margin Zone. In: Miller, R.McG. (Ed.), The Geology of Namibia, 2, pp. 13.69–13.134.

Hoffman, P.F., Macdonald, F.A., 2010. Sheet-crack cements and early regression in Marinoan (635 Ma) cap dolostones: regional benchmarks of vanishing ice-sheets? Earth and Planetary Science Letters 300, 374–384.

Hoffman, P.F., Schrag, D.P., 2002. The snowball Earth hypothesis: testing the limits of global change. Terra Nova 14, 129–155.

Hoffman, P.F., Kaufman, A.J., Halverson, G.P., 1998. Comings and goings of global glaciations on the Neoproterozoic tropical platform in Namibia. GSA Today 8, 1–9.

Hoffman, P.F., Halverson, G.P., Domack, E.W., Husson, J.M., Higgins, J.A., Schrag, D.P., 2007. Are basal Ediacaran (635 Ma) post-glacial "cap dolostones" diachronous? Earth and Planetary Science Letters 258, 114–131.

Kahle, C.F., 2002. Seismogenic deformation structures in microbialites and mudstones, Silurian Lockport Dolomite, northwestern Ohio. U.S.A. Journal of Sedimentary Research 72, 201–216.

Kennedy, M.J., Christie-Blick, N., 2011. Condensation origin for Neoproterozoic cap carbonates during deglaciation. Geology 37, 319–322.

Le Heron, D.P., 2012. The Cryogenian record of glaciation and deglaciation in South Australia. Sedimentary Geology 243–244, 57–69.

Le Heron, D.P., Cox, G.M., Trundley, A.E., Collins, A., 2011. Sea-ice free conditions during the early Cryogenian (Sturt) glaciation, South Australia. Geology 39, 31–34.

Le Heron, D.P., Busfield, M.E., Kamona, F., 2013. An interglacial on snowball Earth? Dynamic ice behaviour revealed in the Chuos Formation, Namibia. Sedimentology 60, 411–427.

Loyd, S.J., Corsetti, F.A., 2010. The origin of the millimetre scale lamination in the Neoproterozoic Lower Beck Spring Dolomite: implication for widespread, fine-scale, layer-parallel diagenesis in Precambrian carbonates. Journal of Sedimentary Research 80, 678–687.

Martín-Chivelet, J., Palma, R.M., López-Gómez, J., Kietzmann, D.A., 2011. Earthquake-induced soft-sediment deformation structures in Upper Jurassic open-marine microbialites (Neuquén Basin, Argentina). Sedimentary Geology 235, 210–221.

Miller, R.McG., 2008. The geology of Namibia. Neoproterozoic to Lower Palaeozoic, volume 2. Ministry of mines and energy, Windhoek, Namibia.

Mulder, T., Razin, P., Faugeres, J.C., 2009. Hummocky cross-stratification-like structures in deep-sea turbidites: Upper Cretaceous Basque basins (Western Pyrenees, France). Sedimentology 56, 997–1015.

Nogueira, A.C.R., Riccomini, C., Sial, A.N., Moura, C.A.V., Fairchild, T.R., 2003. Soft-sediment deformation at the base of the Neoproterozoic Puga cap carbonate (southwestern Amazon craton, Brazil): Confirmation of rapid icehouse to greenhouse transition in snowball Earth. Geology 31, 613–616.

Owen, G., Moretti, M., Alfaro, P., 2011. Recognising triggers for soft-sediments deformations: current understanding and future directions. Sedimentary Geology 235, 133–140.

Planavsky, N., Grey, K., 2008. Stromatolite branching in the Neoproterozoic of the Centralian Superbasin, Australia: an investigation into sedimentary microbial control of stromatolite morphology. Geobiology 6, 33–45.

Pruss, S.B., Bosak, T., Macdonald, F.A., Mclane, M., Hoffman, P.F., 2010. Microbial facies in a Sturtian cap carbonate, the Rasthof Formation, Otavi Group, northern Namibia. Precambrian Research 181, 187–198.

Riding, R., 2011. The nature of stromatolites: 3,500 million years of history and a century of research. In: Reitner, J., Queric, N.V., Arp, G. (Eds.), Advances in Stromatolite Geobiology: Lecture Notes in Earth Sciences, 131, pp. 29–74.

Rose, C.V., Maloof, A.C., 2010. Testing models for post-glacial 'cap dolostone' deposition: Nuccaleena Formation, South Australia. Earth and Planetary Science Letters 296, 165–180.

Schieber, J., Bose, P.K., Eriksson, P.G., Banerjee, S., Sarkar, S., Altermann, W., Catuneanu, O., 2007. Atlas of Microbial Mat Features Preserved Within the Clastic Record. Elsevier (288 pp.).

Shield, G.A., 2005. Neoproterozoic cap carbonates: a critical appraisal of existing models and the plumeworld hypothesis. Terra Nova 17, 299–310.

Simonson, B., Carney, K.E., 1999. Roll-up structures: evidence of in situ microbial mats in Late Archean Deep Shelf environments. Palaios 14, 13–24.

Tojo, B., Katsuta, N., Takano, M., Kawakami, S., Ohno, T., 2007. Calcite–dolomite cycles in the Neoproterozoic Cap carbonates, Otavi Group, Namibia. Geological Society, London, Special Publication 286, 103–113.

Tucker, M.E., 1977. Stromatolite biostromes and associated facies in the late Precambrian Porsanger Dolomite Formation of Finnmark, Arctic Norway. Palaeogeography, Palaeoclimatology, Palaeoecology 21, 55–83.

Wright, P., 1990. Carbonate depositional systems I: marine shallow-water and lacustrine carbonates. In: Tucker, M.E., Wright, V.P., Dickson, J.A.D. (Eds.), Carbonate Sedimentology, pp. 137–163.

Yoshioka, H., Asahara, Y., Tojo, B., Kawakami, S., 2003. Systematic variations in C, O, and Sr isotopes and elemental concentrations in Neoproterozoic carbonates in Namibia: implications for a glacial to interglacial transition. Precambrian Research 124, 69–85.

**APPENDIX B**

MM2  MM1

25  20  15  10  5  1

20 units
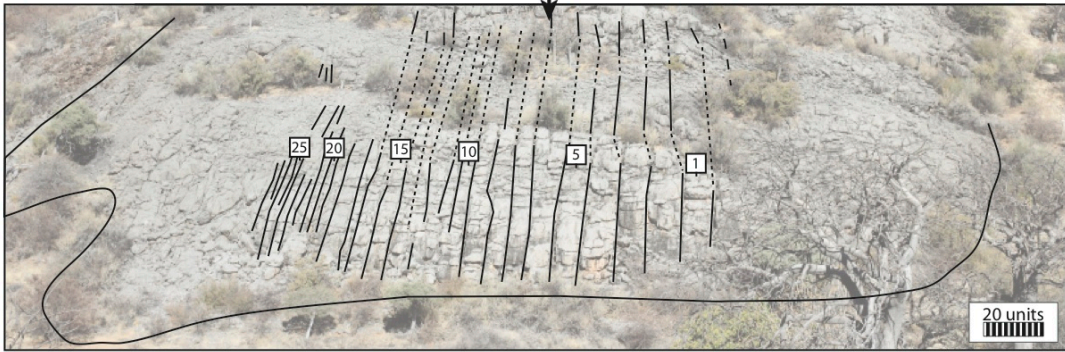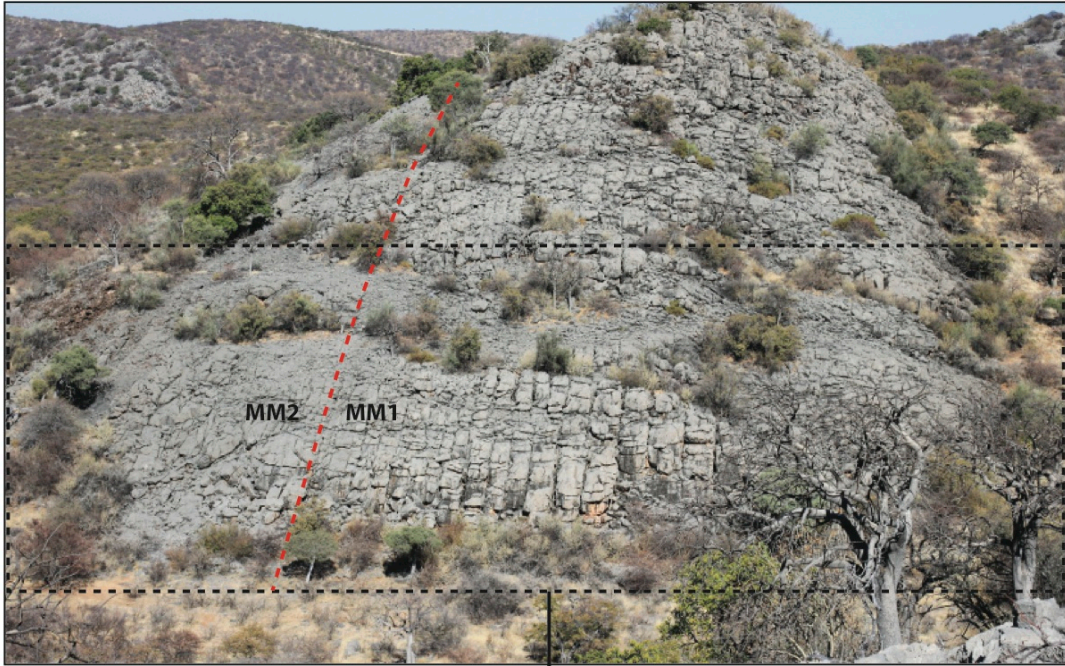
| i (bed #) | hi | R(hi) | i-R(hi) | (i-Rhi))^2 |
|---|---|---|---|---|
| 1 | 10 | 26 | -25 | 625 |
| 2 | 12 | 28 | -26 | 676 |
| 3 | 9 | 23 | -20 | 400 |
| 4 | 11.5 | 27 | -23 | 529 |
| 5 | 9.5 | 24.5 | -19.5 | 380.25 |
| 6 | 9.5 | 24.5 | -18.5 | 342.25 |
| 7 | 6.5 | 19.5 | -12.5 | 156.25 |
| 8 | 7 | 21 | -13 | 169 |
| 9 | 7.5 | 22 | -13 | 169 |
| 10 | 4 | 14 | -4 | 16 |
| 11 | 4 | 14 | -3 | 9 |
| 12 | 6.5 | 19.5 | -7.5 | 56.25 |
| 13 | 3.5 | 11.5 | 1.5 | 2.25 |
| 14 | 4 | 14 | 0 | 0 |
| 15 | 6 | 18 | -3 | 9 |
| 16 | 5.5 | 16.5 | -0.5 | 0.25 |
| 17 | 3 | 10 | 7 | 49 |
| 18 | 5.5 | 16.5 | 1.5 | 2.25 |
| 19 | 3.5 | 11.5 | 7.5 | 56.25 |
| 20 | 2.5 | 8.5 | 11.5 | 132.25 |
| 21 | 2 | 6.5 | 14.5 | 210.25 |
| 22 | 1.5 | 5 | 17 | 289 |
| 23 | 2.5 | 8.5 | 14.5 | 210.25 |
| 24 | 2 | 6.5 | 17.5 | 306.25 |
| 25 | 1 | 2.5 | 22.5 | 506.25 |
| 26 | 1 | 2.5 | 23.5 | 552.25 |
| 27 | 1 | 2.5 | 24.5 | 600.25 |
| 28 | 1 | 2.5 | 25.5 | 650.25 |

| | sum |
|---|---|
| n^2= 784 | 7104 |

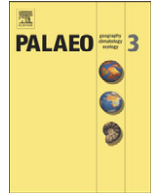| r'= | -0.944 |
|---|---|

For n=28 and $\alpha$= 0.05, the theorical R=0.33.

At Rasthof Farm, $|r'|$ > R, $H_0$ is rejected, beds are becoming thinner.

**APPENDIX C**

# Neoproterozoic ironstones in northern Namibia: Biogenic precipitation and Cryogenian glaciation

D.P. Le Heron [a,*], M.E. Busfield [a], E. Le Ber [a], A.F. Kamona [b]

[a] Department of Earth Sciences, Queen's Building, Royal Holloway University of London, Egham, Surrey, TW20 0BY, UK
[b] Geology Department, University of Namibia, Windhoek, Namibia

## ABSTRACT

The precipitation of Cryogenian ironstones has been attributed to a spectrum of mechanisms ranging from virtually instantaneous "rusting of the seas" in response to post-snowball Earth ice meltback, to localised hydrothermal activity during fragmentation of Rodinia. The former model presupposes that ironstone deposition took place following peak glaciation. In the Chuos Formation of the Otavi Mountain Land, northern Namibia, ironstone facies precede, and are vertically gradational into, diamictites. Evidence for glaciation in the diamictites includes 1) dropstone textures, 2) subglacially deformed and attenuated, thinly stratified diamictites, supported by 3) the co-occurrence of soft-sediment striations. The underlying ironstones contain evidence for tractional processes (large-scale cross bedding) and biogenic growth (stromatolites) in strata rich in magnetite and hematite. Using the analogy of acidophile biomats in modern acid mine drainage environments, where photosynthetic bacteria construct stromatolites, fixing $CO_2$ and Fe intracellularly, it is suggested that Cryogenian acidophile biomats did likewise, triggering ironstone precipitation and local $CO_2$ drawdown, thereby facilitating concomitant glaciation.

© 2012 Elsevier B.V. All rights reserved.

## 1. Introduction

Yeo (1981) first proposed that Neoproterozoic ironstones resulted from hydrothermal activity in small, Red Sea-type rift basins, during the breakup of Rodinia. Conversely, their unusual recurrence in the Cryogenian, following a 1.1 billion year stratigraphic hiatus, led many studies to invoke a direct association with concomitant snowball-type global glaciations (Hoffman and Schrag, 2002). Martin (1965) proposed that Namibian ironstones in the Chuos Formation were deposited due to stagnation under an ice cover. In a global context, this concept was expanded by Kirschvink (1992) who suggested that toward the end of snowball event, where weathering and oxidation of the oceans was inhibited under a carapace of global ice cover, "rusting of the seas" led to deposition of a ferruginous blanket of marine sediment. This hypothesis, however, inadequately accounts for the intra-glacial stratigraphic occurrence of ironstones, particularly in older Cryogenian glacial successions (e.g. Eyles and Januszcak, 2004; Eyles, 2008; Le Heron et al., 2011).

In their recent review of Neoproterozoic chemical sediments, Hoffman et al. (2011) identified three alternative mechanisms of ironstone precipitation under a snowball Earth pretext: 1) ferrous versus euxinic anoxia under a cover of sea ice, 2) subglacial, sulphate-rich ferrous waters, and 3) localization of oxidative titration. This latter mechanism follows from Hoffman and Halverson (2008) who envisaged oxic meltwater plumes, discharged into ferrous basin waters at ice-shelf grounding-lines. These mechanisms require ocean anoxia induced by overlying ice, and do not consider the possibility of non-glacially-induced anoxia, nor fault-related fluids as a source of soluble iron.

Namibia (Fig. 1a) is an excellent natural laboratory in which to test hypotheses of Cryogenian ironstone deposition. The Chuos Formation is a diamictite-rich sedimentary unit of Cryogenian age associated with iron formations whose correlatives are widely distributed across Namibia. The objectives of the present paper are twofold: 1), to present sedimentological evidence for biologically mediated ironstone precipitation in the Chuos Formation and 2) to demonstrate that this ironstone precipitation preceded deposition of observed glaciogenic deposits, based on field observations. Konhauser et al. (2002) argued that chemolithotrophs or photoferrotrophs (bacteria) had the potential to generate most, if not all the ferric iron in Archaean banded iron formations. Those authors did not infer an intracellular iron fixing mechanism, and bacterial precipitation of iron is rarely entertained as a depositional mechanism in younger (Neoproterozoic) strata. Additionally, the implications of this evidence for Cryogenian glacial cycles are discussed, suggesting that in the Chuos, at least, ironstone deposition heralded ice sheet growth.

## 2. Study area and stratigraphy

The Otavi Mountain Land, in northern Namibia, is an area of extensive outcrop of Neoproterozoic strata at the southern margin of the Owambo Basin (Fig. 1b). The strata comprise two laterally extensive glacial successions, belonging to the Chuos Formation (older Cryogenian) and Ghaub Formation (younger Cryogenian) (Hoffmann

---
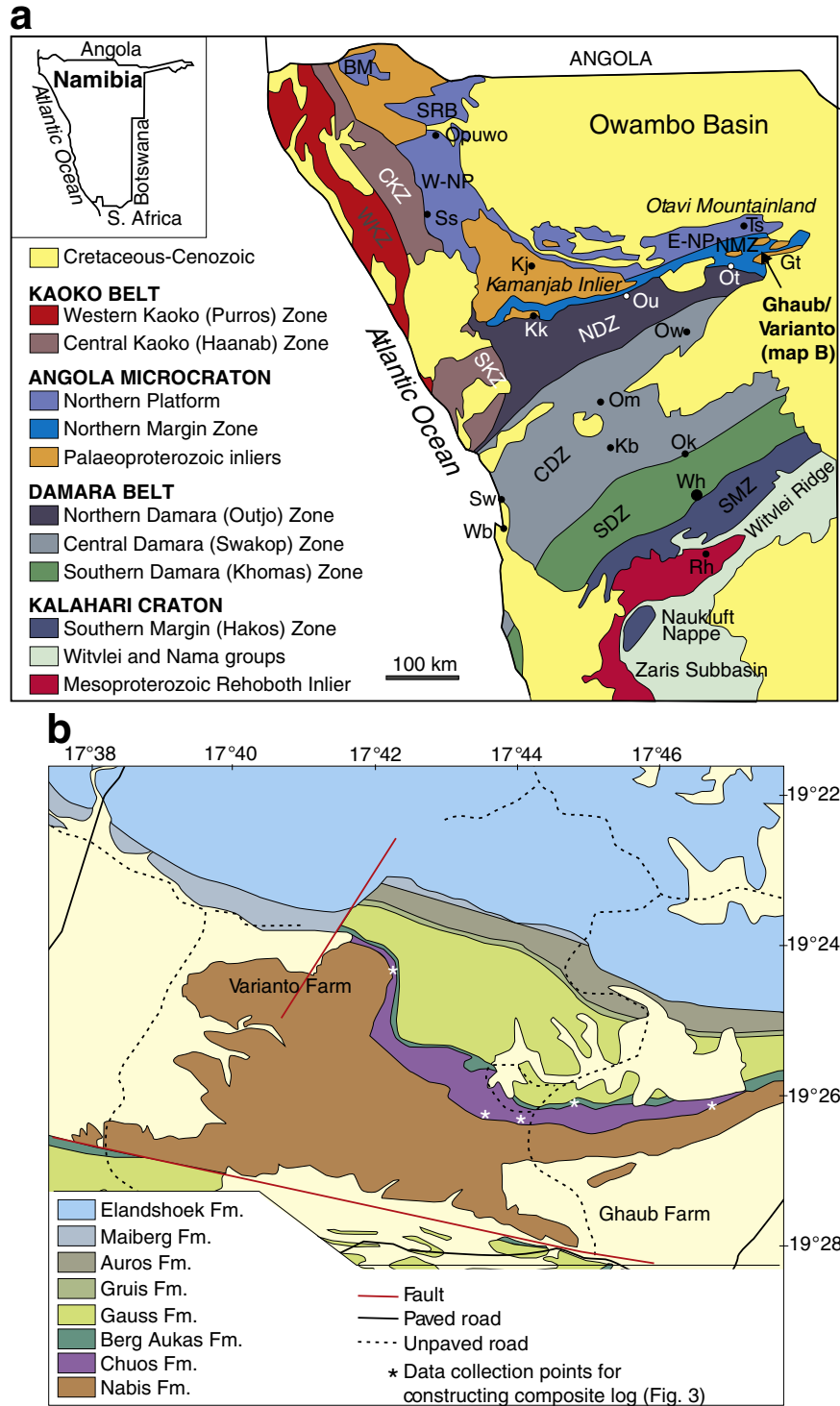
Fig 1. a: Geotectonic map of Namibia showing the location of the Otavi Mountain Land belt at the southern flank of the Owambo Basin (after Hoffman and Halverson, 2008). b: Location of the Ghaub and Varianto farms in the Otavi Mountain Land in northern Namibia. Note the location of observations used to compile the composite section in this small region (Fig. 3). Geological base map after Geological Survey of Namibia (2008).

and Prave, 1996) (Fig. 2). The Ghaub Formation has been subject to extensive scrutiny with a spectrum of arguments as to its genesis through purely gravitational instability (Eyles and Januszczak, 2007), and as to its glaciogenic signature (e.g. Bechstadt et al., 2009; Domack and Hoffman, 2011). The Chuos Formation, meanwhile, has been neglected by comparison to younger mineral rich carbonate strata above (e.g. Kamona and Günzel, 2007). Earlier analyses of the Chuos Formation concentrated on meta-sediments in the vicinity of its type

section south of Windhoek and in the Damara Belt (Gevers, 1931; de Kock and Gevers, 1933; Martin et al., 1985; Henry et al., 1986; Badenhorst, 1988). More modern stratigraphic analyses several hundred kilometres to the west of the Otavi Mountain Land demonstrate that the Chuos Formation is cradled in a rift-related, fault bounded palaeotopography (Hoffman and Halverson, 2008), and hence its substrate also changes along strike, across the southern flank of the Owambo Basin. In the area of Ghaub and Varianto farms, the study
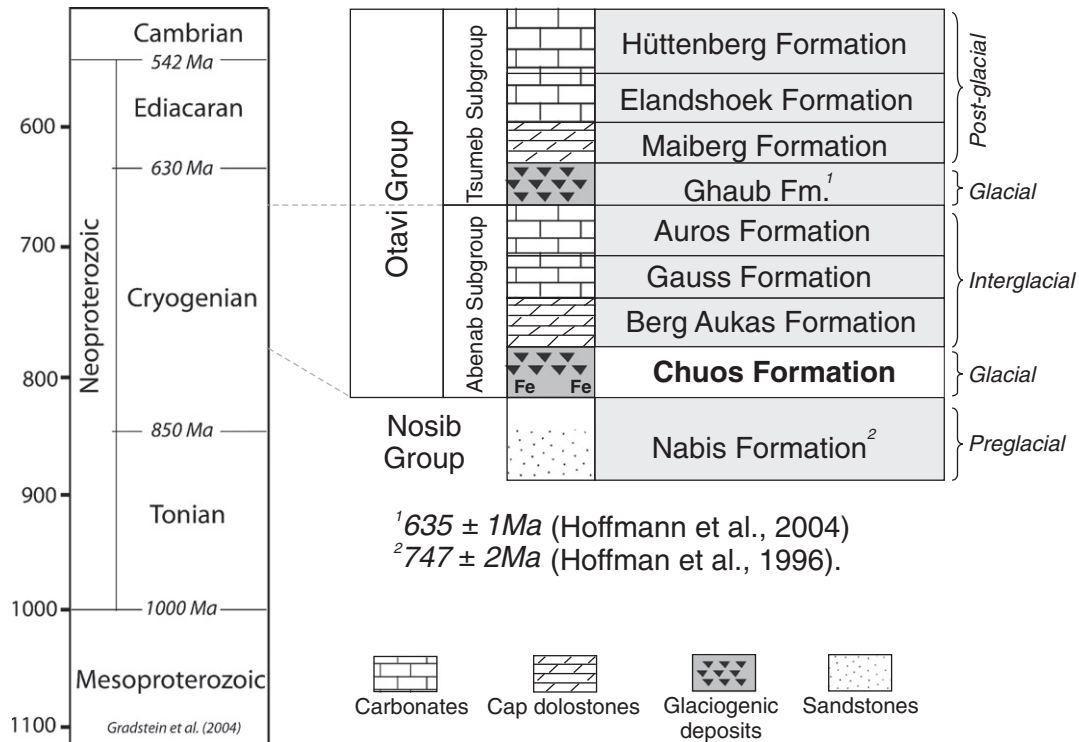
**Fig. 2.** Stratigraphy on the Cryogenian succession exposed in the Ghaub and Varianto farm areas of the Otavi Mountain Land. Stratigraphic hierarchy and formation names after Hoffmann and Prave (1996). U–Pb ages from the Askevold Formation (Hoffman et al., 1996) are from further west: this formation is not preserved beneath the Chuos Formation in the present study area.

interval comprises the Nabis Sandstone Formation of the Nosib Group, overlain by the Chuos Formation and succeeded by the Berg Aukas Formation (Fig. 2). This particular area has been mapped at the 1:250,000 scale (Geological Survey of Namibia, 2008). Age constraints include 747 ± 2 Ma from the Naauwport volcanics, locally beneath the Chuos Formation (Hoffman et al., 1996) and 635 ± 1 Ma from ash beds in the younger Ghaub Formation (Hoffmann et al., 2004). Owing A composite stratigraphy, assembled from observations from closely spaced localities over 12 field days (Fig. 1B), is included in this paper (Fig. 3) as the basis for our descriptions and interpretations.

## 3. Description of strata

The Chuos Formation rests on a ~1 km thick succession of conglomerates and sandstones of the Nabis Formation which crops out as part of the E–W striking Nosib Anticline (Fig. 1). Thickly bedded clast- and matrix-supported conglomerates bear rounded clasts of meta-sedimentary quartzite, vein quartz, red-weathering quartz-porphyry, brown-weathering metavolcanics with quartz amygdales, and dark grey-weathering quartz-feldspar agglomerate: these conglomerates fine up to parallel-laminated sandstones.

An angular unconformity can be demonstrated between the Nabis and Chuos formations, expressed as differences in dip of beds above and below the contact (Fig. 3). In the Ghaub and Varianto farm areas, the Chuos Formation is divisible into 1) an ironstone member at the base and 2) a diamictite member above (Fig. 3). Ferruginous phases in the ironstone include (1) isolated magnetite crystals, (2) magnetite crystal clusters, (3) magnetite stringers along cross-bed foresets and (4) botryoidal hematite (Fig. 4).

Ironstone facies include cross-bedded, coarse-grained sandstones, texturally comparable to the uppermost Nabis sandstones, intercalated with bedding-orthogonal dome structures of 5–10 cm amplitude (Fig. 5a–d) spaced up to 1 m apart. The dome structures often contain crinkly laminae which at the flanks dip at 75° with respect to underlying

and overlying bed boundaries (Fig. 3: 8 m, 16–18 m, 22–24 m, and 29–31 m). Internally, the dome structures are composed of sand- to granule-grade laminae intercalated with hematite-rich microcrystalline laminae (Fig. 5e–f). Intercalation of these lithologies occurs on a millimetre scale. Thickening of the sand- to granule-grade laminae into interdome areas is demonstrable; these truncate underlying laminations at the dome flanks (Fig. 5f). Between the domes, the intercalation is also preserved in bedding parallel, crinkly centimetric bands (Fig. 3: 4–7 m). These are compositionally identical to the laminations in the domes, and are incorporated as clasts in the overlying diamictite member (Fig. 6a). In our study area, Hedberg (1979) observed "ferruginous concretions and Liesegang rings … in the lower part of the unit" (p. 55). These are restricted to the ironstone member, forming triangular-shaped nodules (Fig. 6b) as well as globule-shaped concretions (Fig. 6c). The Liesegang laminae can be demonstrated to crosscut both the dome structures and the inter-dome crinkly laminae. They can be clearly distinguished from sedimentary laminations as no grain size changes are apparent between the rings.

The contact with the overlying diamictite member is highly gradational and concordant (Fig. 3, 34 m). The diamictites, which retain magnetite content throughout, are often poorly bedded, but locally well stratified (Fig. 3). Clasts are randomly oriented, and occur in several population sets. The first, in the <5 cm diameter range, comprises sub-rounded to angular meta-sandstone clasts. The second, in a 5–25 cm diameter category, comprises very well rounded meta-sandstones and quartzites, identical to those in the Nabis Formation. A third population of clasts is restricted to the topmost beds of the diamictite, where a zone of comparatively more exotic clasts occurs. These include granite gneiss, mica schist, hornblende schist, mudstone and andesite. Finally, scattered clasts of ironstone are scattered throughout (Fig. 6a).

Near the top of the Chuos Formation (Fig. 3), well stratified diamictites are common (Fig. 6d). Clast-rich and clast-poor domains are intercalated on the centimetre-scale (Fig. 3). Clasts show evidence

for attenuation parallel to stratification; some are fractured and intruded by the diamictite matrix (Fig. 6e). Asymmetric folds, and pervasive lineations trending 162°, deform the deposit. These decimetre to metre-thick intensively sheared intervals intercalate with relatively undeformed diamictite (Fig. 3: 46 m, 48 m, and 52 m) that contains large lonestones with unequivocal impact structures beneath them (Fig. 6f). Soft-sediment striated surfaces, implying transmission of shear in unconsolidated sediments akin to a sliding deck of cards (Sutcliffe et al., 2000; Le Heron et al., 2005) also occur at intervals (Fig. 3, 48 m; Fig. 6g).

## 4. Interpretation of strata

The Nabis Formation is interpreted as an alluvial fanglomerate succession (Miller, 2008). The angular unconformity between the Nabis and Chuos formations can be seen in the wider context of regional-scale studies in northern Namibia thought to reflect progressive downcutting beneath the latter formation in a rift-related scenario (Eyles and Januszczak, 2007). Elsewhere in northern Namibia, in the Khowarib Fold Belt, a stratigraphic unit known as the Ombombo Subgroup is sandwiched between the Nabis and the Chuos formations (Hoffman and Halverson, 2008). This may suggest either non-deposition of the Ombombo Subgroup in the Ghaub/Varianto farm areas, or deeper erosion beneath the Chuos Formation in this area.

In the basal ironstone member, the cross-beds are interpreted to record the migration of clastic bar systems building out both to the north and to the south. Evidence for classic tidal indicators (e.g. de Vries Klein, 1970) are absent, and bidirectionality may point to subtle switching in gradient, e.g. in response to rift-related slope changes. Whilst the occurrence of magnetite crystals along cross-bed foresets might imply that the crystals were reworked before the succession was lithified, a post-diagenetic origin cannot be discounted.

The dome structures with crinkly laminae are interpreted as stromatolites. In this interpretation, stromatolites are considered "macroscopically layered authigenic microbial sediments with or without abiogenic precipitates" (Riding, 2011, p. 31). Whilst a conservative view is that the biogenic role in the development of stromatolites can only be demonstrated with fossil examples of the dome-building microbes (Buick et al., 1981), emphasis is normally placed on interpretation of the overall stromatolite morphology to infer a microbial control on dome construction (e.g. Awramik et al., 2005). The high dip angle at the dome flanks (>75°) with respect to the bed bases is beyond the angle of repose expected in mechanically or chemically deposited sediments (Hofmann et al., 1999). The dome structures bear no resemblance to soft-sediment deformation structures in other iron formations where delicate flame structures are common in underflow deposits (e.g. Le Heron et al., 2011), or convolute beds/liquefaction structures formed in subglacial settings (Le Heron et al., 2005). However, the high dip angle at the flanks of the dome structures can be explained by the deposition of a sticky, microbially-deposited precipitate to bind the intercalated sand- to granule-sized laminae at a steep angle. In this context, the sand to granule-grade laminae at the dome flanks, and bound in crinkly laminae in the inter-dome areas, is interpreted as mechanically deposited, abiotic sediment (Hofmann et al., 1999). This interpretation accounts for both lateral pinch-out of such laminae against dome flanks and thickening into the inter-dome areas (Fig. 5e, f), because abiotic laminae would be expected to accumulate in local depocentres. Local scour by weak currents in the inter-dome areas explains truncation of the hematite laminations (Fig. 5e, f).
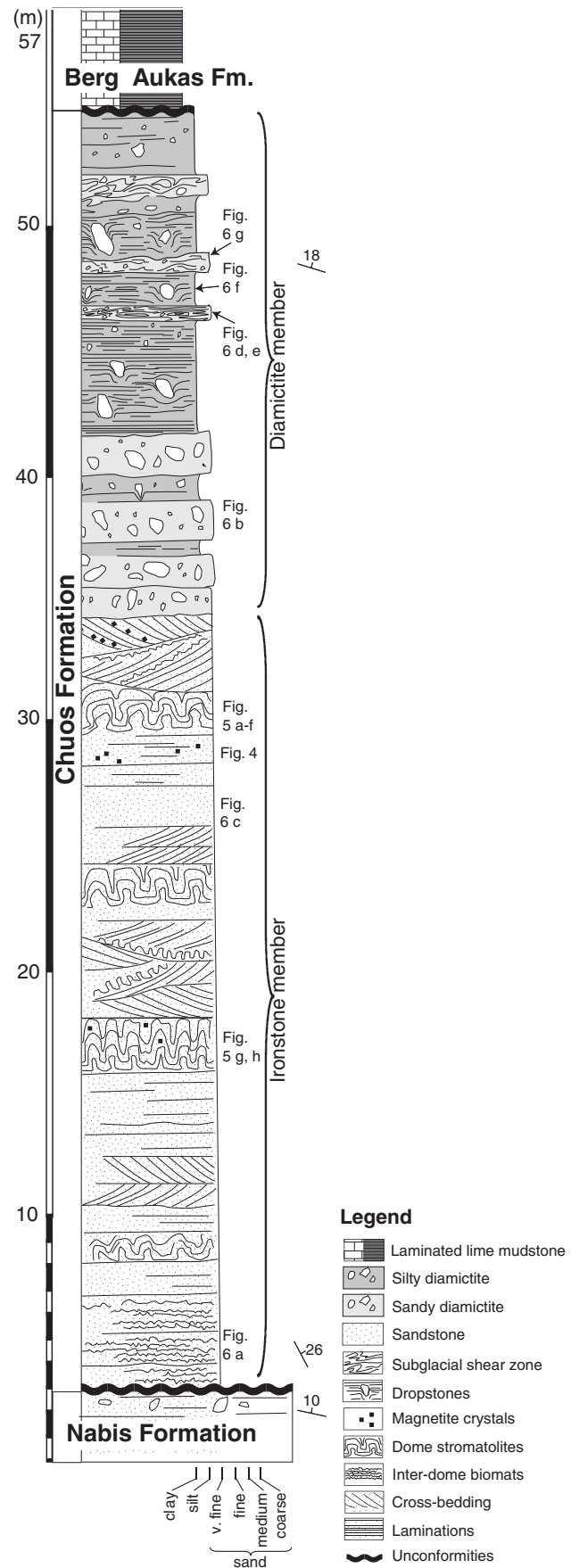


Fig. 3. Composite section of the Chuos Formation cropping out in Ghaub and Varianto farms. Note the angular unconformity with the underlying Nabis Formation and the concordant contact with the Berg Aukas Formation above, together with the informal subdivision of the Chuos Formation into ironstone and diamictite members. The location of photographs and accompanying illustrations in Figs. 4–7 is shown next to the log.
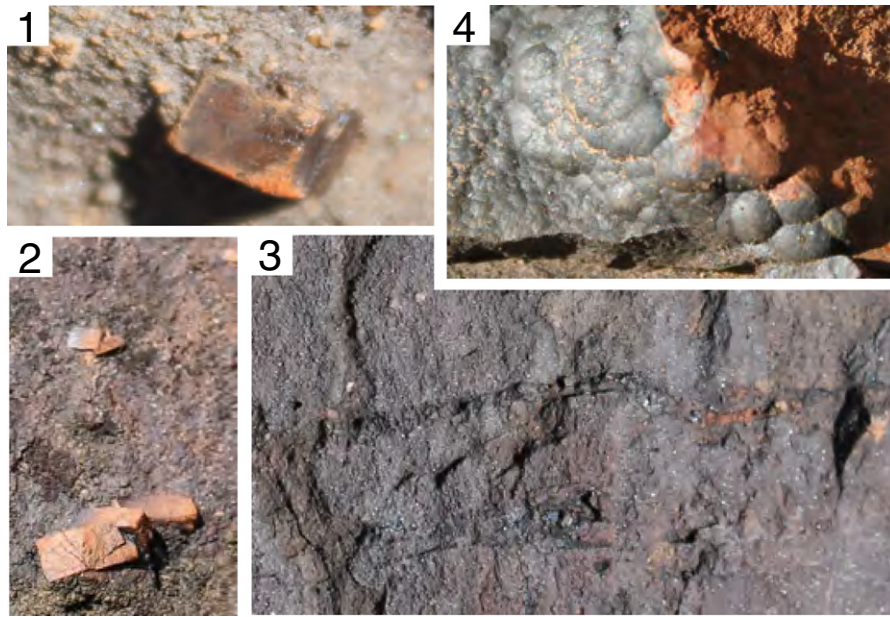
**Fig. 4.** Ferruginous phases in the lower informal member of the Chuos Formation: 1, isolated magnetite crystals (field of view 1 cm across); 2, magnetite crystal clusters (field of view 0.5 cm across); 3, magnetite stringers along bedding planes (field of view 5 cm across); 4, botryoidal hematite (field of view 2 cm across).

On the basis of the above, given their ferruginous composition, the stromatolites are interpreted as acidophile microbialites, locally reworked by current activity. Acidic conditions play a key role in the activity of iron-fixing bacteria (Brake et al., 2002). These organisms harness energy through oxidation of dissolved Fe (II), which remains stable under low-$O_2$ and low pH conditions (Konhauser et al., 2005, 2011; Bekker et al., 2010). Bacteria therefore adapt either to water column anoxia (microaerophiles) or more acidic conditions (acidophiles), analogous to the pH values of ~2 surrounding modern acid mine drainage (España et al., 2007). The acidophile tendencies of these framework-building organisms stand in contrast to the cynanobacterial stromatolites' characteristic of many Neoproterozoic strata (Tewari and Seckbach, 2011), yet they fix $CO_2$ through photosynthesis (Brake et al., 2002). Whilst magnetite can develop during diagenesis or epigenetically (McCabe et al., 1983), it is also possible that this phase may also represent biogenic sedimentation by analogy to magnetotactic stromatolites both modern and ancient elsewhere (Chang et al., 1989; Stolz et al., 1989): this interpretation is tentative because it is noted that crystal forms in those examples are usually microscopic. Regardless, an abiotic diffusional origin of the hematite Liesegang rings must be assumed, thus implying some limited epigenetic dissolution and re-precipitation of iron oxide phases. Based on the above, it is highlighted that stromatolites in the Chuos Formation were probably constructed by a different type of microbial community to the much more common carbonate stromatolites (Tewari and Seckbach, 2011).
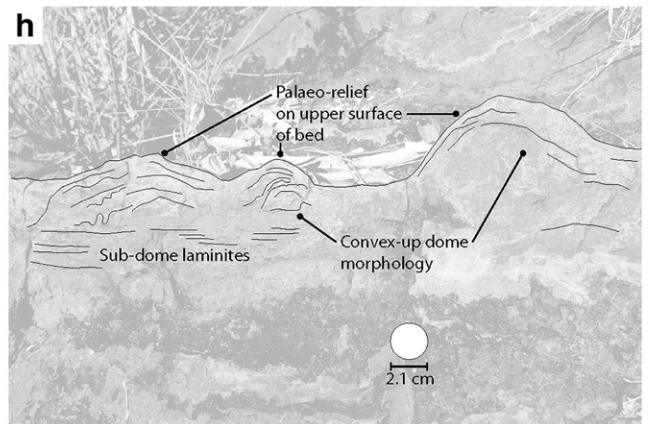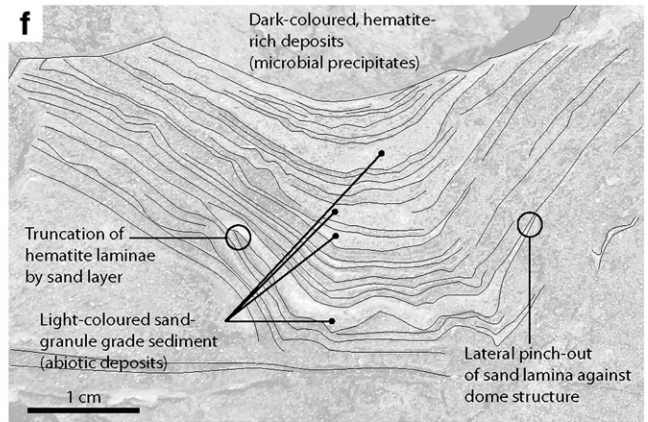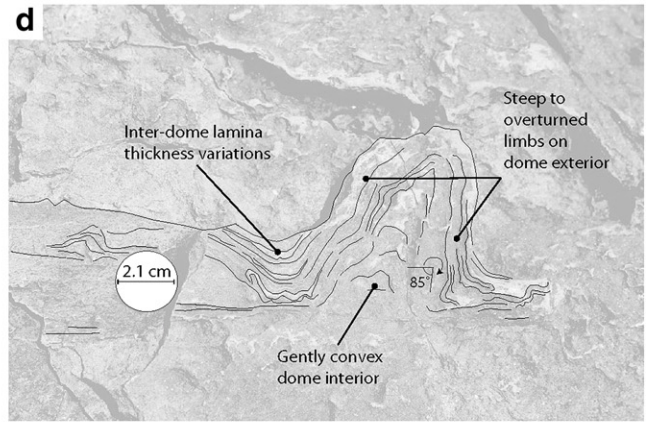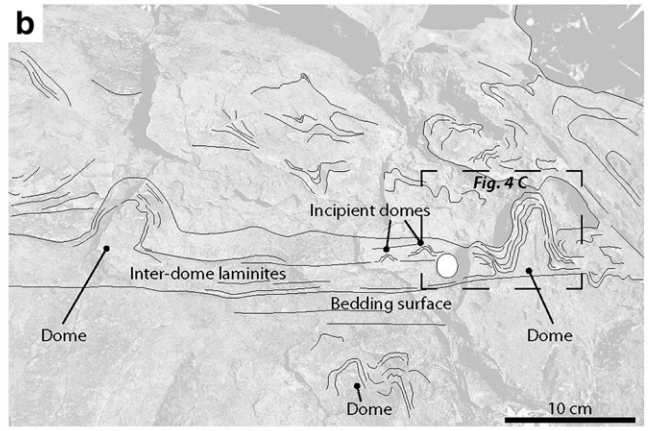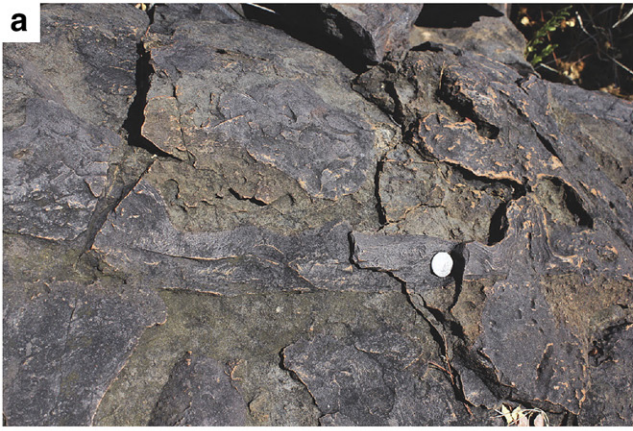
The inclusion of meta-sandstone clasts within the diamictite implies extensive reworking of the Nabis Formation at Ghaub and Varianto farms, but the occurrence of schists and meta-granites toward the top of the succession may suggest erosion down to deeper crystalline basement levels; ironstone clasts in the diamictite member reflect cannibalisation of the underlying ironstone member. The stepwise increase in clast size up section in the overlying diamictites, coupled with poorly developed stratification, could be cited as evidence for non-glaciogenic debris flow sedimentation (Eyles and Januszczak,

2007), but evidence for glaciation in the Chuos diamictites is compelling. Attenuated, lozenge-shaped to lenticular clasts in those diamictites are strongly indicative of subglacial shear (van der Wateren et al., 2000). Fractured clasts, injected with diamictite matrix, are interpreted to record reduction of clast strength and brittle failure under high hydrostatic stresses beneath a confining sediment/ice load. The impact structures beneath pebble to boulder-sized lonestones represent ice-rafted debris (IRD). The commonly cited mechanism of rafting by sediment gravity flows (e.g. Eyles and Januszczak, 2007) is rejected due to the absence of imbrication in the outsized fraction, and the lack of correlation between bed thickness and maximum clast size. Finally, the occurrence of soft-sediment striations within sand-prone levels of the stratified diamictite is interpreted as intra-diamictite slip-planes, akin to a sliding deck of cards (Sutcliffe et al., 2000; Le Heron et al., 2005) (Fig. 6h) induced by an overlying ice mass. The co-occurrence of dropstone textures in the diamictites and sub-glacial shear zones allow us to tentatively propose that these strata represent sub-ice sedimentation, in a similar model to that of the younger Ghaub glaciation of northern Namibia (Domack and Hoffman, 2011). In the model, sub-ice marginal wasting (explaining the dropstones) and subglacial shear structures record oscillation of a dynamic grounding line.

## 5. Discussion: global context of ironstone and diamictites in the Chuos Formation

The concordant and gradational nature of the boundary between the ironstone and diamictite members is important as it allows a temporal connection between them to be inferred, and for a cryptic unconformity or disconformity to be rejected. In the Otavi Mountain Land, the succession initially lacks evidence for glacial processes (ironstone member), with glaciogenic strata becoming more evident upward (the diamictite member). Cannibalisation of shelf successions during subsequent glacial advances commonly destroys the record of

**Fig. 5.** Examples of dome stromatolites in the ironstone member of the Chuos Formation. a and b: General outcrop photograph and sketch of dome structures growing almost orthogonally to bedding surfaces. Note the steep angle of the flanks of the dome structures, and relatively flat inter-dome area with incipient, small-scale domes in between. c and d: Photograph and sketch of area outlined in b. Note that the interior/core of the dome structure is gently convex with the angle of dip increasing up-structure. e and f: Photograph and sketch of area outlined in d. Note the interlamination of sand- to granule-grade laminae (light coloured) and microcrystalline hematite laminae (dark coloured). Note that the former show thickening into the inter-dome area, pinch out onto the dome flanks, and truncate underlying laminae. These properties indicate a mechanical (i.e. abiotic) origin for the sand- to granule-grade laminae. g and h: Photograph and sketch of further examples of dome stromatolites and associated laminites. Note in these examples the lower profile of the domes and gentler dips at the dome flanks. Stratigraphic position of all photographs shown in Fig. 3.

a

b
Fig. 4 C
Incipient domes
Inter-dome laminites
Bedding surface
Dome
Dome
Dome
10 cm

c

d
Inter-dome lamina
thickness variations
Steep to
overturned
limbs on
dome exterior
2.1 cm
85°
Gently convex
dome interior

e

f
Dark-coloured, hematite-
rich deposits
(microbial precipitates)
Truncation of
hematite laminae
by sand layer
Light-coloured sand-
granule grade sediment
(abiotic deposits)
Lateral pinch-out
of sand lamina against
dome structure
1 cm

g

h
Palaeo-relief
on upper surface
of bed
Sub-dome laminites
Convex-up dome
morphology
2.1 cm

early glacial advances in a basin. For example, in the Pleistocene record, nine phases of deeply incised, subglacial tunnel valleys have been recognised in the North Sea based on crosscutting relationships (Stewart and Lonergan, 2011). Therefore, in Ghaub/Varianto, the gradational and concordant nature of the contact may indicate that pre-glacial ironstone deposition led directly into the Chuos glaciation. Alternatively, if the diamictite member of the Chuos Formation is assumed to represent a final glacial cycle, the ironstone member represents an interglacial succession.

Beyond our study area, some 500 km to the northwest, domed stromatolite structures have also been observed in the Chuos Formation of the Opuwo region (Figs. 1b; 7). Here, as in the Otavi Mountain Land, stromatolite structures occur beneath diamictites but are also intercalated with them on the metre-scale. The extent of microbialite facies in other Cryogenian ironstones is unclear, and potentially awaits recognition, because ferruginous facies in Neoproterozoic strata are globally extensive (e.g. Kirschvink, 1992; Hoffman and Schrag, 2002). Both Macdonald et al. (2010) and Hoffman et al. (2011) argue that ironstones in Cryogenian strata are uniquely associated with the Sturtian glacial event at about 715 Ma, although evidence is emerging of Ediacaran-aged ironstones from Uruguay (Pecoits et al., in press).

The Rapitan Group (Cryogenian) of western Canada is similar to the Chuos Formation in both lithofacies and basin context, representing deposition in a paraglacial rift basin (Young, 1976; Eisbacher, 1985). An iron-rich, dropstone-bearing unit (the Sayunei Formation) is capped by a diamictite unit (the Shezal Formation) (Hoffman and Halverson, 2011). Measured sections (Fig. 3 of Eisbacher, 1985) illustrate that the most complete successions have a basal ferruginous shale sequence bearing occasional dropstones. These deposits pass gradationally upward, via 5–40 m jaspillite-hematite ironstone at the top of the Sayunei Formation, into diamictites. The ironstone is laterally persistent in depocentres (Eisbacher, 1985). Sea-ice removal may have triggered local grounding line advance, resulting in deposition of the Shezal Formation (Eisbacher, 1985): Hoffman and Halverson (2011) recognised this as a possible catalyst for ironstone precipitation. In addition to an abiotic "rusting of the seas" model, a biologically-mediated mechanism was also considered. Once "the ice cover thinned and finally disappeared, anoxic and oxygenic photosynthesis could have precipitated $Fe_2O_3$-precursor from anoxic Fe(II)-rich basin waters" (Hoffman et al., 2011). The biogenic mechanism was dismissed by those authors in favour of an abiotic explanation, although the reasons for such preference are unclear. Such a biogenic mechanism for ironstone precipitation, via for example photosynthetic stromatolites, would be in agreement with our observations in Namibia.

In Death Valley (California), a ferruginous rift basin succession (Petterson et al., 2011), again highly comparable to the Chuos Formation, was deposited. The Kingston Peak Formation (Cryogenian) comprises several kilometres of ferruginous glaci-turbidites, diamictites of mass flow affinity and boulder-sized lonestones (Troxel, 1982; Prave, 1999) interpreted as dropstones (Abolins et al., 2000; Corsetti and Kaufman, 2003), deposited beyond the ice grounding line (Mrofka and Kennedy, 2011). Thus, deep-water, iron-rich facies are considered to represent deposition without direct ice sheet influence, in contrast to very similar deposits in the Mackenzie Mountains.

In South America, stratified Fe and Mn ores occur in the Corumbá rift graben of Brazil and in neighbouring Bolivia, are considered to be of hydrothermal origin, and are intercalated with diamictites (Trompette et al., 1998). Urban et al. (1992) attributed the ores to oxidation of Fe and Mn rich rock flour during retreat of mountain glaciers. On the

Yangtze Platform (south China), banded ironstones in the Fulu Formation are sandwiched between Cryogenian diamictites of the Chang 'an and Silikou formations (Zhang et al., 2011). Tang et al. (1987) interpreted the ironstones as "interglacial" whereas in a subtly different interpretation Zhang et al. (2011, p. 358) view them as the "waning stage of the Jiangkou glaciation". This latter interpretation stands in contrast to our interpretation of the Chuos succession, where ironstones in Ghaub/Varianto farms were deposited during the waxing stage of glaciation.

In Australia, likely temporal equivalents to the Chuos Formation include the Holowilena and Braemar ironstones of South Australia (Le Heron, 2012). These ironstones occur at slightly different levels along strike, and are fault-bounded, allowing, like their counterparts in the Mackenzie Mountains, in Death Valley, and in Brazil/Bolivia, a connection to fault-transmitted fluids to be inferred (Link and Gostin, 1981). Bekker et al. (2010) envisaged the same mechanism for ironstone precipitation in the Otjosondu region of the central Damara Belt in Namibia, citing associated volcanogenic massive sulphide (VMS) deposits (Buhn et al., 1992) and REE values in support. By direct comparison with the Chuos deposits described herein, the Holowilena ironstone lies beneath a succession of diamictites and ice-rafted debris in the overlying Wilyerpa Formation, interpreted as the deposits of glacial (re)advance (Le Heron et al., 2011). Thus, in a similar way, deposition during glacial waxing is envisaged. Our evidence from Ghaub/Varianto farms does not exclude extensional fault systems during breakup of Rodinia (Eyles and Januszczak, 2004) as providing a source of ferrous iron in solution for acidophile biomats. The stratigraphic context of the ironstones does, however, exclude the model of global ice cover inhibiting iron precipitation (Kirschvink, 1992; Hoffman and Schrag, 2002) during a phase of ice wasting because evidence for glacial waxing, and indeed subglacial processes, is apparent in overlying diamictite deposits.

From the global analogues discussed above, it emerges that diamictites generally occur above iron formations in Canada (Mackenzie Mountains), in the USA (Death Valley), in China (Yangtze Platform) and in South Australia; they are intercalated with them in Brazil and in Bolivia. In our study area, note that there is no direct evidence for glacial processes in the ironstones, thereby challenging the long-held view of anoxia induced by an overlying ice sheet. Furthermore, the need to invoke meltwater plumes to oxidise iron as envisaged by Hoffman and Halverson (2008) and Hoffman et al. (2011) is unnecessary, because stromatolite colonies provide an alternative mechanism of seawater oxidation.

Our field observations of stromatolites in the Chuos Formation and their interpretation should also be seen in the context of recent work by Tziperman et al. (2011). These authors suggest that enhanced flux of organic material from the upper ocean to submarine sediments and porewaters, when subject to remineralization under anoxic conditions by sulphate or iron-reducing bacteria, may have changed the alkalinity of ocean waters sufficiently to precipitate siderite and draw down $CO_2$ to initiate a snowball Earth. However, this proposed mechanism is distinct from the process highlighted herein, because it is inferred that photosynthetic (and hence sea-floor surface) biomats played a role in drawing down $CO_2$, at least locally. The occurrence of stromatolites within the ironstones suggests a close analogue to the modern day acidophile biomats that photosynthesise, draw down $CO_2$, and oxidise ferrous iron (Brake et al., 2002; Brake and Hasiotis, 2008).

The above comparison requires the Chuos biomats to have developed in the photic zone. Therefore, it is suggested that rift-sourced iron fed acidophile biomats which in turn fixed iron in a shallow marine

**Fig. 6.** a: Clast of the ironstone member incorporated in the diamictite member: microcrystalline hematite laminae are clearly visible. b: Liesegang laminae, recording limited abiotic diffusional re-precipitation of iron oxides. c: Globular concretions of hematite overprinting stromatolitic domes in the ironstone member. d: Well stratified diamictite, showing intercalation of clast-rich and clast-poor zones, with evidence of augen structures and stratification-parallel attenuation of clasts. This is interpreted as a subglacial shear zone. e: Quartzite clast, shattered and intruded by diamictite matrix, in the same subglacial shear zone. f: Large quartzite lonestone with an unequivocal impact structure, enabling it to be interpreted as an ice-rafted dropstone. g: Soft sediment striated surface in the diamictite member. h: Soft-sediment striated surface for comparison in a similar, subglacially deformed sedimentary succession of Late Ordovician age from Libya (Le Heron et al., 2005). The development of soft sediment striated surfaces implies transmission of shear in unconsolidated sediments akin to a sliding deck of cards (Sutcliffe et al., 2000; Le Heron et al., 2005).
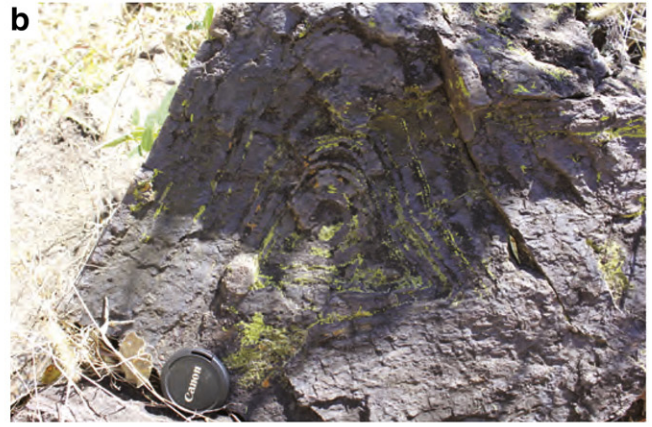
**Fig. 7.** Domed stromatolites, some 500 km west of Ghaub and Varianto farms, in the Chuos Formation of the remote Opuwo area (see Fig. 1B for location). Identical intercalated microcrystalline hematite and sand- to granule-grade laminations appear to confirm that ironstone microbialites are of significant lateral extent in Namibia. Grid reference: 18°43. 828′S 13°43.749′E.

or possibly lacustrine rift basin. Ferrous iron in solution can stimulate photosynthesis by an estimated 500 to 600% (Pierson et al., 1999), and thus the drawdown of $CO_2$ during the formation of these structures may also allow us to tentatively postulate that acidophile biomats played a role in cooling. This, however, presents a paradox. Iron formations typically have extremely low organic carbon contents (Hoffman et al., 2011): $Fe^{3+}$ is also an eager electron acceptor supporting microbial respiration on the seafloor or during shallow burial diagenesis (Walker, 1987). Regardless, ironstones in northern Namibia occur concordantly beneath, and are hence temporally transitional into, glacial diamictites. They were deposited either at the onset of the Sturtian glaciation, or during an interglacial within this snowball Earth episode. In either scenario, they record entry into, rather than exit from, extreme glaciation as more commonly suggested (Kirschvink, 1992; Hoffman and Schrag, 2002).

## 6. Conclusions

- New sedimentological data on the Chuos Formation of northern Namibia reveal that in the Otavi Mountain Land, these Sturtian-age deposits of suspected glaciogenic origin can be divided into two informal members. These are a lower ironstone member, and an upper diamictite member.
- The basal ironstone member, rich in hematite and magnetite, contains 1) evidence for tractional sedimentation (metre-scale cross bedding) and 2) dome structures of 10–15 cm amplitude. These latter structures are characterised by crinkly internal lamination, and at the millimetre scale contain intercalated microcrystalline hematite/magnetite and sand to granule-grade sediment. The dome structures are interpreted as stromatolites probably built from aerotactic and phototactic bacteria. Preliminary mapping suggests that stromatolite intervals extend over at least 500 km of northern Namibia.
- The basal ironstone member shows a gradational contact with the upper diamictite member. This latter unit contains evidence for lonestones with impact structures (interpreted as ice-rafted dropstones), soft-sediment striated surfaces (scratching of an unconsolidated sediment surface beneath a grounded ice mass) and intensely sheared intervals (deformation of a volume of sediment beneath a grounded ice mass). Thus, a strong glacial influence on deposition can be demonstrated.
- By analogy to microbialites in modern acid mine drainage environments, ironstone member stromatolites are likely to have been sustained by photosynthesis, and thus iron fixation and $CO_2$ drawdown may have occurred in tandem. Growth of stromatolites, and

precipitation of ironstones, may thus potentially have promoted local cooling. This mechanism, whilst distinct from the burial model of Tziperman et al. (2011), adds credence to the idea of biologically mediated cooling.
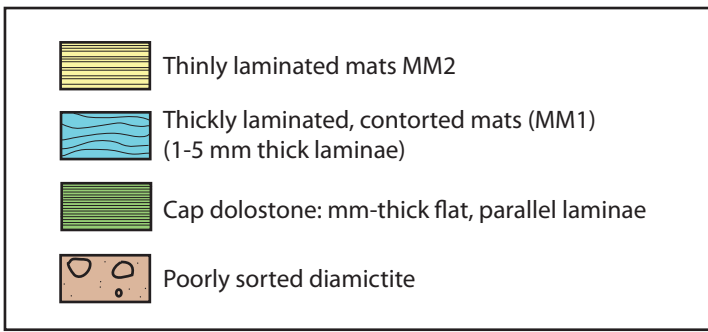
## References

Abolins, M., Oskin, R., Prave, A., Summa, C., Corsetti, F.A., 2000. Neoproterozoic glacial record in the Death Valley region, California and Nevada (in Great Basin and Sierra Nevada), Field Guide. Geological Society of America 2, 319–335.
Awramik, S.M., Grey, K., 2005. Stromatolites: biogenicity, biosignatures, and bioconfusion. Proceedings of SPIE 5906 http://dx.doi.org/10.1117/12.625556 (59060P1–5906P9).
Badenhorst, F.P., 1988. The lithostratigraphy of the Chuos mixtite in part of the southern central zone of the Damara orogen, South-West Africa. Communications of the Geological Survey of SW Africa/Namibia 4, 103–110.
Bechstädt, T., Jäger, H., Spence, G., Werner, G., 2009. Late Cryogenian (Neoproterozoic) glacial and post-glacial successions at the southern margin of the Congo Craton, northern Namibia: facies, palaeogeography and hydrocarbon perspective. In: Craig, J., Thurow, J., Thusu, B., Whitham, A., Abutarruma, Y. (Eds.), Global Neoproterozoic Petroleum Systems: The Emerging Potential in North Africa: Geological Society, London, Special Publications, 326, pp. 255–287.
Bekker, A., Slack, J.S., Planavsky, N., Krapez, B., Konhauser, K.O., Rouxel, O.J., 2010. Iron formation: the sedimentary product of a complex interplay among mantle, tectonic, oceanic, and biospheric processes. Economic Geology 105, 467–508.
Brake, S.S., Hasiotis, S.T., 2008. Eukaryote-dominated biofilms in extreme environments: overlooked sources of information in the geologic record. Palaios 23, 121–123.
Brake, S.S., Hasiotis, S.T., Dannelly, H.K., Connors, K.A., 2002. Eukaryotic stromatolite builders in acid mine drainage: implications for Precambrian iron formations and oxygenation of the atmosphere? Geology 30, 599–602.
Bühn, B., Stanistreet, I.G., Okrusch, M., 1992. Late Proterozoic outer shelf manganese and iron deposits at Otjosondu (Namibia) related to the Damaran oceanic opening. Economic Geology 87, 1393–1411.
Buick, R., Dunlop, J.S.R., Groves, D.I., 1981. Stromatolite recognition in ancient rocks: An appraisal of irregularly laminated structures in an Early Archaen chert-barite unit from North Pole, Western Australia. Alcheringa 5, 161–181.
Chang, S.-B.R., Stolz, J.F., Kirschvink, J.L., Awramik, S.M., 1989. Biogenic magnetite in stromatolites. II. Occurrence in ancient sedimentary environments. Precambrian Research 43, 305–315.
Corsetti, F.A., Kaufman, A.J., 2003. Stratigraphic investigations of carbon isotope anomalies and Neoproterozoic ice ages in Death Valley, California. GSA Bulletin 115, 916–932.
De Kock, W.P., Gevers, T.W., 1933. The Chuos tillite in the Rehoboth and Windhoek Districts, South-West Africa. Transactions of the Geological Society of South Africa 35, 115–118.
De Vries Klein, G., 1970. Depositional and dispersal dynamics of intertidal sand bars. Journal of Sedimentary Petrology 40, 1095–1127.
Domack, E.W., Hoffman, P.F., 2011. An ice grounding-line wedge from the Ghaub glaciation (635 Ma) on the distal foreslope of the Otavi carbonate platform, Namibia, and its bearing on the snowball Earth hypothesis. Geological Society of America Bulletin 123, 1448–1477.
Eisbacher, G.H., 1985. Late Proterozoic rifting, glacial sedimentation and sedimentary cycles in the light of Windermere deposition, western Canada. Palaeogeography, Palaeoclimatology, Palaeoecology 51, 231–254.
España, J.-S., Pastor, E.S., López Pamo, E., 2007. Iron terraces in acid mine drainage systems: a discussion about the organic and inorganic factors involved in their formation through observations from the Tintillo acidic river (Riotinto mine, Huelva, Spain). Geosphere 3, 133–151.
Eyles, N., 2008. Glacio-epochs and the supercontinent cycle after ~3.0 Ga: tectonic boundary conditions for glaciation. Palaeogeography, Palaeoclimatology, Palaeoecology 258, 89–129.
Eyles, N., Januszczak, N., 2004. 'Zipper-rift': a tectonic model for Neoproterozoic glaciations during the breakup of Rodinia after 750 Ma. Earth-Science Reviews 65, 1–73.
Eyles, N., Januszczak, N., 2007. Syntectonic subaqueous mass flows of the Neoproterozoic Otavi Group, Namibia: where is the evidence of global glaciation? Basin Research 19, 179–198.
Geological Survey of Namibia, 2008. Sheet 1916- Tsumeb (1:250,000). Ministry of mines and Energy, Windhoek.
Gevers, T.W., 1931. An ancient tillite in South-West Africa. Transactions of the Geological Society of South Africa 34, 1–17.
Hedberg, R.M., 1979. Stratigraphy of the Ovamboland Basin, South West Africa. Bulletin - University of Cape Town, Precambrian Research Unit 24, 325.
Henry, G., Stanistreet, I.G., Maiden, K.J., 1986. Preliminary results of a sedimentological study of the Chuos Formation in the central zone of the Damara Orogen: evidence

for mass flow processes and glacial activity. Communications of the Geological Survey of South-West Africa/Namibia 2, 75–92.

Hoffman, P.F., Halverson, G.P., 2008. Otavi Group of the western Northern Platform, the eastern Kaoko Zone and the western Northern Margin Zone. In: Miller, R.McG. (Ed.), The Geology of Namibia: Neoproterozoic to Lower Palaeozoic. Ministry of Mines and Energy, vol. 2, pp. 13.69–13.136.

Hoffman, P.F., Halverson, G.P., 2011. Neoproterozoic glacial record in the Mackenzie Mountains, northern Canadian Cordillera. In: Arnaud, E., Halverson, G.P., Shields-Zhou, G. (Eds.), The Geological Record of Neoproterozoic Glaciations: Geological Society Memoirs, 36, pp. 397–411.

Hoffman, P.F., Schrag, D.P., 2002. The snowball Earth hypothesis: testing the limits of global change. Terra Nova 14, 129–155.

Hoffman, P.F., Hawkins, D.P., Isachsen, C.E., Bowring, S.A., 1996. Precise U–Pb zircon ages for early Damaran magmatism in the Summas Mountains and Welwitschia Inlier, northern Damara belt, Namibia. Communications of the Geological Survey of Namibia 11, 47–52.

Hoffman, P.F., Macdonald, F.A., Halverson, G.P., 2011. Chemical sediments associated with Neoproterozoic glaciation: iron formation, cap carbonate, barite and phosphate. In: Arnaud, E., Halverson, G.P., Shields-Zhou, G. (Eds.), The Geological Record of Neoproterozoic Glaciations: Geological Society Memoirs, 36, pp. 67–80.

Hoffmann, K.-H., Prave, A.R., 1996. A preliminary note on a revised subdivision and regional correlation of the Otavo Group based on glaciogenic diamictites and associated cap dolostones. Communications of the Geological Survey of Namibia 11, 77–82.

Hoffmann, K.H., Condon, D.J., Bowring, S.A., Crowley, J.L., 2004. U–Pb zircon date from the Neoproterozoic Ghaub formation, Namibia: constraints on Marinoan glaciation. Geology 32, 817–820.

Hofmann, H.J., Grey, K., Hickman, A.H., Thorpe, R.I., 1999. Origin of 3.45 Ga coniform stromatolites in Warrawoona Group, Western Australia. Geological Society of America Bulletin 111, 1256–1262.

Kamona, A.F., Günzel, A., 2007. Stratigraphy and base metal mineralization of the Otavi Mountain Land, Northern Namibia — a review and regional interpretation. Gondwana Research 11, 396–413.

Kirschvink, J.L., 1992. Late Proterozoic low-latitude glaciation: the snowball Earth. In: Schopf, J.W., Klein, C. (Eds.), The Proterozoic Biosphere. Cambridge University Press, Cambridge, pp. 51–52.

Konhauser, K.O., Hamade, T., Raiswell, R., Morris, R.C., Ferris, F.G., Southam, G., Canfield, D.E., 2002. Could bacteria have formed the Precambrian banded iron formations? Geology 30, 1079–1082.

Konhauser, K.O., Newman, D.K., Kappler, A., 2005. The potential significance of microbial Fe (III)-reduction during Precambrian banded iron formations. Geobiology 3, 167–177.

Konhauser, K.O., Kappler, A., Roden, E.E., 2011. Iron in microbial metabolisms. Elements 7, 89–93.

Le Heron, D.P., 2012. The Cryogenian record of glaciation and deglaciation in South Australia. Sedimentary Geology 243–244, 57–69.

Le Heron, D.P., Sutcliffe, O.E., Whittington, R.J., Craig, J., 2005. The origins of glacially related soft-sediment deformation structures in Upper Ordovician glaciogenic rocks: implication for ice sheet dynamics. Palaeogeography, Palaeoclimatology, Palaeoecology 218, 75–103.

Le Heron, D.P., Cox, G.M., Trundley, A.E., Collins, A., 2011. Sea-ice free conditions during the early Cryogenian (Sturt) glaciation, South Australia. Geology 39, 31–34.

Link, P.K., Gostin, V.A., 1981. Facies and palaeogeography of Sturtian glacial strata (Late Precambrian), South Australia. American Journal of Science 281, 353–374.

Macdonald, F.A., Strauss, J.V., Rose, C.V., Dudás, F.Õ., Schrag, D.P., 2010. Stratigraphy of the Port Nolloth Group of Namibia and South Africa and implications for the age of Neoproterozoic iron formations. American Journal of Science 310, 862–888.

Martin, H., 1965. Observations concerning the problem of the late Precambrian glacial deposits in South West Africa. Geologische Rundschau 54, 115–127.

Martin, H., Porada, H., Walliser, O.H., 1985. Mixtite deposits of the Damara sequence, Namibia, problems of interpretation. Palaeogeography, Palaeoclimatology, Palaeoecology 51, 159–196.

McCabe, C., van der Voo, R., Peacor, D.R., Scotese, C.R., Freeman, R., 1983. Diagenetic magnetite carries ancient yet secondary remanence in some Paleozoic sedimentary carbonates. Geology 11, 221–223.

Miller, R.McG. (Ed.), 2008. The Geology of Namibia: Neoproterozoic to Lower Palaeozoic. Ministry of Mines and Energy, vol. 2.

Mrofka, D., Kennedy, M., 2011. The Kingston Peak Formation in the eastern Death Valley region. In: Arnaud, E., Halverson, G.P., Shields-Zhou, G. (Eds.), The Geological Record of Neoproterozoic Glaciations: Geological Society, London, Memoirs, 36, pp. 449–458.

Pecoits, Aubet, N.R., Gingras, M.K., Poulton, S.W., Bekker, A., Veroslavsky, G., Konhauser, K.O., in press. An Ediacaran iron formation: New evidence for ferruginous late Neoproterozoic seawater. Precambrian Research. DOI: 10.1016/j.precamres.2011.10.002.

Petterson, R., Prave, A.R., Wernicke, B.P., 2011. Glaciogenic and related strata of the Neoproterozoic Kingston Peak Formation in the Panamint Range, Death Valley region, California. In: Arnaud, E., Halverson, G.P., Shields-Zhou, G. (Eds.), The Geological Record of Neoproterozoic Glaciations: Geological Society, London, Memoirs, 36, pp. 449–458.

Pierson, B.K., Parenteau, M.N., Griffin, B.M., 1999. Phototrophs in high-iron-concentration microbial mats: physiological ecology of phototrophs in an iron-depositing hot spring. Applications of Environmental Microbiology 65, 5474–5483.

Prave, A.R., 1999. Two diamictites, two cap carbonates, two $\delta^{13}$C excursions, two rifts: the Neoproterozoic Kingston Peak Formation, Death Valley, California. Geology 27, 339–342.

Riding, R., 2011. The nature of stromatolites: 3,500 million years of history and a century of research. In: Reitner, J., Quéric, N.-V., Arp, G. (Eds.), Advances in Stromatolite Geobiology: Lecture Notes in Earth Sciences, 131. Springer-Verlag, Belin, Germany, pp. 29–74.

Stewart, M.A., Lonergan, L., 2011. Seven glacial cycles in the middle–late Pleistocene of northwest Europe: geomorphic evidence from buried tunnel valleys. Geology 39, 283–286.

Stolz, J.F., Chang, S.-B.R., Kirschvink, J.L., 1989. Biogenic magnetite in stromatolites. I. Occurrence in modern sedimentary environments. Precambrian Research 43, 295–304.

Sutcliffe, O.E., Theron, J.A., Whittington, R.J., Theron, J.N., Craig, J., 2000. Calibrating the Late Ordovician glaciation and mass extinction by the eccentricity cycles of the Earth's orbit. Geology 23, 967–970.

Tang, J.-F., Fu, H.-Q., Yu, Z.-Q., 1987. The stratigraphic horizon, type, and formation condition of Precambrian siliceous iron formation in south China. Ore Geology 6, 1–10 (in Chinese).

Tewari, V., Seckbach, J., 2011. Stromatolites: Interaction of Microbes with Sediments. Springer . 751 pp.

Trompette, R., Alvarenga, C.J.S., Walde, D., 1998. Geological evolution of the Neoproterozoic Corumbá graben system (Brazil). Depositional context of the stratified Fe and Mn ores of Jacadigo Group. Journal of South American Earth Sciences 11, 587–597.

Troxel, B.W., 1982. Description of the uppermost part of the Kingston Peak Formation, Amargosa Rim canyon, Death Valley region, California. In: Cooper, J.D., Troxel, B.W., Wright, L.A. (Eds.), Geology of Selected Areas in the San Bernadino Mountains, Western Mojave Desert, and Southern Great Basin, California. : Geological Society of America Cordilleran Section volume and guidebook. Death Valley Publi. Co., Shoshone, CA, pp. 61–70.

Tziperman, E., Halevy, I., Johnston, D.T., Knoll, A.H., Schrag, D., 2011. Biologically induced initiation of Neoproterozoic snowball Earth events. PNAS 108, 15091–15096.

Urban, H., Stribny, B., Lippolt, H., 1992. Iron and manganese deposits of the Urucum district, Mato Grosso do Sul, Brazil. Economic Geology 87, 1375–1392.

Van der Wateren, F.M., Kluiving, S.J., Bartek, L.R., 2000. Kinematic indicators of subglacial shearing. In: Maltman, A.J., Hubbard, B., Hambrey, M.J. (Eds.), Deformation of Glacial Materials: Geological Society Special Publication, 176, pp. 259–278.

Walker, J.C.G., 1987. Was the Archaean biosphere upside-down? Nature 329, 710–712.

Yeo, G.M., 1981. The Late Proterozoic Rapitan glaciation in the northern Cordillera. In: Campbell, F.H. (Ed.), Proterozoic Basins of Canada: Geological Survey of Canada Paper 81–10, pp. 25–46.

Young, G.M., 1976. Iron-formation and glaciogenic rocks of the Rapitan Group, Northwest Territories, Canada. Precambrian Research 3, 137–158.

Zhang, Q.-R., Chu, X.-L., Feng, L.-J., 2011. Neoproterozoic glacial records in the Yangtze Region, China. In: Arnaud, E., Halverson, G.P., Shields-Zhou, G. (Eds.), The Geological Record of Neoproterozoic Glaciations: Geological Society Memoirs, 36, pp. 357–366.
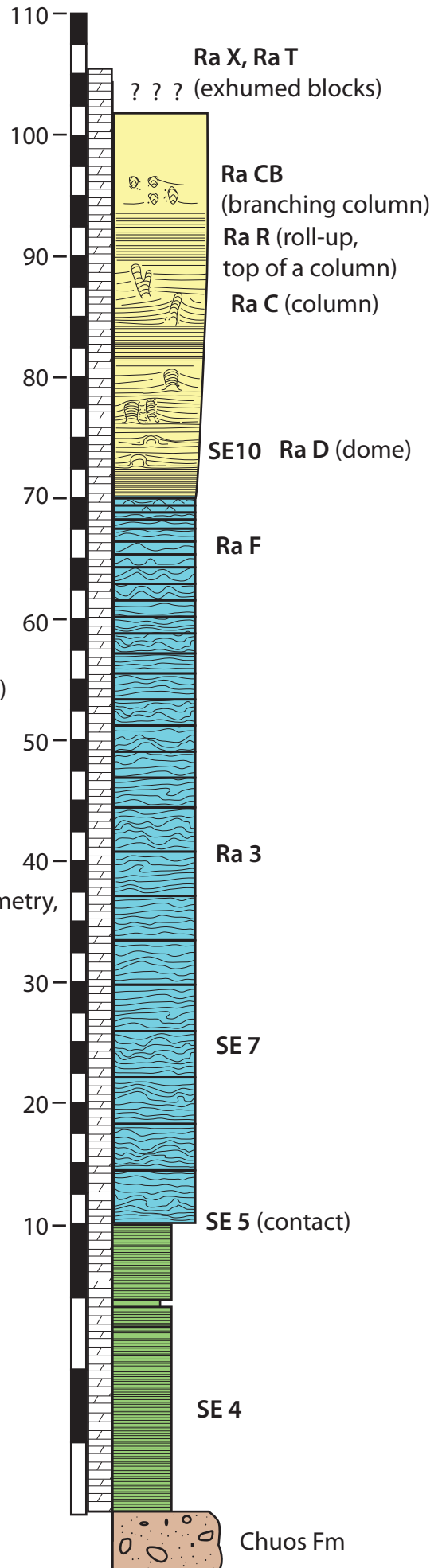
**APPENDIX D**

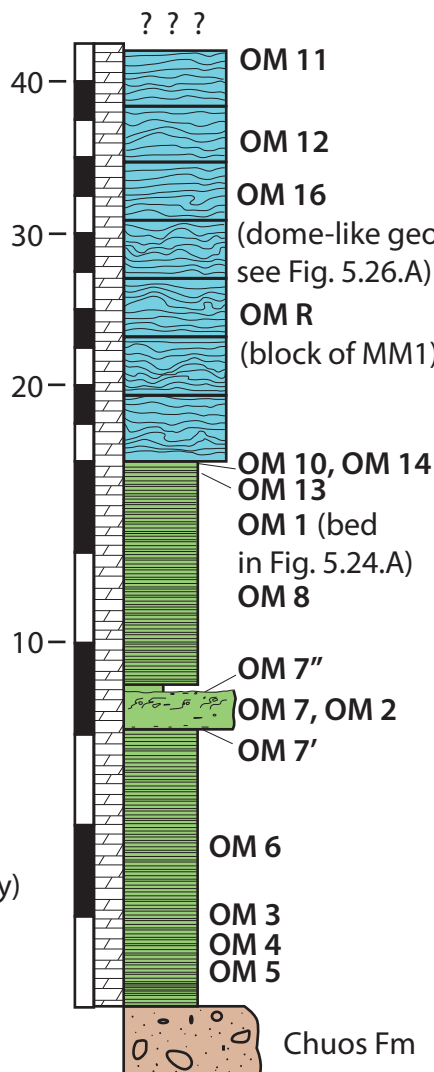**Legend:**

- Thinly laminated mats MM2
- Thickly laminated, contorted mats (MM1) (1-5 mm thick laminae)
- Cap dolostone: mm-thick flat, parallel laminae
- Poorly sorted diamictite

Note: most of samples from the Rasthof Farm area have been destroyed during sample preparation and analyses.

**Scale:** 5 m / 0 m

**Rasthof Farm area**

- Ra X, Ra T ? ? ? (exhumed blocks)
- Ra CB (branching column)
- Ra R (roll-up, top of a column)
- Ra C (column)
- SE10   Ra D (dome)
- Ra F
- Ra 3
- SE 7
- SE 5 (contact)
- SE 4
- Chuos Fm

**Omutirapo area**

OM S and R (block of MM1 found on the slope of the hill)

? ? ?

- OM 11
- OM 12
- OM 16 (dome-like geometry, see Fig. 5.26.A)
- OM R (block of MM1)
- OM 10, OM 14
- OM 13
- OM 1 (bed in Fig. 5.24.A)
- OM 8
- OM 7"
- OM 7, OM 2
- OM 7'
- OM 6
- OM 3
- OM 4
- OM 5
- Chuos Fm

**Okaaru area**

- OP 15
- OP 14
- OP 5
- OP 3
- OP 8
- OP 1, OP 7
- OP 13 (LLH geometry)
- OP 2
- OP 6
- OP 11, OP 10
- Chuos Fm
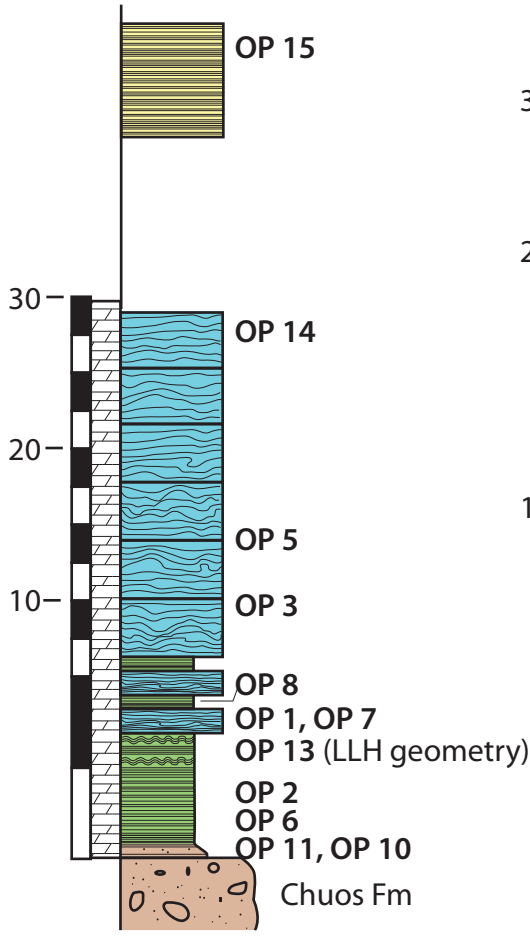
NNW ← 45 km → SSE/WNW ← 80 km → SSE

West      5.5 km      13 km      6.5 km      East
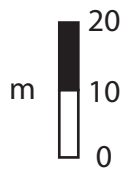
**Log 4**
Varianto Farm

**Top 4**

**CD 4** (exhumed block)

**Log 3**
Ghaub Farm

**Ga 2**

**Ga 1**
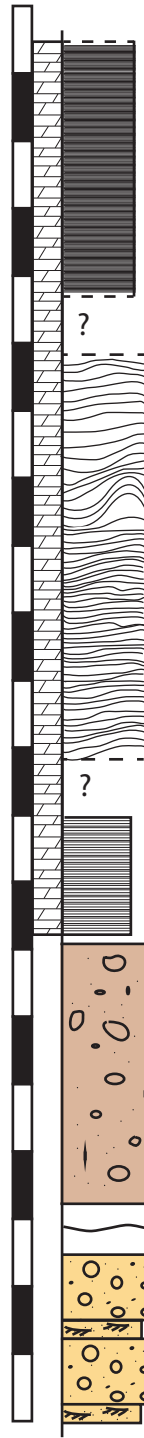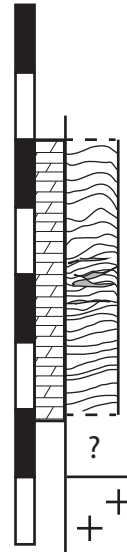
**Log 2**
Nosib Block

**Nosib Farm**

**Log 1**
Road C42

**C42**

Basement

m   20   10   0
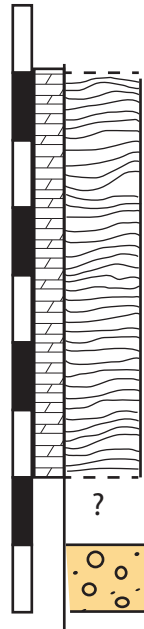
Thinly laminated microbialite
(sub-mm thick laminae)

Thickly laminated microbialite
(2-5 mm thick laminae) - Cuspate Facies

Thickly laminated microbialite
(2-5 mm thick laminae)

Cap dolostone: mm-thick flat, parallel laminae

Poorly-sorted diamictite

Conglomerate

Cross-bedded sandstone